Virginia Polytechnic Institute and State University
Loughborough University

PEGASUS

The First Successful Roadable Aircraft

AGATE General Aviation
Design Competition 2000

Imagine the Pegasus!

Imagine a vehicle that can take you virtually anywhere in the country in departure point to destination point in times unheard of today.

Imagine being able to fly to thousands of destinations which can't be reached by any airline.

Imagine all this and you will find yourself in the world of the ***Pegasus***, the world's first modern "roadable aircraft", a general aviation airplane with all the capabilities of the best four-place, single engine aircraft and with the added utility of having the family car with you at any flight destination.

Imagine being able to avoid high rental costs of airport hangars and tiedowns and parking lot fees for your car while on a flight away from home.

Imagine being able to fly your own plane on vacation or business and not having to worry about being grounded overnight due to weather or limited to certain airports where rental cars are available.

***Pegasus*, the go anywhere, anytime vehicle that makes flying as unfettered as your *imagination*.**

Section 1. Executive Summary

1.1. Introduction

As today's society becomes more demanding and its members become busier, convenience and reliability becomes more important. The Pegasus can provide both to the businessman as no craft could before. Its multipurpose role as both a plane and a car provide many advantages to its user, such as time and money savings, reliability, and the ability to always get to a destination. These are things that the commercial airlines, trains, buses, or a car alone cannot offer.

If the goal of NASA's Advanced General Aviation Transport Experiments (AGATE) Consortium and the Small Airplane Transportation System (SATS) is to make general aviation a viable alternative to current modes of transport, then they must look beyond the current vehicles being offered by the industry. These vehicles, while being safe, use 40 year old technology, are expensive, and do not offer the allure to young pilots that they once did.

Figure 1.1-1 View of the Pegasus in flight

The Pegasus (Figure 1.1-1) has state of the art technology incorporated into the user interfaces and structures. It has a newly designed, efficient, reliable propulsion system. It is designed to be the first successful roadable aircraft in the GA industry, which adds to its appeal to the younger generation who are always seeking something newer, faster, and better.

The AGATE Consortium stresses safety, innovativeness, and user-friendliness. It also calls for designs that will help revitalize the general aviation (GA) industry and provide for more usage of this country's small airports. The Pegasus meets and exceeds all these goals by providing a product that is versatile, yet affordable. It can even be used to fly to small airports where rental cars or taxi services are not available.

The purpose of this vehicle is to exceed the performance of other GA craft on the market by providing the added bonus of door-to-door service. This added convenience will come at a small cost to the user. The price will be comparable to buying a small GA craft and a small, practical car. But, unlike buying both, the car is there when you need to get to the airport and when you land at the other end of the trip.

The general arrangement drawing is shown in Figure 1.1-2.

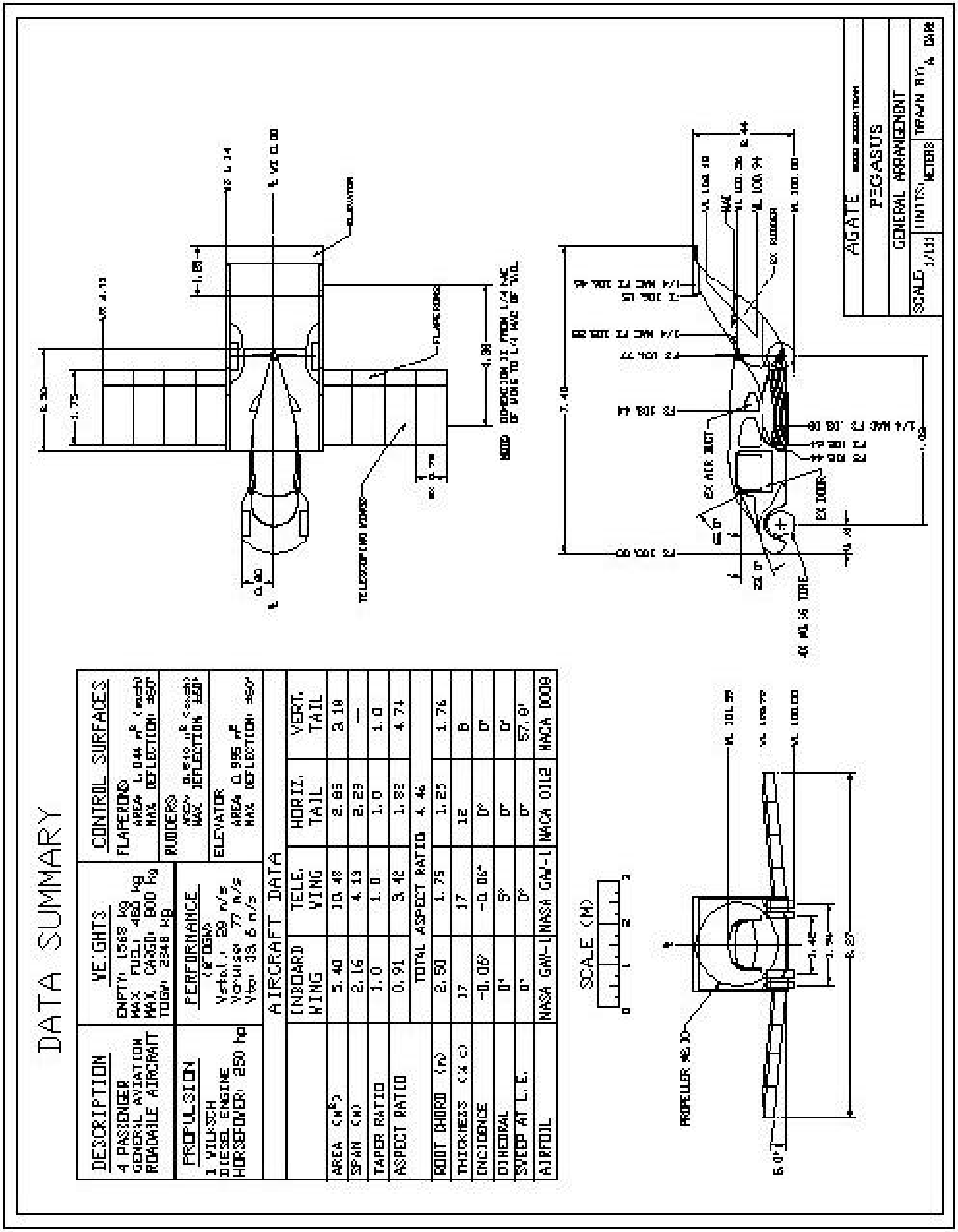

Figure 1.1-2 General Arrangement Drawing

1.2. Performance

If the Pegasus is to succeed it must not only be “roadable” but it must be a viable alternative to existing general aviation aircraft by at least meeting their levels of performance. The performance data shown below reveals that the Pegasus is indeed able to match the performance of popular aviation vehicles such as the Cessna 182 and to excel in several categories. More detail on these performance figures and the assumptions behind them can be found in Appendix K. The cruise altitude used for the calculations was 3000 m (9843 ft) with an 80% power setting.

Table 1.2-1 The Performance of the Pegasus

Normal cruise speed at 3000 meters (9843 ft)	77 m/s	150 kts
Maximum cruise speed at 3000 meters (9843 ft)	84 m/s	163 kts
Sea Level take off ground distance	210 m	690 ft
Sea Level take off with 15 meter (50 ft) obstacle clearance	280 m	920 ft
Sea Level landing ground distance	230 m	755 ft
Sea Level landing distance with 15 meter (50 ft) obstacle clearance	350 m	1148 ft
Sea Level stall speed	28 m/s	55 kts
Maximum rate of climb at sea level	445 m/min	1460 ft/min
Range at normal cruise at 3000 meters (9843 ft)	1528 km	825 nmi
Maximum range at 3000 meters (9843 ft)	1778 km	960 nmi
Maximum endurance at 3000 meters (9843 ft)	9.5 hrs	9.5 hrs

The power versus velocity curves for the Pegasus are shown below as Figures 1.2-1 and 1.2-2.

It is seen from the above table and figures that the Pegasus is very competitive with existing GA aircraft and that there is no serious performance penalty associated with the vehicle’s ability to convert to an automobile for ground use.

The on the road performance of the Pegasus is discussed in a later section of this summary report and in detail in Appendix M.

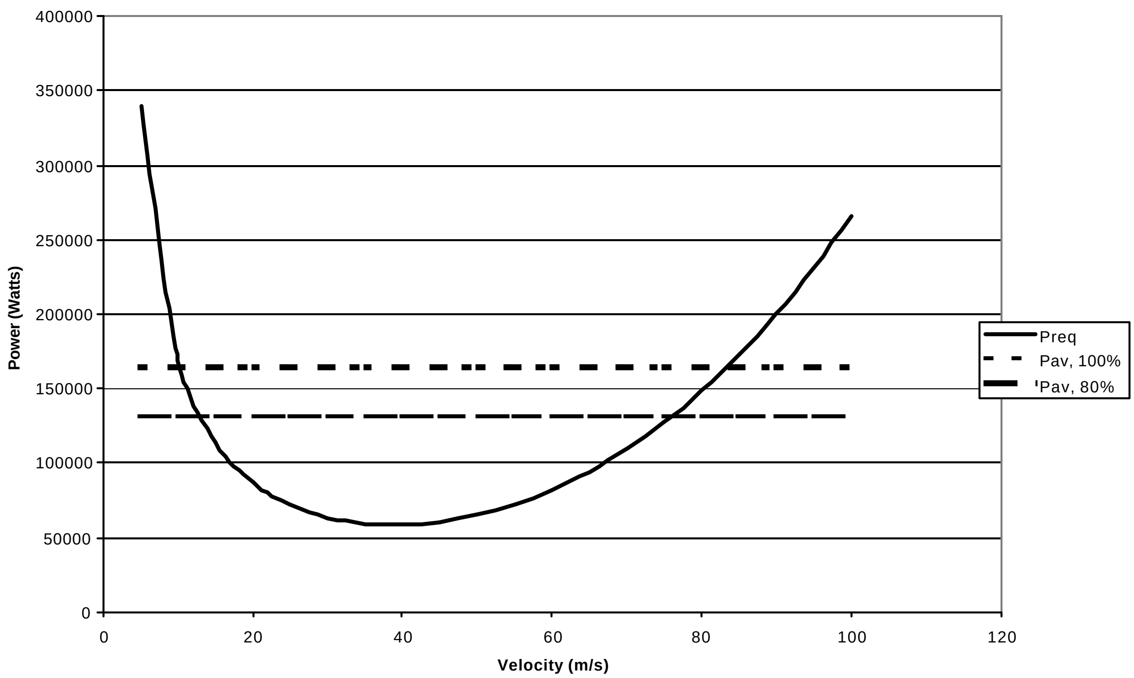

Figure 1.2-1 Power vs. Velocity Curve for Sea Level

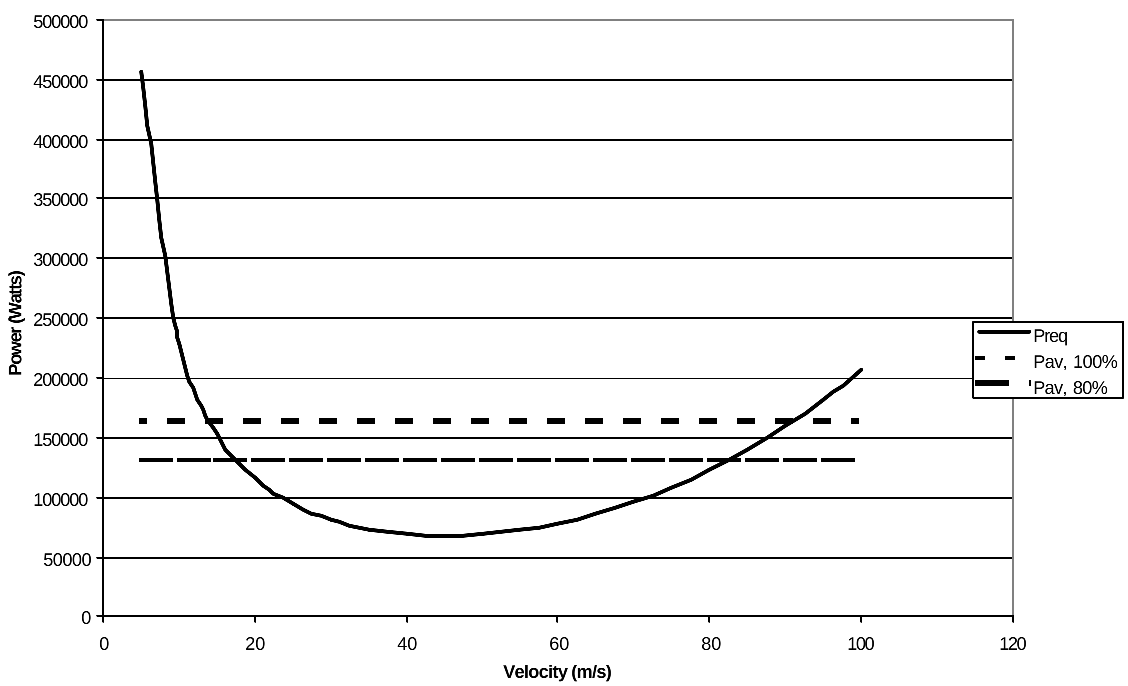

Figure 1.2-2 Power vs. Velocity Curve for 3000 meters

1.3. Aerodynamics

The design of a roadable aircraft presented some unique aerodynamic problems. The lifting surfaces had to be large enough to produce the required lift in the air yet small enough for safe driving on the road. The wing also had to be folded, retracted, or otherwise stored for road use. To find a solution to these issues, aerodynamic configurations not often used in the general aviation industry were examined. The solution included using extending wings. The design uses a low aspect ratio “inboard” wing with telescoping “outboard” wings. Several other uncommon features for increasing lift without increasing wing span were investigated including a Burnelli lifting body, a channel wing, and winglets. The final design used a combination of all these features. Figure 1.3-1 shows a top view of the Pegasus, displaying the lifting surfaces.

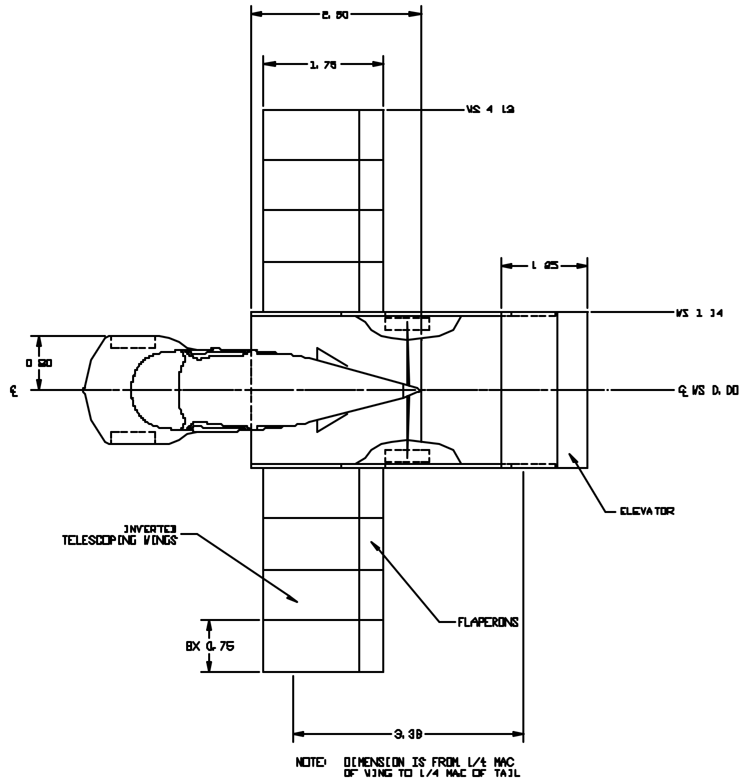

Figure 1.3-1 The Top View of the Pegasus (dimensions in meters)

Based on the performance parameters established for the design, the wing sizes and airfoil section were selected. To meet department of transportation (DOT) and European Community (EC) road requirements, the maximum span of the inboard wing was chosen to be 2.28 m (7.48 ft). A chord of 2.5 meters (8.202 ft) was selected for this inner wing, resulting in an area of 5.7 m^2 (61.35 ft^2). The telescoping wings each had a semi span of 3 meters (9.84 ft) with a chord of 1.75 m (5.74 ft). These sections total 10.5 m^2 (113.02 ft^2) in area, giving a total wing area of 16.2 m^2 (174.4 ft^2). The required size for the horizontal tail was 1.63 m^2 (17.55 ft^2), with a moment arm of 4 m (13.12 ft).

The airfoil section selected for both the inboard and outboard sections is the NASA GA(W)-1 otherwise designated as NASA LS(1)-0417. Figure 1.3-2 shows the airfoil and figure 1.3-3 shows the lift curve slope for this airfoil. This is a 17% thick airfoil with a design lift coefficient of 0.4, and was designed for general aviation applications. This airfoil was selected for its smooth stall characteristics, a high stall incidence angle, and its high lift to drag ratio. Its large thickness was also useful in allowing retraction of the outboard wings into the inboard section. The maximum lift coefficient for the two dimensional airfoil section is approximately 2.0 with zero lift at –4 degrees angle of attack and a lift curve slope of 5.9. For the actual three dimensional airfoil, the maximum lift coefficient is about 1.8 with a lift curve slope of 4.9. The drag coefficient at zero drag for the Pegasus is 0.025, which compares well to today's general aviation craft.

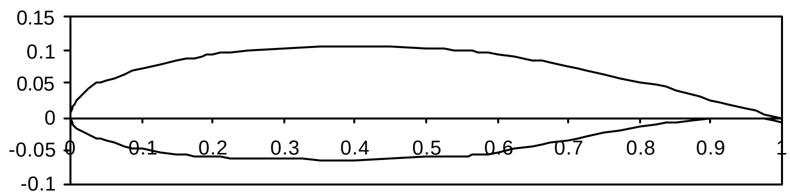

Figure 1.3-2 The GA(W)-1 Airfoil Shape

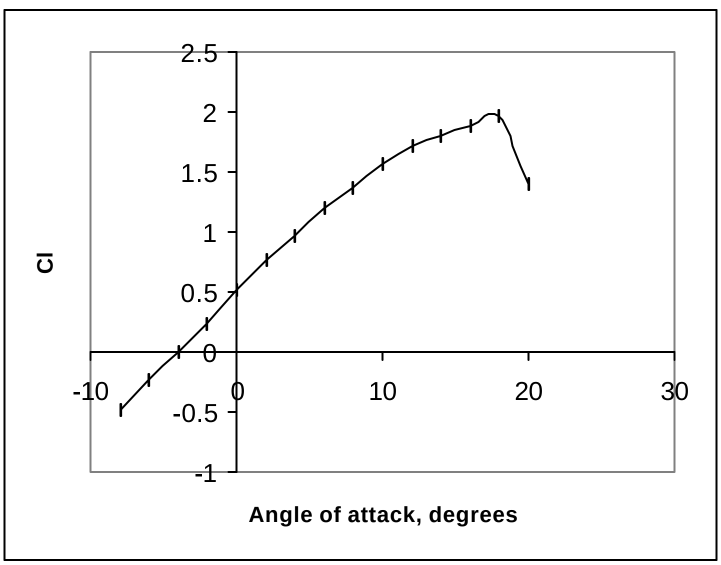

Figure 1.3-3 2-D Cl vs alpha for the GA(W)-1

At a cruise speed of 77 m/s (150 kts), the aircraft's ideal angle of attack is 0.06 degrees. Therefore, the inboard wing was mounted on the fuselage at 0.06 degrees so that the fuselage would remain level in cruise at altitude. The telescoping sections were mounted at the same angle of attack as the inboard section. Wind tunnel tests confirmed that the inboard section of the telescoping wings will stall before the outboard sections due to interference from the main wing, ensuring aileron effectiveness at the onset of stall. To improve lateral stability, the telescoping wing sections were set at a dihedral angle of 5.degrees

The NACA 0012 section was chosen for the horizontal tail. Due to the incidence angle of the vertical tails being used as winglets, the maximum span of the horizontal tail is 2.24 m (7.35 ft). The chord of the tail was calculated to be 1.25 m (4.10 ft). The vertical stabilizers were used as both winglets for the inboard wing and as conventional stabilizers. The optimum thickness to chord ratio for a winglet is 8% according to Raymer[1], so a NACA 0008 airfoil was selected for use in the vertical tail. Calculations of winglet effectiveness showed that the vertical tails needed to be canted at a 1 degrees angle.

The combination of the inboard wing and the propeller can be characterized as a channel wing or more specifically a 'scoop wing', because of the rectangular shape. A channel wing uses the propeller induced flow over the airfoil to increase lift. For the Pegasus' wing, propeller induced lifts of as high as 2200 N (500 lbs) were estimated.

As mentioned above, the vertical stabilizers double as Whitcomb winglets. Whitcomb winglets take advantage of the spill-over vortex at a wing tip or wing juncture to generate a lift-induced thrust. In the flying configuration, the winglets are estimated to generate 80 N (19 lbs) of 'surplus' thrust. This combination of old and new technologies resulted in more than adequate aerodynamic performance to give the Pegasus very competitive flight characteristics and handling capabilities.

1.4. Stability and Control

The Pegasus provides superior handling quality and ride comfort. This craft features conventional rudders on the twin vertical tails, a conventional elevator and full-length flaperons. These control surfaces employ actuators with the fly-by-wire system to provide the needed control power for maneuvering through a wide range of flight conditions. Transitioning from flight mode to ground mode is effortless due to the fly/drive-by-wire system employed by the Pegasus.

Despite the dual role nature of the Pegasus, it remains a well-mannered vehicle while airborn. In addition to its inherent static stability, the Pegasus meets all dynamic stability requirements set in the Military Specification 8785 without augmentation. Add to this the feedback fly-by-wire system, and the result is effortless control without losing the feel of a mechanical system. Refer to Appendix L for details concerning the stability and control analysis for the Pegasus. Road stability is addressed in Appendix M.

1.5. Structures

The structural design of the Pegasus involved innovative approaches to the design of an airplane. The most obvious feature involves the telescoping wing which extends for flight and retracts for driving[2]. Four wing sections telescope into the inner wing and fuselage by way of an internal 12 V motor that retracts the tubular spars, as shown in Figure 1.5-1. Each half of the wing consists of four wing segments of 0.75m (2.46 ft) span composed of an external skin section, which is attached by ribs to two spars (fore and aft). These spar sections are tubular and form the basis of telescopic operation.

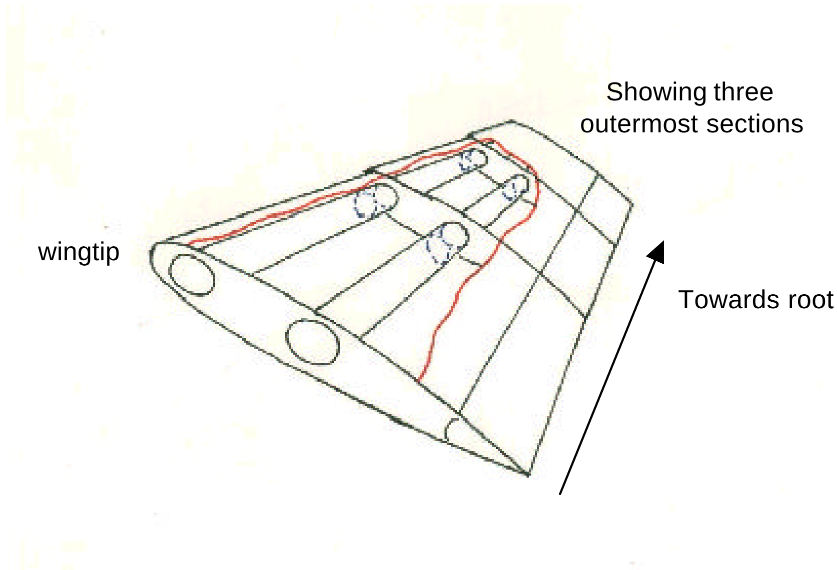

Figure 1.5-1 General Telescoping Wing Schematic

The innermost spar section permanently attached to the structure of the fuselage through a central box section. Alternate sections of the tubular spars are then able to rotate, resulting in a fixed tip most section, which is attached to an endplate. The fixed sections are prevented from rotating by having a rigid attachment to their rib section. The rotating spar segments are attached to their ribs through a ball-bearing joint prevent translational movement. The principle of retraction is shown in Figure 1.5-2. This innovative device is described in more detail in Appendix G.

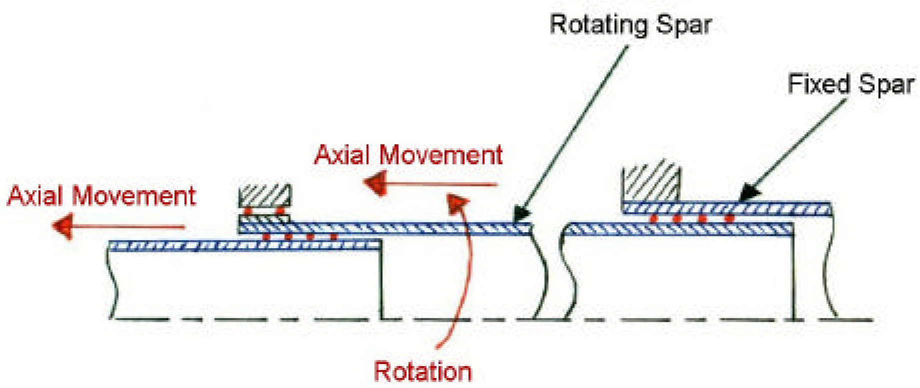

Figure 1.5-2 Telescoping Wing Retraction

The overall vehicle structural design is similar to that of other airplanes. The fuselage consists of main ribs and bulkheads to help define the outer skin and transfer loads. Both sets of landing gear are attached to bulkheads to ensure landing loads can be sustained by the Pegasus. Also, both inboard wing spars are attached to bulkheads, one of which also serves as an engine attachment point and a firewall between the engine compartment and passenger cabin. A general structural layout is seen in Figure 1.5-3.

Safety features included in the aluminum structure of the crumple zone (at the front of the vehicle) include the use of v-shaped grooves or notches along the faces of the forward most longitudinal members. These fold initiators encourage a controlled deformation of the structure upon impact. This protects the passenger compartment from suffering serious distortion.

The structural design also involves an innovative use of composite materials where composites can provide higher stiffness-to-weight ratios and higher strength-to-stiffness ratios than conventional aluminum. This minimizes the weight and can also be cost effective with the implementation of certain manufacturing techniques. Figure 1.5-4 gives a description of airplane components and materials.

Our design will meet all safety requirements of FAR 23 for general aviation planes and NHTSA standards for passenger cars. The load factor diagram determines the normal flight envelope and also the gust envelope for the Pegasus (Figure 1.5-5). This was used to ensure that the airplane's structure would be able to sustain the loads encountered during flight.

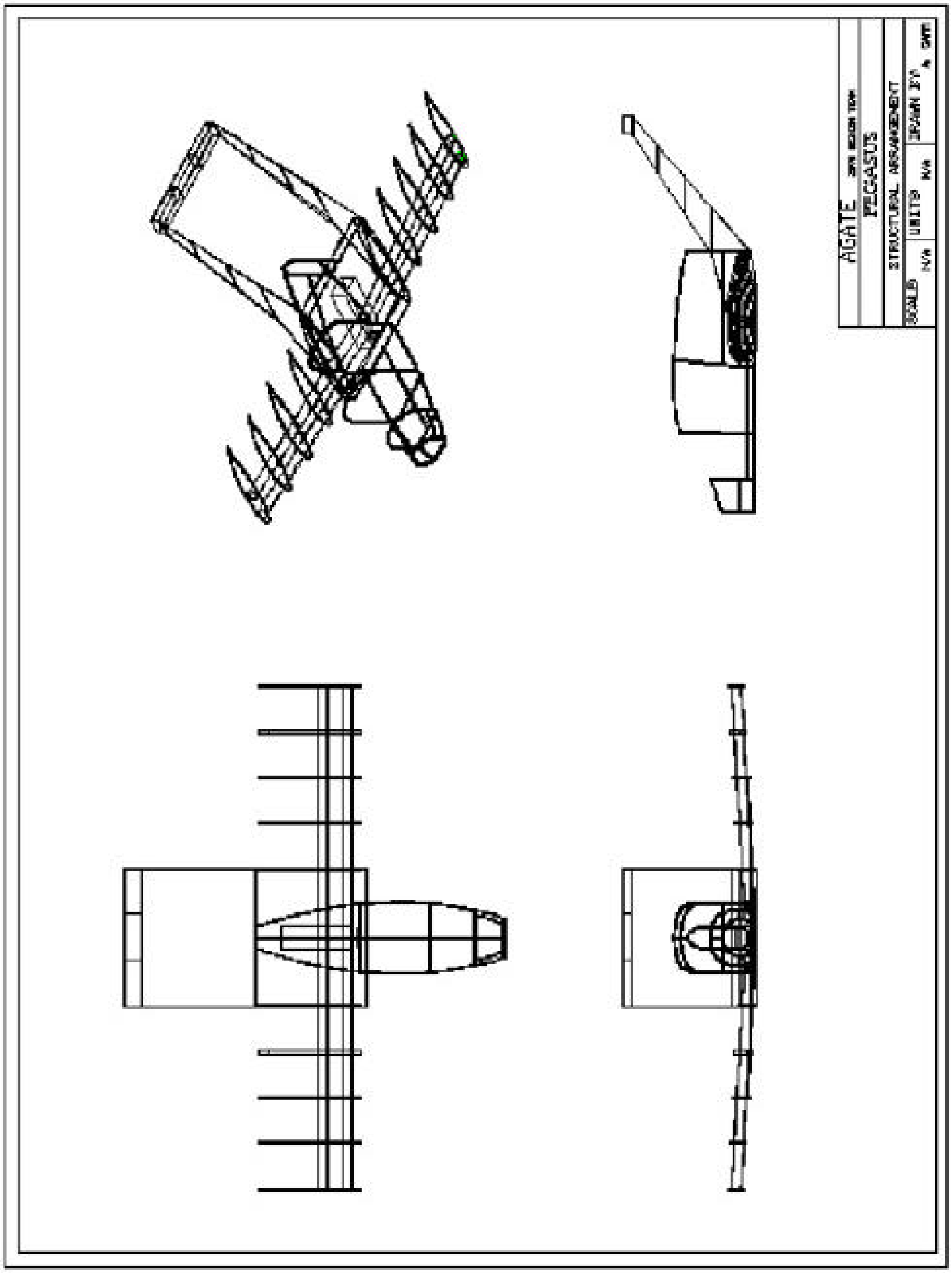

Figure 1.5-3 General Structural Layout

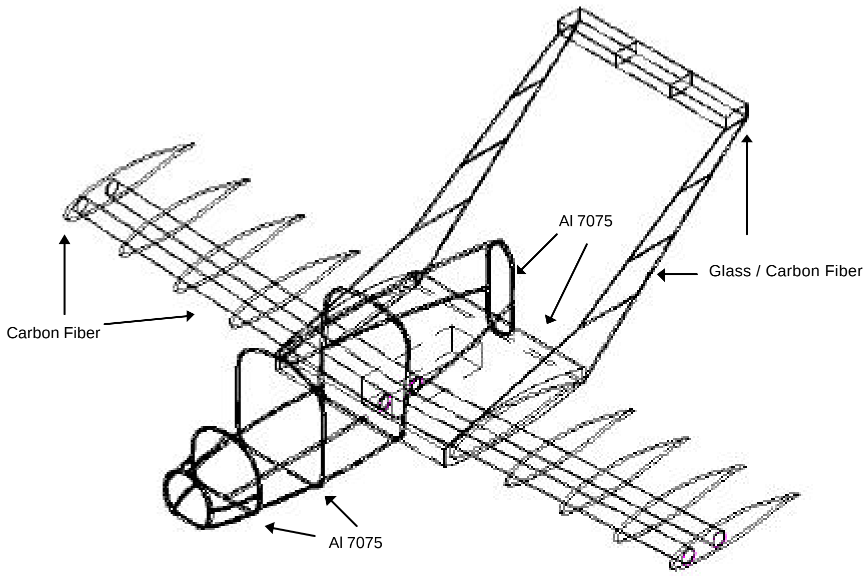

Figure 1.5-4 Material Placement on the Pegasus

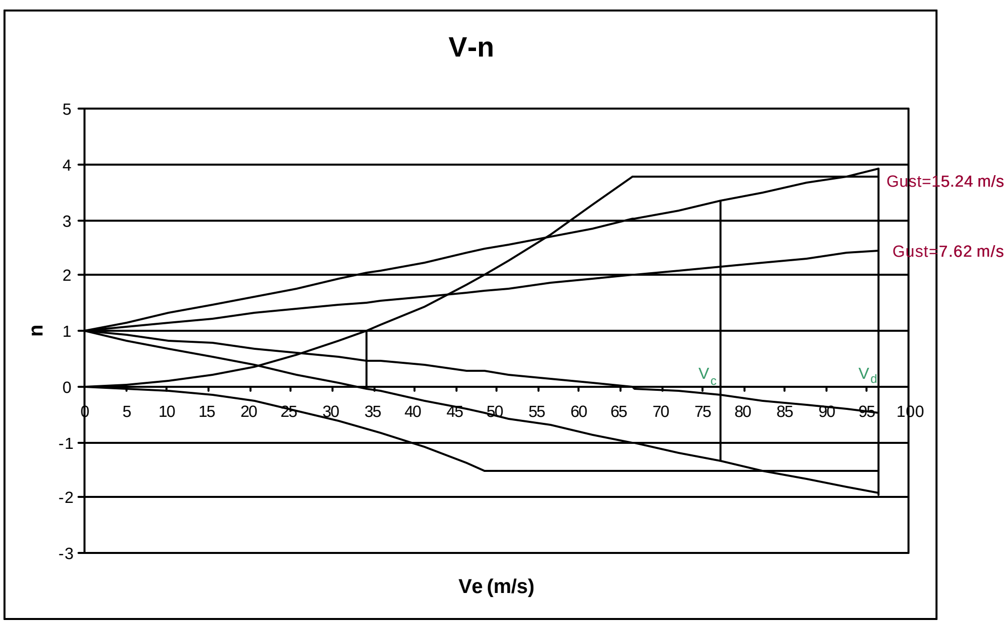

Figure 1.5-5 V-n Diagram

1.6. Propulsion

The engine for a roadable aircraft must meet both the long term, constant revolutions per minute (rpm) demands of an aircraft and the ever changing rpm needs of a car. If an airplane engine, designed for long periods of constant rpm operation, is used in the Pegasus, it must be equipped with a transmission capable of providing power at the varying wheel speeds used in stop and go driving.

The 5-cylinder Wilksch diesel engine (Figure 1.6-1) provides 186 kW (250 hp) of power. This engine is turbocharged and intercooled for increased performance. A strong advantage of this engine is its light weight of 130 kg (287 lb).

Under equal consideration was the availability of AvTur and diesel fuels which are used in the Wilksch engine. Many gas stations in the United States have diesel fuel, so that was not of great worry. Of a random sample of 3738 airports, 2309 (62%) have Jet-A (AvTur) fuel facilities.[2] The availability of these fuels provides support in the choice of engine. Fuel can be found relatively easily for the Wilksh engine and does not limit the goal of providing access to most general aviation sites.

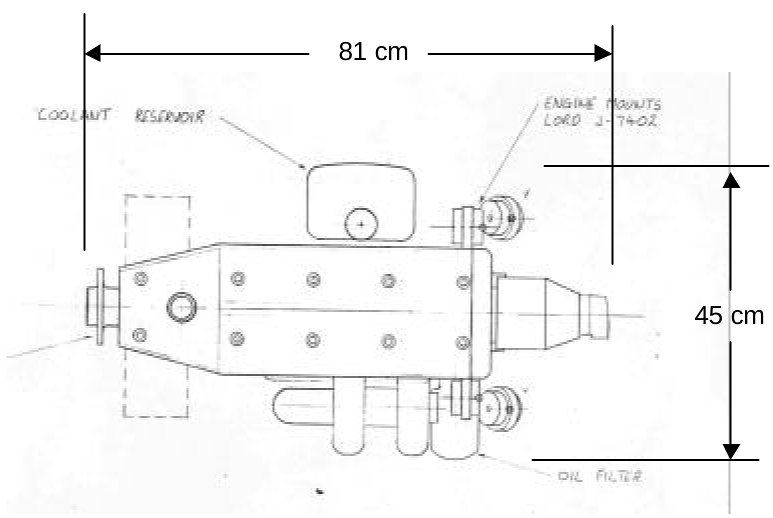

Figure 1.6-1 Top View of Wilksch Engine[4]

Because the Pegasus' design is based on a plane that can be driven on occasion and not for daily commuting, it was decided to use an aircraft engine that employs a modified transmission system for road use. This system, called a continuously variable transmission (CVT) (See Figure 1.6-3) , allows the craft, in automobile mode, to be accelerated by altering the amount of power transferred to the drive wheels instead of by changing the amount of power produced by the engine. The main benefit of the use of the CVT is that it permits the aircraft-based powerplant to be operated at constant speed, thus avoiding the stops and starts of typical driving that would most definitely shorten its lifespan. Unlike most transmissions found in today's automobiles, the CVT is belt driven; this allows for smooth power transfer through an infinite number of drive ratios. The CVT system works by transferring power by means of a specialized steel belt across two variable sized pulleys. The main control module then adjusts the final drive ratio according to information on changes in throttle position, ground speed, and engine RPM provided to it by various sensors.

Figure 1.6-3 Audi CVT [5]

A gearing system connects the engine and the CVT. The main function of this system is to split the power between the propeller and the drivetrain leading to the wheels. Internal to this system is a device called a dog clutch, controlled by the driver, which allows for switching of the power between the propeller and drivetrain. The clutch will be activated from within the cabin just prior to the beginning of the takeoff run.

One major obstacle caused by the location of the engine in this craft was that of cooling. This problem was solved with the use of a liquid cooled engine containing a standard cross-flow radiator cooled by means of an electric fan which draws ambient air in through the side air intake ducts. Due to size constraints, the radiator was limited to approximately 0.14 m^2 (1.5 ft^2), leaving only the fan's motor size to be determined. Using two basic assumptions the motor size was determined using a general heat transfer analysis. The first assumption set the average engine operating temperature at approximately 245°F. The second assumed a worst-case scenario of no added flow due to craft movement and an ambient temperature of approximately 100 °F. This worst-case assumption allows for reassurance that the craft's engine will be protected in case of prolonged static operation.

1.7. Roadability

The Pegasus was designed for good performance in the air and adequate performance on the road. The design emphasis was in safety and handling ease on the road instead of achieving sports car performance. Performance numbers for the ungoverned engine are seen in Table 1.7-1 below.

Table 1.7-1 Roadable Performance of the Pegasus

Performance	
Maximum Speed	160 km/h (99 mph)
0-100 km/h	11 seconds
Min. Stopping Distance (from 80km/h)	43 m
Understeer Gradient (@MTOW)	0.95 + 0.137 + 0.79 a_y deg/g
Rollover Condition (@MTOW)	0.9 g

The design of the suspension provides safety, stability and comfort for the driver and occupants. The four mode suspension is geared toward all probable uses of the craft: road, flight, take-off, and landing.

For the road mode suspension the craft behaves like a typical car. In flight, the wheels semi-retract to reduce drag. For safety, a small amount of the wheel protrudes in the event of an emergency landing. During take-off, the rear wheels retract slightly and the front wheels extend. Upon landing, all wheels fully extend to allow the dampers to absorb the shock of landing.

The front suspension consists of a wishbone configuration and the rear is a trailing arm configuration. The front and rear configurations are depicted in Figures 1.7-1 and 1.7-2.

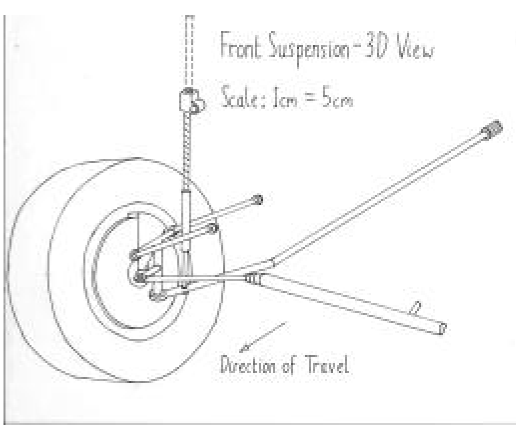

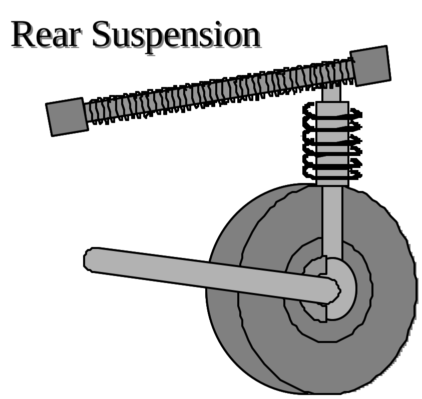

Figures 1.7-1 and 2

A general description of the roadability components chosen for the Pegasus are seen in Table 1.7-2. Automobile type tires were selected based on aircraft and automobile tire selection critieria and discussion with a Michelin engineer.

Table 1.7-2 Roadability Components

System Description	
Tire Designation	P165/75 R14 (Front)
	P175/75 R13 (Rear)
Wheels	TSW Imola Alloys
Front Suspension	Double wishbone with longitudinal torsion bars.
Rear Suspension	Trailing Arm with coil springs.
Damping	Active
Brakes	4 x Disc brakes with floating callipers and electric actuators, mechanical handbrake to rear wheels.
Steering	Motor driven rack and pinion

The active damping system incorporated into the Pegasus allows for variable damping for both the front and rear suspension. The damping ratio can be varied which allows optimization of the vehicle during road mode. This damping ratio is also varied for the different requirements of landing and driving. The damping system allows the wheels to semi-retract.

The simple rack and pinion steering is driven by an electric motor. The electronics in the Pegasus allow the steering to be disconnected for usage during flight.

1.8. Human Factors

The Pegusus is designed to address the need for interior safety and comfort for both aircraft and car. The Pegusus features a spacious, modern cabin with a unique sidestick control system. The emphasis placed on interior layout (Figure 1.8-1), crashworthiness, advanced navigation systems, warning system capabilities, and advanced avionics enhances customer satisfaction.

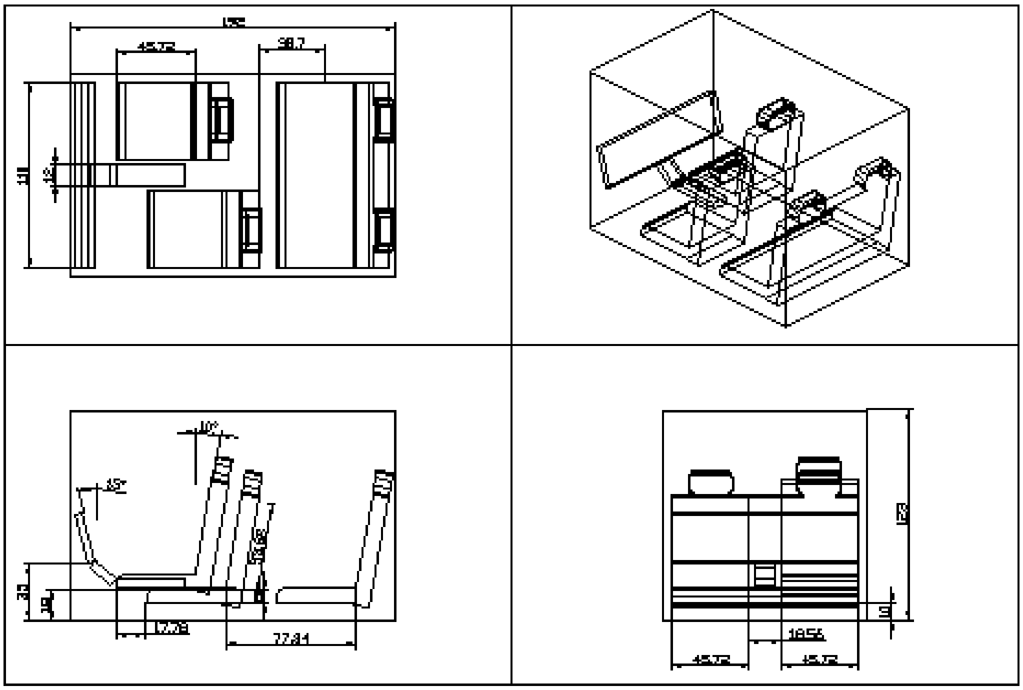

Figure 1.8-1 Cabin Layout

The interior size of the cabin is approximately 2.3 m (7.55ft) in length and 1.2 m (3.94ft) wide. The Pegusus is designed to accomodate passengers from 5th percentile female to 95th percentile male body dimesions based on U.S. Air Force anthropometric data, with a selection of comfortable seats all of which are fully adjustable. Full details are given in Appendix N.

The seat belt system fitted to the Pegasus consists of many features that can be found in practically any automobile. Also, devices are included to ensure that seat belts are in the most effective positions, such as seat belt height adjusters, pretensioners and load limiters. For additional safety, the Pegasus has standard airbags for both front passengers.

In an effort to increase passenger safety and pilot confidence, user friendly instrumentation and navigation equipment is employed, featuring three Liquid Crystal Displays (LCDs). The two outer displays will present information for flying and driving and a center screen will provide the pilot or driver with secondary information including moving maps, and weather and traffic information as seen in Figure 1.8-2. The screens will display various things depending on the operational mode. Efficient integration of information into the instrument panel for both air and car modes provides instantaneous feedback about the status of the vehicle.

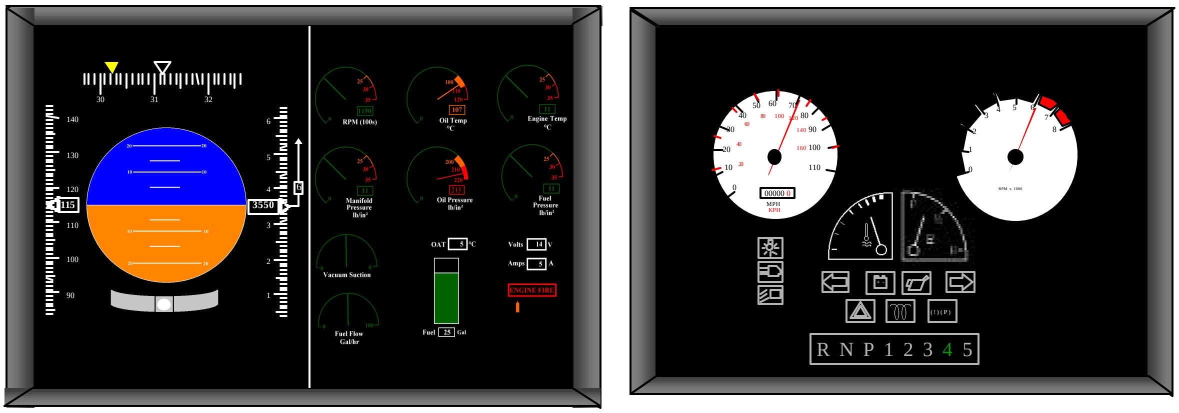

Figure 1.8-2 Example LCD Screens

In meeting the expectations for both flying and driving, the control system employs a sidestick mounted in the door panel. The sidesticks will control roll and pitch in aircraft mode and steering in the car mode. It will also be outfitted with a four-way coolie hat switch to control rudder and elevator trim in flight and in car mode those controls are for turn signals and the high beam lights. Mercedes has proved the safety and ease of use for side stick steering in its SL roadster research vehicle[6]. For steering, the stick moves 20 degrees in each direction and uses force feedback found on modern computer joysticks. The steering is also speed sensitive, so the faster the car is moving the more the joystick needs to be moved.

The Pegusus utilizes a three pedal system with only two pedals being operational in either mode. In flight the Pegasus uses standard rudder pedals linked to electronic transducers which monitor displacement. Between the rudder pedals lies a standard automobile brake pedal. It was decided that the feel of the brake was of paramount importance and so is hinged in a standard manner to give rotational displacement. Whilst the braking is controlled electronically, the feel of the brake is provided by a mechanical spring and damper system. In flight the rudder controls are similar to the accelerator in feel, and the toe brakes at the top of the pedals are hinged as in standard aircraft. In road mode the aircraft toe brake pedal on the accelerator becomes inoperable. Table 1.8-1 summarizes the rules of the stick and pedals in both road and flight modes.

Table 1.8-1 Control Rules

Maneuver	Aircraft Mode	Road Mode
Left Rudder Depressed	Yaw to Left	
Right Rudder Depressed	Yaw to Right	Vehicle Accelerates
Middle Brake Pedal		Vehicle Brakes
Stick to the left	Roll to the left	Vehicle steers to the left
Stick to the right	Roll to the right	Vehicle steers to the right
Stick forward	Nose lowers	No action
Stick back	Nose raises	No action
Coolie Hat Up and Down	Elevator trim	Main and dipped light beam
Coolie Hat Left and Right	Rudder trim	Turn signal

1.9. Systems

The Pegasus acts as both a automobile and an aircraft, utilizing only one set of controls, and can be converted from one mode to the other at the press of a well shielded button. The dual role controls are the first of their kind, and hence, an innovation unseen in roadable aircraft to date. The aircraft produces sufficient power not only for the onboard monitoring and display technology, but also to power control actuators and charge a battery for use in emergencies. Although the aircraft utilizes electrical links between the control actuators with no mechanical backup, the pilot will still have the same sensation as if he or she were flying a mechanically linked aircraft, due to the simple electrical feedback system. Without pilot intervention, the Pegasus monitors all of the utility systems and ensures that the pilot is made aware of the status of all important systems. This means that the pilot is able to concentrate on the primary flying or driving task which makes traveling safer and more pleasurable.

In order for the various components in the Pegasus to function together correctly it has an advanced avionic and electrical system. This collects data in a variety of forms and then processes it prior to either displaying the data or passing it on to other subsystems to utilize. It also allows all of the necessary equipment for each system to be housed together and makes the process of maintaining and repairing the vehicle easier. For the Pegasus the following sub systems were selected:

1. Main Computer: This is the heart of the vehicle avionics system and is responsible for ensuring that all of the data that is transferred among systems via the databus is done so correctly.
2. Displays and Controls Sub-System: This sub-system is responsible for the control inputs for the vehicle and the outputs for the displays.
3. Navigation Sub-System: This subsystem is responsible for providing all of the navigation information for the vehicle from the GPS antenna, the ILS/VOR/DME receivers, the weather data-link and the TCAS system
4. Communications Subsystem: This sub-system contains the air to ground radio, the transponder and the audio entertainment system.
5. Vehicle Utilities Sub-System: This sub-system is responsible for controlling the utilities that are present in the vehicle, such as the electrical and fuel distribution around the vehicle, as well as monitoring the status of the other components that build up the avionics system.

6. Vehicle Control Sub-System: This sub-system takes inputs from the control devices and transfers them into actuator movement, which is monitored and then transferred into feedback inputs to the control devices to provide the driver/pilot with the "feel" of the vehicle.

The Pegasus will be one of the first GA vehicles to utilize the all-electric, i.e. fly-by-wire, aircraft technology currently used in Air Force and other military fighters. There is no need for hydraulics or mechanical linkages, resulting in important weight savings. With continuous monitoring and early fault warnings the Pegasus, will be one of the safest aircraft on the market.

In emergency situations, the vehicle responds and immediately sheds electrical loads and provides the pilot with the information that he or she needs to make an intelligent emergency radio call and then fly the aircraft safely for an emergency landing. Complete details on the Pegasus' systems are given in Appendix O.

1.10. Manufacturing, Maintenance, and Cost

The objective of the manufacturing plan is to produce a product that fits the consumer's needs and desires while staying within set physical and economic constraints. This will be accomplished through "lean manufacturing". The Computer Aided Design (CAD) model will be the base for a 3 plane series of Flight Test-Consumer Models, (FTCM). These prototypes will be used in analytical data collection for future optimization while also collecting consumer input on the design. This is crucial since the product is so revolutionary. Once the design meets aircraft and automobile certification requirements, the optimized product will then be placed into mass production.

Cost was a key factor in the design of a roadable aircraft since the cost needed to be competitive with other general aviation aircraft. It was imperative that the aircraft be designed with amenities and technological advances needed to attract small businesses as buyers, yet the cost had to be affordable.

A sale price of $324,000 is expected. Table 1.10-1 gives a brief summary of the cost.

Table 1.10-1 Cost Summary

Reasearch, Development, Testing and Evaluation Cost	
Engineering, Design and Testing Cost	$13,339
Flight Test and Simulations cost	$57,173
Cost of Overhead	$3,564
	$74,852
Program Manufacturing Cost	
Engineering. Design and Testing Cost	$2,473
Aircraft Production Cost	$205,294
Cost of Overhead	$20,777
	$228,544
Aircraft Estimated Price	**$324,173**

In comparison to other general aviation aircraft, this is a reasonable price based on the amenities and technological advances the Pegasus offers. Table 1.10-2 shows direct comparisons in the standard equipped vehicle prices and features of the Pegasus versus other general aviation aircraft.

As revealed by the table, the standard equipped Pegasus offers many features not found in the base models of the other aircraft. These advanced features such as leather seats, vehicle entertainment, and various navigation aids such as a weather data link system are available in these other aircraft but at extra costs to the buyer. Incorporation of these features into the comparator vehicles would considerably raise the price of each bringing its overall cost close to that of the Pegasus.

Table 1.10-2 Cost Comparison Chart

VEHICLE:	Pegasus	Cessna 182 Skylane	Cirrus SR20	Mooney M20S Eagle	Piper Arrow
PRICE:	$324,000	$227,000	$188,000	$345,000	$230,000
FEATURES:					
4 Passengers	✓	✓	✓	✓	✓
Yoke		✓		✓	✓
Joystick Control	✓		✓		
Advance Avionics System	✓	✓	✓	✓	✓
Mechanical Instruments	✓	✓	✓	✓	✓
GPS (Moving Maps)	✓	✓	✓	✓	✓
LCD Pilot Interface	✓		✓		
Autopilot		✓	✓	✓	
TCAS System	✓				
Weather Data Link	✓				
Leather Seats	✓	✓			
Vehicle Entertainment	✓		✓		
Air Conditioning	✓				
Power Outlet	✓		✓		

Section 2. Background of General Aviation

From the late 1970s until very recently, the GA market was in decline. Reaching its peak in 1978, U.S. manufacturers delivered 18,000 new general aviation aircraft. In 1994, the production of new planes dropped 95%, to under 1000 deliveries[7]. Lawsuits were a major reason for this steady decline. These lawsuits cost the U.S. 20,000 manufacturing jobs and 80,000 support related jobs[8]. Realizing these tremendous losses, the U.S. Congress amended the Federal Aviation Act of 1993. The act allows U.S. manufacturers to compete with foreign companies by reducing the liability risks associated with building general aviation aircraft[8]. In 1998, about 2200 new general aviation aircraft were shipped, indicating the beginning of a revitalization of the market.

The average age of a general aviation aircraft is 27 years and the technology in these aircraft is outdated, sometimes as much as 40 years old[7]. Protected from excessive liability suits, the goal now is to convince U.S. manufacturers to introduce new aircraft using state-of-the-art technologies. Through programs such as the AGATE General Aviation Design Competition, the FAA and NASA hope to stimulate breakthroughs in technology and the application of advanced technology into the general aviation market. A revitalization of the general aviation economy will provide for user-friendly and safer aircraft[7]. A strong consideration in the design of the Pegasus was the available facilities that could be used. The length and conditions of the runways was of utmost concern. Of the total 13,228 airports in the country, 4,712 have runway lights and 4,690 have paved runways (as of 1993). All of these have at least 3000 feet of runway[9]. Also, There are hopes that a world-wide demand for U.S. built, owner-operated small business and personal aircraft will be created, as well.

The first viable attempts at roadable aircraft began in 1937, when Waldo Waterman obtained a patent for his “Arrowbile.” This marked the first accepted design in the field of flying cars. The next big step came when Robert Fulton gained certification from the Civil Aviation Administration in 1946 for his “Airphibian”. This marked the first recognition from an organized flight institution that a combination automobile and aircraft could work. Then, in 1956, Molt Taylor invented the “Aerocar I”. This aircraft was the first to be certified by today’s governing body of aircraft, the Federal Aviation Administration. This proved that a roadable aircraft would be allowed to fly. This certification broke through the beliefs that a prejudice existed in the aviation community against roadable aircraft.

Studies still continue today in roadable aircraft. Paul Moller continues research on his “Skycar” in hopes of someday starting up the flying car industry. Many universities also foster the advancement in this field. With the works of the past and those going on today, a roadable aircraft will be a part of society in the near future.

Section 3. Design Challenges

The task of creating a roadable aircraft presented the Virginia Tech / Loughborough University team with many unique design challenges. These challenges were met along with to the usual challenges associated with both automobile and aircraft design. Major challenges included:

- Meeting both FAR and NHTSA requirements
- Wing storage
- Take-off rotation
- Engine and transmission selection
- Control systems
- Roadability of the design
- Teamwork

One major challenge in the design of the Pegasus involved the need to meet safety and operational regulations for both aircraft and automobiles. This involved researching Federal Aviation Regulations Part 23 for general aviation aircraft as well as the National Highway Transportation Safety Advisory and European Union regulations.

Safety features including airbags, seatbelts, bumpers, and crumple zones were incorporated into the design. Other more basic regulations for aircraft were met including the need for basic instrumentation, lighting, and driver/pilot vision requirements.

The primary structural difficulty in the design of the Pegasus was the need to retract or otherwise store the wing for highway travel. The need for a large wing area for flight, a small span for highway use, and low lift in car mode was addressed by the use of a telescoping wing.

Each outboard wing has four sections with a span of 0.75 m (2.46 ft) each which telescope into the inner wing and fuselage by way rotating/sliding tubular spars. The mechanism is driven by a 12 V motor housed inside a central box in the fuselage.

Another challenge involved rotation for take-off. Normally, the center of gravity of an airplane is located just ahead of the rear landing gear to provide an ease of rotation at take-off. Because the wheel placement on the Pegasus is similar to an automobile wheelbase, the center of gravity falls almost directly between the front and rear wheels. This caused a rotational problem at take-off.

To solve this challenge, the suspension and wheels have been designed to handle four configurations: flight, take-off, landing, and road mode. For take-off, the front wheels extend fully inducing a rotation angle for take-off.

Engines for aircraft and automobiles are designed for different types of operations, making the choice of a propulsion and transmission system difficult. Aircraft engines run at a constant speed for a long time while automotive engines must cycle through wide ranges of rpm. This resulted in questions about engine type, number of engines, type of transmission, and weight constraints. Since the Pegasus was primarily an aircraft, not a car, it was preferable to use an engine designed mainly for aircraft operation.

Ultimately, the Wilksch diesel engine in conjunction with a continuously variable transmission (CVT) was chosen. This engine was chosen for it’s thrust of 186 kW (250 hp) and light weight. The CVT allows the craft, in automobile mode, to be accelerated by altering the amount of power transferred to the drive wheels. The engine is still permitted to be operated at the constant speeds for which it was designed so as to prolong its life.

Selecting control systems for the Pegasus also proved to be a design challenge. Autos and planes do not use the same control systems. A series of systems or one system that would work well with both systems had to be developed. The system also had to be user friendly so anyone would be able to control the aircraft in flight or road mode.

The system chosen has both automobile-like and plane-like features. A joystick is used to control pitch and roll during flight and is also utilized for the steering while on the road. Pedals are used for rudder control with the right rudder also doubling as the accelerator in car mode. An additional pedal is used to control braking. Three Liquid Crystal Displays (LCDs) are utilized to provide both the pilot and driver with necessary and user-friendly instrumentation and navigation equipment.

The roadability of the design meant that systems such as the wheels, landing gear, and suspension had to be designed for flight as well as road travel. The main emphasis was placed on the safety and handling instead of high performance in the road mode. This challenge was met, in part, by development of the four-mode suspension mentioned previously.

In flight, the wheels semi-retract to reduce drag. For safety, a small amount of the wheel protrudes in the event of an emergency landing. During take-off, the rear wheels retract slightly and the front wheels extend. Upon landing, all wheels fully extend to allow the dampers to absorb the shock of landing.

Another important aspect of the roadability was the active damping which allows for variable damping for both the front and rear suspension, thus optimizing the performance of the vehicle. The steering system is a simple rack and pinion arrangement driven by an electric motor. The electronics in the Pegasus allow the steering to be disconnected for use during flight.

Communication within the large, international design group proved to be a difficult task. The team consisted of Virginia Tech students from Aerospace, Industrial, and Mehcanical Engineering, as well as Aeronautical and Systems Engineering students from Loughborough University in England. Electronic mail and teleconferences were the primary modes of communication between members at the two universities. Utilization of the group web page was also an important means of getting up-to-date information about the project.

While the above challenges were the most prominent, many other challenges were presented to the group as the design progressed. These include the need for a strong, lightweight aircraft with good performance characteristics and good aesthetics. The need for a high lift-to-drag ratio, low stall speed, and good stability characteristics also influenced the design decisions.

Overall, this design helps in the revitalization of the general aviation industry by providing a vehicle which can truly be relied upon for travel in any weather and eliminates the needs for auxiliary transport at either end of the air journey. Since the Pegasus is used as both an airplane and car, this added versatility will increase usage of many general aviation airports that lack services such as rental cars, thus expanding the usefulness of many underutilized airports which might otherwise close in the future.

Section 4. Systems Engineering Approach to Design

The successful design of the Pegasus was made possible by a highly integrated team. The multidisciplinary, multilevel, international team consisted of Virginia Tech students from Aerospace, Industrial and Mechanical Engineering, in addition to Aeronautical and System Engineering students from Loughborough University, in England. During the spring semester the team also included sophomore and freshman students. Such a large team, consisting of up to 30 people working in different countries at different levels of education and among different studies in engineering, provided an supportive and dynamic work environment.

The team faced challenges of designing an aircraft that would meet the goal of revitalizing the general aviation industry while maximizing the aircraft's performance, comfort and appearance. The wealth of knowledge available in such a diverse team allowed for all the challenges to be met.

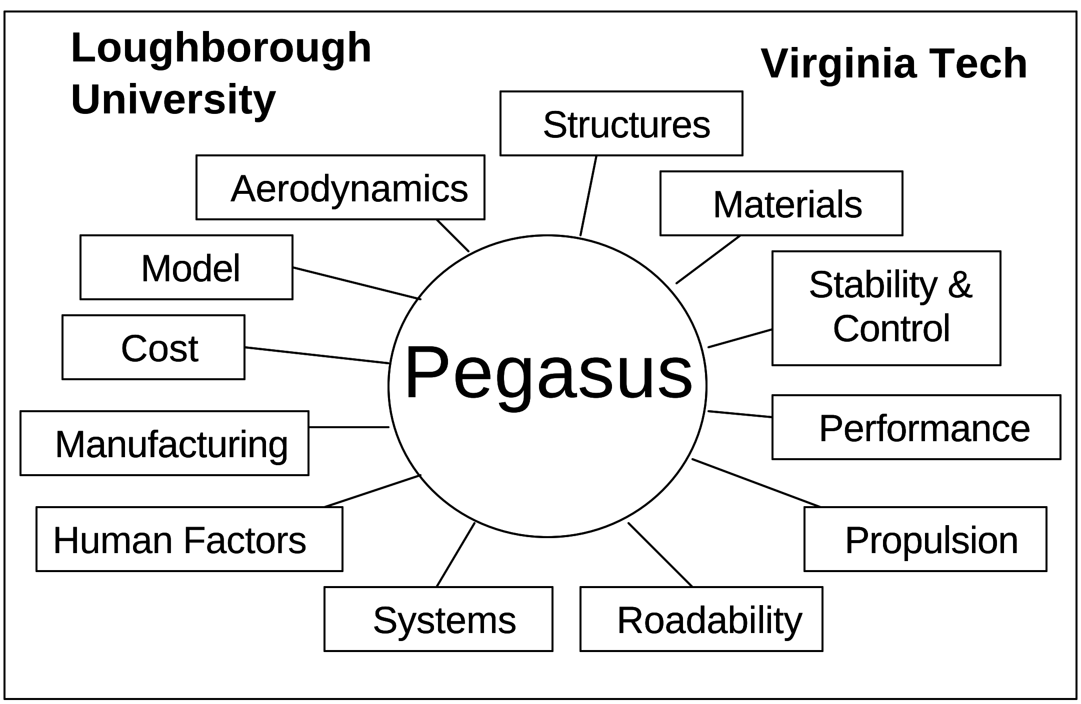

Figure 4.1-1 Pegasus Team Structure Diagram

The team was divided into groups following the well-known concurrent engineering and Integrated Product Team (IPT) approaches, where each IPT or subteam was made up of two or more students from both universities. Each IPT focused on a particular aspect of aircraft design: aerodynamics, stability and control, performance, systems, human factors, propulsion, roadabiltiy, structural mechanics, and manufacturing. The progression through various design stages ensured that each subteam would meet the requirements for their specific discipline, while also making compromises in order to meet the design requirement of other subteams.

As each subteam was comprised of students from both universities the need for communication was crucial. Communication between subteams was also vital as different subteams required information from other teams. Weekly teleconferences, with itemized agendas, facilitated communication between the schools. In addition the teleconferences provided all subteams a common time to speak with other subteams and exchange necessary information. Email and the internet allowed for the communication and exchange of data within the different subteams.

Working with such a large group and across a great distance provided its challenges, but dedication and a clear and valued mission facilitated the completion of the Pegasus.

Section 5. Evidence for Work Completed

5.1. Structures

- V-n Diagram
- Lift Distribution
- Bending Moment Diagrams
- Structural Arrangement
- Telescopic Wing Design
- Selection of Materials

5.2. Propulsion

- Selected engine
- Selected transmission
- Analyzed cooling, chose radiatior and fan sizes
- Selected fuel system
- Designed drive-train
- Designed prop

5.3. Aerodynamics

- Airfoils were selected from set criterion
- wing optimization calculations were performed using lifting line theory
- Initial aerodynamic properties were calculated using an equivalent flat plate assumption
- 3-D aerodynamic property calculations were performed using a vortex lattice method (VLM.m) and methods from Raymer and Torenbeek
- Scoop wing and winglet effect calculations were performed

5.4. Performance

- Standard performance calculations were performed
- Spreadsheet established: Calculates takeoff, climb, velocities, range, endurance, descent, and landing

5.5. Stability and Controls

- Calculated static stability derivatives from geometry.
- Performed dynamic stability analysis.
- Evaluated dynamic modes in accordance with Mil Spec 8785C.

5.6. Roadability

- Front & Rear Suspension Design & Optimization
- Straight Line Road Performance
- Steady-state Cornering Response

5.7. Human Factors and Safety

- Used anthropometric data to develop cabin dimension suitable for an aircraft and car.
- Used the JACK software to assess the suitability of the dimensions.
- Researched/contacted the manufacturers of, the different types of displays and controls that were already being used or could be used, i.e. LCDs, CRTs, analogue displays, mechanical links, Fly by wire, yoke, sidestick, etc.
- Researched the type on extra equipment that was fitted to cars and GA aircraft plus any likely future additions.
- Researched the safety features that should be fitted into the cabin area to meet both the aircraft and automobile regulations.
- Researched different seat options.
- Researched the ingress/egress of the vehicle, including door selection.
- Research pilot training techniques.
- Researched noise issues.
- Researched lighting requirements.

5.8. Manufacturing, Maintenance, and Cost

- Solid Body Computer Modeling
- Facility Layout
- Maintenance
- Manufacturing steps
- Materials Research
- Manufacturing Prototyping
- Composite Research
- Environmental concerns
- Certification Process

Section 6. The Pegasus

In an effort to revitalize the GA industry this design fills the dual role of both a plane and a car, in hopes of tapping a market not previously catered to — small regional businesses.

A roadable aircraft would allow these businesses to utilize local airports near clients, customers, or branch offices and to bypass the increasingly complex and frustrating patterns and demands of airline travel. While these local airports do not typically have all the amenities of large urban airports such as car rentals or shuttles, the pilots of the Pegasus would not need. They could simply convert the plane to the car mode and drive to their nearby destination. By doing this businesses will save time and money otherwise spent on commercial flights and car rentals.

The Pegasus also fills the need of every private pilot to fly to any destination at any time by reasoning the need to spend nights far from home or rent cars when sub IFR conditions prevent take-off. One of the biggest frustrations of being a pilot and owning a plane is that of being grounded due to weather. Many a pilot has cursed his or her way down the highway after being forced to drive instead of fly on the family vacation or other trips or after being forced to rent a car to return home and later rent another car to return to pick up the plane. The Pegasus will truly remove one of the primary hassles of GA flying.

The convenience of being able to fly and drive in the same vehicle almost parallels the automotive industry's sports utility vehicle (SUV) revolution of the last few years. As the population becomes busier, people will need a vehicle that can serve many purposes. The SUV can carry families and baggage and still be functional in the business world by carrying people or equipment to job sites and meetings. The appeal to many people was that these vehicles can go "anywhere." These vehicles are safer than smaller cars and better in bad weather. This surge in SUV sales shows that people do not mind driving large vehicles, such as the Chevy Suburban or the Ford Excursion. The Pegasus has expanded the definition of “anywhere” to the sky, but can still claim all of the advantages of the SUV, while being competitive in the general aviation market.

Typically, small general aviation craft hold four to six passengers and cost in the range of \$140,000 to \$480,000. There are also small regional jets available that cost in the millions of dollars. These jets are out of the price range for individuals and smaller sized businesses. The Pegasus would be available for about the price of a four passenger general aviation craft, while providing more convenience and technology than seen in existing older planes.

By using some of the technology developed under the AGATE program, this design is safer and more user friendly. By using a glass cockpit, it is easy to use GPS navigation, both in the air and on the road. These GPS systems are becoming a common option in many luxury cars, though, and GPS navigation is rapidly becoming the standard in air navigation. Now used even in cellular phones, the price of such systems is dropping drastically. A GPS system can be coupled with such features as inclement weather warnings and updates, as well as traffic and collision avoidance warnings.

One of the big problems in developing a flying car is developing a single control system which will operate both modes and will feel “normal” to the operator in both modes. To make it easier to convert the steering mechanism from air to road, this design uses fly/drive-by-wire. Mercedes has incorporated drive-by-wire into their F200 Imagination concept car[8]. Since flying is typically done with a yoke or a stick, this control should not be a major change for experienced pilots.

A market study was completed at the Virginia Tech airport and the results suggested that pilots wanted the advanced technology mentioned above, but also things like CD players, air conditioning, interior lighting, and cup holders—options that are standard in cars. These things, while adding to the overall cost, will make the Pegasus more marketable and appealing to the public.

Table of Contents

List of Figures and Tables

Symbols

AR : Aspect Ratio of Tire

a_x : Longitudinal Acceleration

a_y : Lateral Acceleration

B

b : Second Coefficient in Tyre Cornering Stiffness Polynomial

b : CoG to Front Axle Distance

b : Span

b_1 : Change in hinge moment due to incidence

b_2 : Change in hinge moment due to control deflection

C

c : Wing chord

c : CoG to rear Axle Distance

C : Celsius

$C_{\alpha f}$: Front Tyre Cornering Stiffness

$C_{\alpha r}$: Rear Tyre Cornering Stiffness

CC_{α} : Cornering Coefficient

C_D : Aerodynamic Drag Coefficient

C_{D0} : Zero Lift Drag Coefficient

cg : center of gravity

C_h : Hinge moment coefficient

C_l : Section lift coefficient

C_L : Aerodynamic Lift Coefficient

C_{La} : Lift Curve Slope

C_{lb} : roll stability parameter

C_{lmax} : Maximum section lift coefficient

C_m : Moment Coefficient

C_{ma} : pitch stability parameter

C_{nb} : directional stability parameter

cog : center of gravity

d : Wire Diameter

D : Coil Spring Overall Diameter

d : Landing Leg / Suspension Deflection

d : Steer Angle of Front Wheels

D : Drag

d : Slope of mean camber line at control point

d : Control deflection

D_A : Aerodynamic Drag

Db_1 : Change in b_1 due to induced camber

Dc : Difference in chord between the two wings

DF_{zf} : Load Change on Front Wheels

DF_{zr} : Load Change on Rear Wheels

d_i : Steer Angle of Inner Wheel (in relation to turn)

d_o : Steer Angle of Outer Wheel

$D_{x`}$	:	Vehicle Deceleration
e	:	Oswald efficiency factor
E	:	Young's Modulus or Modulus of Elasticity
E_c	:	Young's Modulus for composite
E_f	:	Young's Modulus for fiber
E_m	:	Young's Modulus for matrix
f	:	Dihedral angle
F	:	Farenheit
F_b	:	Braking Force
F_b	:	Factor on induced camber contributions to allow for control balance
f_o	:	Rolling Resistance Basic Coefficient
f_r	:	Rolling Resistance Coefficient
f_s	:	Rolling Resistance Speed Coefficient
Ft	:	Feet
Ft/min	:	Feet per minute
F_x	:	Propulsive Force
F_y	:	Lateral Force
G	:	Circulation
g	:	Gravitational Constant (9.81)
G	:	Shear Rigidity
$g/kW\text{-}hr$	:	grams per kilowatt hour (specific fuel consumption)
h	:	Shock Absorber Efficiency

h	:	Height of CoG above Ground
h	:	Drive Train Efficiency
h	:	convection coefficient
h	:	% chord of center of gravity
h_1	:	Height of CoG above Roll Axis
h_f	:	Height of Front Roll Centre above Ground
h_n	:	% chord of neutral point
Hp	:	Horsepower
h_r	:	Height of Rear Roll Centre above Ground
J	:	Polar 2nd Moment of Inertia = pd4/32
k	:	Wahl Stress Correction Factor = (4C-1 / 4C-4)+(0.615 / C)
K	:	Understeer Gradient
k	:	Coefficient for inviscid drag due to lift
K_{at}	:	Understeer Gradient due to Aligning Torque
KE	:	Kinetic Energy
K_{ff}	:	Roll Stiffness of Front Suspension
K_{fr}	:	Roll Stiffness of Rear Suspension
K_{llt}	:	Understeer Gradient due to Lateral Load Transfer
km	:	kilometers
K_n	:	Static Stability Margin
k_q	:	Torsion Bar Rate
k_s	:	Coil Spring Rate
kts	:	Knots

K_{tyres} : Understeer Gradient due to Tyres

kW : kilowatts

k_w : Wheel Rate

L : Length (torsion bar)

l : Ride Frequency

L : Wheelbase

l : Taper Ratio

L : Lift

l : Section lift

L/D : Lift to Drag Ratio

$L_{1/4}$: Sweep angle of quarter chord line

lb : Pounds

$lb/hp\text{-}hr$: pounds per horsepower hour (specifc fuel consumption)

L_h : Sweep angle of hinge line

m : Meters

M : Mach number

m : Viscosity

m : Mass

m/min : Meters per minute

m/s : Meters per second

mac : mean aerodynamic chord

$MTOW$: Max take-off weight

N : Newtons

n : Load

n_a : Number of Coils

nmi : Nautical miles

p : Pneumatic Trail

P : Power

P_{av} : Power available

P_{req} : Power required

P_{RL} : Road Load Power

$\boldsymbol{q}$: Angle of Torsion Bar Twist

q : Dynamic pressure

Q : heat energy produced by engine

r : Distance above the wing median plane

r : Torsion Bar Radius

R : Suspension Ratio

r : Yaw Velocity

R : Turn Radius

$\boldsymbol{r}$: Air Density

r : Distance from vortex filament

$\boldsymbol{r}$: atmospheric density

R_L : Reaction Force on Lower Arm

R_{RL} : Total Road Load Force

$R_{S.SL}$: Effective Radius at Static Load (torsion bar)

R_x / R_{xt} : Rolling Resistance Force

S : wing planform area

s : Seconds

S : Spring Load

S : Reference Area

SD : Stopping Distance

T : Torque

$\boldsymbol{t}$: Shear Stress

t : Track Width

T : ambient air temp

$\boldsymbol{t}$: Time constant

t : Maximum thickness

$\boldsymbol{t}$: Trailing edge angle

t/c : Thickness to chord ratio

$t_{1/2}$: time to half amplitude

t_2 : time to double amplitude

$\boldsymbol{t}_b$: Trailing edge angle

T_e : Engine Torque

t_f : Front Track Width

t_r : Rear Track Width

t_s : Stopping Time for braking application

T_s : surface temp of engine

T_{SL} : Torsion Bar Torque at Static Load

U : Airspeed

U : Free Stream Velocity

u_1 : free stream velocity

u_2 : free stream far behind propeller

v : Maximum Descent Velocity (landing case)

V : Free stream velocity

V : Velocity

$V_{b=0}$: Zero Sideslip Velocity

V_{char} : Characteristic Speed

V_f : Volume fraction for fiber

V_G : Circulation induced velocity

V_o : Initial Velocity in brake application

V_{total} : Vector resultant of the free stream and circulation induced velocities

W : Watts

W : Weight

W : work req'd to cool engine

w_d : Angular Rotation of Wheel = V / r

w_e : Angular Rotation of Engine = 2pRPM / 60

W_f / W_{fs} : Front Axle Load

$W_{f+1/2f}$: Front Passengers + ½ Fuel Weight

W_{fuel} : Fuel Weight

$W_{min\text{-}op}$: Minimum Operating Weight

W_{mtow} : Maximum Take-Off Weight

w_n : undamped natural frequency

$W_{payload}$: Payload Weight

W_r / W_{rs} : Rear Axle Load

W_{sl} : Weight at Static Load

X : Suspension Displacement

x_t : Clockwise location of boundary layer transition

z_d : damping ratio

Abbreviations

ABET: Accreditation Board for Engineering and Technology

AEA: All Electrical Aircraft

AEW: Available Empty Weight

AGATE: Advanced General Aviation Transportation Experiments

AIAA: American Institute for Aeronautics and Astronautics

AMLCD: Active Matrix Liquid Crystal Display

AOA: Angle Of Attack

ASI: American Standards Institute

Avgas: Aviation gasoline

AVTUR: Aviation Turbine Fuel

CAD: Computer Aided Design

CAD: Computer Aided Drafting

CD: Compact Disk

CFRP: Carbon Fiber Reinforced Plastic

CMC: Ceramic Matrix Composite

CNC Computer Numerical Control

CONUS: Contiguous United States

CRP: Carbon Reinforced Plastic

CRT: Cathode Ray Tube

CSD: Constant Speed Drive

CVT: Continuously Variable Transmission

DA: Demonstrator Aircraft

DME: Distance Measuring Equipment

DOT: Department of Transportation

EC: European Community

EFDS: Engine and Fuel Display System

EHA: Electro-Hydrostatic Actuator

EMA: Electro-Mechanical Actuator

EPGS: Electrical Power Generation System

ESDU: Engineering Sciences Data Unit

EU: European Union

F1 Cars: Formula One Cars

FAA: Federal Aviation Administration

FAR 23 : Federal Aviation Regulations Part 23

FAR: Federal Aviation Regulation

FBW: Fly By Wire

FEA: Finite Element Analysis

FTCM: Flight Test Consumer Model

GA: General Aviation

GPS: Global Positioning Satellite

GPS: Global Positioning System

GRP: Glass Reinforced Plastic

HAP: Hazardous Air Pollutants

IBM: International Business Machine

ILS: Instrument Landing System

IPT: Integrated Product Team

JIT: Just In Time

LCD: Liquid Crystal Display

MEA: More Electrical Aircraft

METAR: Meteorological Aviation Routines

MFD: Multi-Functional Displays

MIL SPEC: Military Specifications

MIRA: Motor Industry Research Association

MMC: Metal Matrix Composite

NACA: National Advisory Committee on Aeronautics

NASA: National Aeronautics and Space Administration

NEXRAD: Next Generation Radar

NHSTB: National Highway Safety Transportation Board

NHTSA: National Highway Transportation Safety Advisory

PC: Personal Computer

PFD: Primary Flight Display

PIO: Pilot Induced Oscillations

PMC: Polymer Matrix Composite

R&D: Research and Development

REW: Required Empty Weight

RPM: Revolutions Per Minute

SAE: Society of Automotive Engineers

SATS: Small Airplane Transportation System

SCAPA: Air Contamination Regulatory Agency

SPC: Stsatical Process Control

SSPC: Solid State Power Controller

SUV: Sports Utility Vehicle

TCAD: Traffic and Collision Alert Device

TCAS: Traffic and Collision Alert System

TOGW: Take-Off Gross Weight

US: United States

USA: United States of America

USAF: United States Air Force

VCS: Vehicle Control System

VHF: Very High Frequency

VIPs: Very Important Persons

VLM: Vortex Lattice Method

VMC: Vehicle's Main Computer

VOC: Volitile Organic Compounds

VOR: VHF Omni-Directional Radar

Appendix A. Advisor and Team Member Contact Information

Last Name	First Name	Address	City	State	Zip Code
Anderson	Will	6108 Occoquan Forest Drive	Manassas	VA	20112
Bosen	Trevor	7180 Buckeye Road	Roanoke	VA	24018
Carr	Ashley	846 Newport Terrace	Blacksburg	VA	24060
Cramer	Kevin	2520 Rochester Court	Midlothian	VA	23113
Gassler	Rebecca	300 Jefferson St. #1	Blacksburg	VA	24060
Gray	Dawn	1214 Eagleview Rd.	Goodview	VA	24095
Grissom	Dustin	215 Appomattox Dr.	Simpsonville	SC	29681
Hein	Pam	101 Circleslope Dr.	Simpsonville	SC	29681
Leasure	Dave	441 Cloverdale Circle	Severna Park	MD	21146
Luettinger	Scott	9704 Turnbuckle Dr.	Burke	VA	22015
Marchman	Jim	1825 Azalea Dr.	Blacksburg	VA	24060
Parker	Ryan	17 West Edinburgh Rd.	Ocean City	NJ	08226
Pettersson	Henrik	1502 Walden Dr.	McLean	VA	22110
Prem	Gretchen	1904 Robinway Dr.	Cincinnati	OH	45230
Skinner	Gerard	46758 Woodmint Terrace	Sterling	VA	20164
Stevens	Andrea	2940 Sheephouse Road	Pocomoke	MD	21851
Williams	Ryan	RR4 box 8 LE	Saylorsburg	PA	18353

Apps	Tim	18 Mansion Dr.	Tring	Herts	HP23 5BD	England
Batchelor-Wylam	Chris	The Elms - Picksburn	Doncaster	S. Yorks.	DN5 7XE	England
Birtwhistle	James	Rydal Mount - 36 Briggs Rd.	Barton-on-Humber	North Lincolnshire	DN18 5OH	England
Downey	Michael	2 Plumpton Close - Wrose	Bradford	West Yorks.	BD2 1NJ	England
Goodwin	Russel	258 Wigmore Rd. - Wigmore	Cillingham	Kent	ME8 0L2	England
Kalyan	Gurvinder	4 Reeves Rd	Kings Heath	Birmingham	B14 65Q	England
Panteny	David	137 Clinton Lane	Kenilworth	Warwickshire	CV8 1AY	England
Phillippo	Duncan	8 Garson Rd.- Haydonwick	Swindon	Wiltshire	SN2 3XD	England
Sale	Graham	18 Appleton Dr.	Wilmington	Kent	DA2 7EN	England
Smyth	Rob	Rowan House - Ogwell Green	Newton Abbot	Devon	TQ12 6AG	England
Warren	James	Cedar Glen - Hurtis Hill	Crowborough	E. Sussex		England

Appendix B. Virginia Tech and Loughborough University

Virginia Tech, located in Blacksburg, Virginia, was founded in 1872 as a land grant institution under the Morrill Land Grant Act and has grown to become the state's largest university and lending research institute, offering almost 200 degree programs, $148 million in research projects, and almost 25,000 students. Blacksburg is a small town in Southwest Virginia in the New River Valley where mountains, lakes, rivers, and the shear beauty of the surrounding area provide a fitting backdrop for this superb institution.

Virginia Tech is well positioned to become the model land grant university of the 21st century. Still deeply rooted in its heritage, a Corps of Cadets co-exists with civilian students as they are prepared to be tomorrow's leaders in the armed forces. The Corps has a rich tradition of producing quality leaders and upstanding soldiers that embody the university's motto, Ut Prosim, "That I May Serve."

The 2600 acre university has over 100 campus buildings, hundreds of research laboratories, its own general aviation airport, a 1.8 million volume library, a 55,000 seat stadium, and a communications network that provided voice, video, and computer data transmission to offices, classrooms, laboratories, dormitory rooms, and the community.

Virginia Tech is the home of the state's nationally recognized College of Engineering and research programs. *U.S. News and World Report* ranked the undergraduate engineering program 18th for its quality of education and 28th best public school in the nation[1] All of the engineering programs are accredited by the Accreditation Board for Engineering and Technology (ABET).

Loughborough University is situated in the very heart of England in rural Leicestershire. The University was founded in the market town of Loughborough in 1909, and has grown to become one of Britain's leading universities. With over 10,000 students, Loughborough is made up of 22 academic departments with over 100 institutes and centers, which specialize in different areas of research. The university's academic organization is divided among three Faculties: Engineering, Science, and Social Science and Humanities. Loughborough's academic departments offer undergraduate, postgraduate, and research degrees and most undergraduate degrees include a period of professional or industrial training.

Loughborough University is recognized for it's close links with industry, winning the Queen's Award for it's industrial partnerships with Rolls Royce, BAE Systems, and Ford. The department participates in a multi-disciplinary Systems Engineering program which was developed with British Aerospace Corporation.

Loughborough's reputation in sport training is unrivalled in England and the university has been the training ground for many of the nation's top world class athletes. The 223 acre campus provides a pleasant environment for study with superb sporting and recreational facilities. The campus provides housing for nearly 70% of its students and a rich variety of student extracurricular activities. The modern student's union building is the largest in the country and is the focus of university life for many students. The students union is home to the infamous and elusive Purple Nasty (the working name for the Pegasus project), and provides a wide mixture of clubs and societies.

Loughborough's program in Aeronautical Engineering is one of the largest in Great Britain and is accredited by the Institution of Mechanical Engineers and the Royal Aeronautical Society. A recent survey by The Times ranked Loughborough University as 21st best university in the country, with the Aeronautical Engineering course ranking 5th, and the University achieving joint 1st for teaching quality, alongside Cambridge.

1) http://www.usnews.com

Appendix C. Advisory Sign-Off

As the primary faculty advisors for the Pegasus design project we endorse this report.

Dr. James F. Marchman, III
Professor and Assistant Department Head
Aerospace & Ocean Engineering Department
Virginia Tech

Dr. Gary J. Page
Lecturer
Aeronautical and Automotive Engineering Department
Loughborough University

Appendix D. Evaluation of Educational Experience

The interdisciplinary nature of the AGATE program and the cooperation of several engineering departments at Virginia Tech helped establish the basis for a successful design team. With financial support from The Boeing Company and the Virginia Tech College of Engineering, a collaboration between Virginia Tech and faculty and students at Loughborough University, in England, in an experiment in international aircraft design education was made possible. These factors were essential elements that made this project an overwhelmingly successful educational experience for 16 Virginia Tech engineering students and for 12 engineering students from Loughborough University. These elements and their contribution to the success of this project are discussed below.

A Realistic and Challenging Aircraft Design Project

The desire of every aircraft design professor is to have a challenging aircraft project for a capstone engineering design course. The AGATE General Aviation Design Competition continues to provide an excellent basis for meeting the needs of the traditional senior level, capstone aircraft design course by providing all the elements needed for a thorough design experience. Such a course is important in every engineering curriculum; it is a chance for students to apply much that they have learned in pursuing a degree. The general aviation topic has considerable appeal to students, especially those who may have some involvement in the general aviation field. The desire of the industry to make significant changes in its products, processes, and operating practices adds a real sense of importance to the work of the students, making their design work more realistic and challenging.

An Interdisciplinary Design Experience

In today’s society, it is important for engineering students to learn to work with those of other backgrounds. The AGATE program provides an excellent basis for interdisciplinary design experience at the undergraduate level. This is the fourth year of our use of the AGATE competition in the interdisciplinary design program. This year seniors in Aerospace, Industrial, and Mechanical Engineering at Virginia Tech and in Aeronautical and Systems Engineering at Loughborough University were able to work together using their various academic backgrounds to contribute to the different areas encompassed by the AGATE proposal. The AGATE program continues to make possible the only truly multidisciplinary senior engineering design project at Virginia Tech, and this model has now been successfully expanded to Loughborough University in England.

“Vertically Integrated” Design

“Vertically integrated” design refers to attempts by engineering educators to incorporate elements of design throughout the curriculum. Virginia Tech has, for several years, added a selected number of freshman engineering students to senior design groups in Mechanical and in Aerospace Engineering. This has been a successful experiment which has re-invigorated senior design teams through the mid-year addition of freshmen, forcing the team to re-examine its work and goals as it reviewed them for the new team members. The freshman were not only able to contribute ideas and conduct research for the teams’ work, but they were also able to get an important view of where their education was leading. The AGATE competition provides a vehicle for further expanding the vertical integration project in a multidisciplinary direction, something which works particularly well at Virginia Tech, since engineering students do not enter a major until the end of their freshman year.

The Virginia Tech AGATE team includes 12 seniors from the majors listed above and one sophomore and three freshmen Aerospace engineers. The four underclassmen joined the team at the start of the second semester. The new members quickly became valuable members of a sub-group and began working with the seniors. They helped in running programs and conducting research on different aspects of the aircraft. Since the design incorporates several car aspects, they proved to be as capable of taking on design tasks as the seniors. The addition of the freshmen and sophomore was also timed to coincide with the beginning of an effort to build and test a wind tunnel model of the aircraft design. The underclassman contributed in many other aspects of the design process, becoming full participants of the project.

Preparation for Work in a Global Market

As the Aerospace industry becomes more and more dependent on international cooperation and partnerships in the design and development of aircraft, it was a valuable experience for students at Virginia Tech to work together with students of Loughborough University, England to design a roadable aircraft. The collaboration of the two schools was made possible with financial support form The Boeing Company and the College of Engineering. The support gave 12 seniors from Virginia Tech the chance to visit Loughborough during their Thanksgiving break for a week of intensive aircraft design study with students and faculty at Loughborough. It also permitted a reciprocal visit to Virginia Tech by a team of students and faculty from Loughborough University in April 2000. In the period between the visits the teams worked together via extensive use of e-mail, the internet, and weekly teleconferences.

The participating students learned about the differences between American and European engineering design and management styles and procedures. The trip of team members to England and the U.S. and the team’s sessions with students, faculty, and industry representatives in both countries also helped the participants gain a valuable understanding into the problems and advantages of working in a truly international design team.

Teamwork

Teamwork and team design projects are important objectives for today's engineering students. The AGATE competition allows and basically requires the establishment of a multilevel team structure, similar to a team structure in industry. The participating students were required to develop small group and teams organizational structures and set project objectives and time-lines. This project is significant and challenging in its requirement for an integrated team structure.

Good communications skills were developed as a necessity of team organization and to meet self-imposed deadlines for reports and presentations. Information had to be shared between groups and also between different continents. The team gained valuable exposure and insight into the most effective methods of communication across such a distance. Weekly teleconferences, the world wide web, and email were the only modes of communication between team members at Loughborough University and Virginia Tech beyond the exchange of visits. While this sometimes made communication frustrating, the teams' members worked together and were able to solve the problems presented in the design of the aircraft.

This international teaming represented a new step for the two Universities, since in previous AGATE competitions the collaboration had not extended beyond working in parallel on similar designs.

The international / interdisciplinary team design approach will be continued in the years to come with team members from both Virginia Tech and Loughborough University working together on the same team. Virginia Tech has received a grant from The Boeing Company for continuation and expansion this important program.

Appendix E. Design Evolution

Detailed Final Design Selection

The selection process for defining the detailed final design began with six intermediate concepts, three from the Loughborough team and three from the Virginia Tech team. Students from both schools were grouped into sub-teams for different aspects for the final design, including teams for aerodynamics, weights, cost, performance, and others. The team split into the sub-teams to determine critical issues pertaining to the area of focus of the sub-team. Once a list of critical issues was established the sub-teams ranked each of the six intermediate concepts on a scale of –2 to +2. The critical issues from each sub-team were compiled in a matrix with a weighted sum of the technical areas. Different weighted averages were figured and finally an equally weighted sum was used. The top sum from each of the Loughborough and Virginia Tech designs were selected for final evaluation.

Table E-1 Decision Matrix

		1. GA craft with transmission in wings	2. Lifting Body with telescoping wings	3. Lifting body with folding wings	4. Gyrocopter	5. Car with ducted fans and folding wings	6. Cessna with rotating wings
Structures							
1. Wing Position		-2	-1	-2	0	2	2
2. Aspect Ratio		1	2	1	2	1	1
3. Sweep/Taper		-2	2	1	0	1	2
4. Number of Moving Parts		0	1	0	1	0	1
5. Size of Moving Parts		-2	1	-2	1	-2	-1
6. Wing Loading		1	0	-1	-1	2	1
7. Weight Distribution (Moments)		0	1	-1	-1	1	1
8. Crashworthiness		-1	0	0	2	1	1
Subtotal	1/6	-5	6	-4	4	6	8
Stability and Control/Aerodynamics/Performance							
1. Control in All Aspects (Air)		0	1	1	1	1	1
2. Aft CG for Rotation (Air)		2	0	1	0	-1	1
3. Cross Wind Effects (Road)		-2	0	-1	1	-1	0
4. Low CG (Road)		1	0	1	1	2	-2
5. Central Longitudinal CG (Road)		2	1	1	-1	2	2
6. Reduced Lift (Road)		1	-1	0	2	1	2
7. Clean Flow Over Surfaces and Props (Air)		1	2	1	0	0	2
8. Streamined Frontal Cross Section (Air)		1	1	0	-1	1	1
9. High Aspect Ratio (Air)		1	-2	1	0	2	-1
10. Wing Placement-Mid Wing (Air)		2	0	2	0	0	1
11. Low Profile Drag After Conversion (Road)		1	1	1	1	1	2
Subtotal	1/6	10	3	8	4	8	9
Propulsion							
1. Power		-1	0	0	-1	-1	-2
2. Size, Weight of Engine and Transmission		-1	-2	0	0	-1	1
3. Engine Type (Fuel)		0	0	0	0	0	-1
4. Fuel Efficiency and Range		-1	0	1	0	0	0
5. Cost		0	0	0	-1	0	1
6. Location of Engine and Transmission, Easy Access		0	0	0	0	0	-1
Subtotal	1/6	-3	-2	1	-2	-2	-2
Car							
1. Stability		-2	1	-2	2	1	0
2. Crashworthiness		-2	0	-2	1	1	-1
3. Driver Visibility		0	2	2	2	2	1
4. Road Friendly		-2	1	2	2	2	-1
5. Ease of Conversion		-2	1	-2	0	0	1
6. Aesthetics		-2	0	0	2	2	-2
7. Access		-1	1	2	2	1	2
Subtotal	1/6	-11	6	0	11	9	0
Cost/Manufacturing							
1. Market		0	1	0	1	0	0
2. Development (Outsourcing)		0	-1	-1	-1	0	2
3. Simplicity of Design		-1	1	-1	-2	-1	1
4. Service and Running Costs		-1	-1	1	-1	1	0
Subtotal	1/6	-2	0	-1	-3	0	3
Human Factors							
1. Safety		-2	0	1	1	0	-1
2. Ingress/Egress		-2	-1	2	2	2	2
3. Visibility		-2	2	0	2	1	1
4. Conversion Ease		-2	2	0	2	1	2
5. Asthetics/Noise		-2	1	-1	0	2	-1
Subtotal	1/6	-10	4	2	7	6	3
Total		-3.50	2.83	1.00	3.50	4.50	3.50

As an entire group each sub-team reviewed and explained the rankings the team gave to the final two concepts. Discussions about the mission, resulted in the selection of different aspects from each design for a final concept, almost a hybrid of the two designs.
A decision matrix, shown as Table XXX, was used to refine the six intermediate concepts into a single final concept. The decision matrix consisted of a –2 to +2 ranking system, where –2 was poor and +2 was good. Each of the sub teams evaluated the six intermediate concepts by grading them based on the group's predetermined critical issues. The total scores from each sub team for the six intermediate concepts were then averaged under equal weighting. Intermediate Concept 1 received a total averaged score of -3.50, Concept 2 received a score of 2.83, Concept 3 received a score of 1.00, Concept 4 received a score of 3.50, Concept 5 received a score of 4.50, and Concept 6 received a score of 3.50.

Once the scores for the six intermediate concepts were averaged, the top American concept (Intermediate Concept 2 with an averaged score of 2.83) and the top British concept (Intermediate Concept 5 with an averaged score of 4.50) were chosen to be considered for final refinement. The final concept was then formed through a hybrid of these two concepts based on the positive qualities of each. The driving factor in the selection of the various portions from each concept was the market set forth at the beginning of the design process. The key issues in the design are safety and ease of transformation, since the vehicle is being marketed to small businesses and families.

The final concept of the roadable aircraft, illustrated in Figure XXX, melds the best features from Intermediate Concepts 2 and 5. This design joins the fuselage of Concept 5 and the wings of Concept 2 with some adaptations. The fuselage of Concept 5 was selected due to its aesthetic appeal in the car configuration as well as the dual ducted fan propulsion system. The original Concept 5 cabin interior consisted of a central driving position with two offset rear passenger seats. The cabin was expanded to a four seat conventional cabin to match the selected market. A double width gull-wing door arrangement provides easy ingress and egress. These doors will rotate up to provide access to the front seat, rear bench and aft cargo space.

The ducted fans of this design provide greater road safety than a forward or aft mounted propeller. A drawback of this propulsive arrangement is the nose down pitching moment generated by the location of the thrust line with respect to the center of gravity. The engine that drives the ducted fans and the rear drive wheels was originally located at mid-fuselage. The center of gravity location shifts forward and down to provide better road stability. The crash survivability is also improved since the engine mass is located in front of the passenger cabin. Shafting is the primary drawback to the forward mounted engine. Moving the engine to the front necessitates long drive shafts for both car and airplane configurations.

The lifting surfaces of Concept 2 were improved and blended with the fuselage of Concept 5. The lifting device consists of a main low aspect ratio wing with telescoping sections. The thickness of the high lift, low aspect ratio wing provides convenient stowage of the telescoping wings in automotive configuration. In roadable mode, the vehicle is 2.44 m (8 ft) wide, 2.44 m (8 ft) in height, and 5.18 m (17 ft) in length. The vehicle take-off gross weight is approximately 1591 kg (3500 lb). These dimensions should allow free travel on the road, including parking in garages and spaces. The low aspect ratio airfoil is end plated to reduce three-dimensional effects inherent in such high lift devices. It has a span of 2.44 m (8 ft) and a chord of 3.45 m (11.32 ft), resulting in an aspect ratio of 0.71. By stacking the wings in their stowed positions, the span of each telescoping wing extension was doubled. This increased the overall span of the wing from the 4.33 m (14.2 ft) of Concept 2 to 7.01 m (23 ft) in the final concept. The greater span results in more favorable aerodynamic performance such as lift and range, as well as increased roll stability.

Manual extension of the wings allows maximal span to be achieved, as no machinery is required. This simple telescoping design lends itself to easy conversion between modes. Theoretically, combining the high lift airfoil and telescoping wings will produce sufficient lift for takeoff without significant rotation. The configuration allows the gravitational center to be positioned midway between the front and rear wheels in the road configuration. The front wheels will be articulated to raise the nose of the vehicle from a negative angle of attack in road configuration to a slightly positive angle in the aircraft mode. A negative incidence will generate negative lift to better maintain contact with the road. In aircraft mode, the front wheels will raise the nose allowing the high aspect ratio wing to generate lift during take off should there be inadequate lift to provide take off without rotation.

In flying mode, the controls of the airplane are comparable to current general aviation craft. Large trim tabs compose the trailing edge of the low aspect ratio wing to compensate for the negative pitching moment produced by the thrust line. The craft has a large horizontal tail and elevator to provide pitch stability and control. This control surface will lie in the wake of the ducted fans, assuring flow over the surface and thus pitch control at all times. Twin vertical tails support the horizontal tail with rudders providing control in yaw. Flaperons are situated on the trailing edges of the telescoping wings, generating large moment arms for ample roll control. To keep the wing extensions from stalling, fixed leading edge slots will be incorporated into the airfoil design at their inboard sections.

Once the final concept was decided upon, refinements were made leading to the detailed final design. The primary change from the final concept to the detailed final design was the replacement of the twin ducted fans located on the top of the fuselage with a single unducted propeller located aft of the fuselage. It was found that a larger propeller area was needed to boost the vehicle and the single propeller allowed for this area without exceeding size constraints.

The change in propeller configuration necessitated the movement of the engine from the front of the vehicle to the aft of the fuselage. It was decided that losses associated with shafting from a front mounted engine to a rear mounted propeller were too great. An engine mounted at the aft of the fuselage would minimize these losses and allowing for much greater engine efficiency. The issue of crashworthiness safety of a rear mounted engine was overcome by the installation of firewalls to guide the engine down away from the cabin in the event of an accident.

It was found that the moment caused by the existing tail was not sufficient to control the pitch motion of the Pegasus. Rather than increasing the area of the tail, which would increase profile drag and exceed road width limitations, the moment arm of the tail was increased.

To facilitate driving on the road, the width of the inboard wing was decreased from 2.44 m (8 ft) to 2.28 m (7.48 ft). It was found that an increase in wing area was needed. Instead of the two wings telescoping on top of each other, each wing was made to consist of four 0.75 m (2.46 ft) telescoping sections. This gave an inner wing with a chord of 2.5 m (8.2 ft), a span of 2.28 m (7.48 ft), and an area of 5.7 m^2 (61.4 ft^2). Each outer wings has a chord of 1.75 m (5.74 ft), a span of 3 m (9.84 ft), and an area of 5.25 m^2 (56.5 ft^2). The total resulting area of the wings was 16.2 m^2 (174.4 ft^2).

To decrease the overall drag and strengthen the vehicle structurally, the wheel housings were modified. The rear wheel housings were incorporated into the trailing edge of the inner wing. The housings for the front wheels were incorporated into the fuselage leaving more room for the wheel structures.

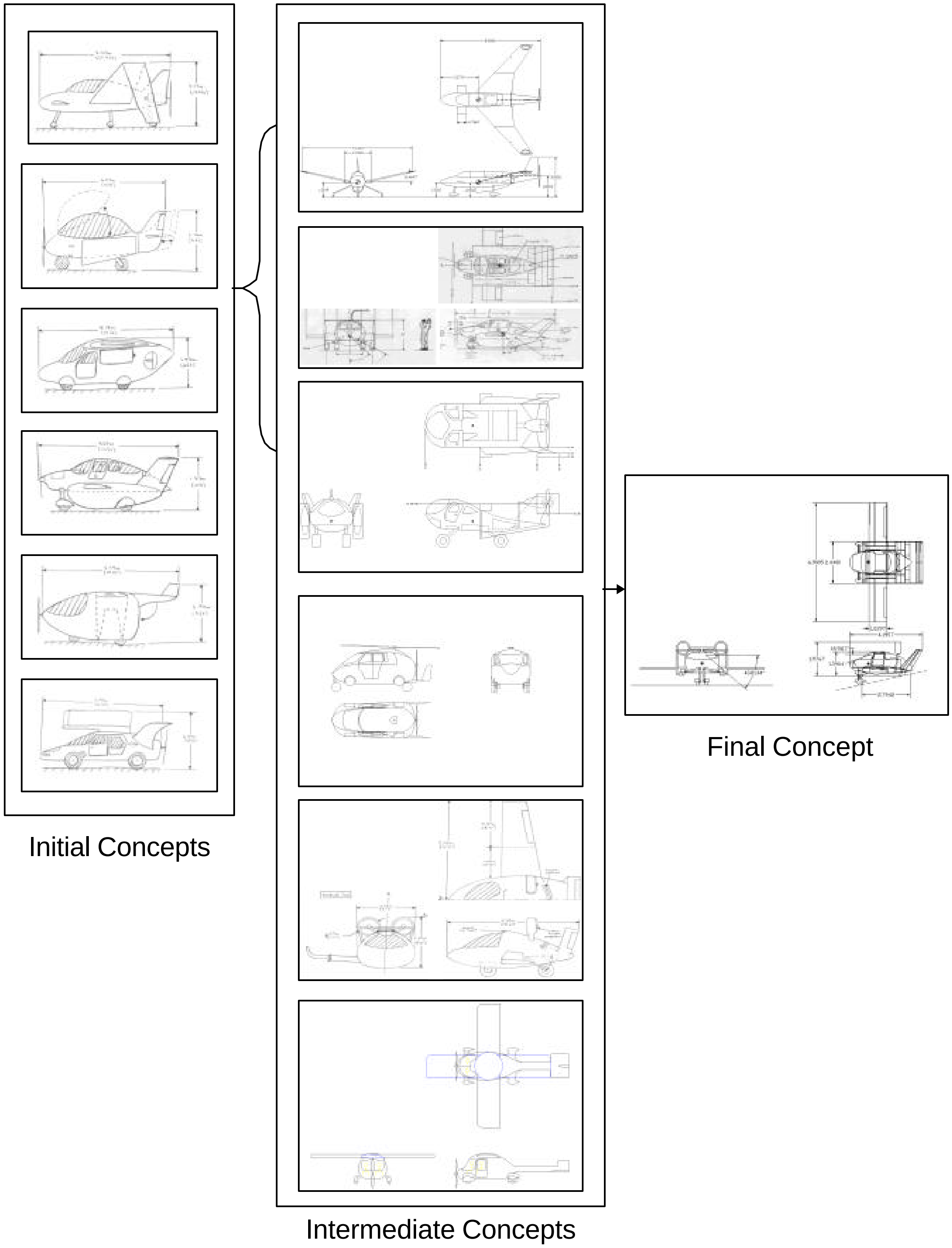

Figure E-1 Decision Tree

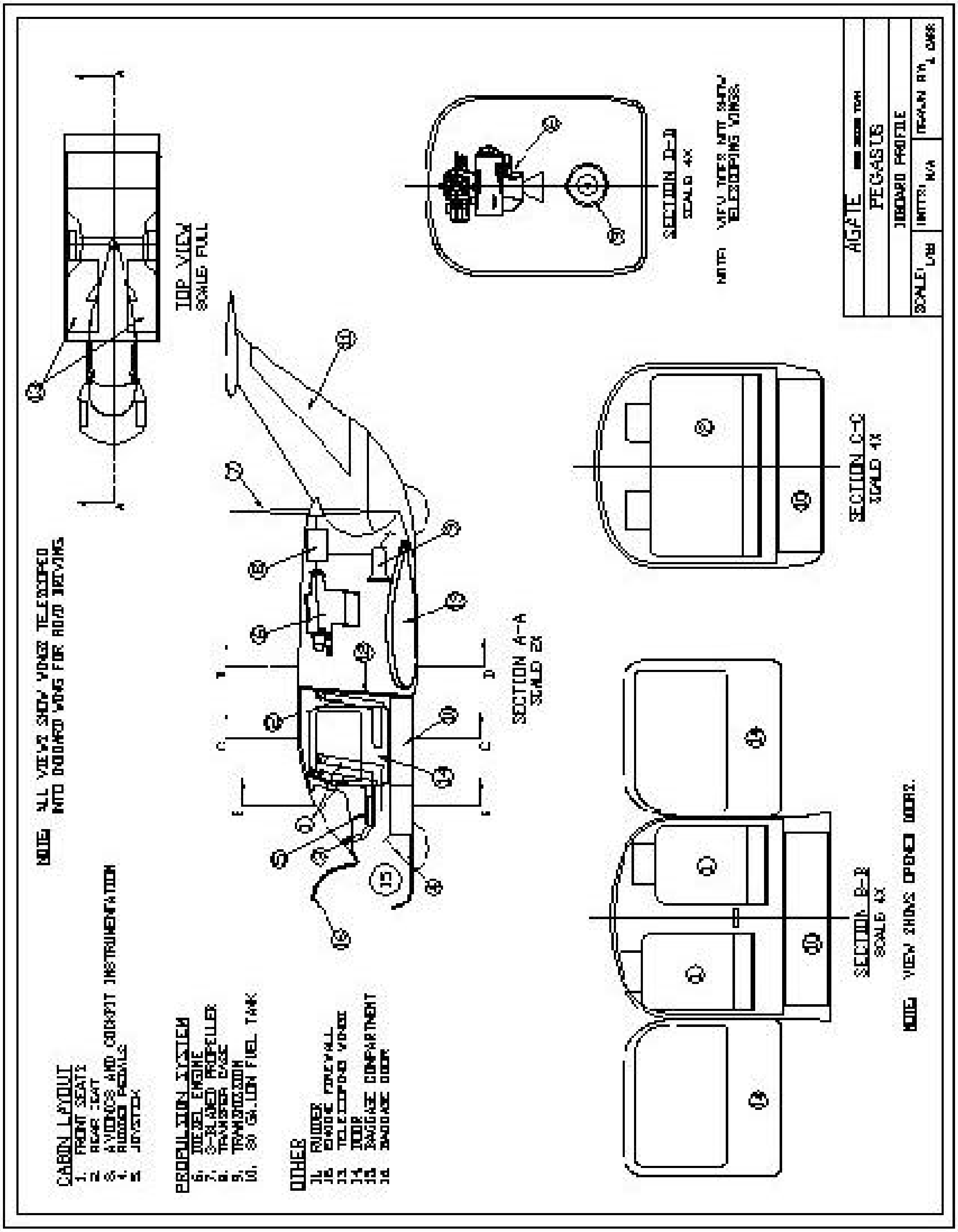

Figure E-2 Inboard Profile

Appendix F. Weights and Balances

F.1. Initial Sizing

The initial sizing for this craft consisted of calculating a take-off gross weight (TOGW) based on the geometry of the craft, some basic aerodynamic characteristics, and parts of the mission profile. The method was based on weight fractions for each part of the mission and the required empty weight. The required empty weight was based on statistical curve fits from Raymer[1] and Roskam[2]. This equation is given as follows:

$$REW = .911 * TOGW^{.947} + 100 \qquad \text{(Eq. E.1)}$$

where REW is the required empty weight in pounds and the 100 at the end is extra equipment added to account for the functionality of a car. This equation is then set equal to the available weight, which is calculated as follows:

$$AEW = TOGW - W_{fuel} - W_{payload} \qquad \text{(Eq. E.2)}$$

where AEW is the available empty weight after the fuel and the payload is subtracted from it. The weight of the fuel is the calculation that uses the inputs mentioned above.

Based on the inputs used, an initial estimation of the TOGW was given to be approximately 1500 kg (3300 lbs).

F.2. Component Weight Estimation

Two different methods were used in the component weight estimations. One was from Raymer[1] and one was from Roskam[2].

The Roskam method for estimation for general aviation craft was based upon Cessna's estimation method. In this, various input parameters such as wing areas, sweeps, thicknesses, number of passengers, moment arms are needed, as well as an initial guess at the TOGW. Then, through iteration, the input TOGW is made to match the end result TOGW.

The Raymer method uses the same concept, but different inputs and different equations. These are also from curve fits done on a large variety of GA aircraft.

The problem with these methods and the roadable aircraft design is that the design is not conventional and would not be expected to fit into those curves well. As a result, some of the equations yielded absurd answers. For example, one equation required the volume of the fuel in the wing. Since the Pegasus has telescoping wings, there is no fuel inside them. This gave a wing weight of less than .5 kg from the equation because conventional GA craft are expected to have fuel in the wings and the amount played a large part in the structural weight of the wings.

To combat this problem, a few things were done. First, as many real weights as possible were used. These numbers included engines, transmissions, propellers, avionics, and furnishings. Then the above methods were used on all other components. Since the two methods used very few of the same inputs, the one that gave the best reasonable estimation was used. In some cases, the inputs for our craft needed for one method were more conventional values, and would therefore give a good result, but if the other method had been used, the result would not have been reasonable. After the methods were applied, the numbers were again looked as to make confirm that they were reasonable. Some were adjusted up or down based on inspection of the design and common sense. Also, some component weights for various general aviation craft were available in the Roskam weights volume[2], so these were used to help make those adjustments.

The end result produced a concept that was 1500 kg. This was very close to the initial sizing estimate. While this is a little heavier than other GA craft in the same size category, this is to be expected because of the extra functionality that it offers. Weight due to the transmission, extra side and front impact protection, quantity and size of wheels and tires all account for this added weight.

Table F.2-1 Component Weight Estimates

Component	Mass (kg)	Weight(lb)
Structure		
Wing	97.73	215.00
Horizontal Tail	13.64	30.00
Vertical Tail	22.73	50.00
Fuselage	159.09	350.00
Main Gear	38.64	85.00
Nose Gear	38.64	85.00
Total	370.45	815.00
Propulsion		
Engine	181.82	400.00
Transmission	138.64	305.00
Propeller	22.73	50.00
Fuel System	20.45	45.00
Total	363.64	800.00
Systems		
Flight Controls	9.09	20.00
Electrical	86.36	190.00
Avionics	45.45	100.00
AC/anti-ice	36.36	80.00
Total	177.27	390.00
Cabin		
Furnishings	52.27	115.00
Variable Weights		
Fuel	218.18	480.00
Front Passengers	145.45	320.00
Rear Passengers	145.45	320.00
Baggage	27.27	60.00
Total	536.36	1180.00
Grand Total	1500.00	3300.00

F.3. Weight and Balance Analysis

From these weights, a center of gravity, c_g, analysis was done. The locations of the components were measured to their c_g, and their moment around the nose was calculated. Then this was divided by the total mass to get the center of gravity location. Shown in Figure E.3-1 is the movement of the cg in various stages of the flight.

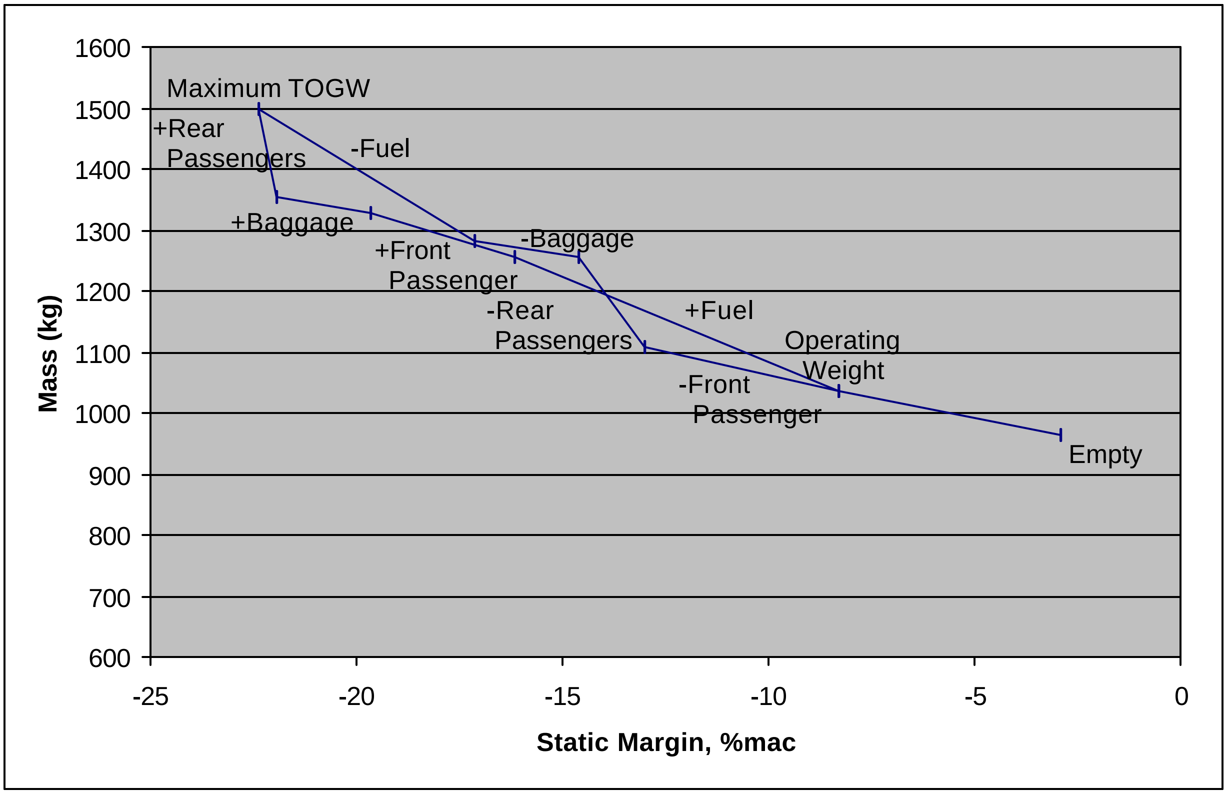

Figure F.3-F.3-1 Cg Excursion Diagram

1) Raymer, Daniel P., Aircraft Design: A Conceptual Approach. Third Edition, 1999.

2) Roskam, Jan, Airplane Design Part V:Component Weight Estimation, 1989.

Appendix G. Structures

G.1. Loads

The Pegasus was designed to structurally meet the regulations of Federal Aviation Regulations (FAR) Part 23 for general aviation aircraft as well as structural requirements imposed by the National Highway Transportation Safety Advisory (NHTSA). The need to meet both sets of requirements governed the structure of the design. The essential structural difference between airplanes and cars is that strength is a major consideration in aircraft while cars focus on stiffness to improve handling and suspension.

FAR Part 23 regulations include gusts of 55 km/hr (50 ft/s). The limiting load factors for the design of general aviation aircraft are given by the following equations:

$$3.8 > n_{pos} \geq 2.1 + \left(\frac{24{,}000}{W_{to} + 10{,}000}\right) \tag{1}$$

$$n_{neg} \geq 0.4 * n_{pos} \tag{2}$$

Table G.1-1 below shows the limit loads imposed by FAR 23 in comparison to the limiting loads the design was subjected to for our design.

Table G.1-1 FAR 23 Limit Loads

	$n_{positive}$	$n_{negative}$
Cruise	3.336	-1.33
Max (FAR23)	3.8	-1.52

A velocity versus load factor diagram was constructed using methods introduced by Niu[1]. Additional gust loads were incorporated into the diagram to produce Figure G.1-1. This diagram was the basis for designing the dimensions of the structural members.

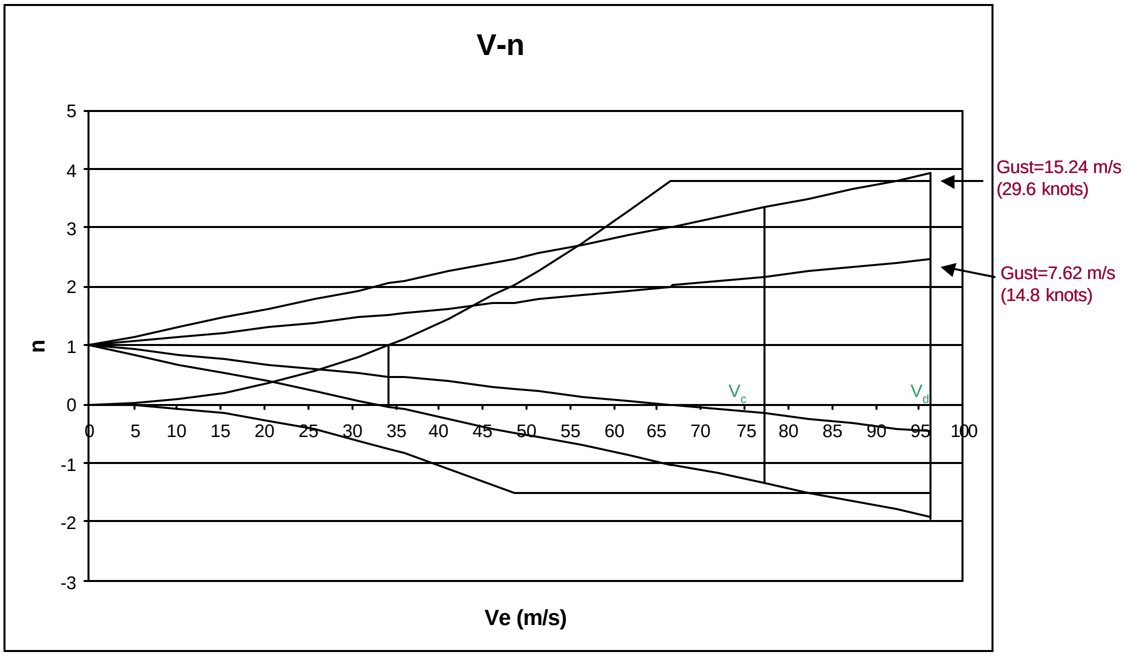

Figure G.1-1 V-n Diagram

Loads and load distributions on the lifting surfaces were determined using the information contained in the V-n diagram. Major loads experienced by airplanes include airloads, inertial loads, landing loads, and powerplant loads. One of these loads will dominate each structural member.

Inertial loads are those that are associated with the resistance of mass to acceleration (Newton's Second Law). Stresses on aerodynamic surfaces are established from accelerations due to maneuver and gust accelerations. Objects in the aircraft experience forces determined by the component's weight times the aircraft load factor.

Landing loads are those associated with the landing of the airplane. This includes the initial shock of touchdown as well as static forces acting while the plane is experiencing forward rolling motion. Landing loads for the Pegasus were calculated in Appendix M.

Powerplant loads are those exerted primarily by the engine and in our case, the transmission as well. The engine mounts must withstand both the thrust and drag forces that are produced by the engine as well as the weight of the engine multiplied by the appropriate load factor. To obtain the design torque for the engine mounts, it was necessary to know the number of cylinders of the engine to ensure a safety factor as well as the maximum torque during normal operation.

Table G.1-2 Engine Loading

# Cylinders	Safety Factor	Max Torque (N-m)	Design Torque (N-m)
5	1.33	660	877.8

Airloads are determined from the total lift acting over the wings and horizontal tail surfaces. Detail on the span-wise load distribution on the wings is presented later. The point loads on the main structure are be defined as the following: lift forces on the wing and elevator, the weight distributed over the wheel base, the propeller thrust and the forces at control surface hinges.

The lift distribution among the two horizontal surfaces was determined through moment equilibrium. The distances between the local aerodynamic centers and the vehicle aerodynamic center were considered moment arms and the resulting second order system was solved. According to this analysis, in cruise, the wing lifts 15,684 N (3307 lbs) (95.9%) and the elevator 678 N (152.4 lbs) (4.1%). These values can be multiplied by the maximum g-force found in the V-N diagram to find the maximum maneuver loads.

The wing loading for the Pegasus was determined to be 968 N/m^2 (1.32 psi) using a total lift of 15.68 kN (3307 lbs) and a wing area of 16.2 m^2 (17.44 ft^2). The total that has been distributed using this method is based on a value of total lift supplied by aerodynamicists.

The span-wise distribution was found for the entire wing, consisting of both the fixed inboard wing and the telescoping outboard wing sections. The total span-wise distribution was calculated using Schrenk's approximation[2] for a conventional wing design, which is based on an average of the actual and elliptical chord distributions. Problems were encountered due to the sharp change in chord between the inboard and outboard sections. The assumptions made will be discussed further.

As seen in Figure G.1-2, the semi-span of the wing is represented by a pair of rectangles, instead of one due to the difference between the inboard and outboard wing chords. Since the same airfoil section is being used for both wing sections, the two-dimensional lift coefficient is the same for each portion and no correction of the chord is necessary.

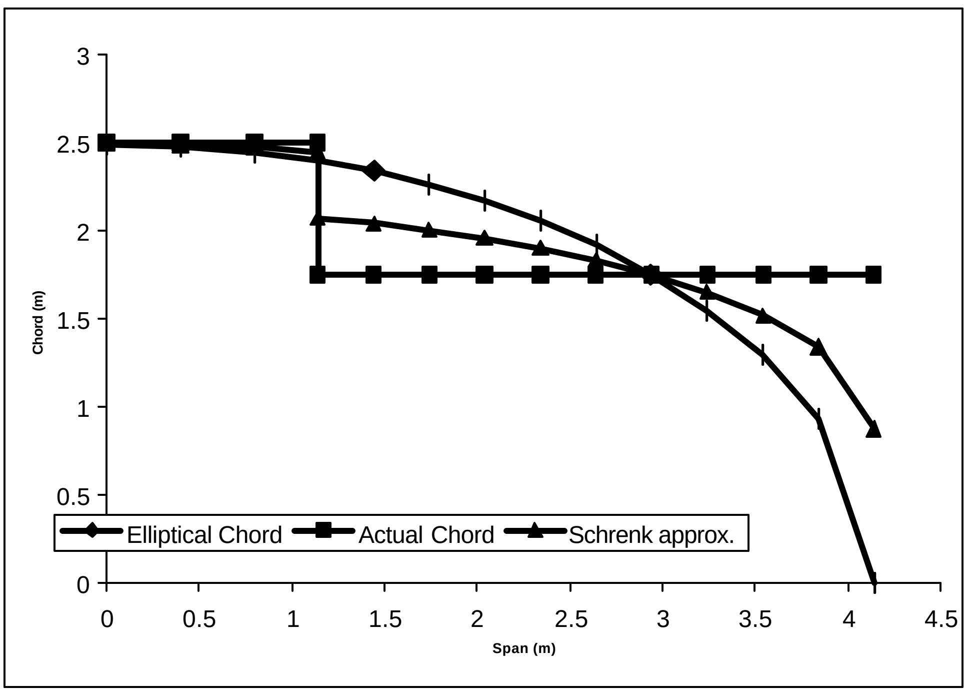

Figure G.1-2 Schrenk approximation of lift distribution

Both wing sections are at the same incidence, so once again no correction of chord is made for varying incidence. The small dihedral angle of the wing has been neglected in all calculations.

The presence of a wing fence between the two sections means that there should be little reduction in three-dimensional lift coefficient due to circulation at the point where the two wings meet. The sudden drop in lift between the two wing sections that can be seen in Figure G.1-2 is purely due to a chord change.

The final assumption is that the fuselage does not have any effect upon the load distribution. This is a safe assumption for most aircraft where the fuselage is a small percentage of the total span. In this case the fuselage is a higher than typical percentage of the total span. Despite this the fuselage is still a sufficiently low percentage for the assumption to be considered valid.

The shear force distribution resulted in the bending moment diagrams shown in Figure G.1-3a and G.1-3b. These diagrams are for the inboard and outboard wing sections respectively. Figure G.1-3c shows distribution of load for a comparable shaped wing constructed in one section.

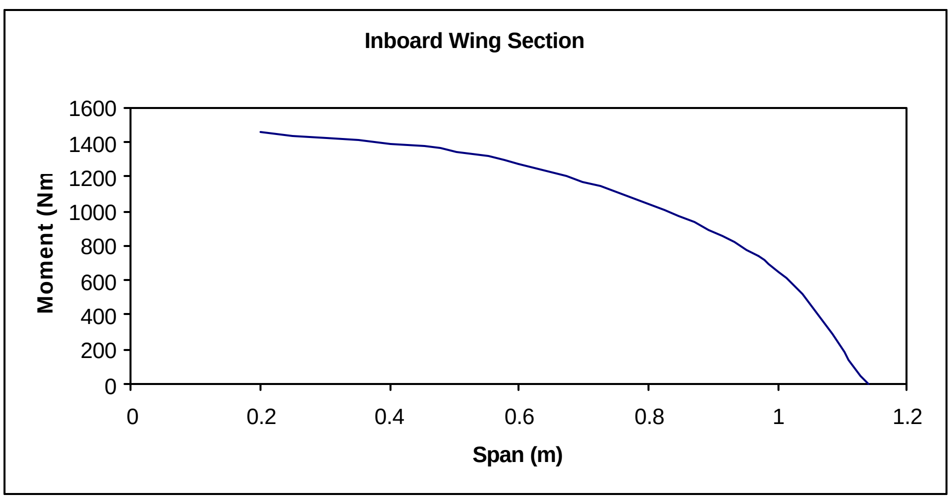

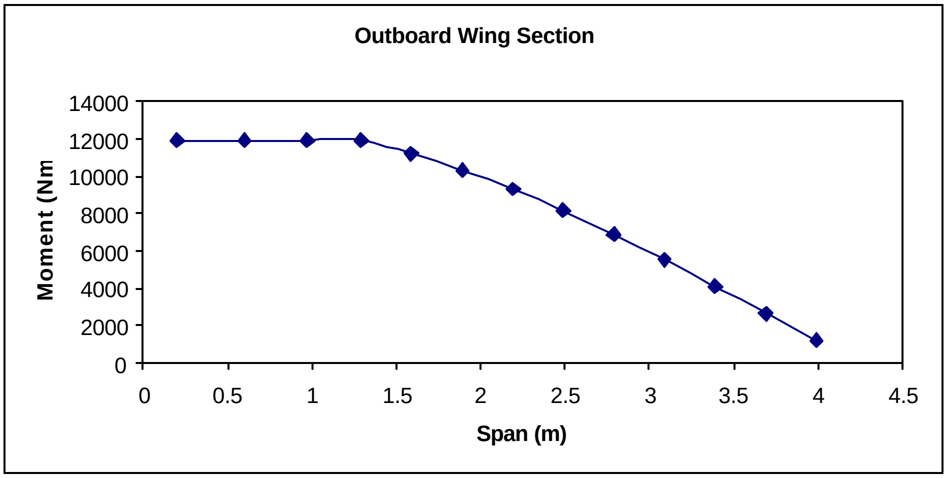

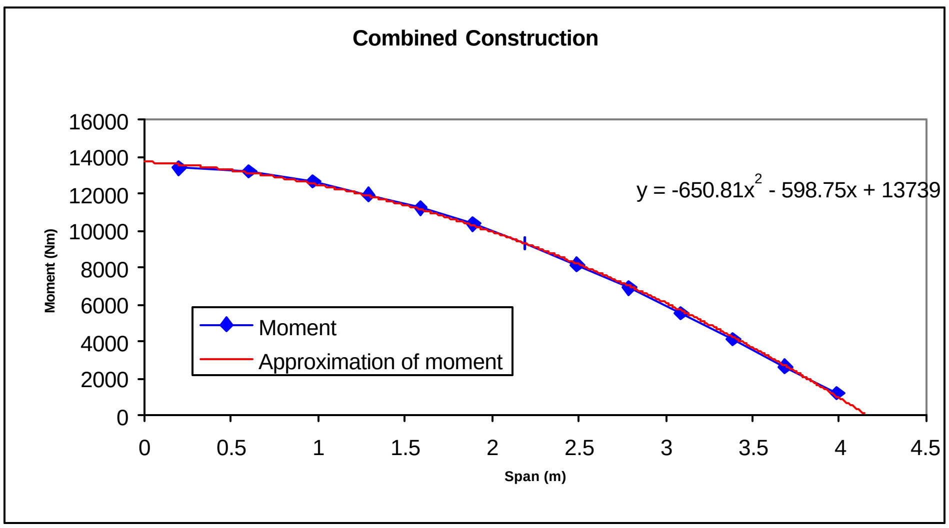

Figure G.1-3 (a-c) (a) Inboard Wing (b)Outboard Wing (c) Combined Moment Diagram

G.2. Arrangement

The general structural arrangement for the Pegasus includes two major sections: the design of the wing and the design of the fuselage. Other important structural considerations included propeller location and loads, landing gear location, and horizontal tail location.

The general arrangement is seen in Figure G.2-1. This arrangement allows all loads to be transferred smoothly between lifting surfaces and the fuselage. Table G.2-1 presents major structural components and locations. Details about the wing design and fuselage design follow.

Table G.2-1 Major structural members and location

Major Structural Member		Number	FS	WS
Fuselage Structure				
Crumple Zone	Rib 1	1	107.87	n/a
	Bulkhead 1	2	128.35	n/a
Passenger Compartment	Rib 2 (doorframe)	3	164.96	n/a
	Bulkhead 2	4	202.36	n/a
Engine Compartment	Firewall	5	202.36	n/a
	Bulkhead 3	6	275.20	n/a
Inboard Wing Spars	Forward Spar	7	202.36	n/a
	Rear Spar	8	275.20	n/a
Telescoping Wing Spars	Forward Spar	9	213.19	n/a
	Rear Spar	10	229.96	n/a
Horizontal Tail	Forward Spar	11	350.79	n/a
	Rear Spar	12	362.20	n/a
Telescoping Wing	Rib 1	13	n/a	44.09
	Rib 2	14	n/a	73.62
	Rib 3	15	n/a	103.15
	Rib 4	16	n/a	132.48
	Rib 5	17	n/a	161.81
Horizontal Tail	Rib 1	18	n/a	14.72
	Rib 2	19	n/a	44.33

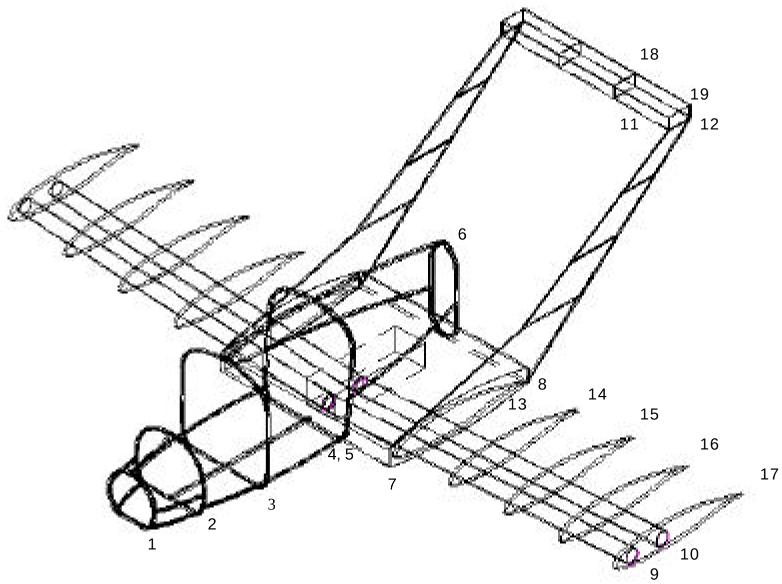

Figure G.2-1 Structural layout

Overall Wing Design

Due to the unique design of a roadable aircraft, the structural design of a stowable or telescoping wing was important. Since the Pegasus has the ability to drive on the highway like an automobile, a system that retracted or folded the wings needed to be devised. Several initial options were discussed, including a folding mechanism or even a sliding mechanism.

One idea considered seriously was to place the two outboard wing sections at different heights and use a retraction system similar to a drawer track (See Figure G.2-2).

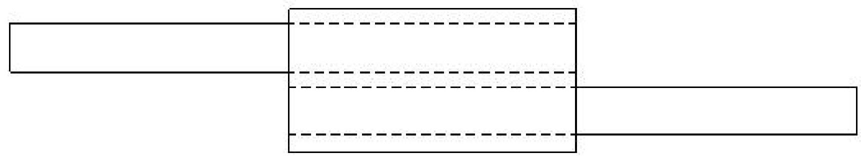

Figure G.2-2 Wing retraction system

During road mode, these two sections would slide into the vehicle and be stored on top of each other inside the vehicle. One major problem encountered with this idea was the need for a large storage space. Other problems involving the mechanism to retract the wings caused this idea to be rejected.

An SAE paper[3] was found that described a telescoping wing which had been designed for use on a flying automobile. This telescoping wing was the only lifting surface for the vehicle, as opposed to our design which also had the inboard section to create lift. Our vehicle, with its inboard sections would require a lower area from the telescoping sections. It was therefore decided to use a telescoping wing similar to this already proven design for the outboard sections.

Telescoping Wing Design

The telescoping wing design varies greatly from traditional wing designs. All components are able to extend and retract telescopically. Figure G.2-3 shows a semi-span of the telescoping wing in an extended configuration. Each half of the wing consists of four wing segments of 0.75m (2.46 ft) span. Each of these segments is made of an external skin section, which is attached by ribs to two spars (fore and aft). These spar sections are tubular and form the basis of the telescopic operation. Inside the inboard section/fuselage is a final spar section.

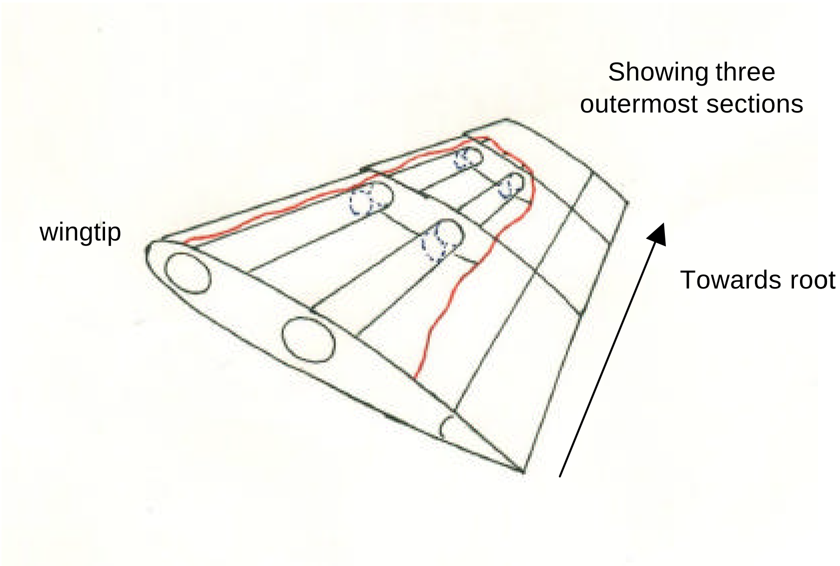

Figure G.2-3 Semi-span of telescoping wing (adapted from Ref 3)

The innermost spar section is held in place by a permanent attachment to the structure of the fuselage, through a central box section. Alternate sections are then able to rotate, resulting in a fixed tip-most section. The fixed sections are prevented from rotating by having a rigid attachment to their rib section, while the segments that are allowed to rotate are attached to their ribs through a ball-bearing joint provided rotational motion only. This principle is shown in figures G.2-4 and G.2-5.

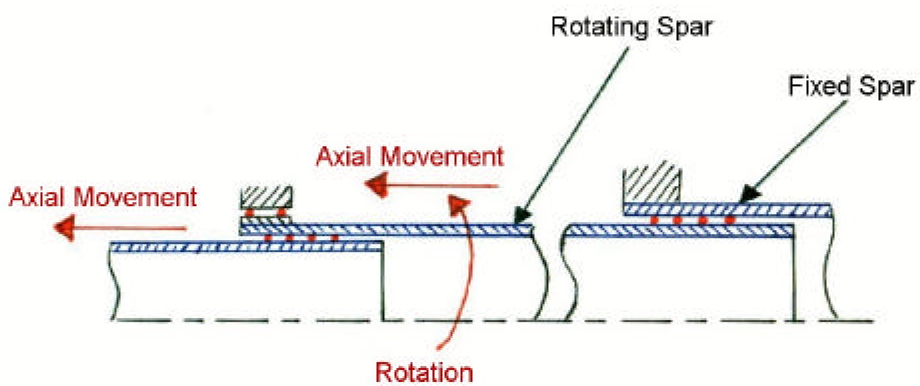

Figure G.2-4 Principles of operation of rotating and non-rotating spars (adapted from Ref 3)]

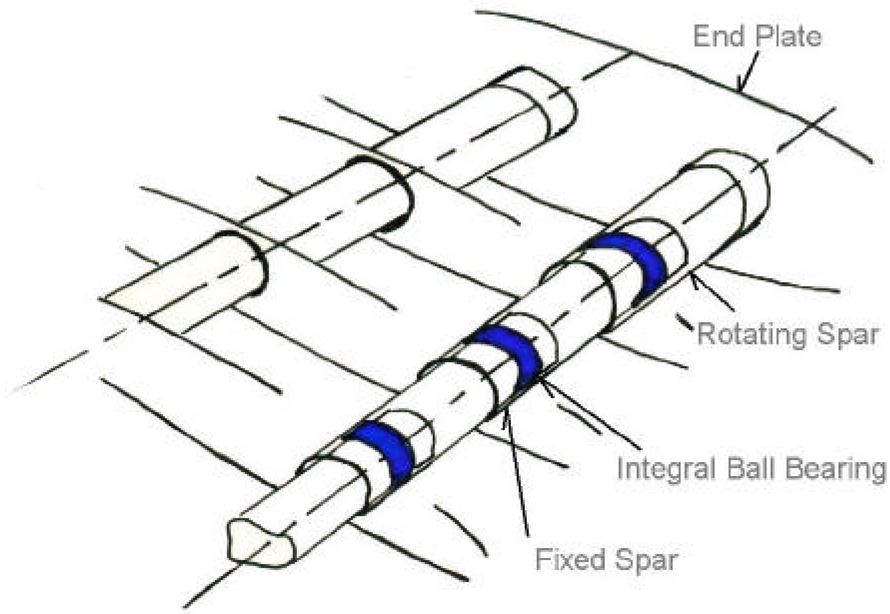

Figure G.2-5 Principles of operation of telescoping wing (adapted from Ref 3)]

Each of the wing sections, from root to tip, is larger than the last, allowing it to move over the previous section, so that the wing can be extended and retracted. Interior and exterior screw threads on each of the sections in matched pairs mean that rotation of the ball bearing mounted sections causes the wing to extend or retract, depending on the direction of rotation.

The rotatable spar sections are driven by a telescopic drive mechanism consisting of tubular frames and rings. This drive mechanism, in turn, is rotated by a set of bevel gears ultimately connected to a 12 V motor housed in a central box section. Alternatively, there is the option to install a manual drive for both cost and weight savings.

During flight, the aerodynamic loads from the wing are transferred to the tubular spars through the ribs. Each spar segment must therefore carry the accumulated loads of each section to that point. Figure G.2-6 shows the wing is a storage/retracted configuration.

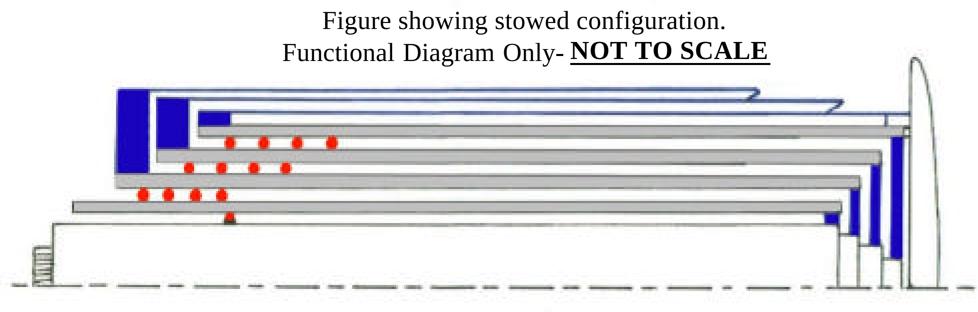

Figure G.2-6 Wing in Stowed Position

The diameter of the spar, as stated previously, is increasing towards the tip. This is so that the chord is decreasing in size at each step. This is the opposite of the method used by Cjakoswki *et al*[3], who preferred a decreasing spar size, and increasing chord, but is addressed in US Patent #4824053. This decreasing chord is considered desirable for aerodynamic reasons.

An important consideration is whether the main component of weight comes from the skin, or from the spar. If the weight were mainly from the spar then it would be desirable to have the chord of the spar increasing. This will move the center of mass of the wing further from the root and hence increase the moment about the chord, increasing the inertia relief of the wing. The wing will not need to be as stiff and for similar diameters a thinner wall can be used, resulting in a lighter wing. The same argument applies for the skin. If this is the heaviest component its center of mass should be the furthest out to increase inertia relief and lighten the wing.

Fixed (Inboard) Wing Design

It would be desirable to share structure between the inboard and outboard sections of wing. However, the need to stow the telescopic wing means that the main spar section will be surrounded by skin and tipwards spar sections when the wing is in roadable mode. The only point at which loads could be transferred to the outboard spar sections would be so close to the centerline of the aircraft as to make it a pointless exercise.

In this case, the inboard wing section has its own more conventional structure consisting of a forward and rear spar. See the general structural arrangement, Figure G.2-1. Since the structure of the inboard wing section must also house the entire telescoping sections for road mode, its main structural elements were placed around the telescoping wing section. This differs from conventional wings that have a forward spar at approximately 0.25c and a rear spar at 0.65c. Our structure was placed at the extreme ends of the inboard wing section.

Because of the close proximity of the wing to the door, there is a slight possibly of having persons climbing over the inboard wing. This was taken into account in the material selection for the upper skin of the wing.

Stringers are included to transfer compressive loads through the top half of the wing box, which will run unbroken through the aircraft. Extra stringers on the outboard wing section will terminate at the fuselage. These stringers will support the extra load of extra impact damage on the inboard wing section, as discussed above. The bottom section will not have continuous stringers, as it is necessary to allow access to the center box of the telescoping wing for maintenance and repair. Two flanges will be used to close the box beam. The rear flange will be well to the rear to avoid the outboard wing section, and as a result a large box section will be created, causing an unavoidable increase in weight.

Fuselage Design

The structure of the fuselage was divided from front to rear by creating four main compartments: crumple zone, passenger compartment, wing box, and engine compartment. These are labeled in Figure G.2-7.

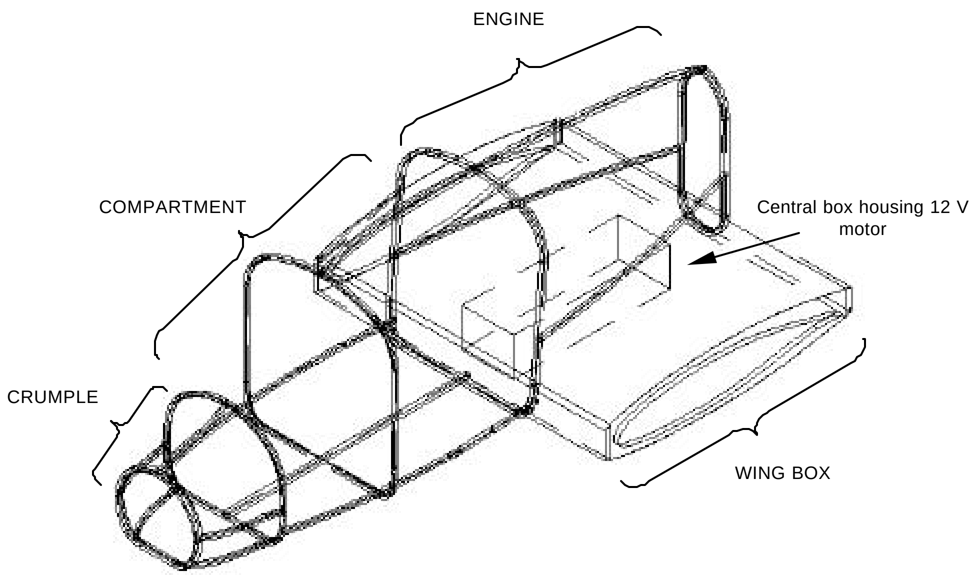

Figure G.2-7 Fuselage Structural Design

The forward crumple zone consists of a composite skin, constructed as part of the main fuselage section, as discussed later in the manufacturing section (Appendix P). The skin at this point will be only lightly stressed, and therefore will consist of fewer laminated sheets. An aluminum sub frame acts as a crumple zone. The brittle nature of the composites was not considered suitable for a crumple zone since the properties of composites degrade substantially with use and time. Therefore, the aluminum sub structure was designed with v-shaped indentions called fold intiators that result in controlled deformations in the event of a crash.

The forward landing gear, consisting of the wheels and suspension, is mounted to the forwardmost bulkhead for support. The steel landing gear, discussed in Appendix M, will be mounted to the aluminum sub frame using conventional bolting methods, to ease repair and maintenance. The composite skin will be mounted to the internal structure using adhesive bonding techniques. Since the loads generated by the landing gear will be eccentric to the joint between frame and skin, a single lap joint will not be suitable, as it will be susceptible to peeling. A scarf of stepped joint will therefore be necessary.

The skin of the passenger compartment is of carbon composite construction. This was chosen because it offers good stiffness and resistance to deformation, thus keeping the passenger cell intact in the event of a crash. An aluminum rib is used to support door loads as well as any loads encountered from the windshield. Two longitudinal stiffeners near the bottom of the fuselage support the cabin floor. Cabin dimensions and interior amenities are discussed in Appendix N.

An aluminum bulkhead marks the end of the passenger compartment. This bulkhead transfers wing loads from the forward spar of the inboard wing to the fuselage. To save weight and structure, the bulkhead is conjoined with a firewall. Both of these structures serve to separate the passenger compartment from the engine compartment.

The firewall is constructed from fiberglass with coatings of sperotex and phenolic resin. The combination of the structures supports the wing loads mentioned previously as well as the engine mounts and loads from the engine and transmission. The rear mounted engine posed safety concerns that were assuaged by placing the firewall at a slight angle. Combined with fold initiators, this allows for the engine to slide under the passenger compartment in the event of a rear end collision.

The wingbox for the inboard wing is a standard carry-through box created by the front and rear structural spars in conjunction with the wing skin. The wingbox carries most of the aerodynamic forces created in flight so that the fuselage internal structure will not be subjected to the majority of the load.

Tail Design

For reasons discussed in the materials section of the report, a carbon-glass-epoxy resin composite is being used in the construction of the tail. This enables a semi-monocoque construction with sparsely located structural supports of carbon fiber shown in Figure G.2-7. A conventional approach to the horizontal stabilizer was taken by having a front and rear spar.

As discussed in the manufacturing section (Appendix P), the composite will be thicker at the root of the tail booms/vertical stabilizers, where the bending moments are greatest, with the number of layers reducing towards the horizontal stabilizer. At the root of the wing, thickness will increase beyond what is necessary purely for bending to allow sufficient area for bonding to the outboard wing section.

Conclusion

This appendix has taken account of the design features and considerations necessary for a finite element analysis to be carried out. In conjunction with the materials section and general drawing it is now possible for a detailed design of the composite skin. Preliminary sizes for sub frames and other structural members, which so far have been scaled from other aircraft can be optimized.

G.3. Materials

Consideration of materials for use in the design of the Pegasus included aluminum, steel, and titanium as well as composite materials such as glass and carbon reinforced plastic (GRP and CRP respectively). Selection criteria used for deciding material selection included cost, manufacturability, durability, weight, damage tolerance, and corrosion resistance. Desirable characteristics of airplane materials include low densities, high strength, good stiffness, abrasion and impact resistantance, and non-corrosiveness. More detail is provided in Appendix H.

G.4. Safety

Safety in the construction of our design is important due to the need to meet both safety regulations for automobiles as well as aircraft. Auto safety regulations were found from NHTSA while aircraft regulations were taken from FAR 23.

One safety approach taken in the structural design included designing the fuselage to absorb the shock from a crash safely. Any impacts taken by the fuselage cause it to deflect and spread the load over distance and time. This was accomplished by utilizing aluminum for the major structural elements instead of composites which tend to be stiff and do not deflect readily.

Also, for safety, the firewall in front of the rear mounted engine was canted slightly. In the event of a rear end collision in automobile mode, the firewall will force the engine underneath the passenger compartment.

Safety features incorporated into our design required by NHTSA include: rear and side mirrors, head and tail lights, lap and shoulder harnesses, air bags, and bumpers. Details about the roadiblity are included in Appendix M. More detail about safety features is provided in Appendix N.

1) Niu, Michael, Airframe structural design: practical design information and data on aircraft structures, 1988.

2) Raymer, Daniel P., Aircraft Design: A Conceptual Approach, Third Edition, 1999.

3 Czajkowski, M; Clausen, G., & Sarh, B., *Telescopic Wing of an Advanced Flying Automobile.* AIAA/ SAE Int. (#975602), 1997.

Appendix H. Materials

H.1.   General Aircraft Materials

Consideration of materials for aircraft structures in general includes conventional metals as well as advanced composites. Selection of materials must depend on the application, but major factors that are considered include yield and ultimate strength, stiffness, density, fracture toughness, fatigue crack resistance, corrosion resistance, temperature limits, producability, repairability, cost, and availability.

The modulus of elasticity for a material is critical in the design of an aircraft structure. This is the relationship between the stress and strain of a material and aids in determining the proportional limit which is the highest stress level at which the strain is still proportional to the stress. The elastic range of a material is where the proportionality between stress and strain is valid. Within this range, the structure does not sustain any permanent deformation, that is, the structure returns to its original state after the load is removed. Shown below in Figure H.1-1is a typical illustration of yield versus ultimate stress and deformation.

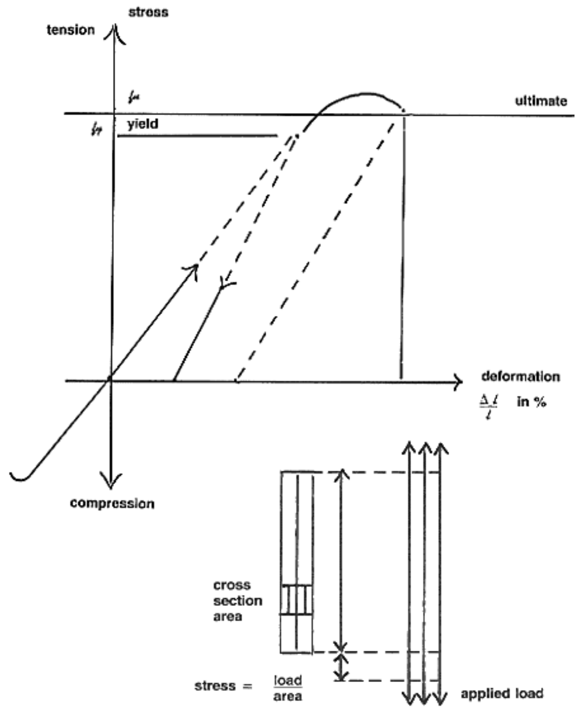

Figure H.1-1 General depiction of stress-strain curve[1]

For aluminum alloys, the ultimate stress is about 1.5 times the yield stress. However, when using composites, a safety factor must be assumed since they fracture suddenly past the proportional limit. Below is Figure H.1-2 showing the differences in the stress-strain curve for wood, aluminum, and composites.

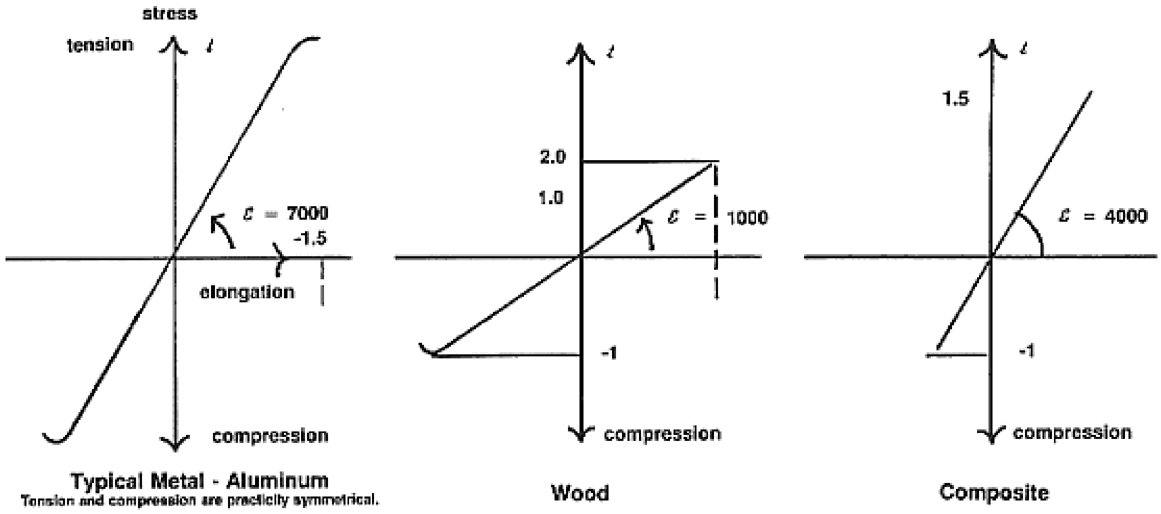

Figure H.1-2 Stress-strain curve comparisons for wood, aluminum, and composites[1]

Table H.1-1 below shows some of the basic mechanical properties of some typical aircraft structural materials.

Table H.1-1 Basic mechanical properties of typical aircraft components

Material	Type	Stiffness (Gpa)	poisson	Ultimate Strength (Mpa)	Yield Strength (Mpa)	Density (g/cm3)	Ustrength/ density	YStrength/ density
Metals								
Aluminium	2024-T3	72.00	0.33	449.00	324.00	2.78	161.51	116.55
	7075-T6	71.00	0.33	538.00	490.00	2.78	193.53	176.26
Titanium	Ti-6Al-4V	110.00	0.31	925.00	869.00	4.46	207.40	194.84
Steel	AISI4340	200.00	0.32	1790.00	1483.00	7.80	229.49	190.13
	300M	200.00	0.32	1860.00	1520.00	7.80	238.46	194.87
Composites								
Carbon Epoxy	T300/5208	140.00		1500.00		1.55	967.74	
	IM6/3501-6	177.00		2860.00		1.55	1845.16	
	AS4/3501-6	140.00		2100.00		1.55	1354.84	
Boron-Aluminum	B/Al 2024	210.00		1500.00		2.65	566.04	
Glass-Epoxy	S2 Glass-Epoxy	43.00		1700.00		1.80	944.44	
Aramid-Epoxy	Kev 49-Epoxy	70.00		1400.00		1.40	1000.00	

H.1.1. Conventional Metals and Plastics

Conventional materials such as aluminum, titanium, steel, plastic, and glass are widely considered for aircraft applications. The following sections give descriptions and properties of these conventional materials. Properties of advanced composites are mentioned in Appendix H section 1.2

Aluminum Alloys

Aluminum alloys, the most common aircraft material, are used extensively in airframes, skins and other stressed members and have dominated the aircraft industry for many years. Aluminum has a good strength-to-weight ratio, is easily fabricated, has a higher initial cost than steel, but has less maintenance, but is tricky to weld. Corrosion problems may exist where aluminum is joined with steel.

After deciding on aluminum for a component, the choice of actual alloy will be based on strength, ductility, ease of manufacture (extrusion and forging), corrosion resistance, ease of protective treatment, fatigue strength, resistance to crack propagation.

There are three main groups of aluminum alloy, and these are summarized below:

1. Derivatives of Y alloy. (Typically 4% copper, 2% nickel and 1.5% magnesium). Included in this group are RR alloys, developed by Rolls-Royce. The quantity of copper is reduced and replaced with extra nickel and some iron. This group retains strength at high temperatures and is therefore more typically used in aircraft engines, rather than in the structure of the aircraft.
2. Aluminum-zinc-magnesium group. Inclusion of zinc and magnesium gives high strength. (Nominal - 2.5% copper, 5% zinc, 3% magnesium 1% nickel) More recent versions eliminate nickel and use chromium and more manganese. These alloys have a tendency to crack in unloaded conditions due to retention of stresses after heat treatment. This problem

reduced by several methods: Adding copper is beneficial. The benefits of adding chromium and manganese are disputed between countries and organizations. The 7000 series (aluminum-zinc-magnesium-copper) meets requirements for high strength and good crack growth resistance as well as possessing adequate toughness. This series therefore finds a great deal of use in compressively loaded structures, such as the upper surfaces of wings. 7075 alloys , especially 7075-T6 are the most commonly used.

3. Nickel free duralumins. These typically consist of about 4% copper, 0.5% magnesium, 0.5%manganese, 0.3%silicon and 0.2% iron. Duralumins are not as strong as zinc bearing alloys. However, they do have good fatigue characteristics. For this reason they are often used on the underside surface of wings where fatigue loads due to cyclic tensile stresses dominate. Natural aging results in better resistance to fatigue and crack propagation than artificially aged, heat treated duralumins. Increasing magnesium content in naturally aged alloys gives mechanical properties between normal and artificially aged duralumin. 2024 alloys are often used as a safe compromise between various requirements.

Recent research has focused on the introduction of lithium into the alloy. Fracture toughness and resistance to cracking is poor, but improving. The main advantage is a reduction of about 10% density. Stiffness is also increased by about 10% and fatigue resistance is improved. Al-Li replacements for both 7000 and 2000 series alloys are anticipated.

Steel

The high density of steel prevents widespread use in aircraft. However, its high strength and stiffness, as well as resistance to wear means it still has a role to play. It is often used in undercarriage and wing root attachments, firewalls, and engine mounts because of its high strength and fatigue resistance characteristics. Steel can withstand high forces, fatigue, and impact with ease of fabrication and low cost. Its poor corrosion resistance means it must be plated for corrosion protection.

At the same time high strengths and stiffnesses are achieved, such as in 300M, other properties are degraded and it is difficult to manufacture into finished components. One solution is to use maraged steels, which would typically be 17-19% nickel, 8-9% cobalt, 3-3.5% Molybdenum and 0.15-0.25% titanium. Carbon content would be unusually low, at just 0.03%. While slightly weaker and less stiff than other steels its strength is still considerable. (0.2% proof- 1400N/mm2 and mod of Ela180,000N/mm2). The cost of the raw material is higher, but it is far easier to manufacture, is less susceptible to cracking and has better corrosion resistance.

Titanium

The use of titanium has increased throughout the aircraft industry, especially in military applications. Titanium has a better strength-to-weight ratio than aluminum and is corrosion resistant. Titanium is also expensive (about five to ten times as much as aluminum) and hard to form. This high cost is primarily due to the difficulty in machining titanium alloys. It can be seriously affected by impurities introduced during forming. It displays good fatigue strength and corrosion resistance, but is difficult to weld. Titanium is also susceptible to stress corrosion cracking.

In terms of density it falls between steel and aluminum, being slightly more than 50% heavier than aluminum. Its ultimate and yield stresses however are close to double those of aluminum. Its fatigue strength / tensile strength is good, along with a generally good resistance to corrosion.

Plastics

Plastics have densities less than half those of aluminium, and therefore have a role for parts which are lightly stressed or have their caracteristics determeined by handling requirements rather than strength. For this reason plastics are often used in windows, although not in pressurised sitautions. There will be requirements for scratch resistance, as well as strength requirements on the windscreen, and plastic is therefore only likely to be found in small side windows.

H.1.2. Composites

Composite use in both business and general aviation planes has increased since the 1980's[2]. A wide variety of composites are available for use today and still more are still being investigated. This section gives an overview of composites for use in aircraft.

A composite is defined as "any multiphase material that exhibits a significant proportion of the properties of both constituent phases that a better combination of properties is realized"[3]. Composites by definition are artificially made and comprised of two phases: a matrix and a dispersed phase. The matrix is continuous and surrounds the dispersed phase which can be particles or fibers.

In fiber-reinforced plastic the dispersed phase is a fiber. This gives a high strength to weight ratio. The modulus of elasticity for a continuous fiber reinforced plastic aligned in the direction of alignment is greater than the modulus of elasticity for a single component and is given by the following equation:

$$E_c = E_m(1 - V_f) + E_f V_f \qquad (1)$$

For transverse loading (opposite of the aligned fiber), the following equation holds:

$$E_c = \frac{E_m E_f}{(1 - V_f)E_f + V_f E_m} \qquad (2)$$

E_c	Youngs Modulus for composite
E_m	Youngs Modulus for matrix
E_f	Youngs Modulus for fiber
Vf	Volume Fraction for fiber

The matrix in fiber-reinforced composites has several purposes. First and foremost it binds the fibers together, but it also transmits and distributes external stresses. The matrix protects the fibers from surface damage that might occur and prevents propagation of brittle cracks between the fibers.

Fibers utilized in these types of composites are generally of small diameter. Typical fibers used are glass (E-glass), carbon, and boron. Some moduli of elasticity for E-glass and carbon are given below in table H.1-3:

Table H.1-3 Values of E for common fibers

	E (GPa)
E-glass	72
Carbon	150-500

Glass reinforced plastic, or fiberglass, is the most widely produced type of fiber-reinforced plastic. This accounts for the material being inexpensive. Carbon- and boron-reinforced plastics are also becoming more widely used. However, both of these materials are expensive.

A hybrid composite consists of two or more fibers embedded in a polymeric resin matrix. Hybrids exhibit better overall properties than those of a single fiber matrix. A common hybrid composite is carbon and glass reinforced. This combination is stronger, tougher, has a higher impact resistance and lower cost as compared with an all carbon or all glass composite. This hybrid composite also does not exhibit catastrophic failure as would be expected. Instead, the carbon fibers fail first and the load is transferred to the glass fibers. Upon the failure of the glass fibers, the matrix sustains the load until ultimate failure.

Composites are becoming more popular for primary aircraft structures. Typically, composite materials yield a weight savings of 25% over conventional aluminum[4]. Most composites used for aircraft are filament reinforced because this gives a great strength-to-weight ratio.

Fiber-reinforced Composite Materials

Fiber composites are suitable for most aircraft structures as they are strong, stiff and light. For aircraft applications they are mostly used in the form of laminates consisting of several unidirectional layers, each aligned in a different direction to provide multi-directional load capability. These composite laminates have excellent fatigue, damage tolerance and corrosion resistance characteristics. In addition laminate constructions can be tailored to give an optimum structural performance by altering the orientation of the various layers.

Fiber-reinforced composites can be broken down into three major groups. Polymer matrix composites (PMC), metal matrix composites (MMC) and ceramic matrix composites (CMC)

Glass reinforced plastic (a CMC) has limited application in the load bearing structure of fixed wing aircraft due to its low stiffness. Kevlar has improved stiffness, but a similar strength. However, Kevlar structures are poor in compression and difficult to manufacture and are therefore not used in primary structures. Boron fiber composites are strong and stiff enough to be used for primary structures, but are expensive. Material properties for these three materials can be found in Table H.1-1.

These composites have been largely superseded by **C**arbon **F**iber **R**einforced **P**lastics (CFRP). CFRPs have comparable material properties to Boron fiber composites, but are considerably cheaper and lighter. CFRP is roughly three and a half to four times stiffer than glass reinforced plastic and twice as stiff as aluminum alloys. The strength is about three times that of aluminum alloys, and approximately the same as glass reinforced plastic.

CFRP does have disadvantages however. It is a brittle material and does not yield plastically in regions of high loading. Strength is reduced by impact damage, even light damage which may not be visible to the naked eye. Over time moisture is absorbed which results in a reduction in compressive strength and other matrix related properties. Finally the properties of CFRP are inherently more random than those of metals. All of these factors mean that a large factor of safety must be used when determining the maximum load possible.

On the positive side, stiffness is affected far less, and is less prone to fatigue damage than metals. CFRP is therefore most valuable in applications where stiffness is the dominating design factor rather than strength.

There are several ways of processing fiber-reinforced composites. Pultrusion is used to create components with continuous length and constant cross sectional shape such as rods, tubes, and beams. Continuous fiber rovings are impregnated with a thermosetting resin and pulled through a die to give the material a desired shape. This continuous process is easily automated and very cost effective. A wide variety of shapes are possible.

Prepreg is the most widely used method of processing fiber reinforced matrices. A continuous fiber reinforcement is pre-impregnated with a polymer resin that is not totally cured. This is stretched into a tape that is supplied to the manufacturer who cures the product. The tape is layered onto a tooled surface. The drawback to this process is the cutting and positioning of the tape must be done by hand. One alternative is to have a machine cut the tape, but it still needs to be hand-positioned. Prepreg is widely used for structural applications.

Filament winding involves continuous reinforcing fibers positioned accurately in a predetermined pattern to form a hollow shape. The fibers are fed into a resin bath and wound onto a mandrel where it is then cured and the mandrel is removed. Various winding patterns are possible. The filament winding process results in a high strength to weight ratio. It is also cost effective and uses not limited to surfaces of revolution are being developed.

Laminar composites are comprised of two dimensional sheets with a preferred high strength direction that are stacked with alternating directions of high strength.

Sandwich panels consist of two strong outer faces separated by a layer of less dense material called a core. The faces bear the in-plane loading and transverse bending stress while the core resists deformations perpendicular to the faces. Aircraft applications include wings, fuselages, and tailplane skins. Typical face materials include aluminum alloys, fiber resin plastics, titanium, and steel. Core materials include foamed polymers, synthetic rubber, and a honeycomb core comprised of hexagonal cells.

Further information on processing and manufacturing is found in Appendix P.

H.2. Usage of Materials

Materials chosen for structural members in the Pegasus were considered from those mentioned in previous sections. Various alternatives were weighed with advantages and disadvantages of each. The final decision on materials used for components is given in Table H.2-1. Shown in Figure H.2-1 is the placement of the materials relative to the structural layout. The next sections give reasoning behind the selection of the materials.

Table H.2-1 Table of material selection

Structure	Component	Material
Crumple Zone	Rib 1	Al 7075
	Bulkhead 1	Al 7075
Passenger Compartment	Rib 2 (doorframe)	Al 7075
	Bulkhead 2	Al 7075
Engine Compartment	Firewall	Fiberglass coated with sperotex & phenolic resin
	Bulkhead 3	Al 7075
	Engine Mounts	Steel
	Fuselage Skin	Carbon Fiber
	Windows	Plexiglass
Inboard Wing	Forward Spar	Al 7075
	Rear Spar	Al 7075
	Top Skin	Al 7075
	Bottom Skin	Al 2024
Telescoping Wing	Rotating Spars	Stainless Steel
	Non-rotating Spars	Carbon Fiber
	Spar Attachments	Al 7075
	Ribs	Carbon Fiber Sandwich
	Skin	Carbon Fiber Sandwich
Horizontal Tail	Forward Spar	Al
	Rear Spar	
	Skin	Hybrid - Glass and Carbon Fiber
Vertical Tail	Skin	Hybrid - Glass and Carbon Fiber
Landing Gear	Overall gear	Steel
	Wheels	Al 7075

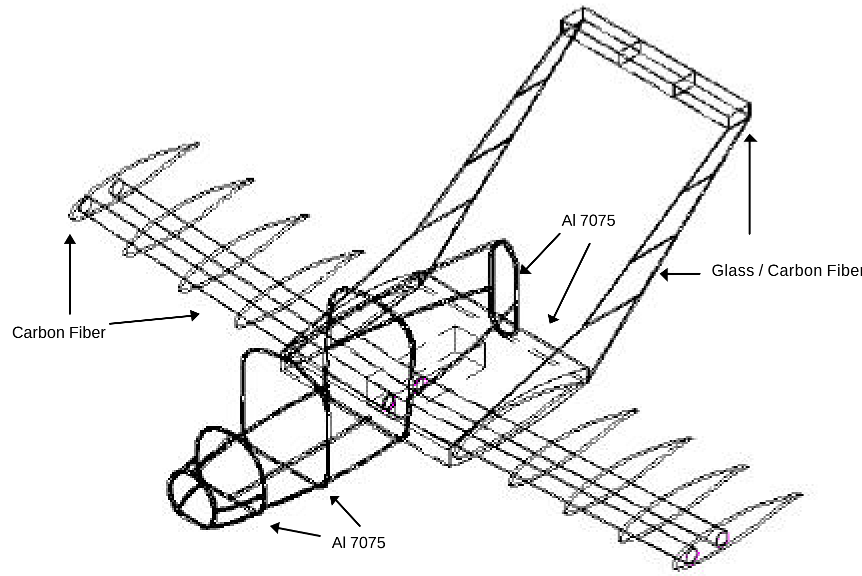

Figure H.2-1 material placement

Fuselage

The underlying fuselage structure is comprised of aluminum ribs, bulkheads and longitudinal members. Aluminum was chosen for several reasons. In comparison to steel, which is used for most car frames, aluminum is more rigid and safer as well as 40% lighter[5]. The passenger compartment also needed to be stiffness for protection in the event of a collision.

Safety features included in the aluminum structure of the crumple zone (at the front of the vehicle) include the use of v-shaped grooves or notches along the faces of the most forward longitudinal members. This ensures a controlled collapse of the structure upon impact. They are called fold initiators and encourage a controlled deformation of the structure. This protects the passenger compartment from suffering serious distortion[6].

The fuselage section of our design is composed of a CFRP skin and was attached to the aluminum structure by aluminum fasteners. Since this structure, in combination with the sub-structure, needs to be crash resistant to meet safety standards, the composite must provide the same level of safety as a metal skin would. Aluminum can sustain greater than 24 times the deformation and greater than 65 times the energy absorption of composites. Composites are generally considered inferior in terms of crash resistance and have high degree of brittleness.

In order to justify our decision of using a CFRP skin for our fuselage, we used a complex aluminum substructure underneath to serve as a crumple zone. Niu[2] states that experience shows that crash protection from critical damage can be provided by appropriate support structure. Our support structure is adequate to prevent critical damage of the passenger compartment.

Further justification of composite usage in the fuselage includes:

- Weight savings (up to 25% compared to Aluminum)
- Can reduce cost or be cost effective
- Have been validated structurally under aircraft environmental conditions

Steps taken to minimize the cost of composites include reducing cost in the areas of fabrication, inspection, and repair. Automated systems assist in the way of cost reduction. More information on manufacturing process is included in Appendix P.

The following chart (Table H.2-2) is a comparison between thermoplastics and metals. Thermosets include epoxies and phenolics both of which are utilized in structural components in our design.

Table H.2-2 Relative advantages of thermosets versus metals (from Ref 2)

	Relative Advantage	
Material Properties	**Thermosets**	**Metals**
Corrosion Resistance	XXX	X
Damage Resistance	X	XXX
Design Flexibility	XXX	X
Moisture Resistance	X	XXX
Physical Properties	XXX	XXX
Specific Strength	XXX	X
Weight Savings	XX	n/a

Note: XXX - best, XX - good, X -fair

The firewall at FS 202.36 shown in Figure H.2-1 was constructed of fiberglass with coatings of sperotex and phenolic resin. Aluminum substructure is also bonded to the composite firewall. Properties of phenolic resin include excellent insulating capabilities and good electrical properties. It is also a load bearing component used to support the engine. It has fair mechanical properties, a high heat resistance (350 F), and is of low to medium cost. The toughness characteristics are poor and it is generally used in secondary structures for cabin interiors for low smoke generation.

The landing gear components mentioned in detail in Appendix M are primarily made from steel due to its high strength and impact loads. The wheels are aluminum. Mounting for the landing gear and suspension will be to an aluminum subframe as composites are not well suited to carrying concentrated bolt bearing loads. Aluminum will therefore be bonded to the composite structure. This bonding type joint is acceptable as there are no high bending mounts being transferred from gear to fuselage.

Wings

The top skin of the inboard wing was comprised of Al 7075 due to its high strength in compression. It was decided to use this due to the impact loads and high compression seen on the upper surface of the wing skin. The lower skin was constructed of Al 2024 because of its fatigue resistant qualities.

The majority of the components of the telescopic wings are composites. The internal structural elements of the telescoping wing include the rotating and non-rotating spars as well as the ribs. The rotating spars are constructed of stainless steel while the non-rotating spars are made of carbon fiber. The ribs are a composite sandwich with a CFRP face. Aluminum reinforcement is used at the spar attachment points. The skin is also composed of a carbon fiber sandwich.

The composite skin mainly carries the bending loads, but in our case due to the shortened span, the skin is subjected to larger amounts of shear. Different plies are used for the different loads seen in skin surfaces such as span-wise direct stresses (0°), shear stresses (45°), and chord-wise direct stresses (90°). Since the number of plies of each orientation varies depending on the application, our telescoping wing skin contains many 45° oriented plies.

Another advantage in using composites for the outboard wing includes easily increasing or decreasing the skin thickness as necessary. The amount of plies determines the thickness and is accomplished by varying the length of the plies used. For instance, on the outboard wing skin, the loads are greater near the root section and less near the tip. Therefore, a thicker skin is used at the root than the tip.

Since composites exhibit poor erosion resistance, the leading edge of the telescoping wing needed to be comprised of a heartier material. It was chosen to bond a metallic layer of aluminum over the leading edges of the telescoping wing sections.

Thin sandwich structures are prone to mechanical impact damage, especially due to frequent, repetitive impacts such as flaps and service doors. This leads to delamination, debonding, punctures, and fluid absorption. Foreign object damage in flight can lead to a whole series of effects. Hail will affect leading edges of control surfaces. All are discussed further under Environmental Conditions.

Tail Surfaces

Both the vertical and horizontal tail sections are composed of a hybrid composite mixture of glass and carbon fiber. Hybrids are useful because they can be tailored for performance requirements and are cost reducing. The carbon / glass hybrid we have chosen exhibits the following qualities:

- Increased impact strength
- Improved fracture toughness
- No galvanic corrosion
- Reduced cost compared to all carbon or all glass composites

The joint where the vertical tail joins the inboard wing will be especially thick to support the loads from both the vertical winglets as well as transferring loads from the horizontal tail. The juncture of the vertical and horizontal tails will be thinner than the root juncture, but not as pronounced as the difference in skin thickness for the telescoping wing.

H.2.1. Certification Of Composites

The certification process for all civil aircraft includes the need for an airworthiness certificate provided the aircraft meets all design and safety regulations for the particular type of aircraft. Our aircraft must comply with all specifications in FAR Part 23 for general aviation aircraft.

Procedures in place to establish the static strength of metal aircraft structure involve a detailed theoretical analysis as well as an abundance of structural testing. For airworthiness standards, full-scale article tests are the most important. Static tests on full scale aircraft include a test to establish that at the design limit load, no unacceptable deformations occur, and a test at ultimate load, upon which failure does not occur. The ultimate load is defined as 150% of the design limit load.

The entire process is outlined in figure H.2-2 below:

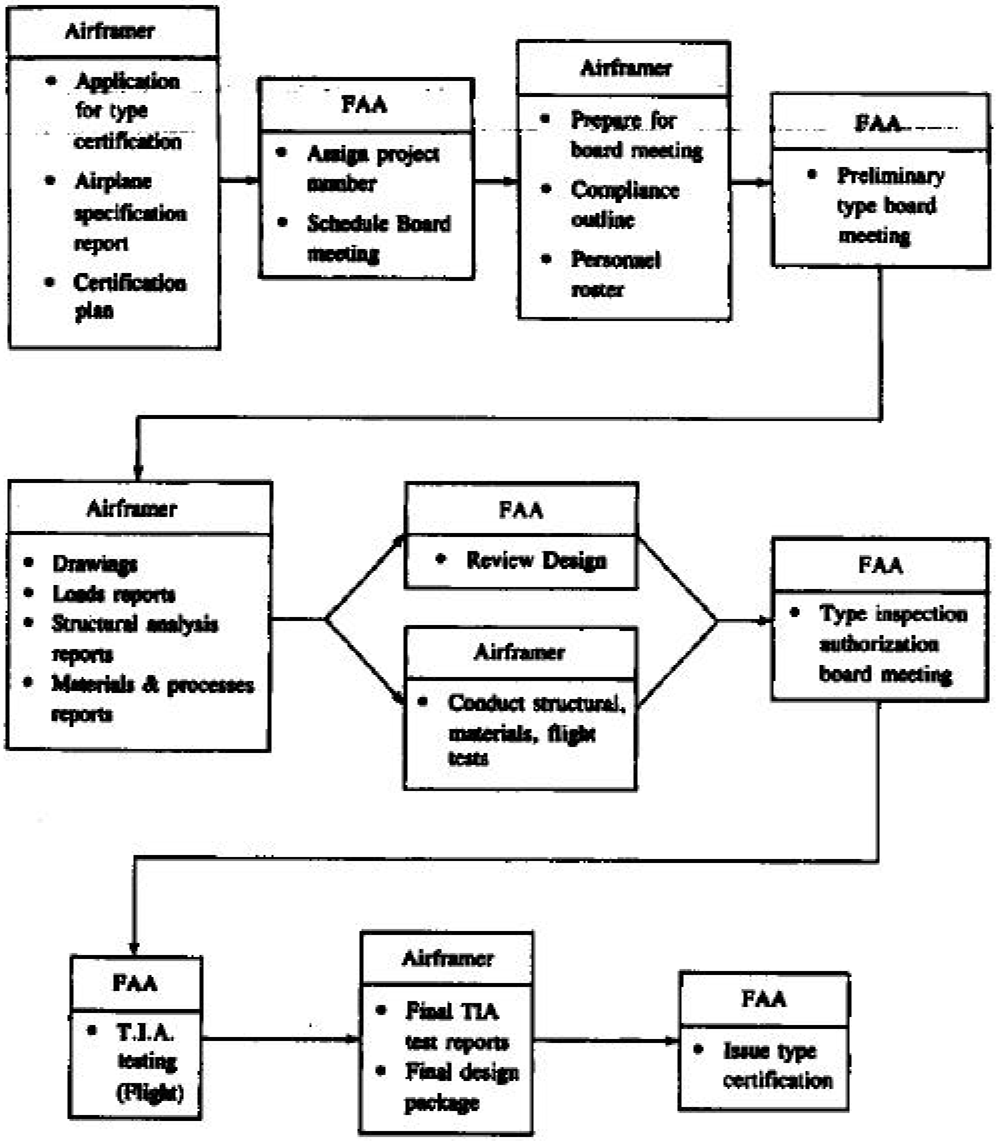

Figure H.2-2 General Outline for Certification of aircraft (from Ref 2)

Certification of composite structures is more complex than of conventional aluminum due to design considerations and variability in the material. Composite structures must be designed to give assurance that a higher risk is not associated with the composite compared to aluminum[7].

Formal requirements for composite structures are still in development, but an advisory circular points out some certification requirements for composites. Advisory Circular 20-107a issued by the FAA in 1984 treats the certification of composite airframe structures. Essentially, the evaluation of safety of the composite must at least meet the level of safety as current metal structures. Other typical constraints imposed on composite structures include:

- 150% design limit load due to a constant stress – strain variation until failure
- Fatigue testing due to variance in fatigue characteristics
- Environmental conditions such as hot / wet and cold / dry due to composite deterioration

More specifically, the advisory circular gives a suggested method of verifying composite structures, but is by no means the only way to certify them. First, environmental effects on design properties of the materials should be established including the most critical exposures to temperature and humidity. Then, the static strength of the materials needs to be demonstrated. This includes ultimate loads tests and subcomponent tests to demonstrate the adequate strength requirements. Any environmental or other effects which may degrade the material must also be addressed. The structures should also be subjected to repeated loads representative of the expected service usage. Also, impact damage should also be addressed.

As suggested by Niu[2], a general outline for substantiating composites is given below in figure H.2-3. This is especially important due to the large amount of composite structures on the aircraft.

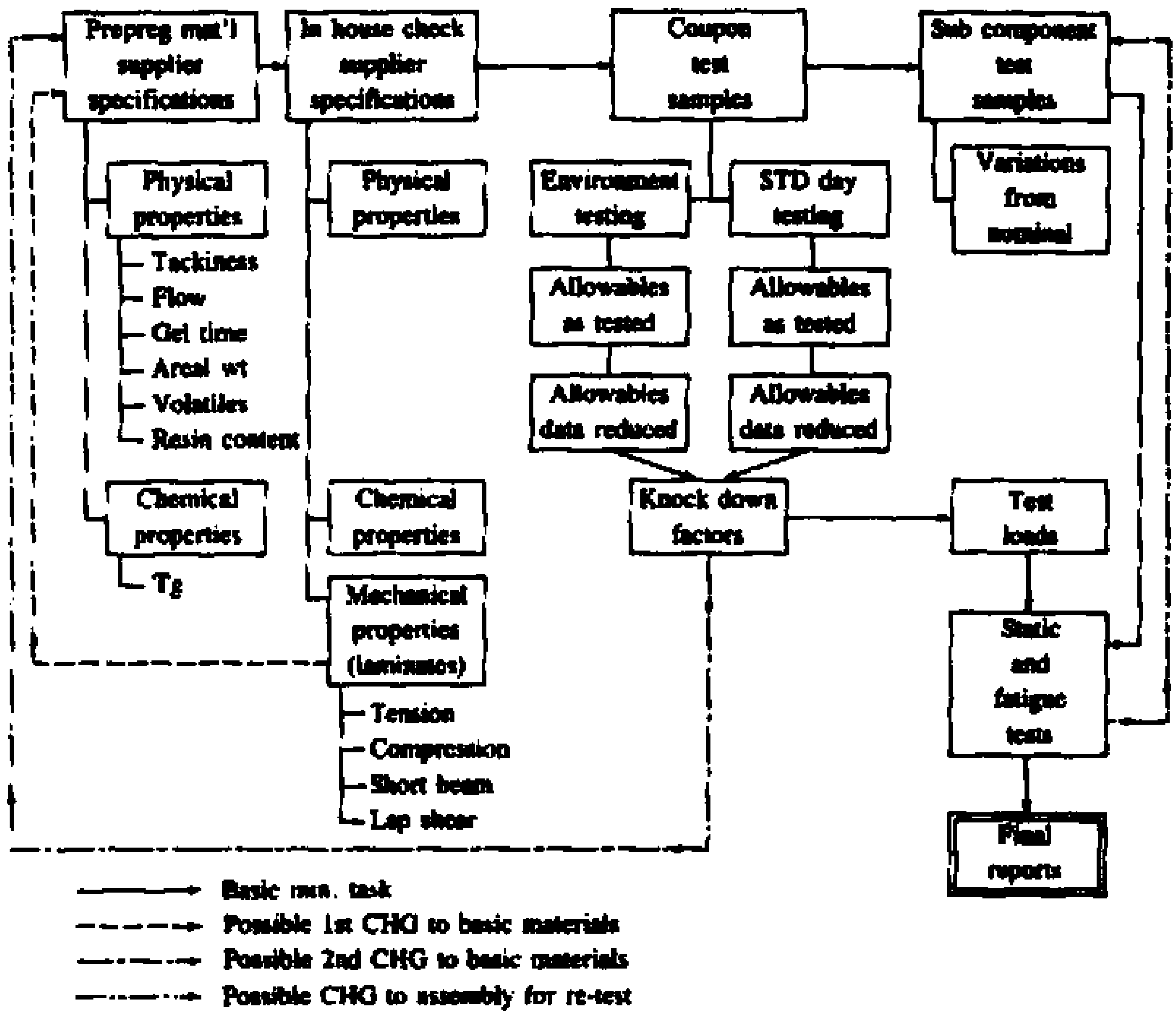

Figure H.2-3 Suggested outline for certification of composites (from Ref 2)

Two main problems seen in testing of composite structures involve allowance for environmental effects and impact of scatter in static and fatigue testing. Since the static strength of composites is degraded due to moisture and temperature effects and possible cyclic loads[7], it is necessary to perform tests to prove that the strength still remains even in the degraded form. More information concerning environmental effects and their impact of composites is discussed in the next sub-section.

One method of testing follows the basic metal aircraft approach. The full scale article tests are conducted in the dry condition while other smaller tests are performed under varying environmental conditions (coupon, subcomponent, and component tests). Other alternatives include testing the full article with increased loadings to allow for environmental effects. Also, it has been suggested to perform full-scale environmental tests.

Demonstrating the fatigue characteristics of composite components is exceptionally more difficult than determining static strength. Full-scale testing on composite structures to date have generally mimicked that of all-metal structures, subjecting the aircraft to cyclic loads for an N number of lifetimes in a normal environment. Again, these tests do not take into account the degradation of the composites due to environmental factors.

H.2.2. Environmental Concerns

Environmental conditions deteriorate composites much more so than metals[7]. Moisture, especially, is a big problem. Moisture diffuses into the matrix causing swelling, softening, debonding, and a loss of stiffness and strength. Water permeability is dependent on the types of resins used. Permeability is highest for epoxy resins and lowest for phenolics.

Water also degrades the mechanical properties and reduces the glass transition temperature which limits the high temperature performance of the composite. Matrix cracking can also occur due to moisture intake. Hot / wet conditions cause plasticity in the matrix while cold / wet conditions cause brittleness. Surface paint, laminate seals, and additional sealant on the composite, all of which will be used in some way or another in our design, aids in preventing moisture from seeping into the matrix.

Other environmental problems occur from impact damage such as hail, rain, and foreign objects[2]. The leading edge components are especially vulnerable. The leading edge components on the Pegasus are protected using an aluminum coating.

Lightening is another problem seen with composite structures. Most composites are not conductive or are significantly less conductive than aluminum[2]. The composites suffer large amounts of damage and also can allow large portions of electricity to invade the onboard systems. One solution, implemented in this design, involves bonding aluminum foil strips to the affected surfaces (wings, horizontal tails).

1) www.zenithair.com/kit-data/ht-86-3.html

2) Niu, Michael. Composite Airframe Structures. Conmilit Press Ltd., Hong Kong, 1992.

3) Callister, William D. Jr. Materials Science and Engineering: An Introduction. 3rd Ed. John Wiley & Sons, New York, 1994.

4) Raymer, Daniel P., Aircraft Design: A Conceptual Approach, Third Edition, 1999

5) www.audi.com

6) Munney, M.J. Light and Heavy Vehicle Technology. Butterworth-Heinemann, London, 1998.

7) Hoskin, Brian and Baker, Alan. Composite Materials for Aircraft Structures. American Institute of Aeronautics and Astronautics, 1986.

Appendix I. Propulsion

I.1. Selection Criteria

Propelling the Pegasus presents a unique set of problems. The system has to be designed to propel both an aircraft and an automobile at acceptable speeds and accelerations. Attaining this in one mode should not compromise the performance and stability of the other mode. These considerations were made more difficult by the size and weight of the Pegasus. Several different systems and configurations were considered in order to achieve the propulsion requirements.

I.2. Engine Selection

The largest factors in engine selection were power and number of engines. The Pegasus had to have sufficient power to take off, climb up to cruise altitude of 3000 m (9843 ft) and fly at the set cruise speed of 77.2 m/s (150 knots) at a power setting of 80 percent. From Figure I.2-1, a thrust to weight ratio of 0.3 was chosen.

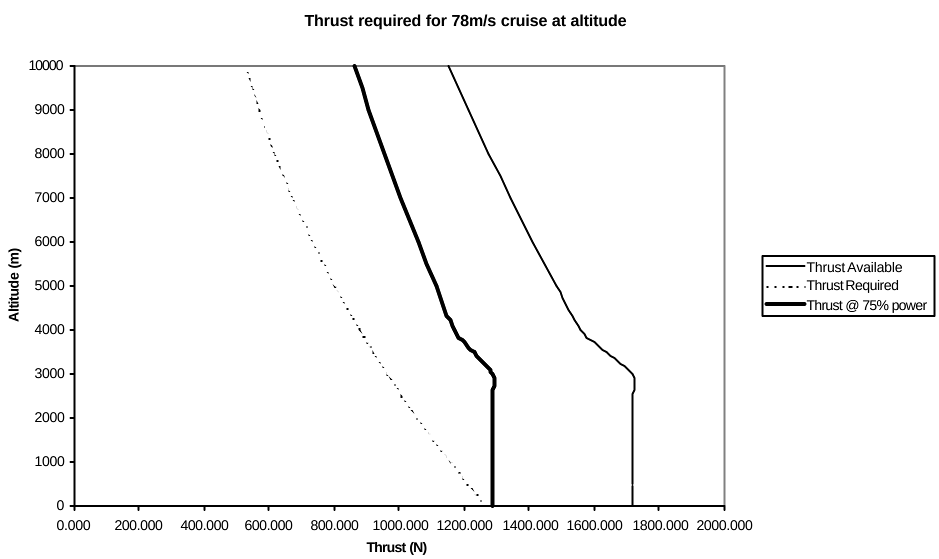

Figure I.2-1 Constraints Diagram

With a Maximum Take-Off Weight (MTOW) of 1500Kg the power that is required to meet these criteria is 155 kW (207 hp).

The number of engines to be used is a key factor in the design. If separate engines were to be used for road use and flight, significant weight would be added. If single engine was used, the problem of engine RPM arises. Aircraft engines are designed to run at a single RPM setting for a long period of time. A car engine is designed to run at a multitude of RPM settings as the automobile accelerates, with a fairly constant RPM while cruising.

Weight also played an important role in determining the engine. An engine powerful enough to propel the Pegasus could be found, but it may be too heavy to make it a feasible choice. By looking at aircraft in the same flying class (single-engine land) and the same market (lower/mid-range general aviation), a list of possible of possible engines was drawn up. The comparisons of weight and power of engines from existing aircraft and development models under consideration are in Table I.2-1.

Table I.2-1 Engine Comparison [1-6]

Engine Model	Current Aircraft Model	Power kW (Hp)	Weight kg (lb)
Continental IO-520	Beechcraft C-55	231 (310)	198 (436)
Lycoming IO-540	Cessna 182 Skylane	216 (290)	198 (437)
Subaru EJ-22	Conversion	119 (160)	134 (295)
Dyna-Cam	In Development	149 (200)	136 (300)
Wilksch	In Development	186 (250)	130 (287)

The engine selected for the Pegasus is the Wilksch 5-cylinder turbo diesel with intercooler. This engine is the choice because it produces the closest to the required power along with an outstanding thrust to weight ratio (0.3) and because of the type of fuel used. The large power as compared to the low weight is well in excess of that specified. The 186kW (250 hp) that the engine delivers exceeds the requirement of 155 kW (207 hp). Due to the turbocharger the engine is flat rated to an altitude of 3000m (9843 ft), this means that the engine power of 186kW (250 hp) is available from sea level up to cruise altitude. Some data on the engine is provided in table I.2-2.

Table I.2-2 Wilksch Diesel Specifications

Dimensions	Length	1050 mm
	Width	450 mm
	Height	640 mm
	Mass	130 kg
Performance	Max Power	186 kW
	Cruise Power (80%)	149 kW
	RPM at Max Power	2700 RPM
	Torque @ Max Power	660 N-m
	Specific Fuel Consumption	270 g/kW*hr

The Wilksch diesel is able to run on diesel and jet fuel. This provides convenience for both aircraft and automotive uses. Most gas stations provide diesel fuel and "in many parts of the world AVTUR (JETA1) is already much more readily available than Avgas."[1] It should be noted that a gas turbine was also considered for this reason, however these currently are not available in the appropriate range. The increased expense associated with turbine engines is also a negative feature.

I.3. Drive Train

A particularly interesting problem was first deciding on the type of propulsion system that would best suit our needs as well as be appealing to the customer. An early possibility that was examined was to use a dual-engine combination, one for road use and a separate powerplant for flight. This combination was quickly discarded in favor of a single engine, due to both weight issues and fuel efficiency. Because of the fact that this craft's design is based on a plane that can be driven on occasion not for daily commuting, it was decided to use an aircraft engine that employs a modified transmission system for road use. The aforementioned system, called a continuously variable transmission (CVT), allows the craft, in automobile mode, to be accelerated by altering the amount of power produced by the engine. The main benefit of the use of the CVT is that it permits the aircraft-based powerplant to be operated at constant speed, thus avoiding the stops and starts of typical driving that would most definitely shorten its lifespan.

Unlike most transmissions found in today's automobiles, the CVT is belt driven, this allows for smooth power transfer through an infinite number of drive ratios. The CVT system works by transferring power by means of a specialized steel belt across two variable size pulleys, an example is shown in Figure I.3-1.

Figure I.3-1 Audi Multitronic CVT[8]

The main control module adjusts the final drive ratio according to information on changes in throttle position, ground speed, and engine RPM provided to it by various sensors. The selected CVT is the Audi Multitronic CVT. This is chosen because it uses a specially designed plate link chain to connect the two pulleys. This chain can withstand a torque of 30.6 m-kg (221 lb-ft). This transmission is approximately the same size and weight as typical automobile automatic transmissions. These dimensions are approximately 99.8 kg (220 lbs), 400 mm (15.7 in) in length and 250 mm (9.8 in) in width. The weight includes transmission fluid. The Audi Multitronic also performs 0.1 s better in acceleration from 0 to 100 km/h (62 mph) than a 5-speed automatic on an Audi A6 2.8. It also has 0.1 L/100 km (4.25 gal/mile) better fuel consumption than a manual transmission[8] on the same vehicle. This CVT also incorporates the differential into the transmission housing.

A gearing system is connected to the powertrain in between the engine and the CVT. The main function of this system is to split the power between the propeller and the drivetrain leading to the wheels. Internal to this system is what is called a dog clutch, controlled by the driver, which allows for switching of the power between the propeller shaft and the drivetrain. The clutch will be activated from within the cabin, and will most likely take place on the runway just prior to takeoff or just after landing. The system used for this will be two gears. One gear will be connected to the output shaft of the engine. This shaft will then run to a dog clutch and the propeller. The gear turns a mating gear that will rotate the automobile output shaft. This shaft will also run to a dog clutch and then to the CVT. When one dog clutch is engaged the other will be in neutral. This will allow for only one driving mechanism to be active at one time.

The downward shaft is integrated into the wheel suspension arms. These shafts run down to the wheels at which point they translate through another 90 degrees (using bevel gears) to drive the wheels. This system is shown in Figure I.3-2.

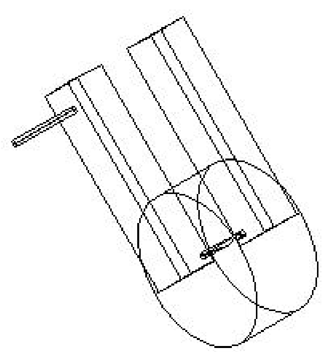

Figure I.3-2 Rear Wheel Drive System

I.4. Propeller Selection

The propeller used must have optimum performance in takeoff, climb and cruise. Because of the less than perfect performance characteristics and the slightly excessive weight of the Pegasus, a special propeller will be designed. The design method was Leonard Newnham's web based propeller design program[9]. This program allows the user to input the engine power, engine speed, aircraft speed, number of propeller blades, angle of attack of propeller, and propeller diameter, then returns the necessary information for the optimum propeller design. The Wilksch diesel engine outputs 186.4 kW (250 hp) at 2700 RPMs. Pegasus's cruise speed is 77.2 m/s (150 knots). The propeller diameter is selected to be at 2 meters (6.56 ft) to give the optimal disc loading. Three blades are selected for the propeller because of the advantages in aesthetics and noise reduction. A three bladed propeller can be run at slower speeds thereby reducing the noise. The propeller angle of attack is optimized in the program by varying the value through a specified range. After these data are input into the program, the designed propeller is output. Manufacture of this propeller can be outsourced to a number of companies specializing in making propellers. The dimensions of length and angle of twist for the selected design are as given in Figure I.4-1 where the height of the squares containing AOA information are 50mm and everything else is scaled off of that.

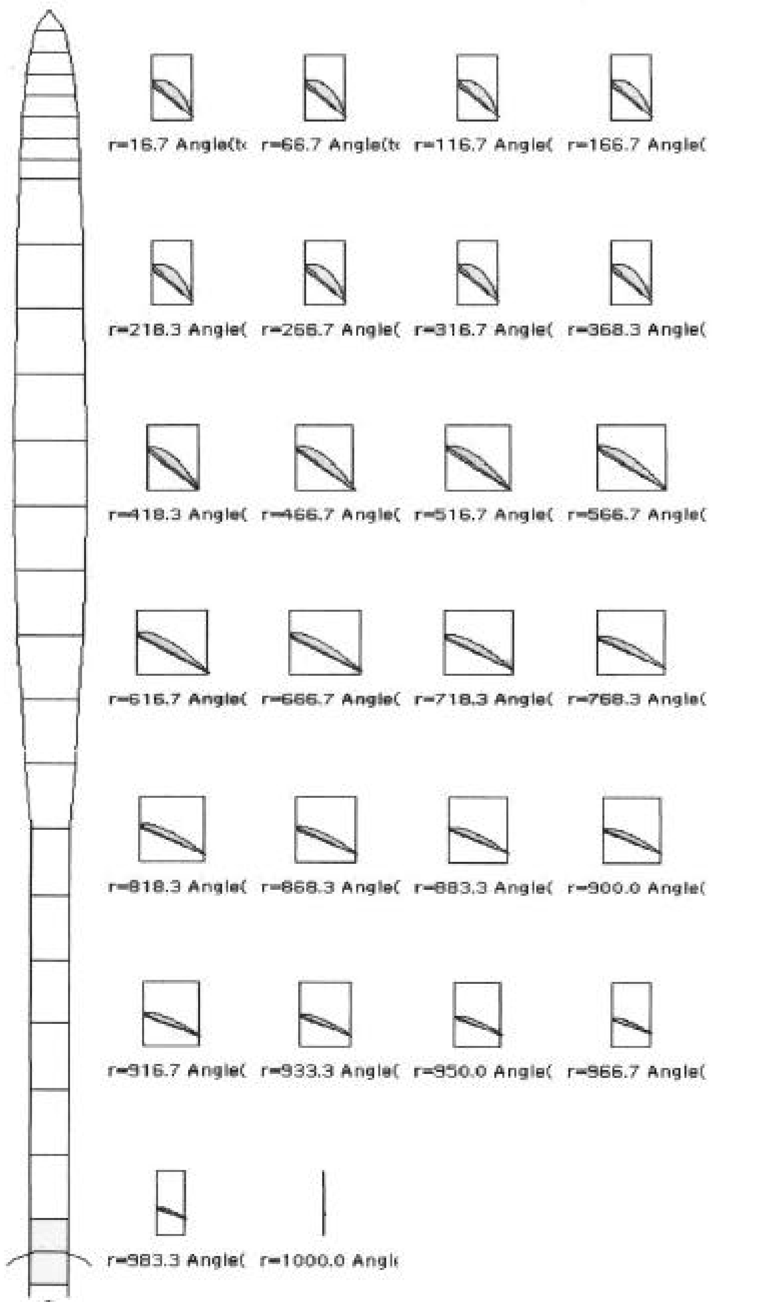

Figure I.4-1 propeller dimensions

I.5. Fuel System

The fuel system will be very simple for the Pegasus. The Wilksch Airmotive diesel engine has a built in fuel pump on it. Fuel lines will be run from the 80-gallon fuel tank in the front of the inboard wings to this pump. This is necessary because the engine is above the fuels tanks and needs to be forced upwards. A fuel drain valve is placed on the side of the Pegasus so that the fuel can be checked for purity. Some disadvantages include some added weight and more moving parts.

I.6. Engine Cooling

One major obstacle caused by the location of the engine in this craft was that of cooling. This problem was solved with the use of a standard cross-flow radiator cooled by means of an electric fan. Due to size constraints the size of the radiator was limited to approximately 0.14m^2 (1.5 ft^2), leaving only the fan's motor size to be determined. Using two basic assumptions the motor size was determined using a general heat transfer analysis. The first assumption set the average engine operating temperature at approximately 245°F. The second assumed a worst-case scenario of no added flow due to craft movement and an ambient temperature of approximately 100 °F. This worst-case assumption allows for reassurance that the craft's engine will be protected in case of prolonged nonmoving operation. The fan motor size was determined using the following equation:

$$W = Q = hA(T_s - T_\infty) \qquad \text{(Eq. H.6.1)}$$

Where **W** represents the amount of power needed to compensate for **Q** amount of heat energy created by the engine. The variable **h** is the convection constant and is determined by the type of radiator and the cooling fluid being used, being water in this case. T_s represents the average surface temperature and T_∞ represents the ambient air temperature. Using the given data along with the aforementioned assumptions it was determined that the minimum amount of fan power required was 280 W (.38 hp). Allowing for a factor of safety, and accounting for assumptions made, it was determined that a 373 W (.5hp) motor would be more than adequate to cool this craft's engine even under the most adverse of conditions.

1) www.wilksch.com

2) www.cessna.com

3) www.dynacam.com

4) www.subaru.cy.net

5) www.tcmlink.com

6) www.lycoming.textron.com

8) www.audi.com

9) http://helios.bre.co.uk/ccit/people/newnhaml/prop/

Appendix J. Aerodynamics

J.1. Introduction

The design of a roadable aircraft presented some unique aerodynamic problems. The lifting surfaces had to be large enough to produce the required lift in the air yet small enough to drive safely and not produce lift on the road. To find a solution to these issues, aerodynamic configurations not often used in the general aviation industry were examined. The solution included using extending lifting surfaces. The design uses a low aspect ratio inboard wing with telescoping outboard wings. Several other uncommon features for increasing lift without increasing wing span were investigated including a Burnelli lifting body, the channel wing, and winglets.

The classic Burnelli lifting body was adapted to a lifting fuselage on a low aspect ratio wing. This provides high lift with a small span. The channel wing was also adapted to fit the needs of the vehicle. In this design, the propeller is at the rear of the low aspect ratio inner wing with endplates and the vertical tails at either side of this wing creating a channel. The propeller pulls high speed air flow over the upper surface of the wing, giving increased lift. The vertical tails of the design start at the middle of the inboard wing and are angled slightly inwards with respect to the fuselage. As such, they act as winglets, increasing the lift to drag ratio of this inboard wing by 15%, according to Raymer[1].

Another design problem experienced was rotation for takeoff. In order to rotate for takeoff, the rear wheels would have to be located just behind the center of gravity, preferably within 15 degrees off of the vertical. However, this would result in an unstable vehicle when operating as a car. It was decided that the rear wheels be placed well behind the center of gravity, as in a conventional automobile, making normal takeoff rotation nearly impossible. To compensate for this, two main options were explored: a high lift airfoil could be used to take off without rotation or rotation could be attained by extending the height of the front wheel suspension.

The fuselage was situated on the main, low aspect ratio wing with the aerodynamic center of the wing behind the center of gravity location of the aircraft. This resulted in a nose down pitching moment for the design. To compensate, a large horizontal tail was introduced.

J.2. Lifting Surface Arrangement

Based on the desired performance parameters established for the design, the wing sizes and airfoil shapes were selected. FAR 23.201 specifies the stall speed not to exceed 31.39 m/s (61 kts) without flaps. Some initial calculations showed for a theoretical C_{Lmax} of 1.5 and a stall speed of 31.39 m/s (61 kts), the total wing area required was 16.2 m^2 (174.4 ft^2). To fit in a lane on the road, the maximum span of the inboard wing was chosen to be 2.28 m (7.48 ft). A chord of 2.5 meters (8.202 ft) was selected for this inner wing, resulting in an area of 5.7 m^2 (61.35 ft^2). The quarter chord of the telescoping outboard wings were placed at the same point as the inboard wing quarter chord. The telescoping wings had a total semi span of 3 meters (9.84 ft), divided into four sections of 0.75 m (2.46 ft) with a chord of 1.75 m (5.74 ft). These sections total 10.5 m^2 (113.02 ft^2) in area, giving a total of 16.2 m^2 (174.4 ft^2) of wing. A diagram of the wing can be seen in figure J.2-1. The size of the telescoping sections were chosen so that they could contract into the inner wing. The required size for the horizontal tail was 1.63 m^2 (17.55 ft^2), which required a moment arm of 4 m (13.12 ft).

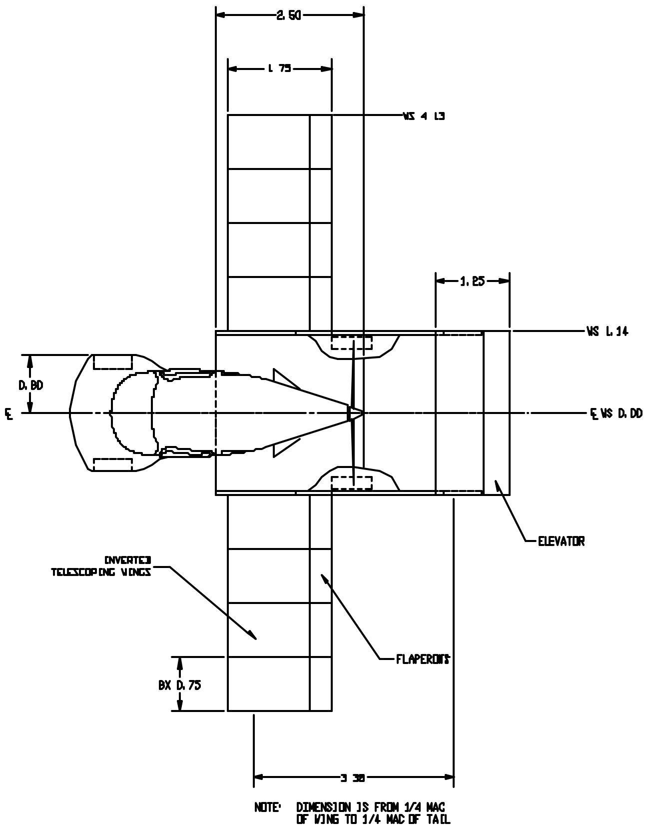

Figure J.2-1 Wing Arrrrangement (in meters)

J.3. Airfoil Selection

Once the initial configuration was selected, airfoils had to be chosen. For the inboard and outboard wing airfoils, several criteria were established. A Reynold's number of 6.0×10^6 was selected for comparing the various airfoils in <u>Theory of Wing Sections</u> by Abbot and von Doenhoff. A high angle of attack, α, for stall was a requirement so that stall would not be likely. For predictable behavior after stall, smooth C_l vs. α behavior was required at stall. For low stall speed, a high C_{Lmax} was desired. A high lift to drag ratio was chosen as a requirement to reduce drag. Along with a large drag bucket, the high lift to drag ratio would ensure better aerodynamic efficiency.

Specific requirements were set for the inboard and outboard sections of the wing. The inboard section was to have high lift at zero angle of attack to be able to takeoff without rotation. A flat bottom was required on the inboard section airfoil so as not to produce ground effect suction, and thereby negative lift, on takeoff runs. For the outboard section, an efficient wing was desired. The following airfoil sections were investigated for the above criteria:

- NACA 2412
- NACA 4412
- NACA 63_1-412
- NACA 63_2-415
- NACA 65_2-215
- NASA GA(W)-1 (LS 0417)
- NASA GA(W)-2 (LS 0413)

Initially, the NACA 4412 and the NASA GA(W)-1 (LS 0417) were selected for the inboard and outboard sections of the wing, respectively. The 4412 met the above requirements and had a flat bottom. The GA(W)-1 was an efficient high lift airfoil which fit the requirements for the outboard section. This outboard wing was set at an incidence angle of 2 degrees to generate greater lift without rotation during takeoff. This solution to the takeoff rotation issue had some problems. First, taking off without rotation would require a long takeoff ground run. Second, setting the outboard wings at 2 degrees incidence caused them to stall early.

Instead of taking off without rotation, it was decided to takeoff with artificial rotation. The front gear would extend to raise the vehicle nose, setting the wings at 8^o, their takeoff angle. This allowed for the use of a more efficient, higher lift airfoil as it no longer had to have a flat bottom.

The airfoil section that was selected for both the inboard and outboard sections is the NASA GA(W)-1 otherwise designated as NASA LS(1)-0417. Figure J.3-1 shows the GA(W)-1 airfoil. This is a seventeen percent thick airfoil with a design lift coefficient of 0.4, and has been designed for general aviation applications. Some of the main features of the airfoil (taken from a NASA technical note[3]) are listed below:

- The airfoil has a good lift to drag ratio (around 90, for M=0.15) at a lift coefficient of 1 for improved climb performance.
- The airfoil has a large upper surface leading edge radius of about 0.06c. This attenuates peak negative coefficient of pressure values and hence delays stall of the section to high angles of incidence.
- The airfoil is contoured to provide uniform chordwise loading for a lift coefficient of 0.4. Aft loading is increased by the use of aft camber greater than that found on the NASA 6-series of airfoils.
- The blunt trailing edge provided with approximately equal upper and lower surface slopes moderates upper surface pressure recovery and hence postpones stall to high angles of incidence.
- The airfoil section experiences a gradual stall, of a turbulent trailing edge type.

Figures J.3-2 and J.3-3 show the two dimensional aerodynamic properties of the airfoil. The GA(W)-1 produced more lift and less drag than the NACA 4412 at the same Reynolds number and angle of attack. At a cruise speed of 77.2 m/s (150 kts), the ideal angle of attack for the GA(W)-1 is 0.06 degrees. Therefore, the inboard wing was mounted on the fuselage at 0.06 degrees, so that the fuselage would remain level in cruise at altitude. The telescoping sections were mounted at the same angle of attack as the inboard section. The inboard section of the telescoping wings should stall before the outboard sections due to interference from the main wing. This ensures aileron effectiveness at stall. To improve lateral stability, the telescoping wing sections were set at a dihedral angle of 5 degrees.

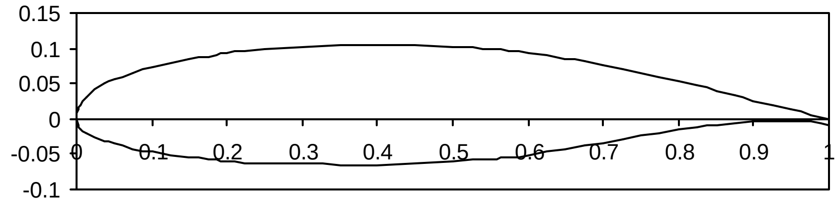

Figure J.3-1 GA(W)-1 airfoil

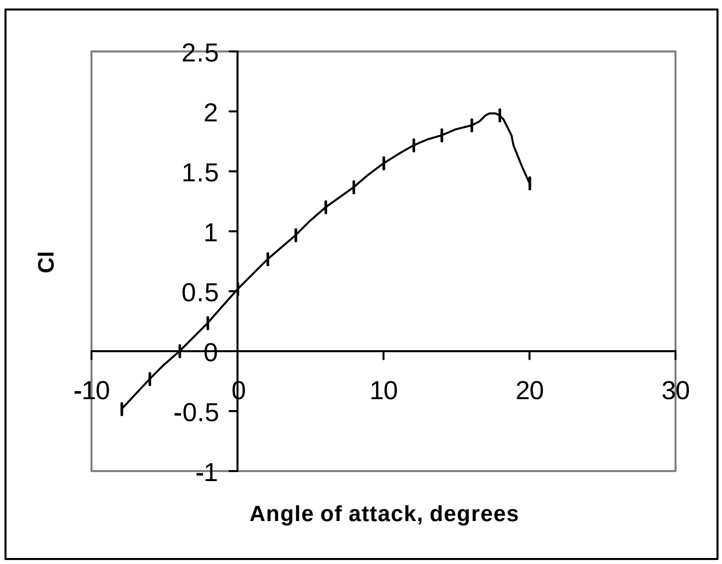

Figure J.3-2 2-D Cl vs. alpha for GA(W)-1 airfoil section

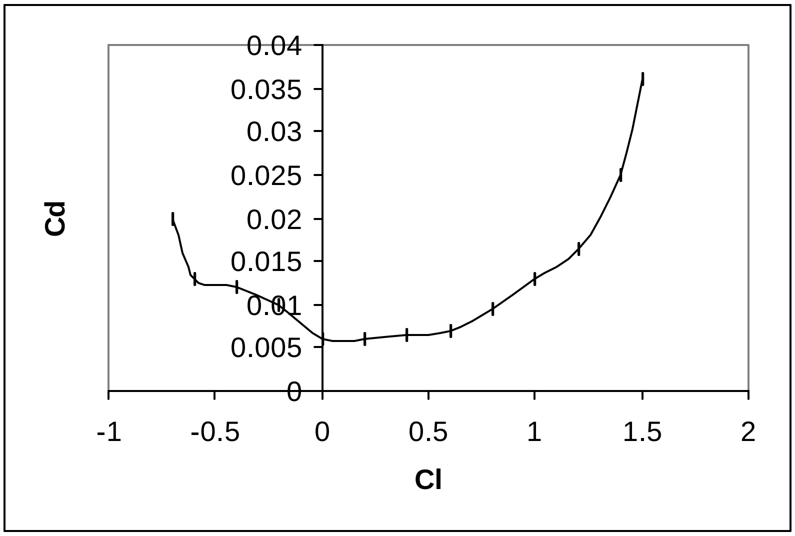

Figure J.3-3 2-D Drag Polar[2]

The GA(W)-1 airfoil caused a nose down pitching moment, which further worsened the initial nose down pitching moment of the design. The moment arm of the horizontal tail was limited by the automobile's parameters, so other options had to be explored to solve the pitching moment problem. Some of the configurations analyzed were adding a canard, having a fold-out horizontal tail, a telescoping horizontal tail boom, and extending the tail moment arm. For simplicity and weight, it was decided to extend the design's overall length to 7.4 m (24.3 ft). This configuration compromises the size of the car on the road, but proves beneficial in the air.

For the horizontal tail, a symmetrical airfoil was desired. A NACA 0012 was chosen for the horizontal tail. Due to the incidence angle of the vertical tails being used as winglets, the maximum span of the horizontal tail is 2.24 m (7.35 ft). The chord of the tail was calculated to be 1.25 m (4.10 ft). For the vertical tails, their use as winglets had to be considered in selecting an airfoil section. The optimum thickness to chord ratio for a winglet is 8% according to Raymer[1], so a NACA 0008 airfoil was selected for use in the vertical tail. Table J.3-1 shows a summary of the lifting surfaces selected.

Table J.3-1 Lifting Surfaces

surface	span (m)	chord (m)	airfoil
inboard wing	2.28	2.50	NASA GA(W)-1
outboard wing	6.00	1.75	NASA GA(W)-1
horizontal tail	2.24	1.25	NACA 0012
vertical tail	1.80	0.906	NACA 0008

J.4. Channel Wing

The overall effect of the placement of the propeller above the low aspect wing is to promote attached flow in even the most extreme angles of attack. However, the propeller does contribute a lift constituent in the same fashion as the channel wing introduced by Custer[4]. Because the wing in the [vehicle name] is not a channel but a flat-based scoop, the aerodynamic configuration has been dubbed the scoop wing.

The scoop wing's contribution to the vehicle performance was analyzed using the actuator disk model of propellers, as demonstrated in Yates[BBB]. In this model, the propeller induces a step increase in the static pressure of the fluid at the propeller plane, while the velocity increases gradually from asymptotes in the free stream fore and aft of the propeller plane. This model is shown in Figure J.4-1.

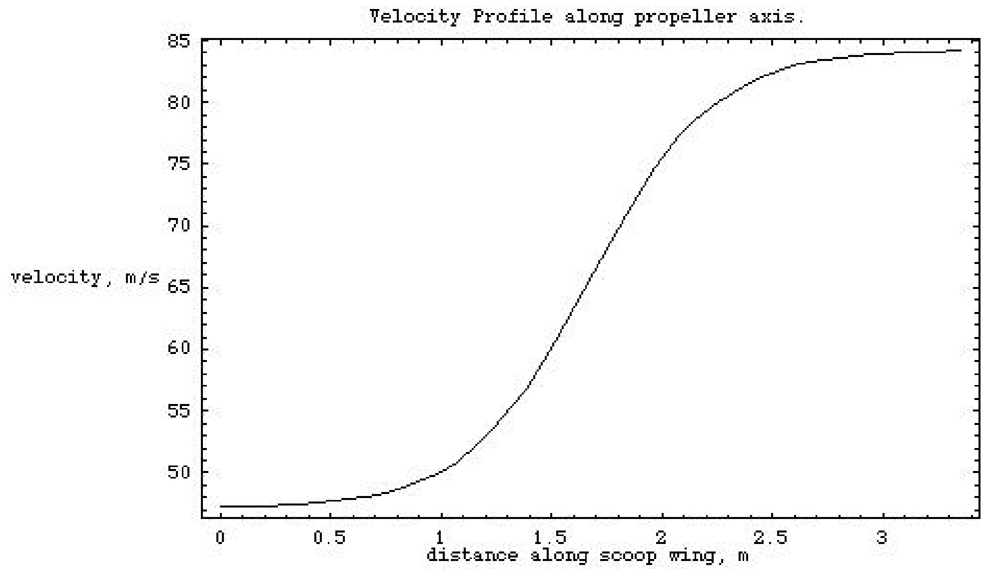

Figure J.4-1 The velocity profile according to the actuator disk model. Propeller plane is at the mid-point (x=1.675m).

The asymptotic values of the velocity fore and aft of the propeller, u_1 and u_2 are related to the thrust through the following relations: At cruise, the thrust and drag are equal and opposite. Solving the relation for the free stream velocity, we find

$$u_1 = \sqrt{\frac{2 \times Thrust}{C_D \, \boldsymbol{r} S}} \qquad (1)$$

where C_D is the drag coefficient for the entire aircraft, $\boldsymbol{r}$ is the density, and S is the wing planform area. The velocity far behind the wing is given directly by the actuator disk model as

$$u_2 = \sqrt{\frac{2 \times Thrust}{\boldsymbol{r} \times A}} \qquad (2)$$

where A is the propeller disk area, and $\boldsymbol{r}$ is the density of the flow.

A hyperbolic tangent curve was fit to the two asymptotes to generate the 3-D profile, with a propeller at 50% chord, is shown in Figure J.4-2.

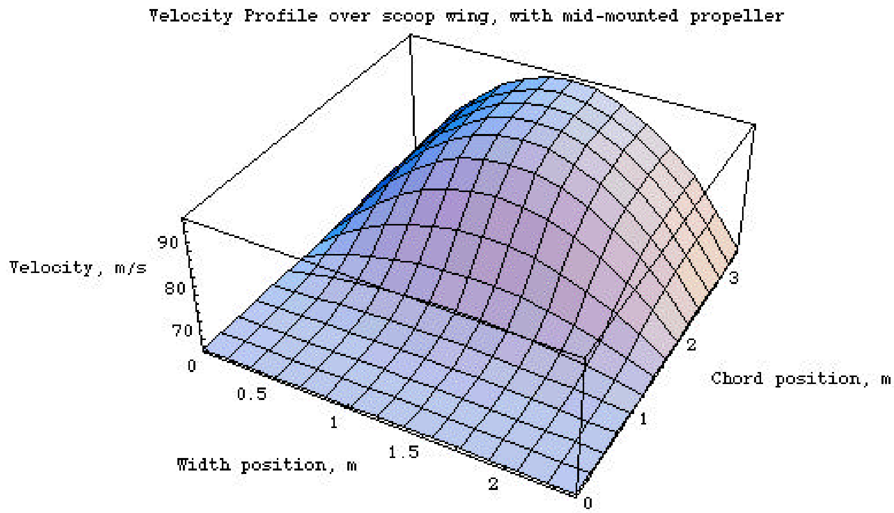

Figure J.4-2 The velocity model on the low aspect ratio wing for a mid-mounted propeller.

From a form of Bernoulli's equation, the pressure coefficient profile corresponding to the velocity profile can be found. The pressure coefficient distribution on the wing for a mid-mounted propeller is shown in Figure J.4-3.

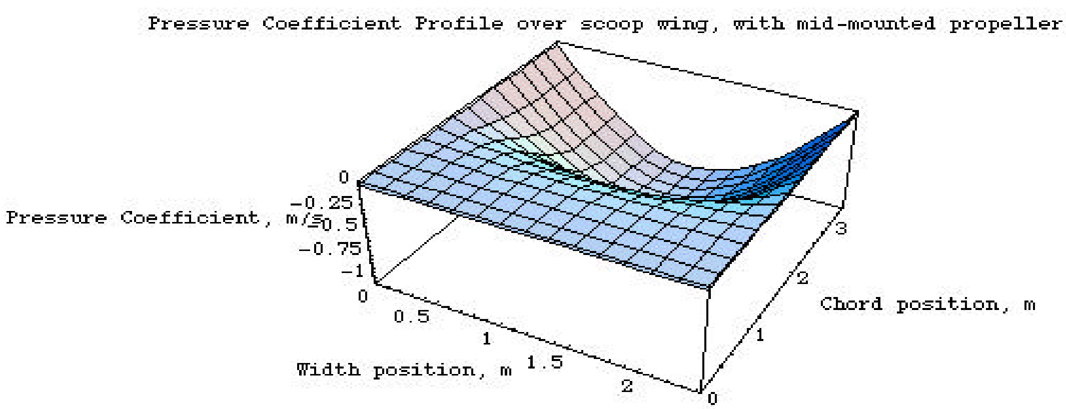

Figure J.4-3 The pressure coefficient distribution over the low aspect ratio wing.

These pressure coefficients could be integrated to find a lift coefficient and ultimately, a lift produced by a certain engine thrust and propeller placement. The lift was calculated for all reasonable propeller placements and an assortment of thrusts. This lift graph is shown in Figure J.4-4.

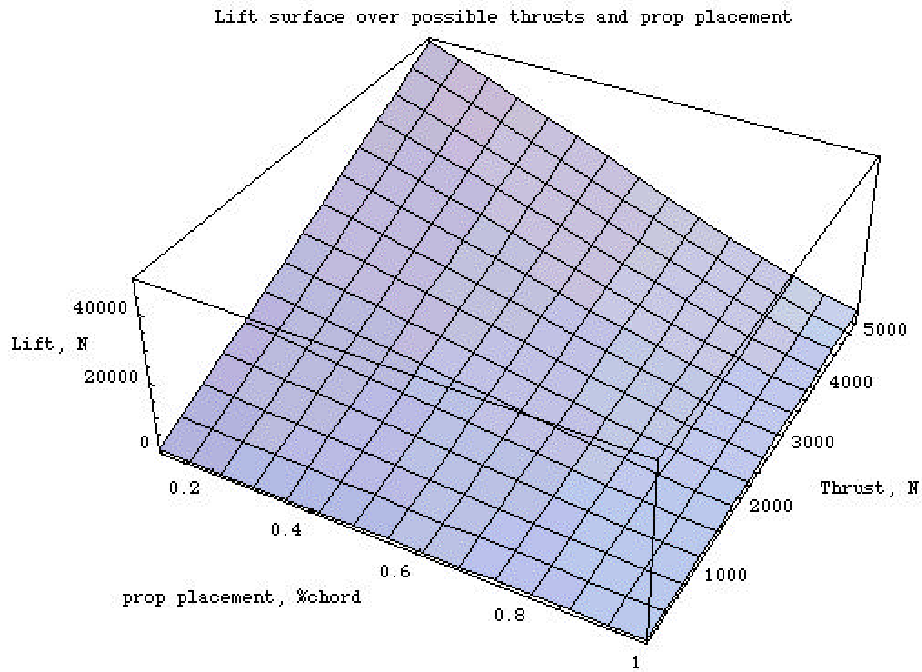

Figure J.4-4 The lift corresponding to all propeller placements and thrusts.

To apply this analysis to the design of the Pegasus, the low aspect ratio wing's geometry must be defined as well as the thrust and the placement of the propeller. For our configuration, with the propeller at 85% of the chord behind the leading edge, the propeller induced lift is 2321 N.

J.5. Winglets

The two endplate positions and sizes were originally determined according to the required control power in the rudders. Two other advantageous phenomena were identified with this configuration:

The two vertical plates could augment the aerodynamic performance of the low aspect ratio wing. By blocking spanwise flow, the plates could preserve the lift coefficient of the interior wing beyond that possible in an ‘unfenced wing’ of similar aspect ratio.

The two endplates could function as Whitcomb winglets, boosting the wing’s lift to drag ratio by 10-15%.

The second possibility was investigated to compare the potential performance gains with the required configuration modifications to convert the plates to winglets.

An analytical model based on the vortex generated by the junction of two semi-infinite wings of different chords was developed. Like our configuration, both semi-infinite wings have the same section lift coefficient, C_l. The analytical representation of our wings is demonstrated in Figure J.5-1. At the junction, a vortex is generated as a result of the two differently sized semi-infinite vortices about the two wings. This ‘delta-vortex’ branches from the junction and extends (theoretically) forever. A winglet takes advantage of this vortex to generate a thrust. However, the winglet’s shape must be optimized so that the drag of the winglet is not greater than the winglet-produced thrust.

In optimizing the winglet’s geometry, it is first necessary to quantify the circulation resulting from the discontinuity at the junction. Bertin and Smith[5] state that the 2-D lift, *l*, and circulation, *G*, of an inviscid continuous flow are related by

$$l = rV_\infty \Gamma \qquad (1)$$

where V_∞ is the free stream velocity. The 2-D lift of a wing such as the one in our model can be expressed as the following [5]:

$$l = C_l \frac{1}{2} r V_\infty^2 c \ . \qquad (2)$$

The wing chord is given by c and the density is given by ρ. Combining equations 1 and 2, we can find the circulation strength of the vortex generated by a change in chord Δc:

$$\Delta\Gamma = \frac{1}{2} C_l V_\infty \times \Delta c \,. \qquad (3)$$

This vortex induces a spanwise velocity above (and below) the wing in the direction of the wing with the larger chord. The vortex induced velocity is given by

$$V_\Gamma = \frac{\Gamma}{2\pi r} \,. \qquad (4)$$

The distance above the wing plane is denoted by r. Therefore at any station r above the wing, the velocity field is completely defined as shown in the box in Figure J.5-1:

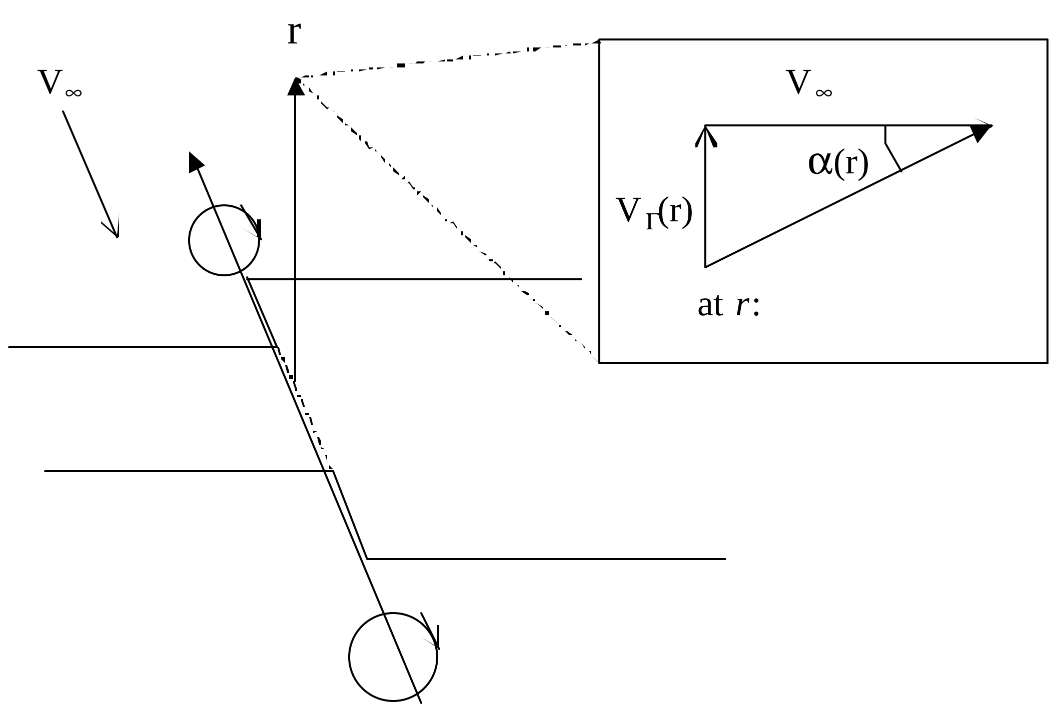

Figure J.5-1 The analytical model of the main wings of the Pegasus.

$$V_{total}(r) = \sqrt{V_\infty^2 + \left(\frac{\Gamma}{2\pi r}\right)^2} \qquad (5)$$

$$\alpha(r) = Tan^{-1}\left(\frac{\Gamma}{2\pi r V_{\infty}}\right) \qquad (6)$$

The angle between the local flow and the free stream is denoted by α. The chord distribution as a function of *r* was also defined. For analysis and manufacturing ease, a symmetric airfoil was assumed. At any station *r* the situation depicted in Figure J.5-2 is exposed. Another angle is defined, *an*. This is the angle between the local velocity vector and the airfoil. With a fixed chord distribution, this distribution of this angle can be optimized for maximum overall thrust.

To define this thrust as a function of *an* was therefore of primary interest. The ‘section thrust’ at each station was found by the following relation, which proceeds from Figure J.5-2:

$$t(r) = l(r)\sin(\alpha(r)) - d(r)\cos(\alpha(r)). \qquad (7)$$

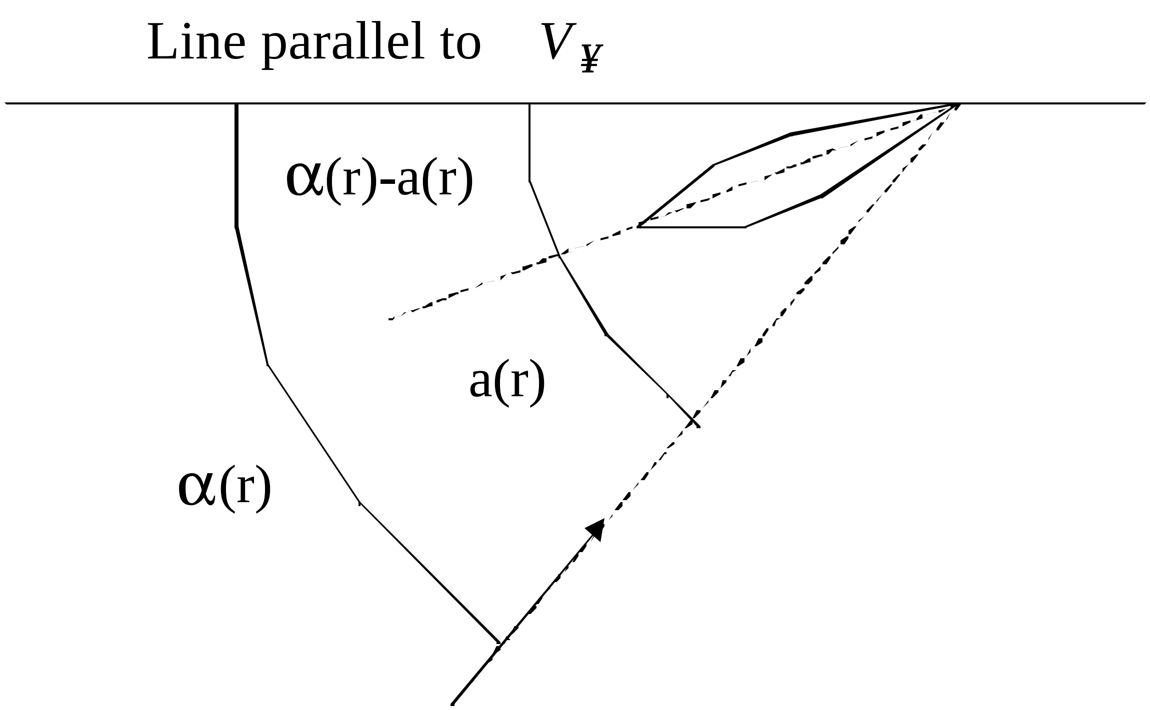

Figure J.5-2 The velocity, pertinent angles and the winglet cross-section at an arbitrary station.

Section lift and drag are denoted by l and d respectively. The section lift was found through typical 2D airfoil theory [5]:

$$l(r) = \frac{1}{2}\rho V_{total}(r)^2 c(r) \times [2\pi(an(r))]. \qquad (8)$$

Section drag was found using a conventional drag polar. The zero-lift drag was ignored in the analysis because the endplate dimensions are fixed. However, the lift-induced drag was closely examined, such that its detraction from the thrust was not catastrophic. In fact, in optimizing the thrust we did not necessarily minimize the drag, nor maximize the lift. Their interaction in the form of equation 7 was optimized. This said, the section drag at each station is given by [5]

$$d(r) = \frac{1}{AR \times e}\left[\frac{2l(r)}{\rho V_{total}(r)^2 c(r)}\right]^2. \qquad (9)$$

The aspect ratio, AR, is that of the winglet. The Oswald efficiency factor, e, is taken to equal 0.9. Equations 7, 8 and 9 can now be integrated over the entire winglet to find the optimal winglet angle of attack at each station. This information could then be used to find the best winglet twist, given by

$$\alpha(r) - an(r). \qquad (10)$$

Because the chord distribution in r is a piecewise defined function, the optimization had to be done numerically, which generated a grid of points rather than a function. The graph of the results of this optimization is given in Figure J.5-3. Subtracting this angle from the local induced angle of attack exposes the best physical twist of the winglet – this distribution is shown in Figure J.5-4.

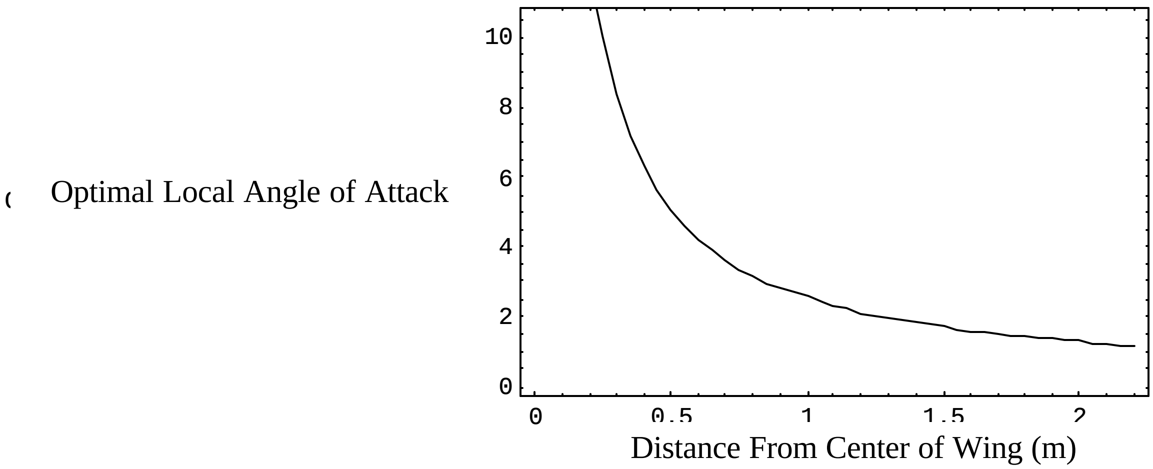

Figure J.5-3 The optimized local angle of attack of the winglet at all stations.

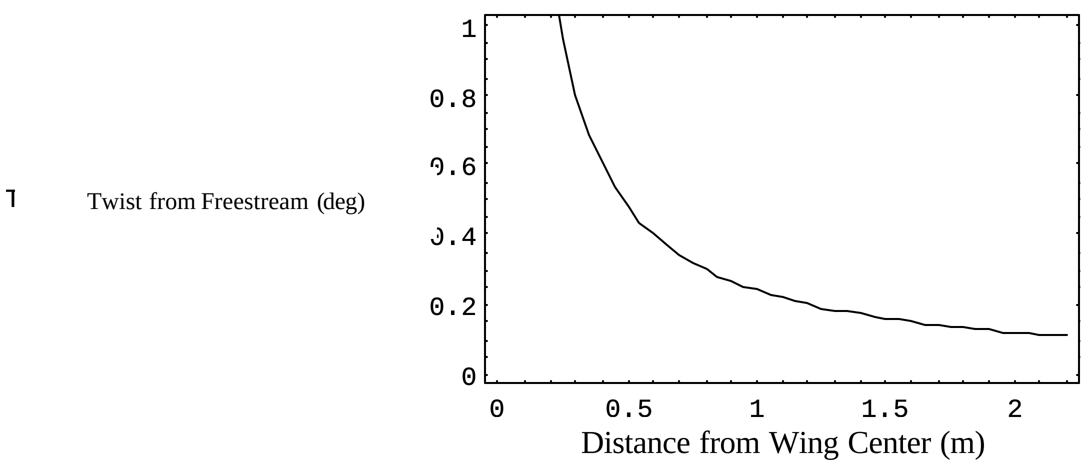

Figure J.5-4 The optimal twist of the winglet relative to the free stream.

The most curious fact about the winglet twist distribution is that the twist is so shallow compared to conventional winglet designs. Typically, a winglet has a base twist of 4 to 5 degrees. However, our ‘winglets’ are much larger, with lower aspect ratios (0.55). The endplates on the Pegasus are more sensitive to over-twist than industrial winglets. If we increase the twist, the thrust decreases and at a certain twist, our thrust becomes a drag.

Integrating equation 7 with the optimized twist distribution we found the maximum thrust possible from each of our winglets at cruise conditions: 41.01 N (9.31794 lbs).
Thus the entire winglet configuration generates 82.02 N of thrust.

The Pegasus without optimized winglets had a *L/D* of 9.8. If we assume that the lift and weight are equal at cruise, than this thrust corresponds to a 5.5% increase in the *L/D* ratio.

J.6. Lift

Two Dimensional Airfoil Section Characteristics

The two dimensional data for the airfoil section used, the NASA GA(W)-1, has been taken from charts of airfoil lift coefficient against airfoil angle of incidence for different Mach numbers and different Reynolds numbers. The maximum lift coefficient and the lift curve slope was found for three different flight conditions, cruise, take off / landing and stall.

The charts used for the calculation of the two-dimensional characteristics were taken from a NASA technical note[6]. The charts that were used and the readings that were taken from them depended upon the Mach number and the Reynolds number at the particular flight condition being looked at. The flight conditions looked at were at altitudes of 0 and 3000m. The speed of sound is given by:

$$a = \sqrt{gRt} \qquad (1)$$

Where,

ã = 1.4

R = Gas constant = 287 J/kg•K

t = Static temperature (288.2 K at sea level, 268.7 K at 3000m)

Thus the speeds of sound at sea level and at an altitude of 3000m are 340.3 m/s and 328.6 m/s respectively.

Reynolds Number is given by:

$$R_e = \frac{V\bar{c}}{\boldsymbol{n}} \qquad (2)$$

Where,

V = Velocity

$\bar{c}$ = Mean Aerodynamic Chord

õ = Kinematic Viscosity (1.461×10^{-5} m^2/s at seal level and 1.863×10^{-5} m^2/s at 3000m)

The mean aerodynamic chord was based upon area and is calculated as follows:

$$\bar{c} = \frac{(c_1 S_1 + c_2 S_2)}{S} \qquad (3)$$

Where,

c_1 = Chord of outboard wing. (1.75m)

c_2 = Chord of inboard wing. (2.5m)

S_1 = Area of outboard wing. (10.5m^2)

S_2 = Area of inboard wing. ($5.7m^2$)

S = Total wing area. ($16.2m^2$)

Thus the mean aerodynamic chord is 2.014m

There are three flight conditions that have been looked at, these are:

Stall Speed:

The stall speed for the aircraft was specified to be 55 knots (28.3m/s) at sea level. The stall speed Mach number is therefore 0.082 and the Reynolds number is 3.86×10^6.

Take Off and Landing:

Take off speed is 1.2 times the stall speed and landing speed is 1.3 times the stall speed, giving 33.6m/s and 36.4m/s respectively. Thus the take off and landing Mach numbers are 0.099 and 0.107 respectively. The Reynolds numbers for the take off condition is 4.63×10^6, and for the landing condition is 5.02×10^6.

Cruise:

The cruise speed was specified as 150 knots (77m/s) at a cruise altitude of 3000m. Hence the cruise Mach number is 0.234. Cruise Reynolds number is 8.32×10^6.

The charts of lift coefficient against angle of incidence available (NASA[6]) are for M=0.1, M=0.15, M=0.2, M=0.28. So for the cruise condition the chart for M=0.2 will be used. For all other conditions the chart for M=0.1 will be used.

Take off, landing and stall.

Figure J.6-1 shows the coefficient of lift plotted against angle of incidence for M=0.1 and for a Reynolds number of 3.7×10^6. This is fine for the stall condition, but the Reynolds numbers for the other flight conditions are slightly higher. As can be seen from figure J.6-2 higher Reynolds numbers increase the maximum lift coefficient, but the lift curve slope (gradient) stays roughly constant at the lower incidences. So higher values of maximum lift coefficient will have to be estimated for the take off and landing flight cases.

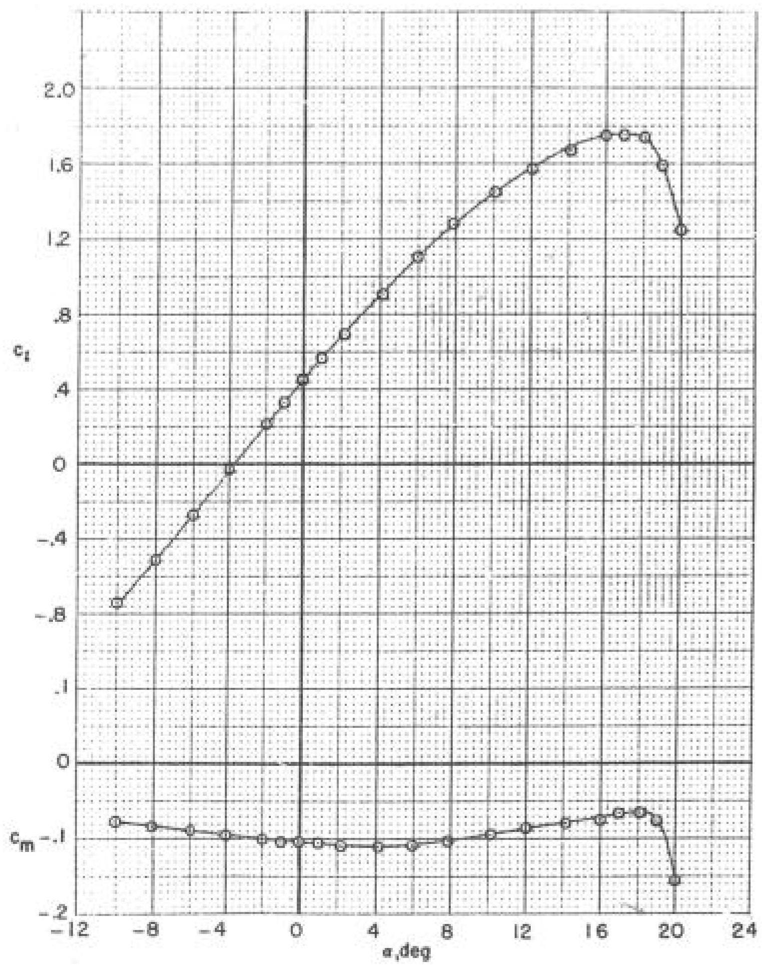

Figure J.6-1 2-D lift curve slope for stall, take off / landing[6]

The gradient of the graph gives the airfoil lift curve slope, this gradient was taken at approximately 0° of incidence.

Cruise condition.

The following chart, figure J.6-2, shows lift coefficient plotted against angle of incidence for M=0.2 at various Reynolds numbers.

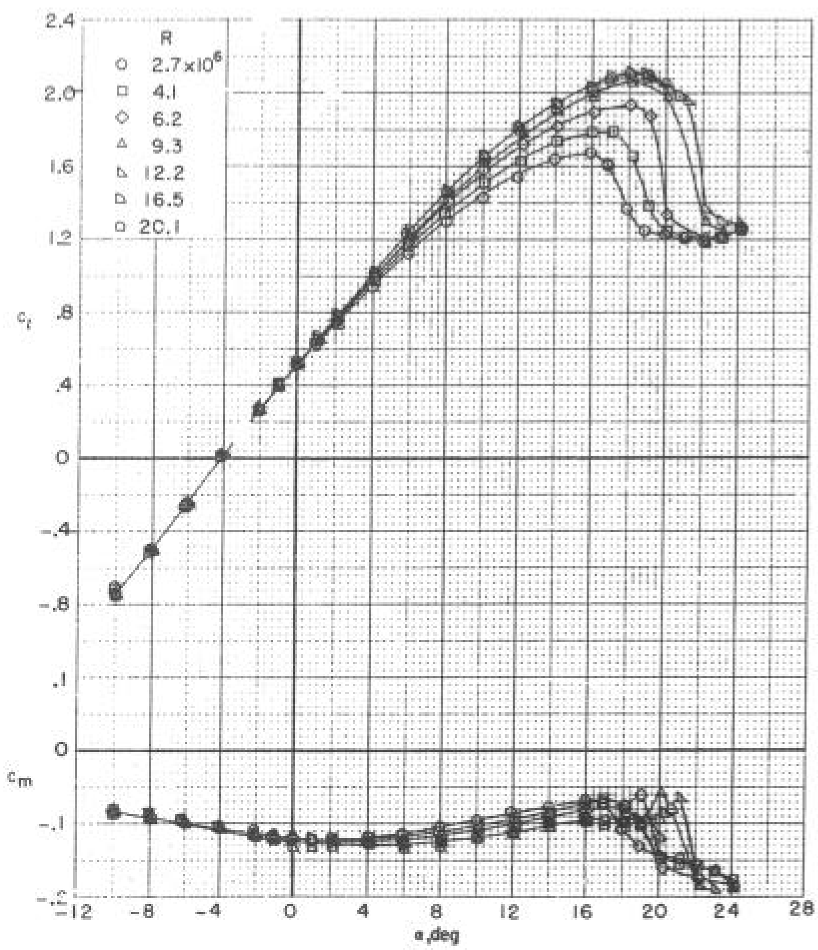

Figure J.6-2 2-D lift curve slope for cruise[6]

From this chart the lift curve slope (gradient) for a Reynolds number of 8.32×10^6 was found to be 7.0 rad^{-1}. The maximum lift coefficient was found to be 2.02. These two-dimensional airfoil characteristics are summarized in table J.6-1 below:

Table J.6-1 2-D airfoil characteristics

Flight Case	Max 2-D lift coefficient (C_{lmax})
Cruise	2.02
Take off / Landing	1.95
Stall Speed	1.75

Three Dimensional Wing Characteristics

The 3-D lift curve slope and maximum lift coefficient for the wing with no high lift devices can now be looked at. Again the same three flight conditions were looked at.
The following equation by Raymer[1] was used to give the three-dimensional (3-D) lift curve slopes:

$$\frac{dC_L}{d\alpha} = \frac{2\pi A_e}{2 + \left[4 + \frac{A_e^2\beta^2}{\eta^2}\left(1 + \frac{\tan^2\Lambda_t}{\beta^2}\right)\right]^{1/2}} \frac{S_{exp}}{S} F \qquad (4)$$

Where,

$\frac{dC_L}{d\alpha}$ = 3-D lift curve slope

A_e = Effective aspect ratio. (Including effect of winglets and endplates)

$\beta^2 = (1 - M^2)$ (M = Mach number)

Λ_t = Sweep of wing at maximum thickness (= 0. As there is no sweep on wing.)

S_{exp}= Exposed wing area (12.95m^2)

$F = 1.07\left(1+\frac{d}{b}\right)^2$ = Fuselage lift factor

d = Fuselage diameter (1.3m)

b = Wing span (8.28m)

$$\eta = \frac{dC_l}{d\alpha}\frac{\beta}{2\pi}$$

$\frac{dC_l}{d\alpha}$ = Two-dimensional lift curve slope

The two-dimensional lift curve slope, and Mach number can be taken from earlier in this section from table J.6-1.

Aspect ratio, $A = \frac{b^2}{S} = 4.23$

The effect of the winglets on the inboard section has been accounted for by multiplying the aspect ratio by 1.055, this gives, effective aspect ratio, A_e = 4.46. The factor of 5.5% was calculated in the winglet section earlier in this appendix. For the wing maximum lift coefficient another equation from Raymer[1] was used.

$$C_{L\max} = 0.9C_{l\max}\cos\Lambda_{1/4} \qquad (5)$$

Where,

$\Lambda_{1/4}$= Sweepback at quarter chord (=0, as there is no sweepback)

Thus for the flight conditions looked at earlier, the wing lift curve slopes and maximum lift coefficients in table J.6-2 were found.

Table J.6-2 3-D wing characteristics

Flight Case	3-D Lift Curve Slope ($dC_L/dá$)	Maximum 3-D lift coefficient (C_{Lmax})
Cruise	4.97	1.818
Take off / Landing	4.92	1.755
Stall Speed	4.92	1.575

Implementation of High Lift Devices

It was decided that with the telescopic wing that full span flaperons could be used on the trailing edge of the outboard wing. It was thought that separate ailerons and flaps would be more complicated and have an increased weight penalty, because of the use of the telescopic wing. Leading edge devices were thought to be unnecessary and also have too large a penalty with complexity and weight. The flaperons used were decided to be of the plain flap type, with the gap between wing and flap sealed to minimize losses. For plain flaps it was found from Raymer[1] that the optimum flap chord to airfoil chord ratio was 0.25. However due to ground clearance issues, it was decided that the flap chord to airfoil chord ratio would be 0.2.

Effect of Plain Trailing-Edge Flap Deflection on Airfoil Section Lift

Using theory from Torenbeek[7] the increase in the maximum and the zero angle of attack lift coefficients, due to the deflection of plain trailing-edge flaps, can be calculated. All theory and charts in this section are from Torenbeek.[7] The effect trailing-edge flaps have on section lift can be seen in figure J.6-3 below:

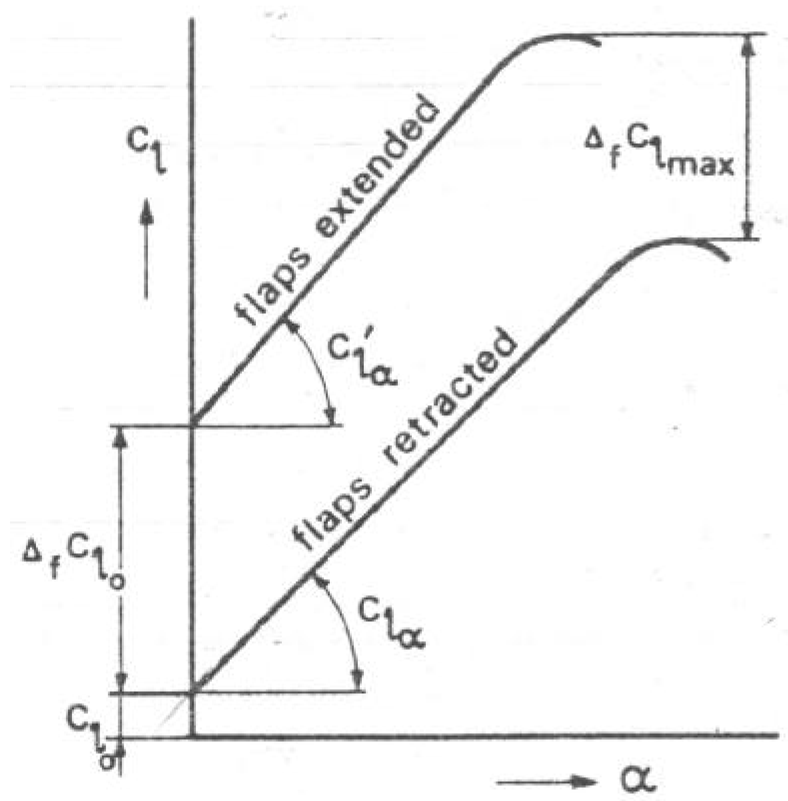

Figure J.6-3 Effect of trailing-edge flaps[7]

As can be seen the effect the flaps have is made up of an increase in lift coefficient at zero angle of attack, an increase in maximum lift coefficient and a change in the lift curve slope. For the airfoil section at zero angle of attack, the increase in lift coefficient is given by:

$$\Delta_f C_{lo} = \eta_\delta \alpha_\delta C_{l\alpha} \delta_f \qquad (6)$$

Where,

η_δ = Lift effectiveness factor.

$C_{l\alpha}$ = Two-dimensional lift curve slope (Radians^{-1}).

δ_f = Flap deflection (in Radians).

$$\alpha_\delta = 1 - \frac{\theta_f - \sin\theta_f}{\pi} \text{ = Theoretical flap lift factor.} \qquad (7)$$

$$\theta_f = \cos^{-1}\left(2\frac{c_f}{c} - 1\right) \qquad (8)$$

c_f = chord of flap.

c = Chord of airfoil without flap deflection.

The lift effectiveness factor, which accounts for differences between practical and theoretical cases, is taken from the following figure J.6-4:

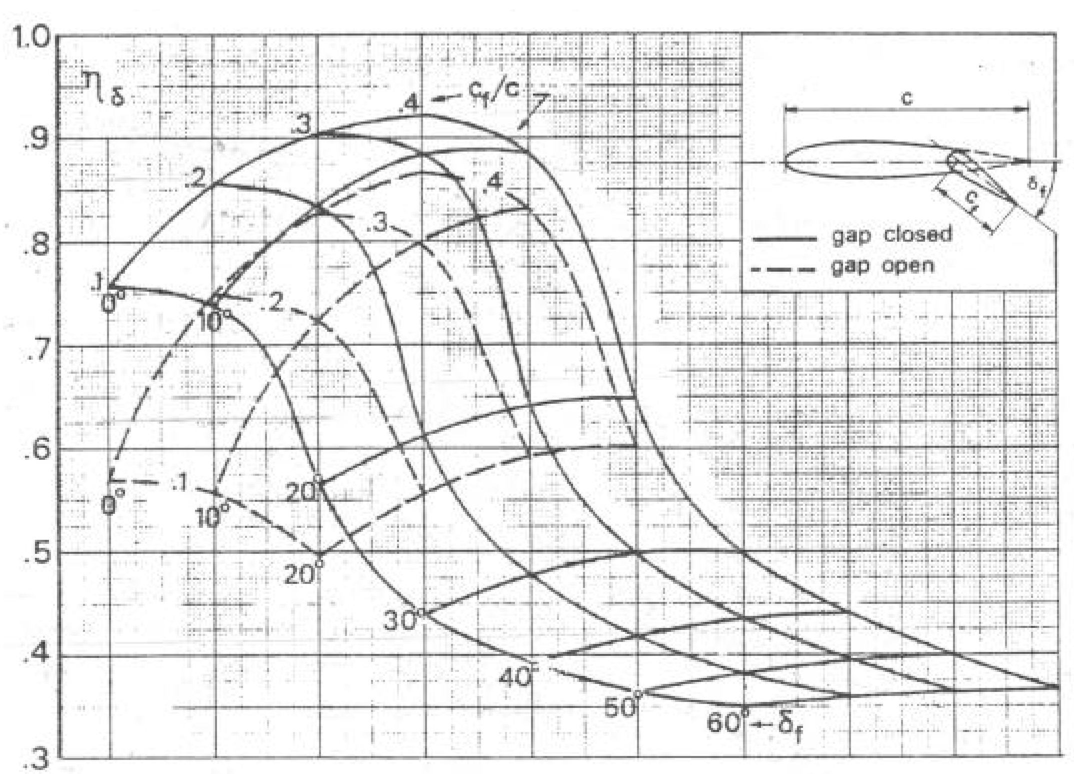

Figure J.6-4 Lift effectiveness factor[7]

The flap chord to airfoil chord ratio is 0.2, and the range of flap deflections are from 0º to 60º. It has been assumed that the gap between the flap and wing is closed. The increase in maximum lift coefficient is given by:

$$\Delta_f C_{l\,\max} = \left(\frac{c'}{c} C_{l\,\max}\right)_{d_f = 0} + \Delta_f C_{lo} - C_{l\,\max} \qquad (9)$$

Where,

C_{lmax} = 2-D maximum lift coefficient. (Taken from table J.6-1)

c’ = Chord of wing with flap deployed.

The chord of the wing with flaps deployed will actually decrease as plain flaps are being used. This is shown in figure J.6-5 below:

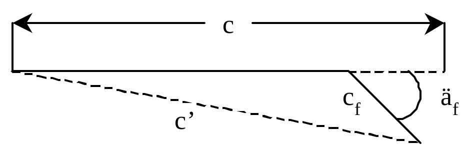

Figure J.6-5 Reduction of chord length

$$c' = \sqrt{\left(c - c_f + c_f \cos \boldsymbol{d}_f\right)^2 + \left(c_f \sin \boldsymbol{d}_f\right)^2} \qquad (10)$$

The airfoil section was considered with flap deflections from 0º to 60º in 10º increments. For these flap deflections the following was found and table J.6-3 was generated:

c_f = 0.4375 m

$á_ä$ = 0.6090 Radians

Table J.6-3 Effect of flap deflection on 2-D characteristics

Flap Deflection ($ä_f$) (degrees)	$ç_ä$	c’ (m)	$Ä_f C_{lo}$	$Ä_f C_{lmax}$

10	0.860	1.746	0.579	0.574
20	0.625	1.733	0.842	0.822
30	0.490	1.712	0.990	0.946
40	0.425	1.683	1.145	1.068
50	0.390	1.647	1.314	1.195
60	0.370	1.604	1.496	1.327

These results are for the take off / landing configuration, however the values do not change too much for the other flight cases. These values have than been used in the next section to determine the effect of the flaps on three-dimensional wing lift.

Effect of Plain Trailing-Edge Flap Deflection on Wing Lift

The theory and charts pertaining to the calculation of the three-dimensional effects of flaps has also been taken from Torenbeek[7]. This theory is used to calculate the increase in wing maximum lift and zero angle of attack lift coefficients, as well as the change in the wing lift curve slope, due to the deflection of trailing-edge plain flaps. For the wing at zero angle of attack:

$$\Delta_f C_{Lo} = \Delta_f C_{lo} \left(\frac{C_{L\alpha}}{C_{l\alpha}} \right) \left[\frac{(\alpha_d)C_L}{(\alpha_d)C_l} \right] k_b \qquad (11)$$

Where,

$\Delta_f C_{Lo}$ = Increase in 3-D lift coefficient at zero angle of attack.

$\Delta_f C_{lo}$ = Increase in 2-D lift coefficient at zero angle of attack.

$C_{L\alpha}$ = 3-D lift curve slope without flaps. (Radians^{-1}).

$C_{l\alpha}$ = 2-D lift curve slope without flaps (Radians^{-1}).

(á$_{ä}$)C_L = 3-D flap effectiveness factor.

(á$_{ä}$)C_l = 2-D flap effectiveness factor.

k_b = Flap span effectiveness factor.

The two-dimensional lift curve slope values can found in table J.6-1. The three-dimensional lift curve slopes can be taken from table J.6-2. The two-dimensional flap effectiveness factor, together with the aspect ratio can be used to determine the ratio of (á$_{ä}$)C_L to (á$_{ä}$)C_l (or K_c) with figure J.6-6

$$(\boldsymbol{a}_d)C_l = \boldsymbol{h}_d \boldsymbol{a}_d \quad (12)$$

The terms ç$_{ä}$ and á$_{ä}$ are defined and calculated earlier in this section.

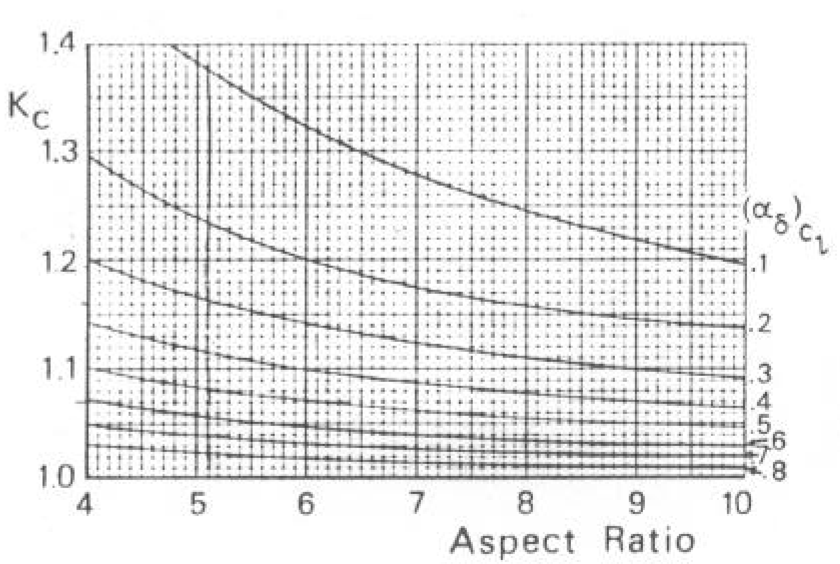

Figure J.6-6 Graph for the determination of the factor K_c[7]

The effective aspect ratio of the wing is 4.46, the calculations for this can be found earlier in this section. The span effectiveness factor (k_b) is taken from figure J.6-7:

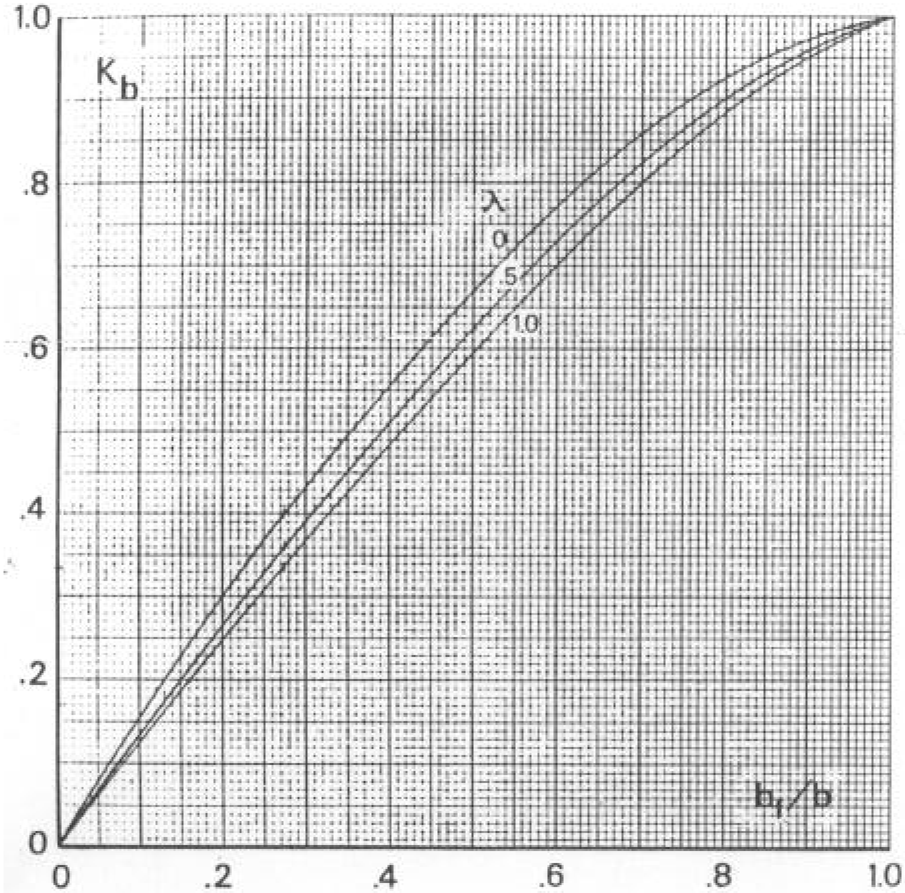

Figure J.6-7 Span effectiveness factor, k_b[7]

The method of finding the factor kb is best explained using figure J.6-8:

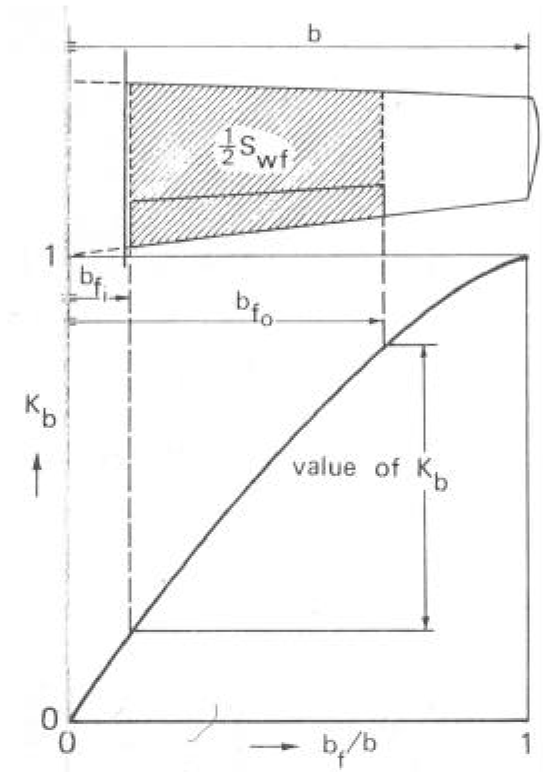

Figure J.6-8 Explanation of span effectiveness factor[7]

The taper ratio, ë is taken as 1. This is because the flaps are only present on the outboard sections that have no noticeable taper. The wingspan is 8.28m. The total flap span is 6m. Hence the factor kb is 0.655

For the maximum lift coefficient, the following equation was used:

$$\Delta_f C_{L\max} = 0.92\Delta_f C_{l\max}\left(\frac{S_{wf}}{S}\right)\cos\Lambda_{1/4} \qquad (13)$$

Where,

Ä$_f$C$_{lmax}$ = Increase in 2-D maximum lift coefficient due to flaps

S_{wf} = Wing area affected by trailing-edge flaps

Because there is no sweepback, Ë$_{¼}$=0º

Values for the increment in two-dimensional maximum lift coefficient can be found in table J.6-3. The change in three-dimensional lift curve slope is given by:

$$C_{L\alpha}' = C_{L\alpha}\left(1 + \frac{\Delta_f C_{Lo}}{\Delta_f C_{lo}}\left[\frac{c'}{c}\left(1 - \frac{c_f}{c}\sin^2 \delta_f\right) - 1\right]\right) \tag{14}$$

Where,

$C_{L\alpha}'$ = 3-D lift curve slope with flaps deflected

$C_{L\alpha}$ = 3-D lift curve slope with flaps retracted

c' = Chord of wing with flaps deflected

All other terms are defined earlier in this section.

Thus from these equations table J.6-4 was generated for the take off / landing condition:

Table J.6-4 Effects of flap deflection

Flap Deflection (δ_f) (degrees)	$\Delta_f C_{Lo}$	$\Delta_f C_{lmax}$	C_{Lmax}	$C_{L\alpha}'$
10	0.286	0.337	2.092	4.897
20	0.435	0.482	2.237	4.833
30	0.527	0.555	2.310	4.727
40	0.628	0.627	2.382	4.587
50	0.723	0.701	2.456	4.433
60	0.830	0.779	2.534	4.270

Wing Stall Characteristics

In order to ensure that the wing had good stalling characteristics, it was decided that the inboard section of the wing should stall first. In order to accomplish this a number of ideas were looked at that would keep the flow attached to the outboard sections of the wing up to higher angles of attack than the inboard sections.

It was seen that the junction between the two wings should, at high incidences, cause the inboard section of the telescoping wing to stall first. If however the wind tunnel tests proved this to be incorrect, then it may be necessary to introduce another method of ensuring the outboard sections stalled at higher incidences than the inboard sections. Fixed slots at the leading edge of the outboard wing were considered however it was decided that these would be hard to implement on a telescoping section, and that the performance losses in cruise would be unacceptable. Another solution would be to have vortex generators on the outboard sections to prevent separation, however the telescoping sections again mean that this would be very difficult to implement. Another idea was to have washout or wing twist on the wing. This would be accomplished by having the outboard wing set at a negative incidence relative to the inboard wing. This was considered less complex than having each individual wing component twisted, as this would have been harder to stow.

Calculations based upon theory from Torenbeek[7] have been used to calculate the zero-lift angle for the entire wing if –2 degrees of twist was used. From Torenbeek[7] the wing zero lift angle is given by:

$$\alpha_{Lo_r} = \alpha_{lo_r} + \alpha_{o_1}\varepsilon_t \qquad (15)$$

Where,

α_{Lo_r} = Three-dimensional zero lift angle of attack of wing at wing root

α_{lo_r} = Two-dimensional zero lift angle of attack of wing root section å$_t$ = Wing twist at tip of wing (=-2º)

$$\boldsymbol{a}_{0_1} = -\int_0^1 \frac{\boldsymbol{e}}{\boldsymbol{e}_t} L_a \, d\boldsymbol{h} \qquad (16)$$

å = Aerodynamic wing twist. (=0º for inboard section, =-2º for outboard section.)

$$L_a = C_1 + (C_2 + C_3)\frac{4}{\boldsymbol{p}}\sqrt{1-\boldsymbol{h}^2} \qquad (17)$$

$$\boldsymbol{h} = \frac{y}{b/2} \qquad (18)$$

y = Distance out along span of wing from centerline

b = Span of wing. (8.28m)

C_1, C_2 and C_3 are taken from the following figure J.6-9:

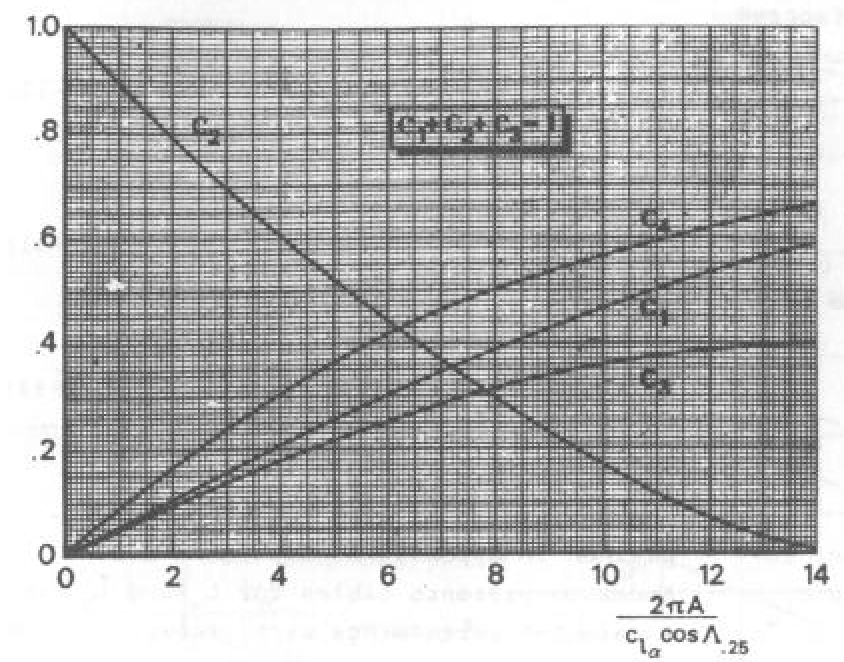

Figure J.6-9 Factors used for wing twist effect[7]

Aspect ratio, A = 4.46

$C_{lá}$ = 6.9 or 7.02 for take off / landing and cruise conditions.

Because of the closeness of the results only the take off / landing case has been looked at.

Hence,

$C_1 = 0.24$

$C_2 = 0.56$

$C_3 = 0.2$

At the intersection between the inboard and outboard wings,

$$\boldsymbol{h} = \frac{1.14}{8.28/2} = 0.275$$

Because the aerodynamic wing twist is zero for the whole of the inboard section, and is constant for the length of the outboard section, equation (16) becomes:

$$\boldsymbol{a}_{0_1} = -\int_{0.275}^{1} L_a \, d\boldsymbol{h} \tag{19}$$

$$\therefore \boldsymbol{a}_{0_1} = -\int_{0.275}^{1} \left(C_1 + (C_2 + C_3)\frac{4}{\boldsymbol{p}}\sqrt{1-\boldsymbol{h}^2} \right) d\boldsymbol{h}$$

$$= -\left[C_1\boldsymbol{h} - (C_2 + C_3)\frac{4}{3\boldsymbol{p}}\left(1-\boldsymbol{h}^2\right)^{3/2} \right]_{0.275}^{1}$$

$$= -\left[C_1 - \left(0.275C_1 - (C_2 + C_3)\frac{4}{3\boldsymbol{p}}\left(1 - 0.275^2\right)^{3/2} \right)\right]$$

$$= -0.160$$

The two-dimensional zero-lift angles of attack of the wing root section were taken from figures J.6-1 and J.6-2 for the different flight conditions and are:

Take off / Landing, α_{lo_r} = -3.6º

Cruise, α_{lo_r} = -4.2º

Therefore using equation (15), the three-dimensional zero-lift angles of attack of the wing at wing root would be:

Take off / landing, α_{Lo_r} = -3.28º

Cruise, α_{Lo_r} = -3.88

However as no wing twist will be used unless needed after the wind tunnel test then the two-dimensional values will be equal to the three-dimensional zero-lift angles of attack. These values can be used to give a wing setting angle on the fuselage, depending upon the lift coefficient required at a specific flight condition. The flight condition considered was at take off with 30 degrees of flap deflection this resulted in the wing setting angle to be 2 degrees in order that the plane could rotate at take off.

Ground Effect

Because the aircraft has a low ground clearance in ground roll, the effect due to ground clearance will be large. The image vortex system will induce a velocity distribution at the airfoil in the opposite direction to the freestream velocity, which will result in a reduction of lift. However this effect may be negated by the fact that there will be an induced upwash, which will reduce the angle of incidence required in obtaining a certain lift coefficient. Overall, the last effect will be the most noticeable, giving an improved performance in the take off and landing conditions.

Charts of lift coefficient against angle of attack for the different flight conditions.

Figures J.6-10 and J.6-11 show the three-dimensional lift curve slope for the aircraft in the cruise condition and in the take off / landing condition with the effect of flap deflection shown. The stall characteristics of the wing are hard to predict and the wind tunnel tests will provide more indicative results of the stall region.

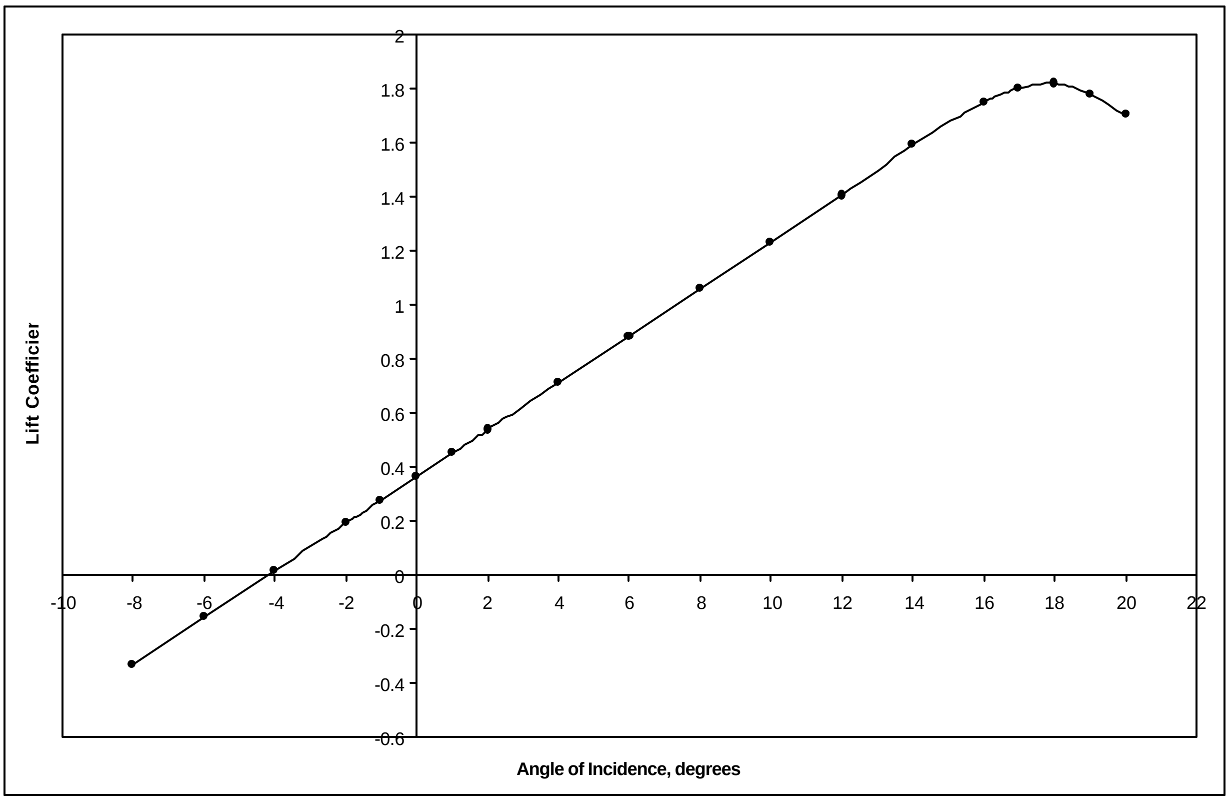

Figure J.6-10 3-D Lift curve slope for wing at cruise.

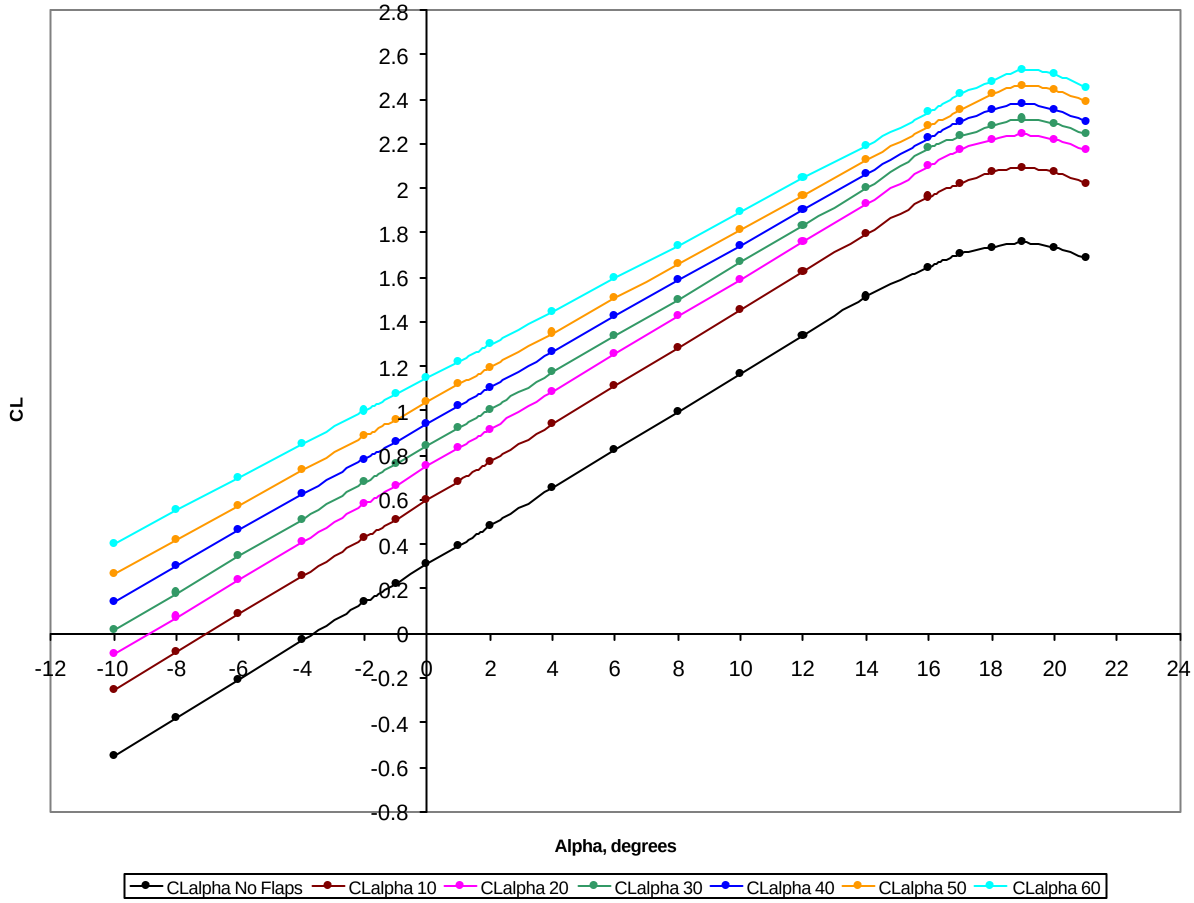

Figure J.6-11 3-D Wing lift curve slope at take off and landing.

Figure J.6-11 shows the effect of flap deflection at the take off / landing condition. As can be seen the maximum lift coefficient increases and the lift curve slope decreases with increased flap deflection.

Horizontal Tailplane

The horizontal tail has a chord of 1.25m and a span of 2.28m this gives a physical aspect ratio of 1.82. It has been assumed that the rudder fins act as large endplates, and that the tail surface will be slightly affected by the propeller wash. The endplates will affect the tail surface so it will act more like a two-dimensional wing, and the propeller wash will increase the effective aspect ratio. With this in mind it was decided that there would be an increase in the aspect ratio of the horizontal tailplane of 30 percent. This resulted in the effective aspect ratio being 2.37.

For the NACA 0012 airfoil, that is to be used for the horizontal tailplane, the two-dimensional lift curve slope was found to be 6.2, and the maximum lift coefficient was found to be 1.6. These values were taken from a chart of lift coefficient versus angle of incidence from Abbot and Doenhoff[444]. Using equation 4 from earlier in this section, the three-dimensional lift curve slope can be calculated. The fuselage lift factor can be taken as 1 as can the ratio of exposed tail area to the reference tail area. This gives a three-dimensional lift curve slope of 2.9.

The two-dimensional maximum lift coefficient was also calculated in the same manner as the wing and was found by multiplying the two-dimensional value by a factor of 0.9. This gave a maximum three-dimensional value of 1.44.

The effect of the elevator was assumed to be in the same manner as the flaps on the main wing. The elevator chord to tailplane chord ratio was decided to be 0.35 and it was assumed that it was a plain flap type of elevator, the reasons behind the selection of the elevator type and size can be found in section 5 of this appendix.

Using the theory pertaining to the calculation of the effect of trailing-edge flaps earlier in this section the effect of the elevator on the three-dimensional maximum lift coefficient (Table J.6-5) and lift curve slope (Figure J.6-12) for the horizontal tailplane were found to be as follows.

Table J.6-5 Effects of elevator deflection on the lift coefficient

Elevator Deflection	Increase in 3-D C_{Lo}	Increase in 3-D C_{Lmax}	3-D C_{Lmax}	3-D dC_L/d▶ for horizontal Tail
10	0.336	0.616	2.056	2.884

20	0.522	0.892	2.332	2.821
30	0.629	1.008	2.448	2.715
40	0.757	1.155	2.595	2.578
50	0.874	1.279	2.719	2.422
60	0.981	1.359	2.799	2.251

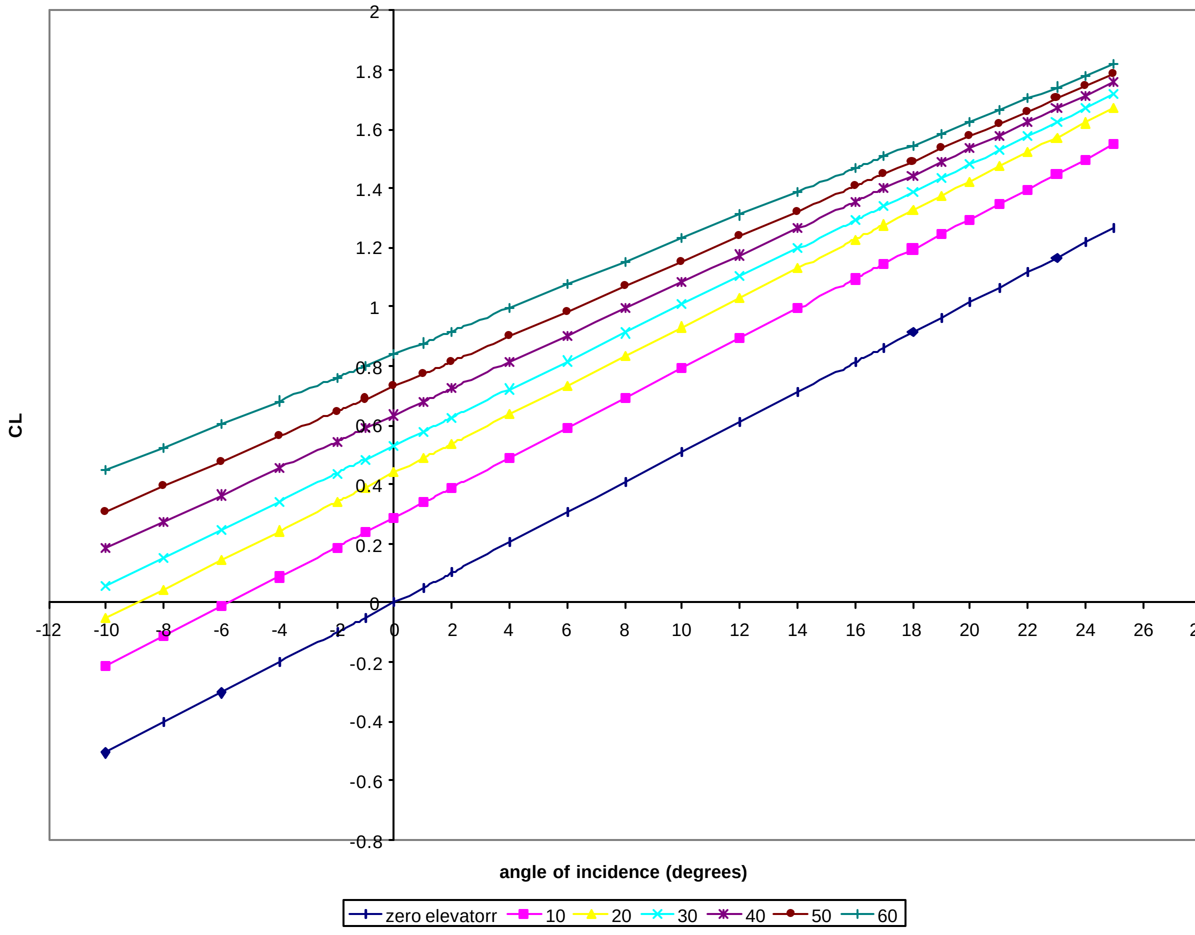

Figure J.6-12 variation of three-dimensional lift coefficient with angle of incidence with varying elevator deflections

As can be seen from figure J.6-12, the lift curve slope is quite small, resulting in stall being delayed to very high incidences. This shallow lift curve slope is due to the low aspect ratio of the horizontal tail surfaces.

Vertical Tailplanes

The vertical tailplanes will use a NACA 0008 airfoil section, and will have a span of 1.8 meters, a chord of 0.9 meters, a sweepback of 59 degrees and a taper ratio of 0.26. This gives a physical aspect ratio of 2, and assuming the tailplane and fuselage increase the effective aspect ratio by a factor of 1.2, the effective aspect ratio will be 2.4. From Abbot & Doenhoff[444] the two-dimensional lift curve slope is 6.19 per radian, and the maximum lift coefficient is 1.6. Again using the theory given earlier in this section pertaining to the conversion to three-dimensional characteristics, this time the surface has sweep, so the lift curve slope and maximum lift coefficient includes the factor for sweep. This results in a three-dimensional lift curve slope of 3.22 per radian and a maximum lift coefficient of 0.742.

The effect of the rudder on the characteristics of the vertical tailplanes is again assumed to be similar to the flaps effect on the wing, The rudder chord to section chord ratio is 0.35, and spans from 10 percent to 90 percent of the span of the vertical tailplane. Using the theory given earlier in this section for the effect of flaps, the effect of the rudder on the lift coefficient (Table J.6-6) and lift curve slope (figure J.6-13) were found to be as follows:

Table J.6-6 Effects of rudder deflection on the lift coefficient

Rudder deflection (degrees)	Increase in 3-D CLo	increase in 3-D CLmax	3-D CLmax	3-D dCL/dα
10	0.317	0.318	1.059	3.200

20	0.492	0.892	1.634	3.134
30	0.593	1.008	1.749	3.024
40	0.713	1.155	1.897	2.881
50	0.824	1.280	2.021	2.717
60	0.925	1.360	2.102	2.538

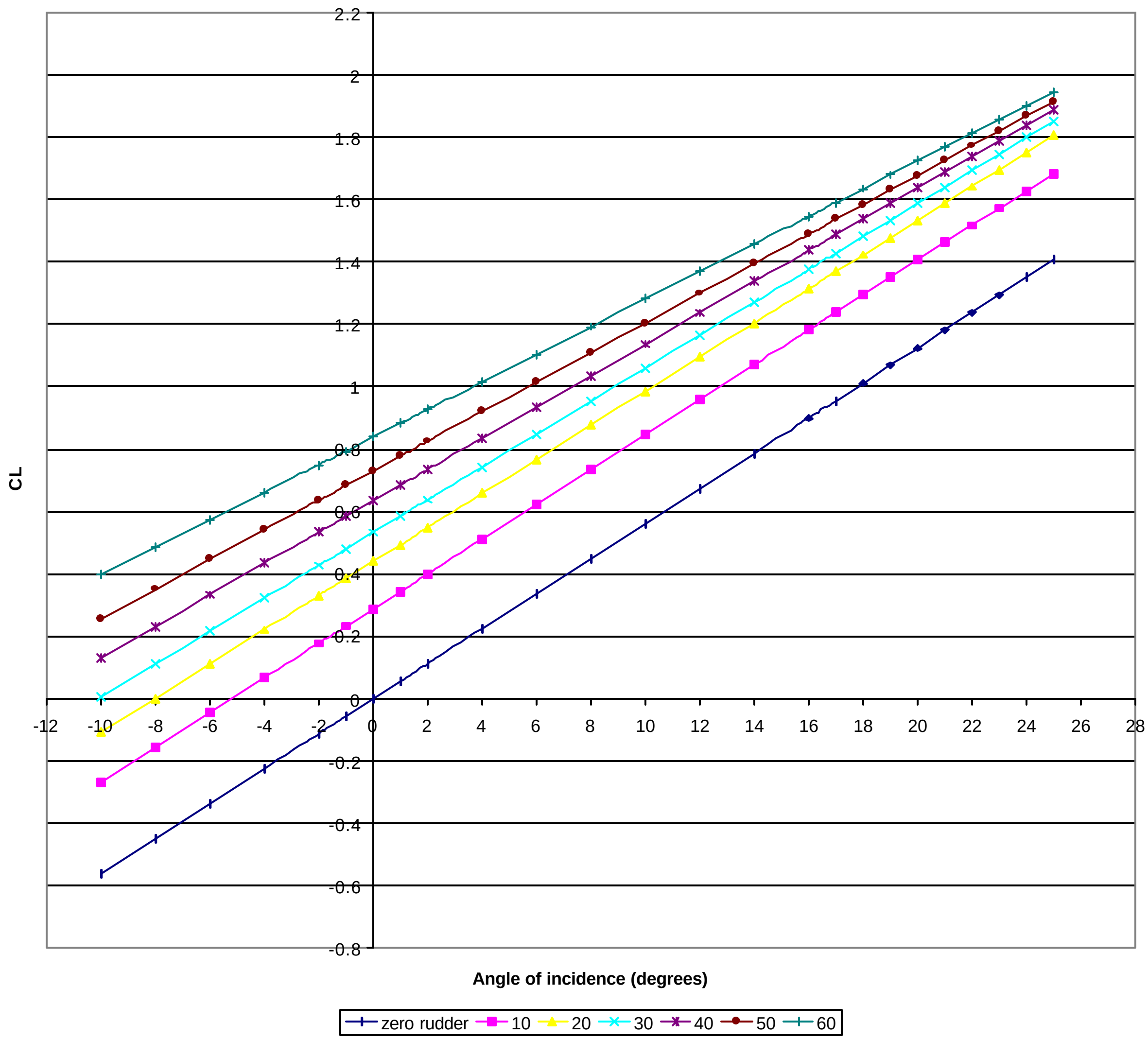

Figure J.6-13 effect of the rudder deflection on the fin lift

J.7. Drag

In order to assess the performance of any aircraft an estimation of the drag force in all configurations and flight conditions is required. The optimization of the vehicle will involve the detailed design of all external surfaces to minimize drag.

At the very earliest stages of the design process the configuration of the vehicle will not have been finalized, making accurate drag estimation impossible. However, even at this stage, the performance will need to be assessed for the design process to continue. The first estimation of the drag was based purely on the study of similar type aircraft. This in itself presented problems, as the layout is unique. The need for safe, efficient road travel was always going to incur some drag penalty over conventional general aviation aircraft. It was possible to obtain an estimation of this penalty from the study of existing roadable aircraft, but this served to highlight another problem. Very nearly all readily available information on general aviation aircraft relates to outdated designs, with no indication of the effect of advances in manufacturing, construction and design that have occurred in recent years and are likely to occur in the near future.

These arguments led to the conclusion that, as a first estimation, it would be reasonable to assume that the increase in drag associated with the dual role of the design would be offset almost completely by recent and future improvements in technology. The first working estimation of the profile drag coefficient was 0.025 with the lift induced drag coefficient being assumed to be a function of lift coefficient, aspect ratio and the Oswald efficiency factor, i.e.

$$C_D = 0.025 + \frac{C_L^2}{(\pi \times A \times e)} \qquad [1]$$

Where

C_D = Total drag coefficient

C_L = Aircraft lift coefficient

A = Aspect ratio

$$e = 1.78 \times (1 - 0.045 \times A^{0.68}) - 0.64 \qquad [2]$$

As the design process moved on, the geometry of the vehicle began to be defined, but without knowledge of the drag of the components, optimization could only be based on guesswork. The clear need for a breakdown of the drag of the various structures was established. At this stage this was only done for the profile drag, while the lift induced drag was calculated using the above expression. The profile drag of each component was estimated using it's wetted area multiplied by form factors, interference factors and estimated skin friction factors. This method, although rough, immediately highlighted the landing gear as a problem area, contributing 52% of the profile drag in cruise configuration. This was due to the front wheels being exposed to the flow in all configurations. The addition of fairings to the side of the fuselage allowed the wheels to be almost completely retracted from the flow, with very little added complexity as the front wheels were already moveable to facilitate rotation-free take off.

The profile drag breakdown method described above helped with the definition of the undercarriage, and gave some indication of the drag of other components, but was not really up to the job of optimizing areas such as the windshield. Also the lift induced drag, which usually contributes most of the drag in flight, was too generic to show the effect of alterations properly.

Several methods of estimating the drag (profile, vortex and boundary layer dependant) exist, most using large amounts of empirical data, based on component geometry. The ESDU data sheets provide a good range of tried and tested data, based on the summation of a series of simple geometrical shapes. The methods presented allow for the calculation of the vortex induced drag and the boundary layer dependant drag of wings, fuselages and other components.

Using these methods it was possible to highlight and if necessary redesign the components, or parts of components, which were producing the most drag.

The profile drag of the wing was calculated using empirical data for the wing drag coefficient[8]. The boundary layer lift dependent drag rise was calculated using:

$$C_{Db} = K_1 \times C_L^2 \qquad [3]$$

Where

C_{Db} = boundary layer dependant drag coefficient

K_1 = Factor estimated using figure J.7-1 of reference [9]

The vortex drag was calculated using:

$$C_{Dv} = \frac{1+\delta}{\pi \times A} \times C_L \qquad [4]$$

Where

$1 + \delta$ = Lift dependant drag factor based on taper ratio[10]

The low wing position on the fuselage was always going to give a small increase in drag over a mid-winged design. Torenbeek[7] suggests the effect is:

$$C_D S = C_F \times C_L \times c_r \times D_f \qquad [5]$$

Where

$C_D S$ = Drag area

C_F = Skin friction coefficient

C_L = Lift coefficient

c_r = Root chord

D_f = Fuselage diameter

This provided an estimate of the low wing drag increase of 1.8 drag counts at cruise, which when compared to the advantages of the low wing, such as good undercarriage mount position and low center of gravity, is too small to justify a redesign. One simple method of decreasing the interference of the wing and fuselage was to add a leading edge fillet to reduce the vortices produced at the sharp wing-fuselage intersection. The weight penalty and cost associated with such a modification is minimal and is easily outweighed by the drag reduction. A similar fillet would be desirable on the outboard wing, but the practicalities of attaching it to an extending wing make it uneconomical. The inboard wing only extends 200mm beyond the leading edge of the outboard wing, so it is unlikely that a fillet would have a very great effect, even if it were possible.

The design of the horizontal tail, with fins at either end means that the fins will act as endplates on the tail, reducing the tip vortices. At certain incidences the tail will be in the propeller wash, which will also change the flow pattern over the tail. Torenbeek[7] suggests an increase in effective aspect ratio of as much as 50% for areas of wings in the propeller wash. Taking these two factors into account it was decided to increase the effective aspect ratio of the horizontal tail by a factor of 1.5. Due to the short tail arm the lift (and so the drag) generated by the horizontal tail is greater than is usual for GA aircraft, so this increase in aspect ratio should help to bring the value in line with that of competitor aircraft. The drag of the tail was calculated using the same equations as the wing, but with the different section and aspect ratio.

The profile drag of the winglets has been integrated with the fin, as it is not clear where one starts and the other finishes. The effect of the winglets has been calculated elsewhere in the aerodynamics section. The lift dependant drag of the fins has been assumed to be zero in straight and level flight.

To calculate the drag of the fuselage it was necessary to break it down into component parts, with the drag of the windshield and wheel fairings being calculated separately. The body could then realistically be modeled as an axisymmetric body of rotation with a tangent to give afterbody and a forebody which most closely resembled body 7 of reference [11]. With these considerations it was then possible to calculate the profile drag of the fuselage:

$$C_{Do} = \lambda \times C_f \qquad [6]$$

Where

C_F = Mean skin friction coefficient

$$\lambda = K_{tr} \times K_M \times \lambda_G \qquad [7]$$

K_{tr} = Transition position factor [12 figure 4]

K_M = Mach number factor [12 figure 6]

λ_G = Body geometry factor [11 & 12]

The vortex induced drag of the fuselage was calculated using:

$$C_{Dv}S = 0.15 \times \alpha_f^{\,2} \times V^{2/3} \qquad [8]$$

Where

V_f = Volume of the fuselage

α_f = Fuselage angle of attack

The windshield profile drag was estimated as 0.08[7], based on windshield area.

It has already been noted that the profile drag of the undercarriage is likely to be very significant. In cruise configuration only the lower part of the wheel is exposed to the flow. In landing and take off not only is the wheel exposed, but the suspension forks, the drive shaft casing and the steering cable are also exposed. As these struts are not exposed in cruise it was not worthwhile fairing them so their effect is very significant. The fairing profile drag is given by:[13]

$$C_{Do} = \frac{0.07 \times S_f}{S} \qquad [9]$$

Where

S_f = fairing frontal area

S = Reference area

The exposed wheel profile drag is given by:

$$C_{Do} = 0.55 \times \frac{C_D}{C_{Do}} \times \frac{b \times h_w}{S} \qquad [10]$$

Where

b = Width of the wheel

h_w = Exposed height of wheel

$\frac{C_D}{C_{Do}}$ = Based on wheel diameter/width and given by figure J.7-1 of reference [14]

The strut drag is given by:

$$C_{Do} = 1.2 \times \frac{l_s \times d_s}{S} \times R_1 \times R_2 \times R_3 \qquad [11]$$

Where

l_s = Strut length

d_s = Strut diameter

R_1 = Strut inclination factor[13 figure 4]

R_2 = Strut/strut interference factor[13 figure 5]

R_3 = Strut/body interference factor[13 figure 6]

In the take off and landing configurations the trailing edge flaperons are deflected, which produces a very significant drag increment. The flaps are plain flaps so experimental data is readily available. Reference [14] figure J.7-1 shows the profile drag of plain flaps for different deflections and flap chord to wing chord ratios. The vortex drag increment is given by:

$$C_{Dv} = (w + z) \times \Delta c_L{}^2 + v \times C_L \times \Delta c_L \qquad [12]$$

Where

Δc_L = Change in lift coefficient due to flap deflection

v, w = Vortex drag factors[7 figures G-21 & G-22]

$$z = \frac{0.07}{(1+\lambda)} \times 1.3^2 \times \frac{b_f}{b} \qquad [13]$$

λ = Taper ratio

b_f = Flap span

b = Wing span

Several other calculations have been included to take account of factors such as the drag control surface gaps, surface roughness and the drag of various unspecified airframe installations. The latter refers to antennas, lights, windshield wipers, instrumentation etc. It is impossible to predict the drag of these separately at this stage, so a generic term has been used based on similar aircraft[7].

The calculations shown above are an outline of the method used to find the drag of the aircraft; the methods in the references require many more inputs and calculations to find the various factors. The results of these calculations is a drag breakdown of the complete aircraft.

The lift induced drag coefficients change so much with C_L that they are not worth showing at one particular flight condition, so they are shown as a drag polar. The profile drag of the various components are shown below in table J.7-1.

Table J.7-1 Profile drag coefficients based on reference area of 16.2 m^2

	Cruise	**Landing**	**Take off**
Inboard wing	0.002321	0.002321	0.002321
Outboard wing	0.006138	0.006138	0.006138
Flaps		0.044074	0.035648
Horizontal tail	0.001557	0.001557	0.001557
Fins and winglets	0.001983	0.001983	0.001983
Fuselage	0.003884	0.003903	0.003904
Fuselage/wing interference	0.001859	0.001859	0.001859
Low wing drag correction	0.000188	0.000611	0.000717
Engine cooling drag	0.000009	0.000015	0.000017
Total front undercarriage	0.002178	0.012645	0.012202
Rear undercarriage	0.000622	0.004512	0.003154
Windshield	0.001481	0.001481	0.001481
Surface roughness	0.001200	0.001200	0.001200
Total control gaps	0.000291	0.000291	0.000291
Airframe installations	0.000390	0.000390	0.000390
Total profile drag	**0.024100**	**0.082974**	**0.071763**

The profile drag is clearly only part of the story. The total drag contains the vortex-induced drag and the boundary layer lift dependant drag. These values are best presented in graphical form as a so-called drag polar. This is shown below.

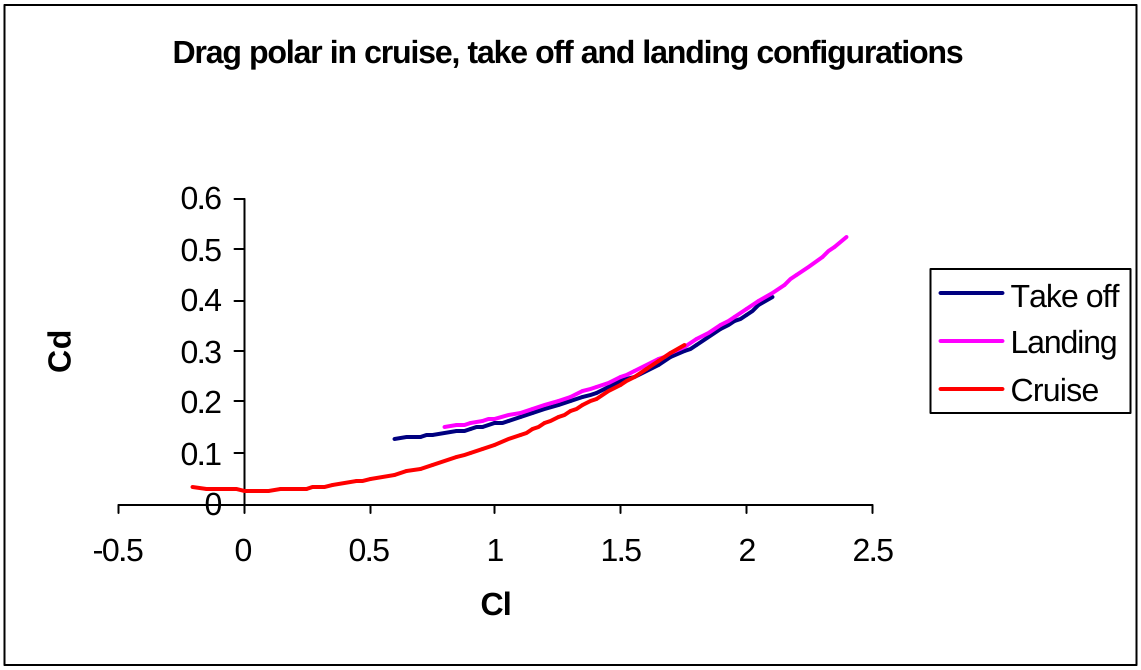

Figure J.7-1 Drag coefficient against lift coefficient of the complete aircraft based on a reference area of 16.2m^2.

J.8. Vortex Lattice Method Analysis

Although lifting line theory could provide reasonable estimate of the lift and induced drag for a geometrically simple, thin wing with high aspect ratio, an improved flow model was needed to calculate those values for a low aspect ratio, complex wing with thickness, like the one chosen for the design. The Vortex Latice Method (VLM) is one such improved flow model. Since the design has a complex, non uniform wing structure, the standard VLM programs could not perform the necessary calculations. Following the Vortex Lattice Method outlined in

J.9. Automotive Aerodynamics

Lift

The geometry of the vehicle will change due to the retraction of the outboard wings. This results in a mean chord of 2.5m and a wing span of 2.28m. The inboard wing section will still produce some lift whilst in the roadable configuration. Using the same theory as described in section 3, the maximum lift coefficient and lift curve slope can be found.

Two-dimensional airfoil lift curve slope and maximum lift coefficient

Assuming the car is at cruise velocity, which was specified as 70 mph (31.3m/s) and at an altitude of 0m, the vehicle will be at a Mach number of 0.092. (Speed of sound at sea level is 340.3m/s). The Reynolds number at road cruise velocity for the wing will be 5.36×10^6. Figure J.6-1 in section J.6 can then be used to give the maximum lift coefficient and the lift curve slope for the airfoil, these are 1.95 and 6.9 respectively.

Three dimensional lift curve slope and maximum lift coefficient

The wing lift produced by the inboard wing during the road cruise configuration was as in the airplane mode calculated using Raymer[111]. Using equations (4) and (5) in section 4.3 the values obtained for the lift curve slope and the maximum lift coefficient were, 1.462 per radians and 1.755 respectively.

The zero lift angle of the wing will be the same as the two-dimensional zero lift angle, as the inboard wing has no twist. This zero lift angle as can be seen from figure J.6-1 in section J.6 is minus 3.6 degrees.

Using this information, a graph of lift coefficient against angle of attack can be plotted for the wing in the road configuration. The graph is shown below in figure J.9-1

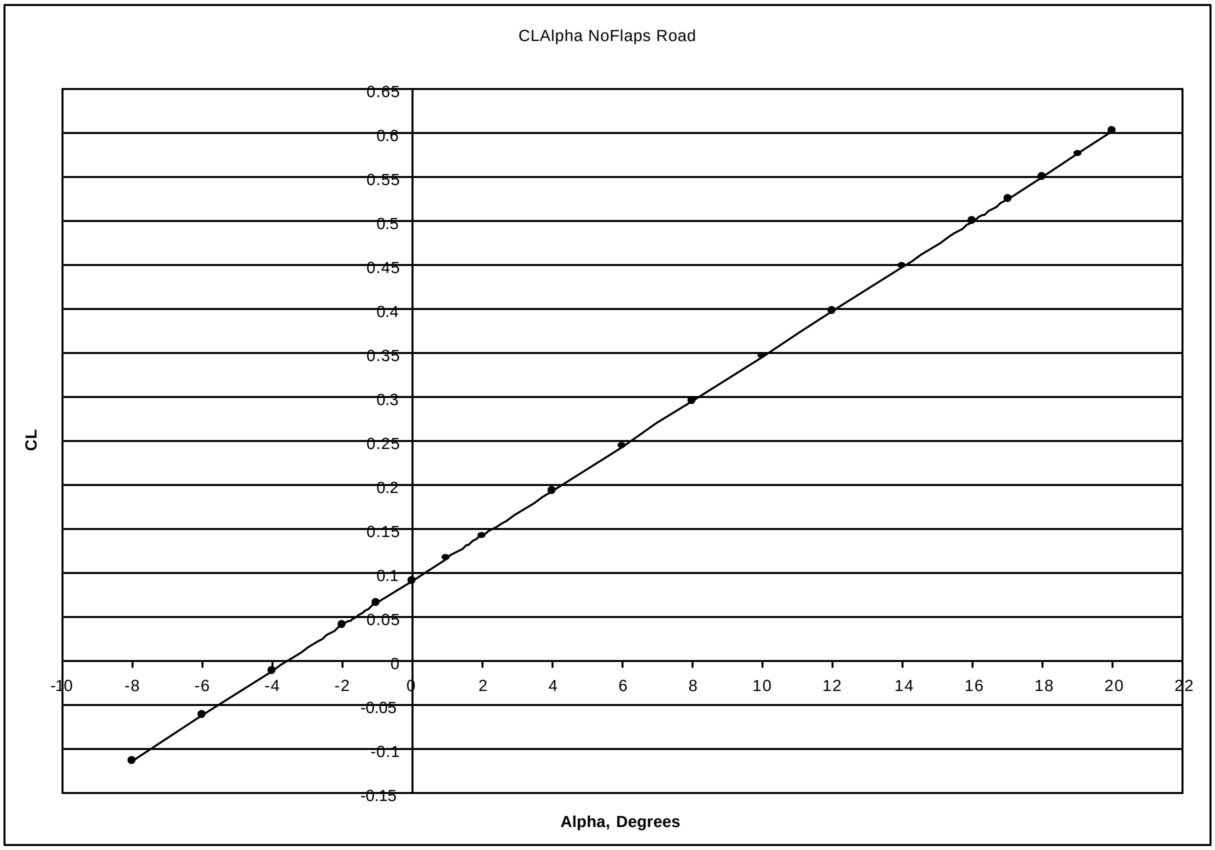

Figure J.9-1 Road 3-D lift curve slope

As can be seen from figure J.9-1 the slope of the graph is very shallow, and results in very small lift coefficients generated by the inboard wing over the angles of incidence that the wing is likely to see. It should be noted that the angle of incidence plotted here is the wing angle. For the aircraft as a whole the wing setting angle on the fuselage must be added.

This wing setting angle will be determined by stability requirements and should be found in appendix K.

Drag

The drag calculations for the road configuration use the same formulae as for the aircraft configurations, but several simplifications are possible. The outboard wings are clearly retracted, leaving only the simple untapered untwisted inboard wing. The tail is assumed to be set at zero incidence, so it only has a profile drag term. The fuselage is at zero incidence, so it also only has a profile drag term. The profile drag breakdown of the aircraft in road configuration is as follows in table J.9-1.

Table J.9-1 Profile drag coefficients based on reference area of 5.7m^2

Wing	0.002321
Horizontal tail	0.001557
Fins and winglets	0.001983
Fuselage	0.003909
Fuselage/wing interference	0.001859
Low wing drag correction	0.000079
Engine cooling drag	0.000018
Total front undercarriage	0.003609
Total rear undercarriage	0.002489
Windshield	0.001481
Surface roughness	0.001200
Control gaps	0.000110
Airframe installations	0.000391
Total profile drag	0.021008

It is clearly not relevant to plot the drag coefficients against lift coefficient, even though this is a major factor with the wings at incidence to the flow. Instead a graph showing the variation of drag (N.B. not drag coefficient) with velocity has been included. For completeness the Rolling resistance has also been included. The rolling resistance is principally a function of the weight, as is shown below[7].

$$D_R = K_R \times W \qquad [1]$$

Where

W = Vehicle weight

$$K_R = 0.005 + \frac{0.15}{P} + \frac{0.000035 \times V^2}{P} \qquad [2]$$

Where

V = Velocity (mph)

P = Tire pressure (lb/in^2)

This gives the drag of the tires on the road, which has been added to the aerodynamic drag to produce figure J.9-2.

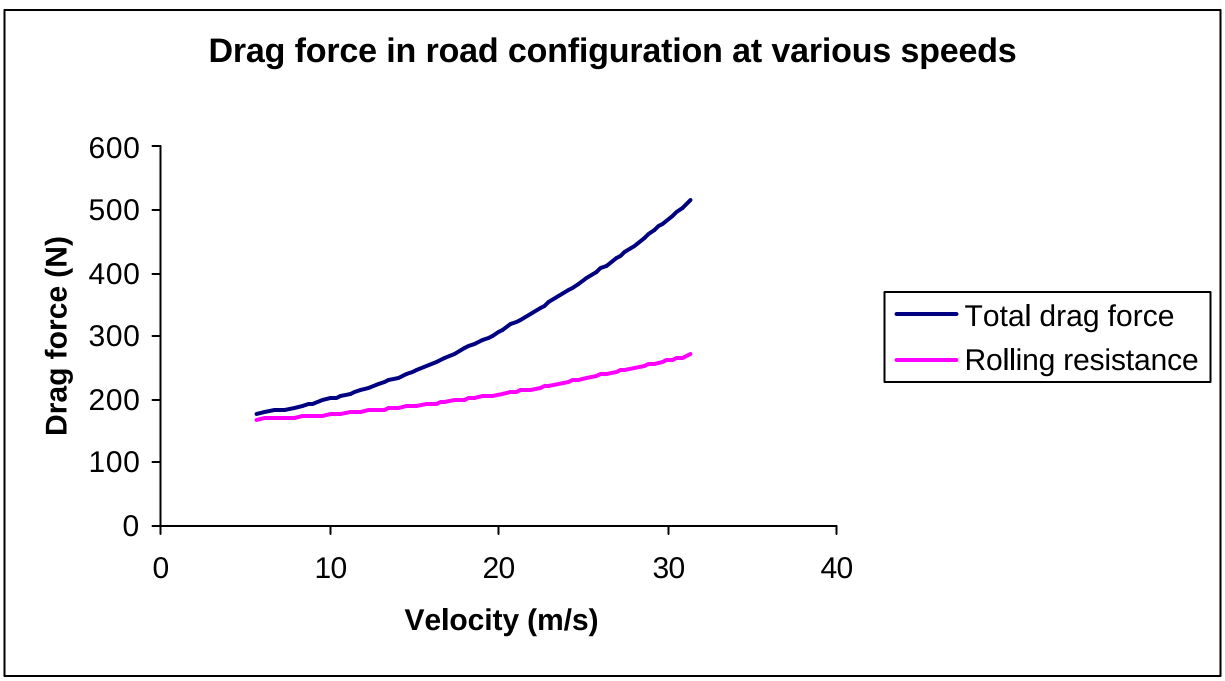

Figure J.9-2 Drag force against velocity in road configuration

J.10. Control Surfaces

The main factor that needs to be considered in the aerodynamics of control surfaces is the plan form layout as shown in figure J.2-1. The reasons for choosing these particular control sizings are discussed in more depth in appendix L.1.1. Due to the short moment arm too the tail section, small rudder and elevator sizes such as 20% would not give sufficient control force to maneuver especially at low speeds such as landing, where the ability to control the aircraft is very important. Because of this and the desire not to have surfaces that are too large (because of drag increases) it was decided to use a 35% control surface chord in relation to the surface chord to which the control is attached.

The increase in lift from the control surfaces has been calculated in Appendix I.4.3, so will not be covered here. The other area of aerodynamics that will need to be considered will by the drag increase because of the control surfaces. For stability and control the ideal decision for the control surface a gap between the control surface and the rest of the wing being unsealed will be desirable, as the drag will decrease the moment on the surface. From an aerodynamics point of view however this is bad as even a small gap can lead to large increases in drag and decrease in lift. In wind tunnel experiments it has been shown that even with a small gap between the control surface and the rest of the wing, it will lead to a large drop in the amount of lift produced. This drop in lift will be for the entire wing as the lift produced forward of the quarter chord line will actually increase, but around the gap near the back of the wing the lift will drop which will give an increase in the nose up pitching moment. This will not be a problem for our airfoil as it currently has a nose down pitching moment, but the decrease in lift produced will be significant and so the gap around the control surface will have to be sealed.

The other aerodynamic decision will be the choice of airfoil sections for the horizontal and vertical tail sections. The sections chosen are the NACA 0012 for the vertical section and a NACA 0008 for the horizontal. The NACA 0008 section will produce less drag than the 0012 due to its decreased thickness. However due to the large size of the horizontal tail and large moments that it will produce will means that it will have to be supported by a strong structure. This structure will have to be contained in the fin, so as a structural compromise an increase in drag will be accepted so that the thicker NACA 0012 can be used to house the structure to support the horizontal tail.

1) Raymer, Daniel P., Aircraft Design: A Conceptual Approach, Third Edition, 1999

2) Abbot and von Doenhoff, Theory of Wing Sections, 1959

3) NASA TN D-7428 “Low speed characteristics of a 17% thick airfoil section designed for general aviation applications”.

4) C.L. Gunther, J.F. Marchman III, R. Van Blarcom, "Comparison of Channel wing theoretical and experimental performance.", 1999

5) Bertin, J.J., Smith, M.L., Aerodynamics for Engineers, Third Edition, 1998

6) NASA Technical Note TN 18

7) Egbert Torenbeek , ‘An Introduction to Subsonic Aircraft Design’, 1982

8) ESDU data sheet 02.04.02 - Profile drag of smooth wings

9) ESDU data sheet 66032 - Subsonic lift dependant drag due to boundary layer of plane, symmetrical section wings

10) ESDU data sheet 74035 - Subsonic lift dependant drag due to the trailing vortex wake for wings without camber or twist

11) ESDU data sheet 77028 - Introduction to axisymmetric bodies of revolution

12) ESDU data sheet 78019 - Axisymmetric body drag prediction methods

13) ESDU data sheet 79015 - Undercarriage drag prediction methods

14) ESDU data sheet 87024 - Subsonic profile drag prediction methods for plain and single slotted flaps.

Appendix K. Aircraft Performance

K.1. Mission

The goal of the Pegasus design was to revitalize the general aviation industry. If a design as unconventional as a roadable aircraft is to accomplish this feat, it must be able to match or surpass the performance standards of today's general aviation. The pilot of tomorrow will look for a craft that is not only comfortable and convenient, but is also manageable in the air. This is where the Pegasus will appeal to the user.

The performance of the Pegasus was evaluated over a basic general aviation mission. The mission of the Pegasus is to take off, climb to cruise, cruise, loiter, descend, and finally land. In the preliminary design stages, various criteria, based on comparator general aviation aircraft, were set forth for each section of the mission. Table K.1-1 shows the initial desired mission performance of the Pegasus.

Table K.1-1 Initial Mission Criteria

T/O Distance	Climb Rate	Cruise @3000m	Loiter Time	Landing Distance
500 meters	3.556 m/s	77.22 m/s	30 min	500 meters
1640 feet	11.67 ft/s	150kts	30 min	1640 feet

The initial stages of the Pegasus performance design process began with determining weights of the aircraft using sizing codes based on the theories of Daniel Raymer (1) and Jan Roskam (2). Once the final design configuration was chosen these codes were run and the take off gross weight of the Pegasus was determined to be 14715N (3308lb).

Once the weight of the Pegasus was determined, various aerodynamic/propulsion parameters had to be determined based largely on aircraft geometry. An aspect ratio of 4.46 and an Oswald efficiency factor of .92 were calculated giving a K value in the drag polar of .0777. A C_{Do} value of .025 was also calculated. This C_{Do} is about average as compared with other general aviation aircraft. A propulsive efficiency of 88% was assumed. Since the engine was mounted near the rear of the aircraft it was assumed that shaft losses would be somewhat minimal. The static thrust of the engine was assumed constant at 4500N (1011.64lb) and the engine's sea level specific fuel consumption was taken to be 270g/kW-hr (.44lb/hp-hr).

K.2. Maximum and Cruise Velocities

Once the initial sizing and various aerodynamic parameters had been determined, the rest of the performance characteristics were calculated through the entire mission of the aircraft. Plots of the power required and power available versus velocity were generated. It was decided that the Pegasus would cruise at approximately 80% of its maximum power, and thus power settings of 80% and 100% were used to find the cruise parameters of the aircraft at sea level and its cruise altitude of 3000m (9842.5ft). With an 88% propulsive efficiency, 100% power available from the engine is about 165kW (220hp) and 80% power available from the engine is about 132kW (176hp). Figure K.1-1 shows the power available and power required curves versus velocity at sea level.

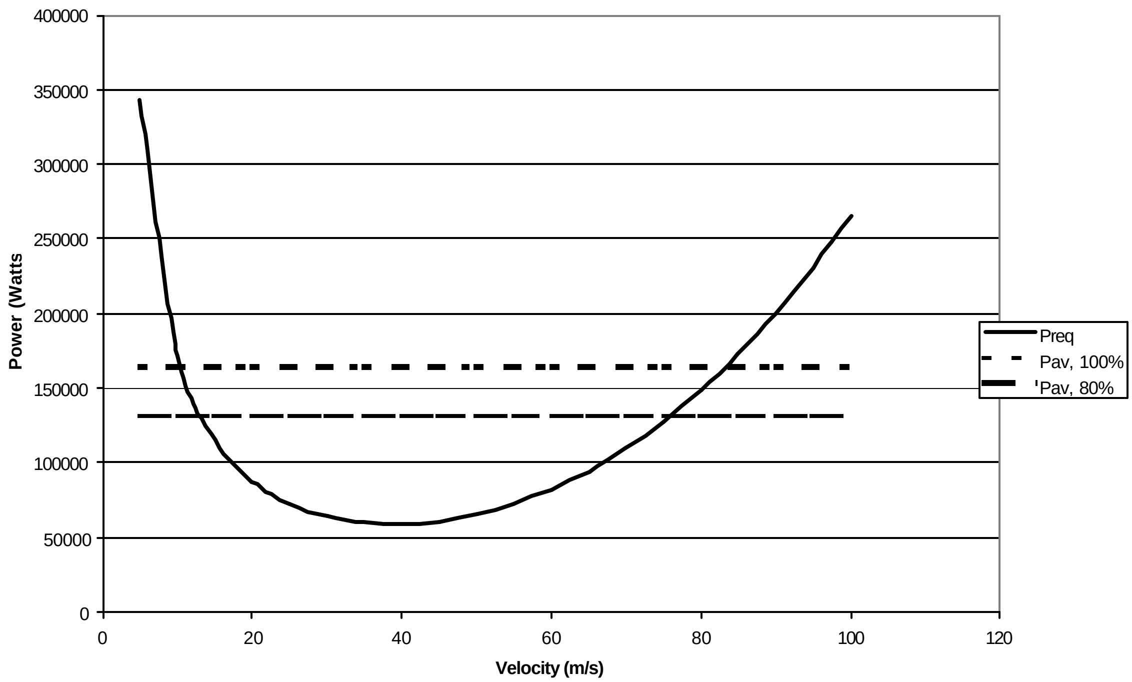

Figure K.1-1 Pav,Preq Vs Velocity At Sea Level

The curve reveals that at sea level the Pegasus cruises at 77m/s (150kts) at 80% power available. This 77m/s (150kts) cruise speed gives the Pegasus a sea level cruise C_L of .25, a sea level cruise C_D of .0298, and an (L/D) for sea level cruise of 8.4. The curve also reveals that the maximum sea level speed of the Pegasus is 84m/s (163kts).

Figure K.1-2 shows the power available and power required curves versus velocity at the Pegasus's cruise altitude of 3000m (9842.5ft).

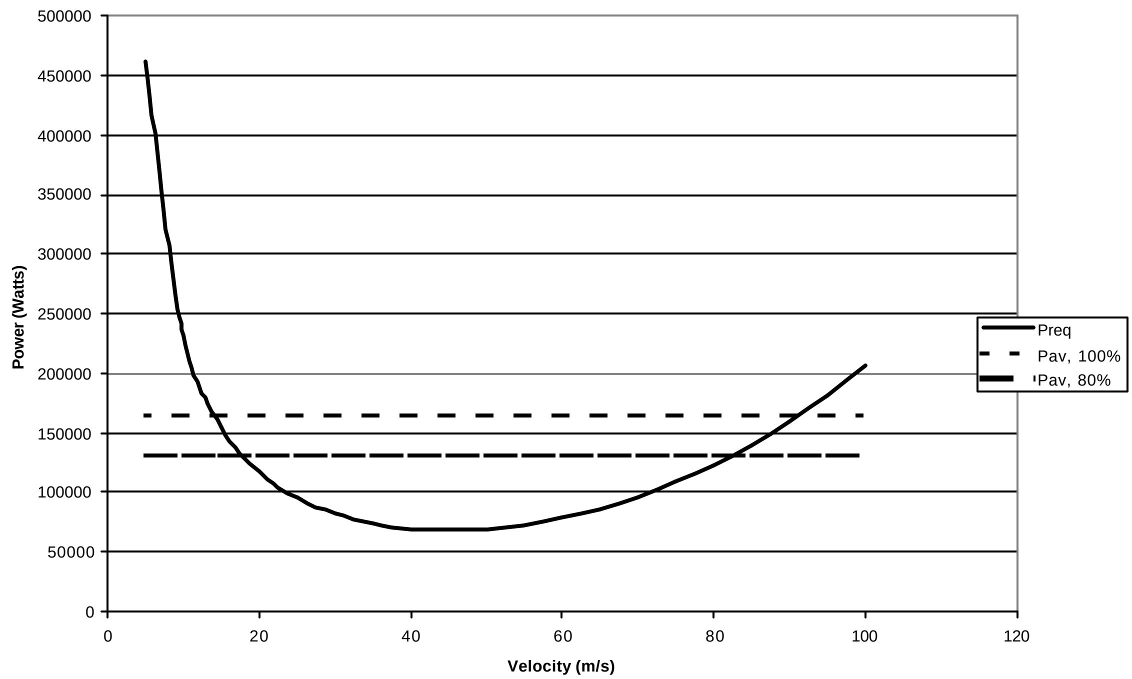

Figure K.1-2 Pav,Preq Vs Velocity At 3000m

The graph shows that at its cruise altitude the Pegasus cruises at 81m/s (157.5kts) at 80% power available, and has a maximum speed of 92m/s (178.8kts). At the cruise altitude of 3000m (9842.5ft) this 81m/s (157.5kts) cruise speed gives the Pegasus a C_L of .37, a C_D of .0338, an (L/D) of 10.9, and an angle of attack for cruise of .06 degrees. The cruise speed and maximum speed of the Pegasus exceeds that of a Cessna 182, which cruises at a speed of about 72m/s (140kts) and has a maximum speed of 75m/s (145.7kts).

The C_{Lmax} of the Pegasus is about 1.8 without flaps and 2.6 with flaps deflected to 60 degrees (see Appendix I) giving a sea level stall speed of 28m/s (55kts). These values of C_{Lmax} were a bit high largely due to the small area of the wings. To counterbalance this problem the

GA(W)-1 airfoil section was chosen for the wings due to its high lift/high C_{Lmax} capabilities. The stall angle of attack was then determined to be 19 degrees.

K.3. Take-Off

Takeoff performance was a major concern throughout the design process. Because of the plane's relatively large weight and size it was assumed the Pegasus would require long distances for takeoff. For takeoff performance a ground friction coefficient of .02 (asphalt) was assumed and a takeoff speed 20% higher than the sea level stall speed of 28m/s (55kts) was used. This takeoff velocity of 33.6m/s (65.3kts) gave a C_L for takeoff of 1.4 and a takeoff angle of attack of about 11 degrees without flaps and 6 degrees with flaps deflected to 10 degrees (see Appendix J). The required takeoff ground roll of the Pegasus was calculated to be 210m (689ft) in a time of approximately 11s. The total take off distance, ground roll distance plus the distance required to clear a 15.24m (50ft) obstacle at the end of a runway while climbing at 425m/min (1395ft/min), was calculated to be 280m (920ft) in a time of about 13s. The Cessna 182, which has a takeoff gross weight slightly lower than the Pegasus of about 13800N (3110lb) with a takeoff power of about 170kW (227hp), requires a ground roll of 230m (755ft). Thus the Pegasus once again matched the performance of the Cessna.

K.4. Climb

Another major concern throughout the design process was the Pegasus's performance in climb. The Pegasus again was able to meet the standards set in industry. Figure K.1-3 shows the plot of the Pegasus's climb rate versus velocity at sea level.

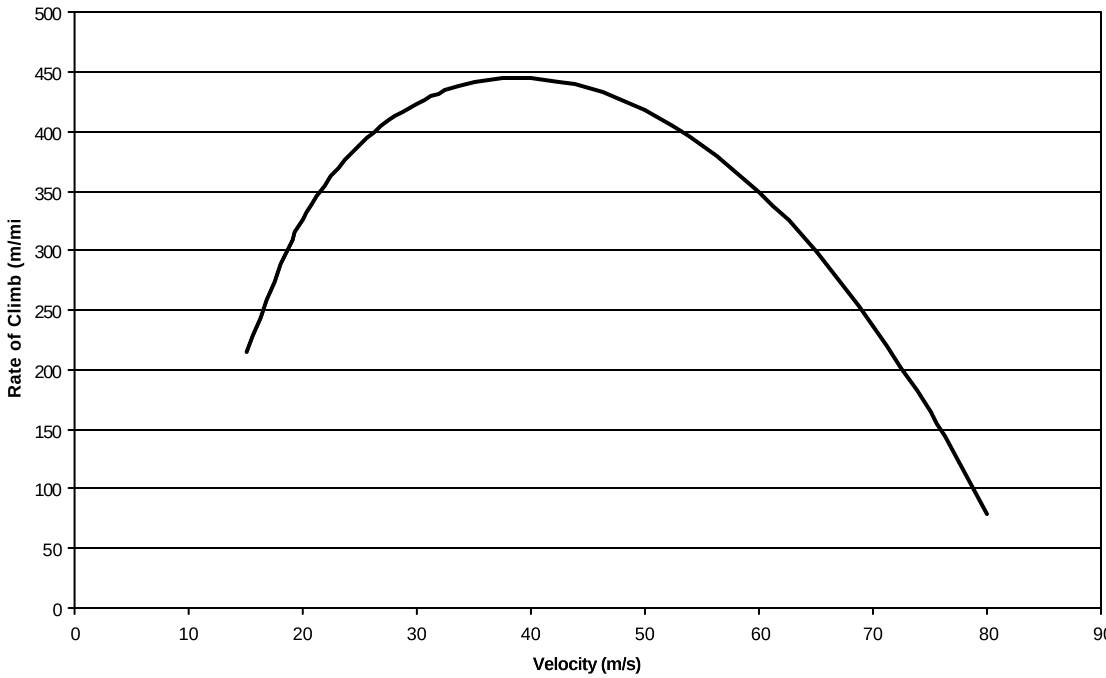

Figure K.1-3 Rate of Climb Vs Velocity At Sea Level

The maximum rate of climb of the Pegasus at sea level conditions is about 445m/min (1460ft/min) at a speed of 40m/s (77.7kts). This climb rate is very competitive in the general aviation market. Figure K.1-4 shows the plot of maximum climb rates at various altitudes. This plot reveals that the Pegasus can still climb at about 230m/min (755ft/min) through its cruise altitude of 3000m (9842.5ft) up to its absolute ceiling altitude of approximately 6600m (21650ft). The maximum climb rates of the aircraft stay somewhat high up through the cruise altitude of 3000m (9842.5ft) due to the turbo diesel engine (see Appendix H.2). The engine maintains a constant power from sea level up to about 3050m (10000ft).

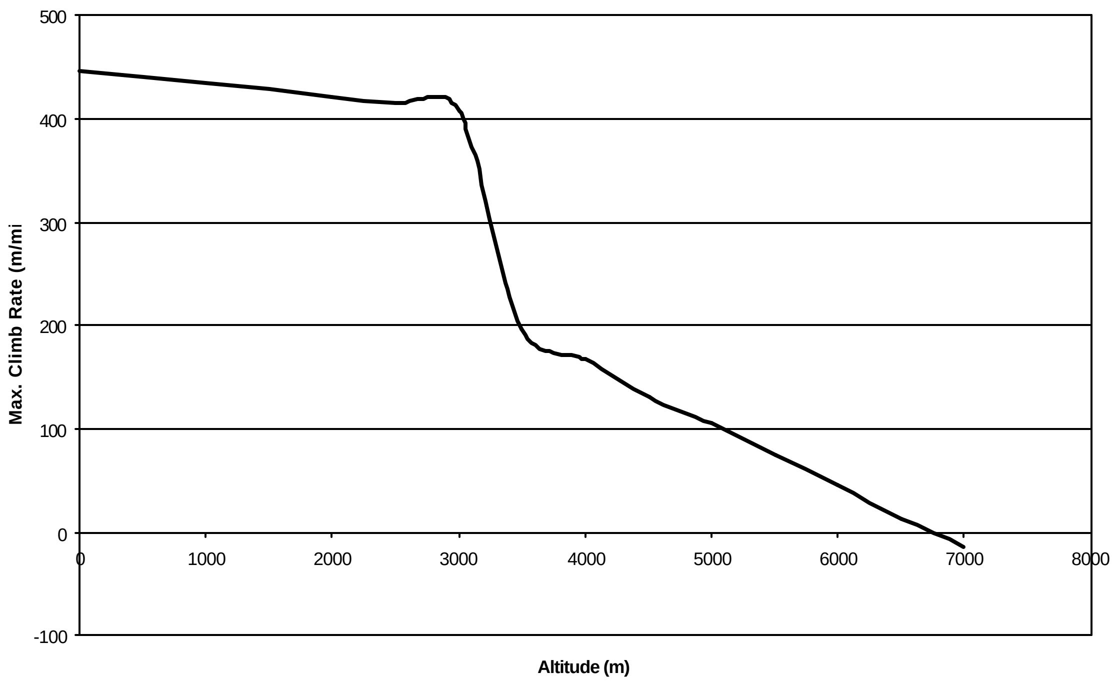

Figure K.1-4 Maximum Climb Rate Vs Altitude

K.5. Range and Endurance

Once it was determined that the aircraft would have adequate climb capability to its cruise altitude of 3000m (9842.5ft), range and endurance values were calculated to determine the efficiency and performance of the Pegasus in flight. These values were calculated first at cruise conditions and then at conditions for maximum range and endurance. In cruise the Pegasus has a range of 1528km (825nmi) and an endurance of 5.7 hours. The maximum range of the Pegasus, calculated at minimum drag conditions, is 1778km (960nmi) and its maximum endurance is 9.5 hours. These numbers are similar to current general aviation aircraft. Despite the Pegasus's relatively low aspect ratio wing and extra weight its performance met the demands of the general aviation market.

K.6. Glide and Rate of Descent

Figure K.1-5 shows the maximum engine off gliding characteristics of the Pegasus. Maximum gliding range occurs at minimum drag conditions. As the plot shows the Pegasus can glide approximately 35km (19nmi) from its cruise altitude of 3000m (9842.5ft) and over 60km (32.4nmi) from its absolute ceiling altitude of about 6600m (21653.5ft). These values may seem somewhat low as the plot was derived at the maximum takeoff gross weight of the vehicle. In flight conditions the aircraft would be able to glide farther distances at lighter weight configurations.

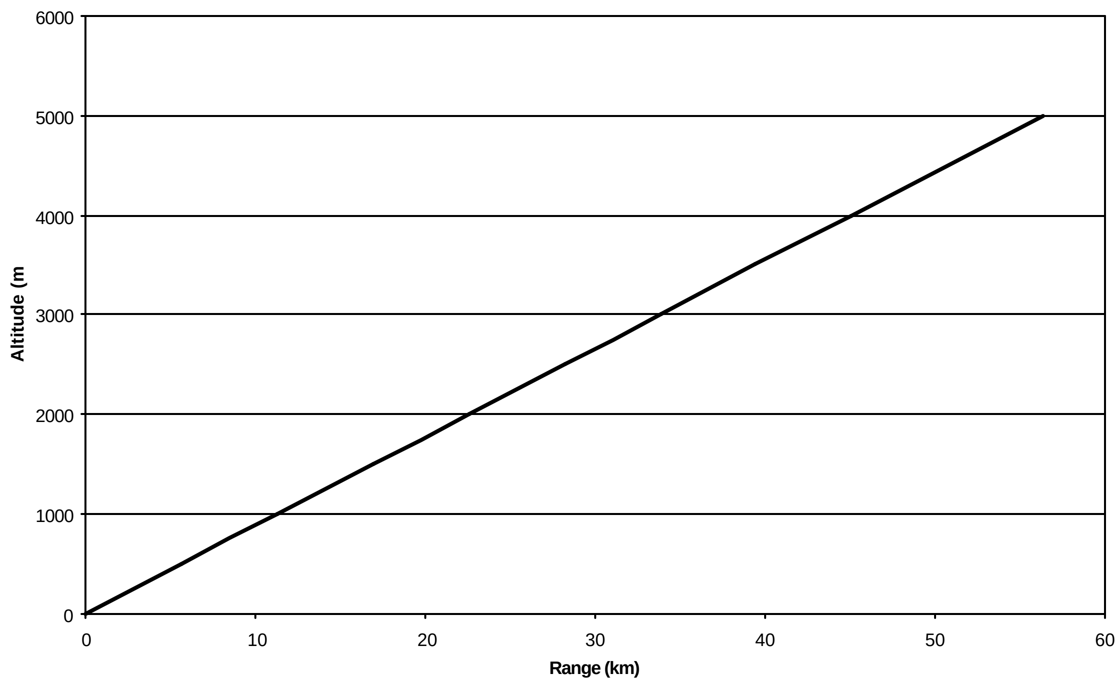

Figure K.1-5 Gliding Range (max) Vs Altitude

Figure K.1-6 shows the rates of descent of the Pegasus at various altitudes. As the plot reveals, the Pegasus descends somewhat rapidly, about 4.5m/s (14.76ft/s) from its cruise altitude of 3000m (9842.5ft) and above 5m/s (16.4ft/s) from its approximate absolute ceiling altitude of 6600m (21653.5ft). Once again these descent rates may seem high, but like the gliding ranges observed above, this plot was derived at the maximum takeoff gross weight of the vehicle. In flight conditions the aircraft would descend at slightly lower rates.

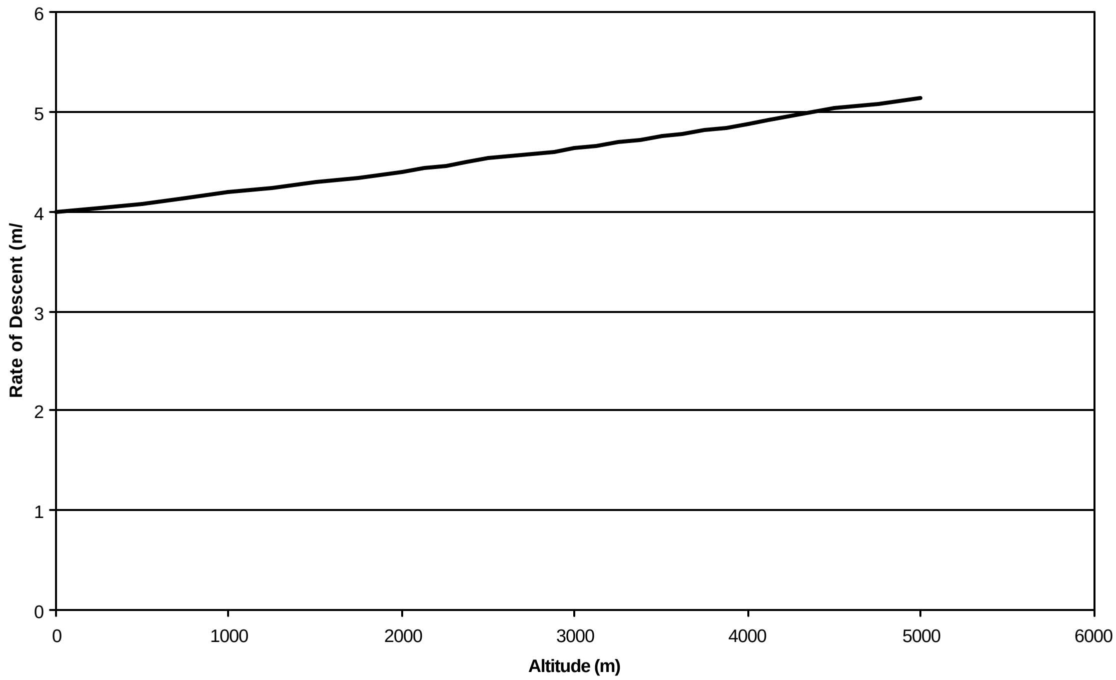

Figure K.1-6 Rate of Descent Vs Altitude

K.7. Landing

Finally the landing characteristics of the Pegasus were determined. The aircraft touches down at approximately 30% more than the sea level stall speed of 28m/s (55kts), a touchdown speed of 36.4m/s (70.7kts). This touchdown velocity gives a C_L for landing without flaps of 1.02 and an angle of attack for landing without flaps of 7 degrees. Once the touchdown speed was determined, the landing roll distance was calculated assuming once again a ground friction coefficient of .02 (asphalt) and application of brakes at 80% of the touchdown speed giving a braking friction coefficient of .5. The ground roll of the Pegasus was then calculated to be 230m

(754.6ft). The total landing distance required, the landing ground roll distance plus the distance required to clear a 15.24m (50ft) obstacle at the beginning of the runway while descending at a rate of 4m/s (see Appendix J.1.6), was calculated to be 350m (1148ft). With the deployment of 30% flaps the C_L for landing increases to about 1.1 leading to a touchdown speed of about 33.9m/s (65.89kts). The landing ground roll with flaps deflected, calculated the same as above, was 215m (705ft). The total landing distance required with 30% flap deflection was calculated to be 325m (1066ft).

From the performance data of the Pegasus it is evident that it can perform equal to or better than current general aviation aircraft. Therefore the comfort and convenience being sought by tomorrow's pilot will be attainable in the Pegasus without surrendering manageability and performance.

1) Raymer, Daniel P., Aircraft Design: A Conceptual Approach, Third Edition, 1999.

2) Roskam, Jan, Airplane Design Part V:Component Weight Estimation, 1989.

Appendix L. Aircraft Stability and Controls

When designing the Pegasus, the goal was to create a vehicle that would be competitive with any other airplane in the general aviation market. Consequently, the stability and handling qualities need to be equal or superior to those of general aviation aircraft.

Initial control surface sizing was performed using the method provided in Raymer[AAA]. The horizontal and vertical tails were optimized for dynamic stability requirements with the roadability requirement in mind. Based on empirical results in Thurston[BBB], the horizontal tail volume coefficient was sized to be greater than 0.55 and the vertical tail volume coefficient greater than 0.30. Examination of comparable aircraft led us to refine the horizontal tail volume coefficient from 0.55 to 0.35. This allows reduction of the overall length to better meet roadability requirements while maintaining acceptable stability characteristics.

L.1. Control Surface Configuration

Like the majority of general aviation aircraft the control surfaces to be used for control in yaw and pitch will be a rudder and elevator. Due to the low wingspan of the aircraft and small wing area of the aircraft combined with the need to take off and land from a relatively short runway full span flaps are required. This leaves no space for separate ailerons, so two solutions to this problem were considered. The first of these is the use of full span flaperons, and the second would be the use of spoilers.

The spoilers have a large drag penalty associated with and drastically reduce the amount of lift produced by the wing when they are deployed. This could have serious consequences when the aircraft is required to roll when at speeds close to the stall speed on landing and takeoff when a large amount of lift is required.

The other option is flaperons and the feasibility of these depends on the type of flap system used. On a small general aviation aircraft complex flap systems are not practical and the extra lift they produce is not required. In general, plain flaps are used for aircraft of this size, and they will be relatively easy to install on the telescoping wing. The plain flaps will also be suitable for use in roll control, making a plain flap system used as a flaperon a feasible solution. When landing, the amount of roll control will be reduced if the flaps are at full deflection, but by reducing the flap incidence on one wing a roll maneuver will still be possible.

General recommendations for the rudder and elevator areas suggested for a general aviation aircraft are between 25% and 45% of the respective surface areas (e.g. horizontal and vertical tails). This aircraft will not need to perform rapid yaw and pitch maneuvers and a large control surface area will also produce more drag so 45% of the area will not be used. The plane does have fairly short moment arms to the tail so a 25% control surface will be too small. This suggests that an area of 35% of the vertical tail for the rudder size, and 35% of the horizontal tail surface for the elevators are sensible values.

When calculating the required area for the flaperons a smaller area is suggested. Due to the need for roll ability when travelling at low speeds with the flaps extended, is essential to make sure that at stall the flap is not fully extended. The suggested maximum size for flaps is 35% of the wing area but again due to drag penalties associated with control surfaces, this size flap will not be ideal. So a compromise on flap size suggests that full span flaperons at 20% of the wing area will be used.

In both the yawing and pitching modes the aircraft will be required to be trimmed, so that if flying in a strong crosswind or if a desired incidence is to be flown the pilot will not have to keep the control surfaces held at a small deflection. This function is normally achieved with the aid of trim tabs. These are small sections at the rear of the main control surface, which can be set to a different deflection to the rest of the control surface. This means that small changes to yaw or pitch can be made without the necessity of continual control pressure. Since this aircraft has no need to roll at a constant rate for a prolonged period of time and the complexity they would add to the telescoping wing, it was decided that trim tabs on the flaperons would not be required and would add structural complications to the telescoping section.

L.2. Longitudinal Static Stability

Size constraints dominated the center of gravity (CG) limits. The aft limit without fuel, baggage or pilot resides at -8.53% of the mean aerodynamic chord (MAC) giving positive pitch static stability margins ($K_n = h_n - h$) of 36.4% during takeoff and 36.2% at cruise. This provides ample static stability.

The longitudinal static stability parameters for takeoff, cruise and landing were measured from Figures J.6-1 and J.6-2. Table L.2-1 provides calculated values for cruise and takeoff conditions. The pitch derivative ($C_{m\alpha}$) is stable when negative.

Table L.2-1 Longitudinal Stability Parameter Data

Flight Conditions	Cruise	Takeoff	Landing
Altitude (m)	3000	0	0
Density (kg/m^3)	0.909	1.226	1.226
Mach Number	0.237	0.1363	0.1477
$C_{m\alpha}$	-0.279	-0.140	-0.140

L.3. Longitudinal Dynamic Stability

The Pegasus was analyzed for longitudinal dynamic stability using the method suggested by Render.[1] Results meet the Military Specification 8785C level 1. Level 1 implies that the aircraft has satisfactory flying characteristics with no more than minimal pilot compensation.

Table L.3-1 provides calculated values of damping ratio (ξ_d) and undamped natural frequency (ω_n) for cruise, takeoff and landing conditions. Table L.3-2 provides calculated values of damping ratio (ξ_d) and time constant (τ) for cruise, takeoff and landing conditions.

Table L.3-1 Short period results

Short Period Pitching Oscillation				
Flight Conditions	Cruise	Takeoff	Landing	Mil Spec
ξ_d	0.350	0.574	0.573	0.35 - 1.3
ω_n	3.758	1.358	1.358	N/A

Table L.3-2 Phugoid results

Phugoid				
Flight Conditions	Cruise	Takeoff	Landing	Mil Spec
ξ_d	0.116	0.107	0.060	> 0.04
τ	109.2	48.0	48.0	N/A

L.4. Lateral-Directional Static Stability

The lateral-directional static stability parameters were calculated using aircraft geometry equations from Lutze[2] and Etkin[3]. Table L.4-1 provides calculated values for cruise and takeoff conditions. The directional stability parameter ($C_{n\beta}$) is stable when positive, the roll stability parameter ($C_{l\beta}$) is stable when negative.

Table L.4-1 Lateral-Directional Stability Parameter Data

Flight Conditions	Cruise	Takeoff	Landing
Altitude (m)	3000	0	0
Density (kg/m^3)	0.909	1.226	1.226
Mach Number	0.237	0.1363	0.1477
$C_{n\beta}$	0.0702	0.1020	0.0926
$C_{l\beta}$	-0.0269	-0.0311	-0.0302

L.5. Lateral-Directional Dynamic Stability

The Pegasus was analyzed for lateral-directional dynamic stability using the method suggested by Render,[1] data from Engineering Sciences Data Unit (ESDU) data sheets and the static derivatives of Appendix L1.4. Results meet the Military Specification 8785C level 1 except for the Dutch roll mode which meets level 2. Level 1 implies that the aircraft has satisfactory flying with no more than minimal pilot compensation. Level 2 implies that the aircraft has acceptable flying qualities with some increase in pilot workload or degradation in performance. Category B covers normal flight operations including climb and descent. Category C covers takeoff and landing operations.

Table L.5-1 provides calculated values of time to half amplitude ($t_{1/2}$) and time constant (τ) for cruise, takeoff and landing conditions. Table L.5-2 provides calculated values of time to double amplitude (t_2) for cruise, takeoff and landing conditions. Table L.5-3 provides calculated values of time to half amplitude ($t_{1/2}$), undamped natural frequency (ω_n), damping ratio (ξ_d) and the product of natural frequency and damping ratio for cruise, takeoff and landing conditions.

Table L.5-1 Roll subsidence results

Roll Mode				
Flight Conditions	Cruise	Takeoff	Landing	Mil Spec
$t_{1/2}$	0.067753	0.1157	0.118949	N/A
♦	0.097748	0.1669198	0.171607	< 1

Table L.5-2 Spiral Mode Results

Spiral Mode				
Flight Conditions	Cruise	Takeoff	Landing	Mil Spec
t_2	72.90252	16.748788	18.1028	> 20 (Cat. B) > 12 (Cat. C)

Table L.5-3 Dutch roll results

Dutch Roll Mode				
Flight Conditions	Cruise	Takeoff	Landing	Mil Spec
$t_{1/2}$	6.345887	10.67685	10.67685	N/A
♦	1.527954	2.4756845	2.598842	N/A
♦ n	4.113608	2.5379588	2.417687	> 0.4
⌘d	0.026562	0.0255798	0.026852	> 0.02
♦ n⌘d	0.109266	0.0649206	0.064921	> 0.05

L.6. Control and Hinge Moment Stability

The hinge moment is a useful quantity giving guidance about the moments on the control surface and therefore how easy they will be to deflect and how capable the aircraft will be when sustaining a constant yaw or pitching maneuver. To calculate this value ESDU data sheet 89009 (REF [4]) has been used. Several other data sheets have been used and these are identified in the method described below. This calculation described the hinge moment for an unbalanced elevator. It was originally for a plain flap, but plain flaps, rudders and elevators can be modeled in the same way.

Below is the nomenclature list used in the hinge moment equation.

A = aspect ratio

a_1 = lift curve slope with angle of attack

a_2 = lift curve slope with control deflection

b_1 = change in hinge moment due to incidence

b_2 = change in hinge moment due to control deflection

Δb_1 = change in b_1 due to induced camber

C_H = hinge moment coefficient

C_L	=	lift coefficient
c	=	wing chord
F_B	=	factor on induced camber contributions to allow for control balance
G1,G2,G3	=	functions used in induced camber contributions
t	=	maximum thickness
α	=	incidence from zero lift angle
δ	=	control deflection (downwards is positive)
$\Lambda_{1/4}$	=	sweep angle of wing quarter chord line
Λ_h	=	sweep angle of control hinge line
τ	=	the trailing edge angle(assumed to be 15 degrees)
τ_b	=	the trailing edge angle found by associating it with the thickness of the airfoil at 95% and the thickness at 99% and calculating the angle from these two points
x_t	=	the clockwise location of boundary layer transition (assumed to be 0.3)

The subscript T denotes values for incompressible inviscid flow

The superscript $*$ denotes properties for a standard airfoil section

The subscript 0 denotes two dimensional values.

STEP 1: The first step is to find a value for the two dimensional lift curve slope $(a_1)_0$ for the relevant control surface, which is found from REF[5].

$$\frac{(a_1)_0}{(a_1)_{0T}} = \frac{0.1 + (1.05 - 0.5x_t \,/\, c)\tan(\tfrac{1}{2}\boldsymbol{t}\ )}{(\log_{10})^{[1-2.5\tan(\frac{1}{2}t_a)]}}$$

$$(a_1)_{0T} = 2\boldsymbol{p} + (4.75 = 0.02\boldsymbol{t})\, t/c$$

This then enables a value for $(a_1)_0$ to be found, for a general airfoil.

STEP 2: Next a value for $(a_2)_0$ which is the two dimensional lift curve slope with control surface deflections, this is found by using data from REF[6].

$$C_L = (a_1)_0[\alpha + \delta(a_2)_0/(a_1)_0]$$

As $(a_1)_0$ is known for the wing or reference surface which means that C_L will be able to be found, and hence $(a_2)_0$.

STEP 3: Next $(a_1)_0^*$ and $(a_2)_0^*$ have to be found. These are done by using the same method as in steps 1 & 2. The only difference is instead of using τ a value called τ' is used which is given by:

$$\tau' = 2\tan^{-1}(t/c)$$

STEP 4: Using REF[7] $(b_1)_0$ must be determined, this value is the rate of change of hinge moment coefficient with incidence for a two dimensional airfoil.

$$(b_1)_0 = (b_1)_0^* + 2[(a_1)_{0T}^* - (a_1)_0^*](\tan \tfrac{1}{2}\tau_b - t/c)$$

The coefficient of $(b_1)_0^*$ is found by two graphs (figures 1 & 2) in REF[7] which uses t/c, c_f/c and $(a_1)_0^*/(a_1)_{0T}^*$.

STEP 5: Using the same procedure as in 4 but using $(a_2)_0^*/(a_2)_{0T}^*$ instead of $(a_1)_0^*/(a_1)_{0T}^*$, a value for $(b_1)_0$ can be found. The coefficient $(b_2)_0$ represents the rate of change of control hinge moment with control surface deflection. The subscript 1 denotes changes due to incidence, and the subscript two represents changes due to control surface deflection.

For this estimation a plain unbalanced control surface is being used, this means that the values obtained in steps 4 & 5 for $(b_1)_0$ and $(b_2)_0$ will be the actual values for the control surfaces.

STEP 6: According to REF[4] the next step to this calculation is to find a $dC_L/d\alpha$ for the relevant control surface. This is however not required in this case as this value has already been estimated in Appendix I 1.4.3, which gives a $dC_L/d\alpha$ of 3.2 per radian.

STEP 7: Next functions G1 and G2 have to be calculated, these two functions have little significance in direct terms with the aircraft but are needed in the calculation for the induced camber contribution. The full span induced camber contribution parameter can be found from figure 1 for REF[4], and also equals the following:

$$= \frac{2pbG_1}{F_B (a_1)_0 \cos\Lambda_h}$$

From REF[4] figure 3 it is possible to find out the part span induced camber contribution parameter, which is equal to the following:

$$= \frac{2pbG_2}{F_B (a_1)_0 \cos\Lambda_h}$$

From figure 4 found in REF[4] the further part-span induced camber contribution can be determined, this is also equal to the below equation.

$$= \frac{2pbG_3}{F_B (a_1)_0 \cos\Lambda_h}$$

STEP 8: Calculate the hinge moment coefficient derivatives b_1 and b_2. The first part of this is to calculate the contribution to induced camber Δb_1.

$$\Delta b_1 = G_1 + G_2$$

Therefore the hinge moment coefficient derivative b_1 or $\partial C_H/\partial\alpha$ is given by:

$$b_1 = \frac{(b_1)_0}{(a_1)_0}\left(\frac{dC_L}{d\alpha}\right)\cos\Lambda_h + \Delta b_1$$

The other hinge moment coefficient derivative b_2 or $\partial C_H/\partial\delta$ is given by:

$$b_2 = \left[(b_2)_0 - \frac{(a_2)_0}{(a_1)_0}(b_1)_0\right]\frac{\cos\Lambda_h}{(\beta^2 + \tan^2\Lambda_{1/4})^{1/2}} + \frac{(a_2)_0}{(a_1)_0}(b_1 + G3)$$

Using the above method to calculate a value for b_1 for the rudder a value of 0.445rad^{-1} was found. For a steady hinge moment throughout a maneuver and so that control power demand is not excessive, a maximum value of 0.33 is normally recommended, thus the above value is high. This means that the assumption that an unbalanced control surface would be used is not realistic, and some form of control balance will have to be utilized to limit the plane's hinge moment.

Remedy for control problem

For large control surface deflections and at speeds approaching the maximum velocity the control surfaces will require large forces to turn them. For this aircraft which will use a fly by wire system with no mechanical linkage to the control surfaces, the rudder and elevator will be powered by actuators. This means that large hinge moments will be feasible, as the actuators will still be able to deflect the control surfaces. It will be a good idea though to minimize the hinge moments as this will reduce the power needed to be produced by the actuator resulting in a smaller actuator and less electrical power required. The smaller actuator will be achieved by balancing the control surfaces to reduce the hinge moment. There are several different ways to balance a control surface, these are an overhanging balance, internal balance, beveled trailing edge and tabs.

The overhung balance is often used in small airplanes due to its simple concept. The hinge is positioned so that it pivots at about 30% of the control surface chord, so that at high deflection there will not be such a high moment about the hinge due to the trailing edge being 70% of the chord behind the hinge rather than 100% for an unbalanced wing. This results in a smaller distance that the control surface force acts about. By using a rounded leading edge on the control surface, and then leaving the gap between the airfoil section will also reduce the moments but this reduction will be due to a frictional increase producing an opposing moment to the hinge moment. This will however increase the profile drag produced by the wing, which is not desirable.

The next option is the internal balance, which is sealed completely inside the control surface. Like the overhung balance a moment is produced which is in the opposite rotation to the hinge moment, having the resultant effect of reducing the hinge moment. The overhung balance can produce non-linear characteristics even at relatively small deflections, where the internal balance does not have this problem. The greatest problem with the internal balance is it interferes with the structure inside the control surface. Because the wing that this system will be installed upon will be telescoping, the structure will have to be hollow. As the flaperons will have to retract together, the insides of the control surfaces will also have to be hollow consequently there will be no room inside the flaperons to house the internal balance.

The next balance is the beveled trailing edge, which is the simplest form of control balance. By increasing the angle that the top and bottom surfaces of the control surface at the trailing edge the hinge moment can be slightly reduced. This method is generally only utilized in conjunction with another balance solution unless only a small amount of hinge moment reduction is required. The characteristics of the beveled edge balance are always non-linear unless the control gap is sealed, which would be difficult for the telescoping wing. When manufacturing this type of control balance, it is not always possible to achieve the desired trailing edge angle, even though structurally this would not be a problem. The mean chord for the control surface would be effectively reduced due to the implementation of a beveled edge balance, which would reduce the effectiveness of the control surface.

There are two types of tabs available, these are a servo tab and a balanced (geared) tab. Both of these tabs utilize the same method to reduce the hinge moments. Both tabs have an independently hinged surface over the rear 20% of the control surface. These tabs can be deflected in the opposite sense to the rest of the control surface producing a small force in the opposite direction to the hinge moment. Because this force is acting at a relatively large moment arm from the control surface hinge, a large moment is produced opposing the hinge moment, with the resultant action of reducing the hinge moment. The main difference between the geared tab and the servo tab is that the pilot's input to the control surface deflection is applied directly to the tab with the servo tab, and with the geared tab it is applied to the main control surface. This is shown below in Figure L.6-1 with the balanced tab on the left and the servo tab on the right.

Figure L.6-1 Diagram of geared tab and servo tab

These tabs are very effective at reducing the hinge moments without seriously degrading the effectiveness of the control surface, as long as the rear tab does not get much larger than about 20% of the control surface chord. Like many other solutions to the balance of the control surfaces this method fails when the feasibility of it when installed on telescoping wing. Even though it would not be impossible to set up a geared, or servo tab it would be very complicated and would not be necessary for an aircraft of this size with it's required maneuver rates.

Taking all of these factors into account about the advantages and disadvantages of each form of control balance, a simple overhung balance will be used. This can be used in conjunction with other balances such as the beveled trailing edge but this should not be required. By recalculating the hinge moment with the overhung balance it will be possible to find out if the balance will be effective in reducing the hinge moment to a magnitude of less than 0.3. The overhung balance due to its simple concept will be easily adaptable for use on the telescoping wing.

L.6.1. Changes in hinge moment due to control balance

The control balance reduces the hinge moment by reducing $(b_1)_0$ and $(b_2)_0$, and hence b_1 and b_2. The method for carrying out this reduction was found from REF[GGG] and is outlined here. For an overhung control surface the two graphs labeled figure1 and figure 2 in REF[GGG] are all that is needed. The greatest reduction in hinge moments is achieved for a rounded control surface leading edge, so that is what will be used.

These new values of $(b_1)_0$ and $(b_2)_0$ are then used in step 8 of the previous calculation.

These yield a value of b1 = -0.0786 for the elevator (as this is full span there is no b2). For the rudder b_1 = -0.159 and b_2 = -0.112. These values are both small enough to be feasible to be controlled by the actuators, allowing a steady pitch and yaw rate.

1) Render, P.M. Aircraft Stability & Control. Loughborough University, 1999.

2) http:// aoe.vt.edu/~lutze/AOE3134

3) Etkin, Bernard, and Lloyd Duff Reid. Dynamics of Flight: Stability and Control. 3rd Ed, 1996.

4) ESDU data sheet 89009

5) ESDU data sheet W.01.01.05

6) ESDU data sheet C.01.01.03

7) ESDU data sheet C.04.01.01

Appendix M. Roadability

M.1. Introduction

The Road Vehicle Design Specification addresses all issues that affect the ability of the designed vehicle to travel safely and legally on the road, meeting or exceeding all regulations and requirements.

Given that the design is for a roadable aircraft, a concern for the roadability of the vehicle must underlie all design activities. This underlying concern is clearly evident in the evolution of the vehicle configuration to a baseline level; the baseline design was arrived at as a result of continuous trade-offs between road and air vehicle requirements.

Upon progression from the baseline to the detailed design stage, the project group formed a number of sub-groups with specific objectives. Each of these sub-groups was responsible for addressing both the air and the roadable components of their agenda. The roadability sub-group was responsible for developing all components of the vehicle relating specifically to travel on the road. The Road Vehicle Design Specification can be sub-divided into three main areas:

- Design and integration of the road systems of the vehicle including steering, brakes, and suspension / landing gear.
- Calculation of the vehicle performance in terms of velocities, acceleration, braking, handling, and rollover.
- Proof that the vehicle will meet US and EC transport regulations and standards.

M.2. Road Systems Design

The road systems are those components that directly affect the ability of the vehicle to drive safely on the road; namely the steering, suspension, and brakes.

The road systems serve a dual purpose; firstly as the vehicle suspension, steering and braking systems when in road configuration, and secondly as the vehicle undercarriage when in flight configuration. In order to meet the requirements of both cases it was necessary to make trade-offs in order to optimize the system to provide adequate performance in both configurations. The main considerations for each configuration are tabulated below in table M.2-1.

Table M.2-1 Configurations Considerations

ROAD CONFIGURATION	**FLIGHT CONFIGURATION**
Safety	Absorption of landing loads
Stability & Handling	Ground Stability
Passenger Comfort (ride)	Ground Clearance
Vehicle Lift	Wing Incidence on take-off

The road systems design is biased towards the road configuration due to the complex loadings that must be accounted for in this configuration. In most cases, such as braking and steering, the design for the road exceeds the similar requirements for the air. The suspension represents the greatest challenge and this has been the object of a large proportion of the design efforts.

M.2.1. Wheels/Tires Selection

The tire selection was based on a hybrid between car and aircraft tires. Major considerations were the package size and weight, cornering stiffness (for road handling), and tire deflection (for landing load absorption).

In order to provide suitable performance in the road configuration it was necessary that the rear tires had greater cornering stiffness than the front tires; this was achieved by increasing the rated load index of the rear tires through increasing the section width. This led to section widths of 165mm at the front, and 175mm at the rear. The aspect ratio was a compromise between a low aspect ratio for good cornering stiffness and low rolling friction, and a high aspect ratio to provide maximum tire deflection for landing (Eqn M-1):

(M-1) Aspect Ratio, AR = (Section Height / Section Width) * 100

An aspect ratio of 75% was chosen as a compromise, based on an analysis of car and aircraft tires. To keep the rolling radius of front and rear tires as close as possible, the rear tires have a rim diameter of 13”, and the front tires a rim diameter of 14”. The tire construction is radial, as radial tires represent “the only means of satisfying the increasingly variegated range of operating capabilities demanded of the tires used on today’s passenger cars and heavy commercial vehicles”[1]. This leads to a tire designation of P165/75 R14 (Load Index = 81) for the front tires, and P175/75 R13 (Load Index = 85) for the rear tires (based upon Pirelli P2000’s). The tire pressure was designated as 24psi, front and rear.

The wheels were chosen on the basis of minimum weight and hence TSW Imola alloy road wheels were selected.

M.2.2. Suspension Design Requirements

The suspension was designed according to the following requirements :

- Provide adequate wheel clearances across the load range, in all modes,
- Provide adequate clearance for the flaperons at full deflection,
- Limit package size,
- Maintain minimal wing incidence in road configuration, especially at low weights,

- Provide adequate load absorption for road and landing cases,
- Give good ride response, with similar frequencies front and rear
- Optimize cornering performance to produce understeer across all loading conditions.

The design process was iterative, with minor modifications being made to the geometry and spring design to optimize the vehicle and suspension performance according to the above requirements.

The suspension system operates in four modes; the suspension configuration for each mode is:

Road : The suspension is optimized for road travel.

Take-Off : Rear wheels retract slightly to increase wing incidence by 1°.

Flight : The suspension semi-retracts into the fuselage to reduce drag, whilst still allowing a small amount of the wheel to protrude in case of an emergency landing scenario.

Landing : The suspension fully extends due to the force of the spring and the variable damper is set to provide optimal shock absorption for touch-down.

M.2.3. Suspension Configuration

The front suspension is of an upper wishbone configuration with the lower arm attached to a longitudinal torsion bar (see Figure M.2-1). The two prongs of the upper wishbone and the torsion bar are attached to the vehicle structure. The stub axle / steering swivel are connected to the arms by ball joints. The damper is located on the lower arm and runs between the two prongs of the upper wishbone to attach to the vehicle structure, via a screwjack.

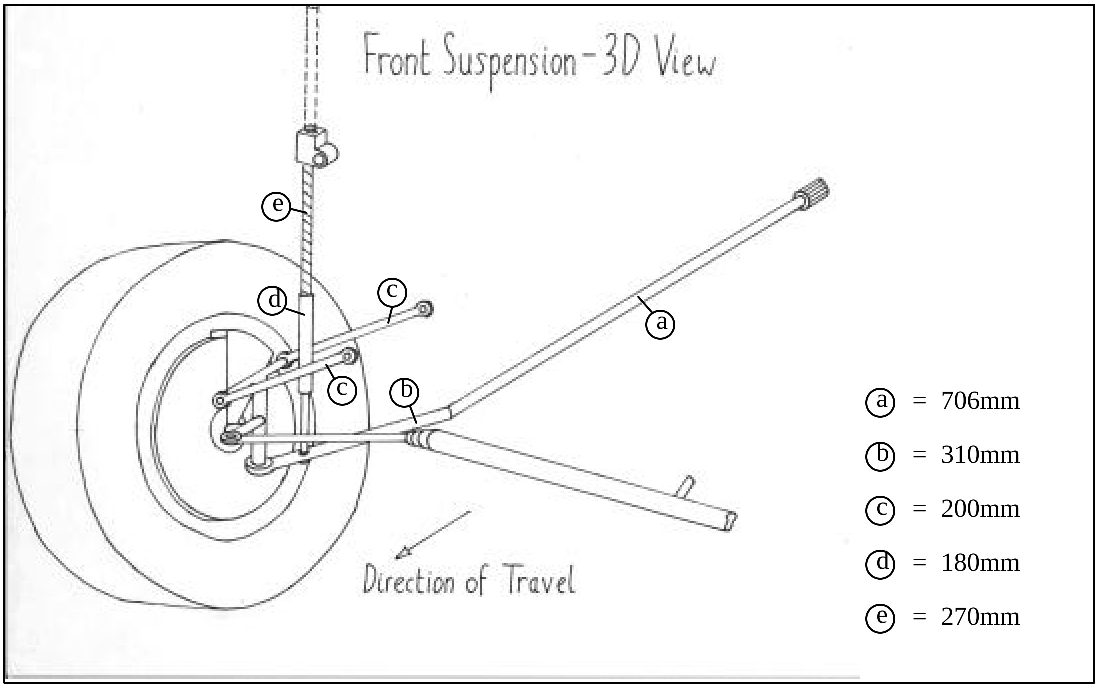

Figure M.2-1 Front Suspension

The rear suspension is of a trailing arm configuration (see Figure M2-2) with a spring/damper unit attached close to the wheel. Given the limited package requirements at the rear wheels the trailing arm attachment is mounted as low as possible. For take-off the rear suspension retracts by 70mm to provide an additional 1° of wing incidence.

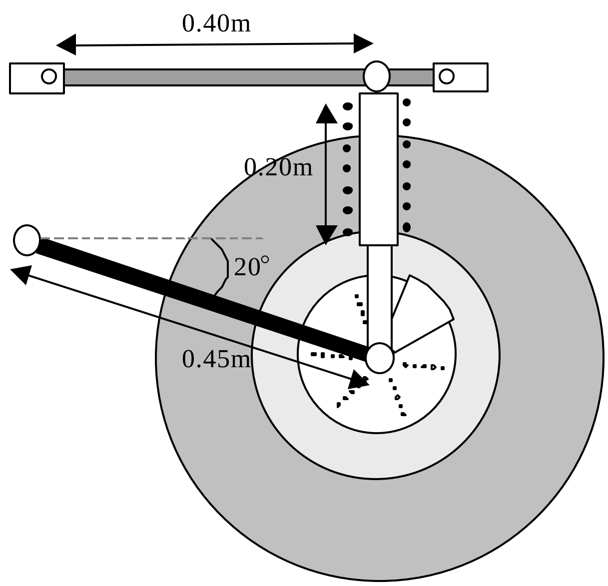

Figure M.2-2 Rear Suspension

The ground clearances, across the load range, in the different modes are as follows in table M.2-2:

Table M.2-2 Ground Clearences

GROUND CLEARANCES		
Mode	**Front (mm)**	**Rear (mm)**
Road	349 – 400	368 – 400
Take-Off	349 – 400	298 – 330
Flight	200	200
Landing	470	500

M.2.4. Damping

Active dampers provide variable damping for the front and rear suspension. This system operates by using a solenoid valve to control the rate of flow of damping fluid and hence alter the damping ratio. The variable damping ratio allows the performance of the vehicle to be optimized when in the road configuration. More importantly, the active damping allows the damping ratio to be varied between the different requirements of the road case and the landing case.

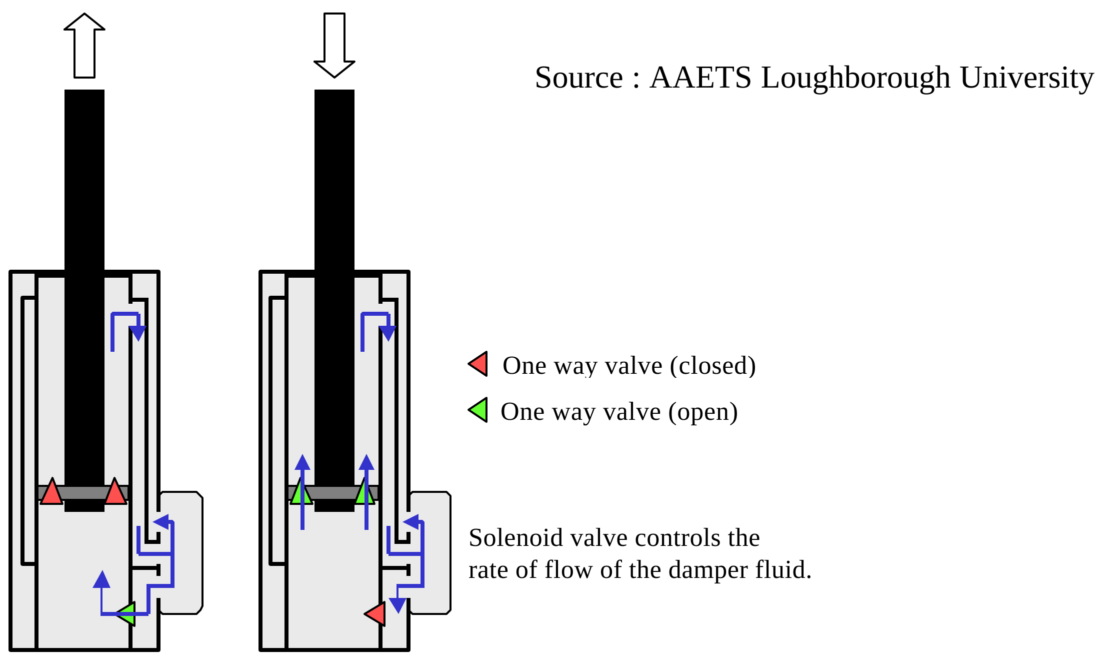

Figure M.2-3 Front and Rear Dampers

The front and rear dampers are used to semi-retract the wheels in flight (refer to figures M2-1 and M2-2). The dampers are connected to the vehicle structure via screw jacks, which allows the damper, and hence the whole wheel unit, to be semi-retracted. The screw jacks are electrically powered with a manual back-up. Each front damper is connected to a single screw jack mounted close to the vertical. Each rear damper is mounted to a longitudinal sliding arm, operated by the screw jack.

The damper lengths may be determined from the maximum suspension deflection divided by the spring ratio (for the damper), giving lengths 0.18m (front) and 0.20m (rear).

M.2.5. Landing Deflection

The aircraft is designed to touch down rear wheels first. The minimum leg deflection was calculated using Eqn's M-2 to M-4:

(M-2) $$KE = Wv^2 \big/ 2g = \boldsymbol{h}.nW\boldsymbol{d}$$

(M-3) $$\boldsymbol{hd} = v^2 \big/ 2ng$$

(M-4) $$\boldsymbol{hd} = \boldsymbol{h}_{tyre}\boldsymbol{d}_{tyre} + \boldsymbol{h}_{leg}\boldsymbol{d}_{leg}$$

A maximum descent velocity for a civil aircraft of 3.05 m/s[XXXM5], and a minimum value for n of 3, were used. The tire efficiency η_{tire} = 0.47[XXXM5], and damper efficiency η_{leg} = 0.65 (estimated). Hence, the vertical travel for the rear suspension arm is required to be at least 0.14m (5.5 in.) to absorb the kinetic energy of landing; given that the damper length is 0.20m this is ample.

M.2.6. Front Geometry and Spring Design

The suspension was optimized through varying the deflection (and hence the wheel rate), and the lower arm length and angle. An initial evaluation, based upon a maximum bump acceleration of 0.5g @MTOW[3] and a maximum shear stress of 800N/mm^2 [4], gave an optimal value for the lower arm length of 0.31m (12.2 in). A ground clearance of 400mm (15.7 in) was chosen as a compromise between the opposing requirements of road and flights operations. Using the values for ground clearance and lower arm length the lower arm angle was determined as 33°. A negative swing arm suspension geometry[3] was initially chosen to reduce the loads on the torsion bar. However, in order to provide good cornering performance it was necessary to raise the front roll center, and hence the geometry was modified to inclined parallel links[3]. With this information the geometry was defined, as shown in the following diagram :

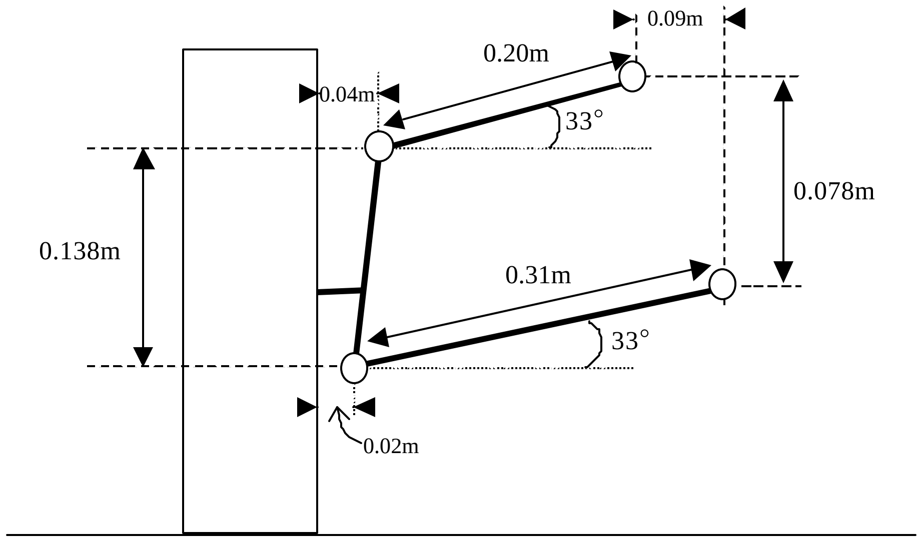

Figure M2-4 (not to scale)

A target value for the wheel rate was estimated from the lateral load transfer performance calculations (see Section M3.9). The suspension static deflection was then optimized, front and rear, to reach a compromise between this requirement and the ground clearance requirements.

The torsion bars were designed using the method described by Dunn[2], summarized in Eqn's M-5 to M-11:

(M-5) $$k_w = \frac{W}{\boldsymbol{d}}$$

(M-6) Ride Frequency, $$\lambda = \frac{1}{2\boldsymbol{p}}\sqrt{\frac{gk_w}{W}} = \frac{1}{2\boldsymbol{p}}\sqrt{\frac{g}{\boldsymbol{d}}}$$

(M-7) $$\frac{T}{J} = \frac{G\theta}{L} = \frac{\tau}{r}$$

(M-8) $$d = \sqrt[3]{\frac{16T}{\pi\tau}}$$

(M-9) $$L = \frac{G\theta \;\; \pi d^4/32}{T}$$

(M-10) $$T_{SL} = R_L a = W_{SL} R_{S.SL}$$

(M-11) $$k_\theta = k_W R_{S.SL}{}^2 + T\frac{dR_S}{dX}$$

Based upon this method, the wheel rate k_W of the front suspension is 29.43N/mm giving an acceptable ride frequency of 1.44Hz, at MTOW, and the following deflections:

Min Operating Weight	-	70.0mm (2.76 in.)
Max Take-Off Weight	-	120.5mm (4.92 in.)
0.5g Bump Acceleration	-	180.7mm (7.13 in.)

Given the geometry of the front suspension the force diagram is as follows (not to scale):

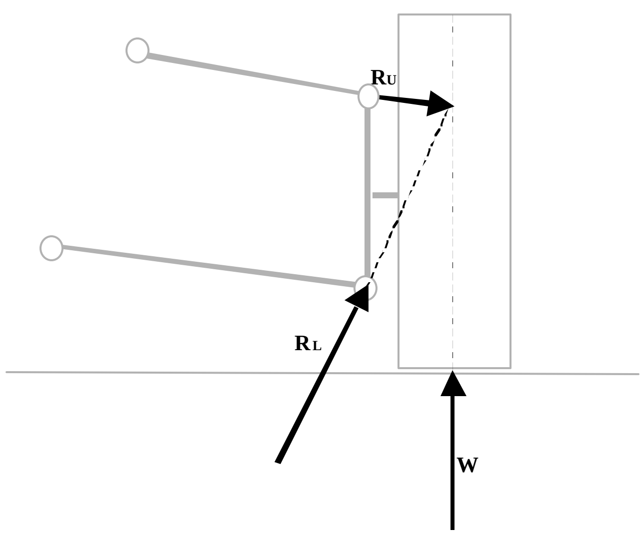

Figure M.2-5 Front Suspension

From the above diagram the angles between the force lines, termed α,β, and δ may be determined. The static deflection at MTOW is used to calculate the suspension geometry for this condition :

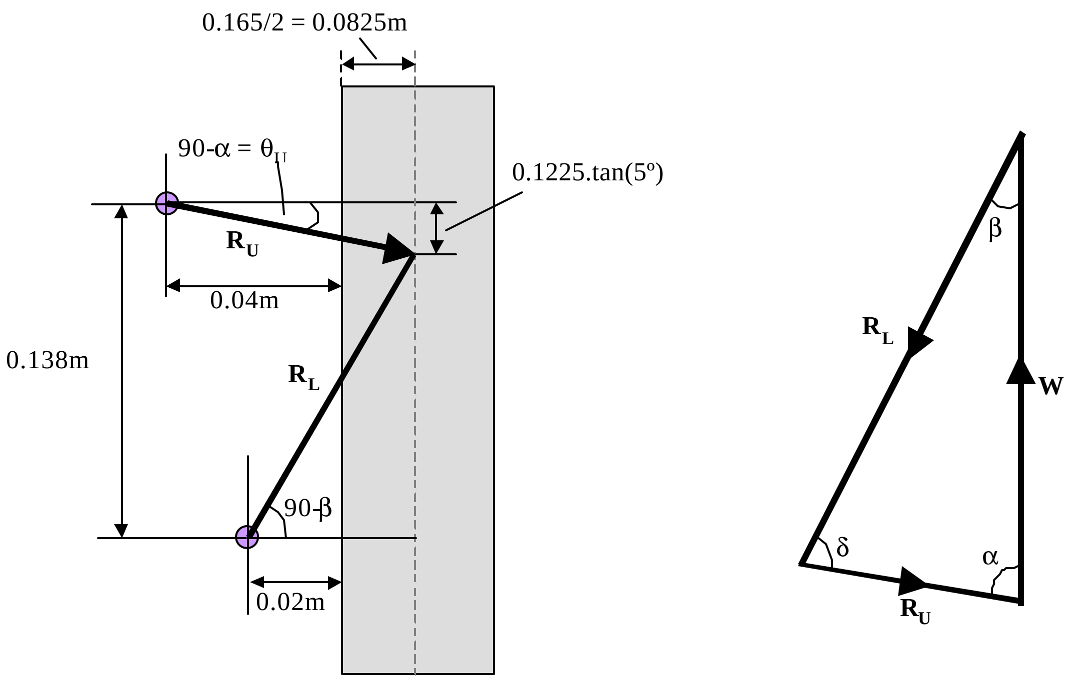

Figure M.2-6 Front Suspension Loading

Using the sine rule :

$$\frac{W}{\sin \delta} = \frac{R_L}{\sin \alpha} = \frac{R_U}{\sin \beta}$$

The dimension, a, may be determined:

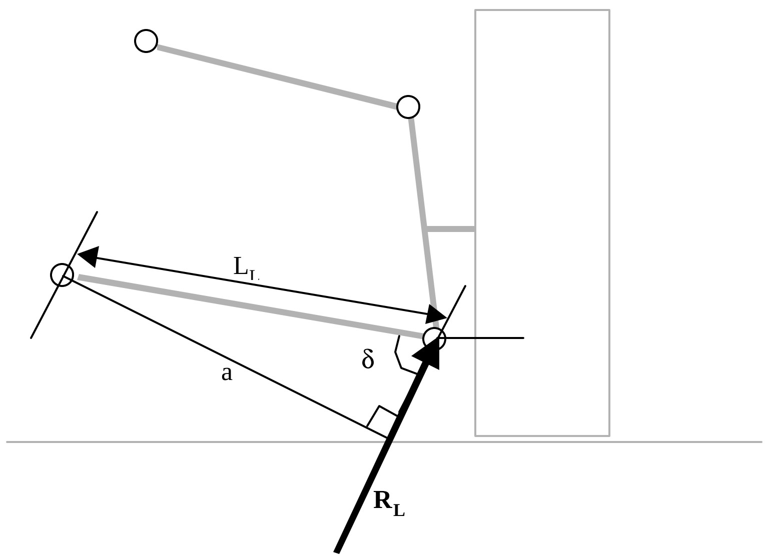

Figure M.2-7 Normal Force on the Front Suspension

Eqn's M-10 and M-11 now give the torsion bar rate k_θ as 2.42 x 10^6 N/rad, leading to a torsion bar diameter of 22.0 mm (0.87 in.) and a length of 706mm (27.8 in.) - based upon a maximum shear stress of 800N/mm^2.

M.2.7. Rear Suspension and Spring Design

The rear suspension geometry is outlined in the following figure :

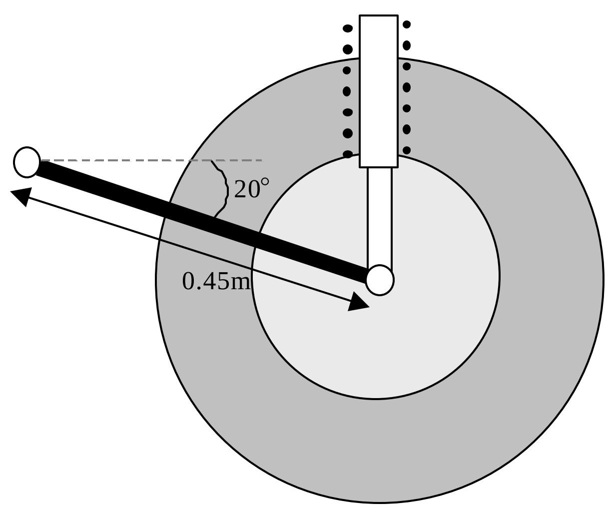

Figure M.2-8 Rear Suspension

The coil springs were designed using the method described by Dunn[2], summarized in Eqn's M-12 to M-15:

(M-12) $$k_s = k_w R^2$$

(M-13) $$\boldsymbol{t} = k\frac{2.55SD}{d^3}$$

(M-14) $$k = \frac{4C-1}{4C-4} + \frac{0.615}{C}$$

(M-15) $$n_a = \frac{Gd^4}{8k_s D^3}$$

Based upon this method, the wheel rate k_W of the rear suspension is 24.87N/mm, giving an acceptable ride frequency of 1.37Hz @MTOW within 5% of the value for the front suspension, and the following deflections:

Min Operating Weight	-	100mm (3.94 in.)
Max Take-Off Weight	-	132mm (5.20 in.)
0.5g Bump Acceleration	-	197mm (7.76 in.)

The spring rate k_S is 24.9 N/mm, leading to a coil diameter of 100mm (3.94 in.), a wire diameter of 12mm (0.47 in.), and a requirement for 8 turns (based upon a maximum shear stress of 800N/mm^2).

For the maximum bump case (0.5g@MTOW) the ground clearance is 303mm (12.04 in), or 233mm (9.26 in) with the rear suspension lowered for take-off. The maximum possible flaperon deflection is 60%, giving a vertical distance of 300mm (11.92 in) downward. Given that the outer wing is mounted approximately 100mm (3.97 in) from the bottom of the fuselage it can be shown that in the worst case scenario the flaperon is 33mm (1.31 in) above the ground.

This state requires a combination of extremes (max. bump, full flap and full control deflection) and will be reached only occasionally and for brief periods; when it is the suspension stops will prevent the flap impacting with the ground.

M.2.8. Steering System

The steering system is operated by a simple rack and pinion arrangement, with the pinion being driven by an electric motor. No mechanical back-up is provided, allowing the vehicle electronics to disconnect the steering from the controls when the wheels are retracted. This system causes a concern over safety and reliability, as the system is not yet certified. Mercedes are pioneering drive-by-wire electronics and it is likely to receive certification within the next decade.

The steering geometry is based on the Ackerman geometry, Eqn's M-16 & M-17:

(M-16) $$\boldsymbol{d}_0 = \tan^{-1}\frac{L}{(R + t/2)}$$

(M-17) $$\boldsymbol{d}_i = \tan^{-1}\frac{L}{(R - t/2)}$$

This gives a maximum outward angle of 30.9° and a maximum inward angle of 37.2°.

M.2.9. Braking System

The braking system architecture consists of floating caliper disc brakes on all wheels. The brakes shall be actuated electronically using electronic actuators, with a mechanical linkage from the rear brakes to the handbrake serving as the secondary and parking brake system.

M.2.10. Wheel Volumes and Attachment Points

The dimensions of the front wheels are 165mm (6.57 inches) width, 603mm (23.74 inches)diameter. The dimensions of the rear wheels are 175mm (6.89 in.), 593mm (23.33 in.) The suspension attachment points are defined using the geometric center of the wheel as a reference point (x,y,z) = (0,0,0), using the following co-ordinate system:

+ve x = longitudinal : towards front of vehicle

+ve y = lateral : towards the centerline of the vehicle

+ve z = vertical : towards the ground

The wheels are mounted 4.02m (13.19 ft) apart. The lateral distance between the centerlines of the front wheels is 1.42m (4.66 ft). The lateral distance between the centerlines of the rear wheels is 1.94m (6.36 ft). At the reference position, i.e. minimum operating weight, the front and rear wheels both provide a distance between the ground and the underbody of the vehicle of 0.4m (15.75 in.).

For the front wheels the range of angles through which the upper and lower arms travel (where +ve is a downward displacement) are:

Upper Arm : 50.4° (full downward wheel deflection) → 10.8°

Lower Arm : 50.4° → 10.8°

The front suspension has four attachment points:

Two upper wishbone attachment points

@ (0.075, 0.290, -0.201)m & (-0.075, 0.290 -0.201)m

Torsion Bar attachment point

@ (-0.706, 0.363 -0.123)m

Damper attachment point

@ (0.0, 0.144, -0.560)m

The whole front wheel has an upward displacement from the reference position of 0.11m (4.33 in.) and a downward displacement of 0.07m (2.76 in.). Throughout its travel the front of the wheel must rotate through 30.9° towards the vehicle and 37.2° away from the vehicle.

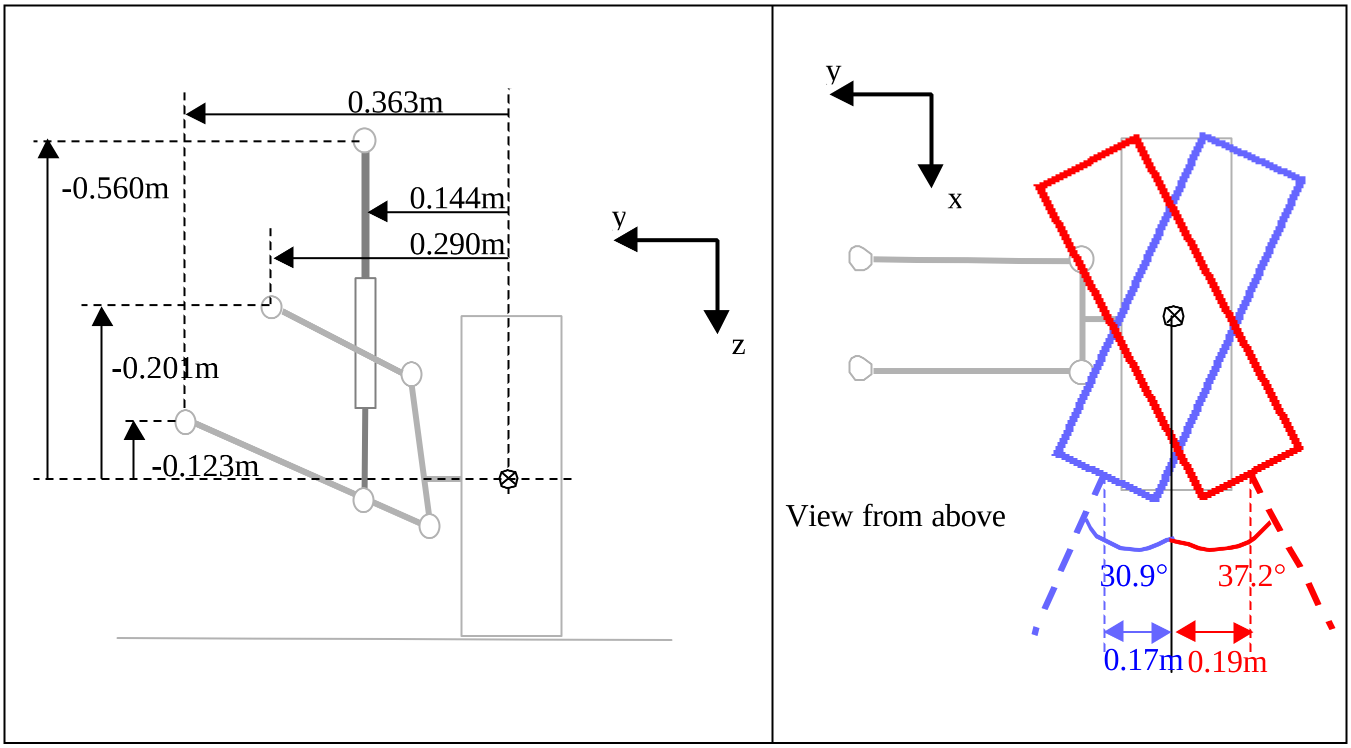

Figure M.2-9 Rear Suspension Schematic

The rear suspension has three attachment points:

Swing arm attachment point (A)

@ (0.423, 0.098, -0.015)m

Two screwjack attachment points, with 50mm clearance (B & C)

@ (0.433, 0.098, -0.394) & (-0.050, 0.098, -0.394)m

The whole rear wheel has an upward displacement from the reference position of 0.097m (3.82 in.) and a downward displacement of 0.10m (3.94 in.).

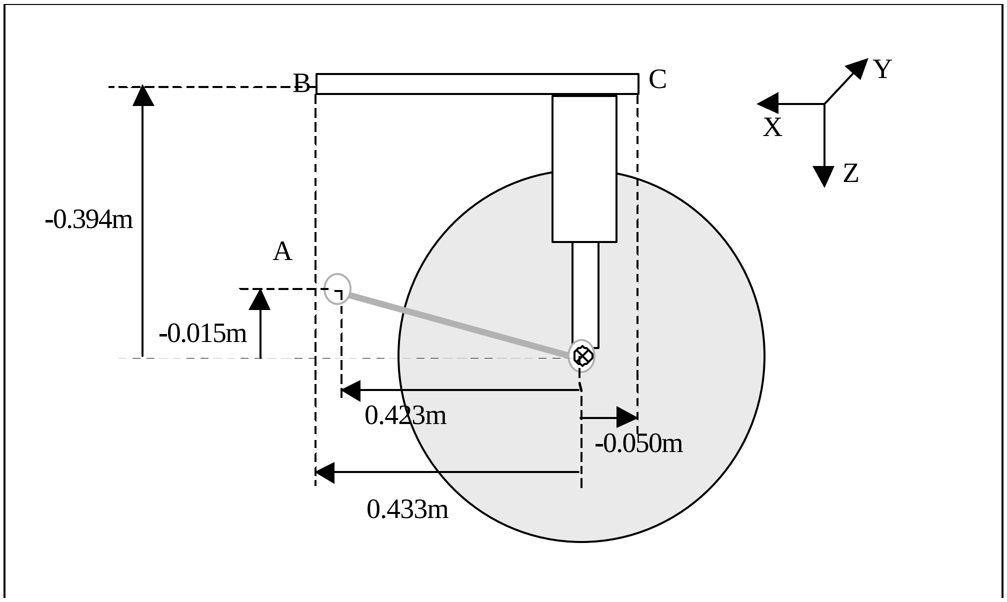

Figure M.2-10 Rear Suspension Positioning

M.3. Vehicle Dynamics

The road vehicle is *not* designed to offer a road performance comparable to modern high performance automobiles. Rather the emphasis for road performance is upon safety and predictable handling. The vehicle performance analysis is based upon Gillespie[3].

M.3.1. Vehicle Loading

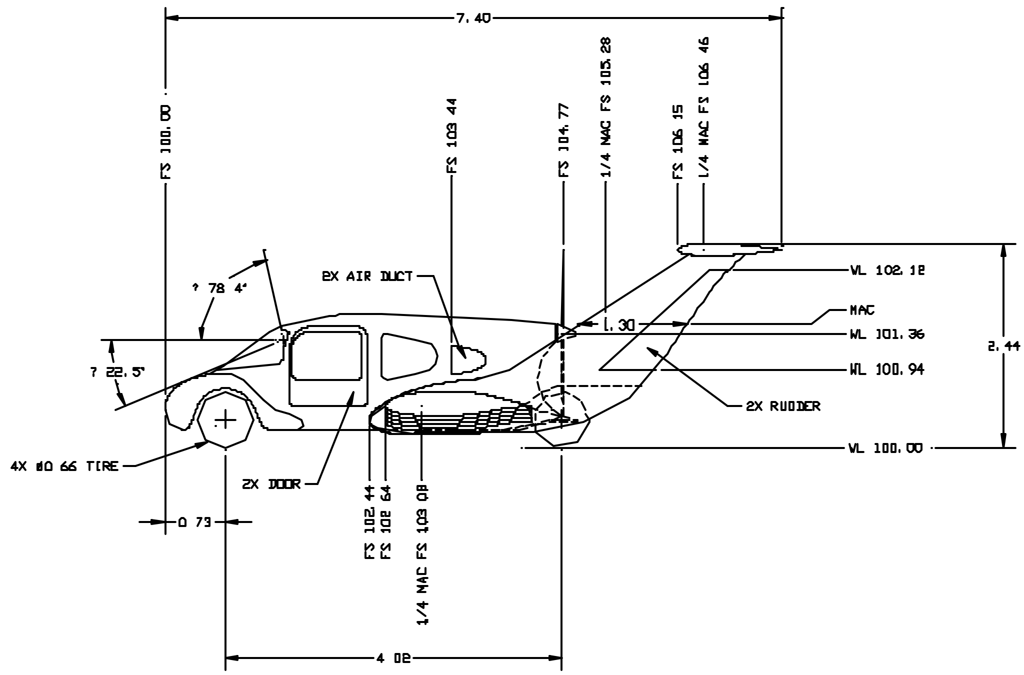

Figure M.3-1 Dimensioned Side View of the Pegasus

For suspension and ride analysis the vehicle must be separated into sprung and unsprung masses. The body is a single lumped mass and each wheel assembly is an unsprung mass of the following magnitude:

Unsprung Mass (each front wheel assembly) = 30 kg

Unsprung Mass (each rear wheel assembly) = 30 kg

Using Eqn's M-18 and M-19:

(M-18) $W_{fs} = W \,.\, (c / L)$

(M-19) $W_{rs} = W \,.\, (b / L)$

the static loads at MTOW, minimum operating weight, and an intermediate value (front passengers + ½ fuel) may be tabularized:

Table M.3-1 Operating Conditions

OPERATING CONDITION	**Mass (kg)**	**CG (m) *1**	**W_{fs} (N)**	**W_{rs} (N)**	**Load Distribution (F : R)**
Min Operating	1047	2.20	4650	5621	45 : 55
Front Passengers + ½ Fuel	1229	2.05	5908	6148	49 : 51
MTOW	1510	1.93	7701	7111	52 : 48

**1 From front axle.*

These operating conditions shall be used, where appropriate, throughout the vehicle performance analysis.

M.3.2. Road Loads

The total road load may be decomposed into the aerodynamic drag (Eqn M-20) and the wheel rolling resistance (Eqn's M-21 & M-22):

(M-20) $$D_A = \tfrac{1}{2}\, \boldsymbol{r} V^2 C_D A$$

(M-21) $$R_{xt} = f_r.W$$

(M-22) $$f_r = f_0 + 3.24 f_s \left(V/100\right)^{2.5}$$

Values for the basic rolling resistance coefficient and speed coefficient may be estimated from Figure M3-2 as $f_o = 0.012$ and $f_s = 0.0075$:

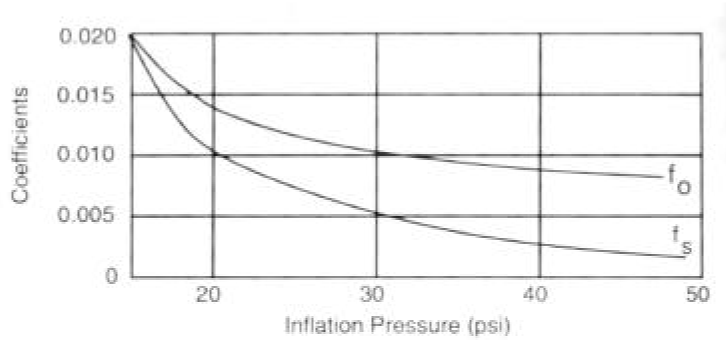

Fig. 4.34 Coefficients for Eq. (4-15).

Figure M.3-2 Tire Rolling Resistance Coefficient

Given a drag coefficient of 0.0275, based upon a 16.22m^2 (174.6 ft^2) reference area, the total road load and its components can be plotted against speed (Graph M 3-1).

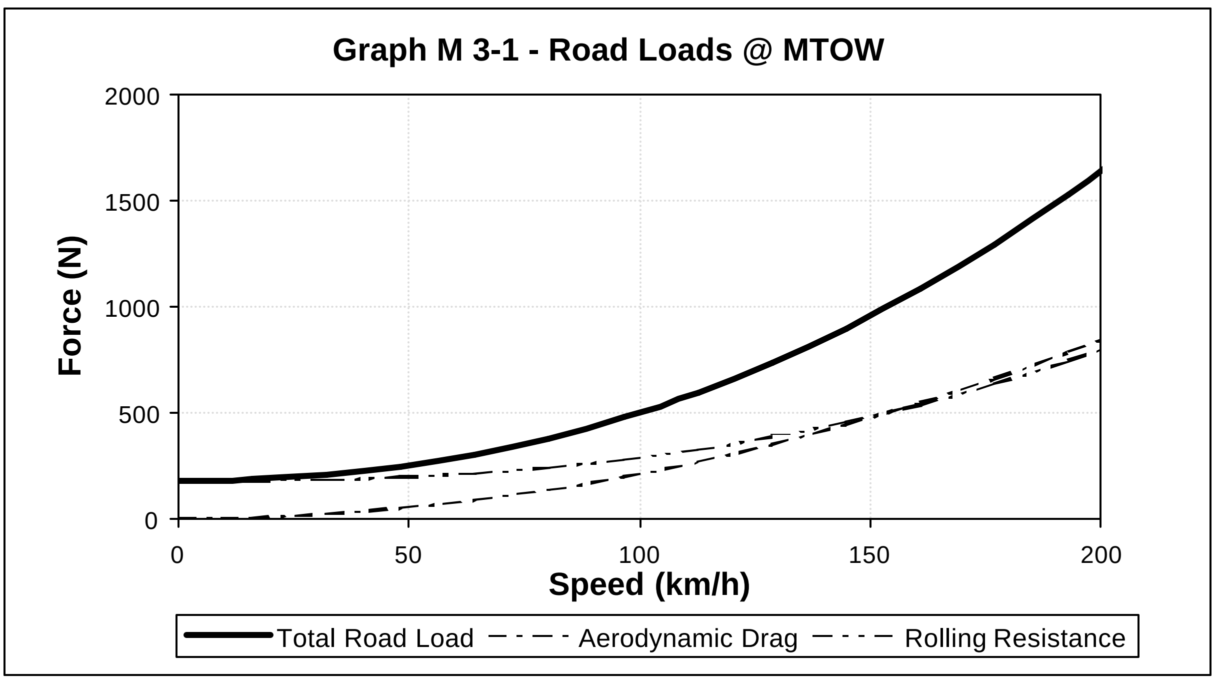

Figure M.3-3 Road Load Power vs. Speed

Using Eqn M-23:

(M-23) $$P_{RL} = R_{RL} \times V$$

the road load power may be plotted against speed (Figure M.3-3).

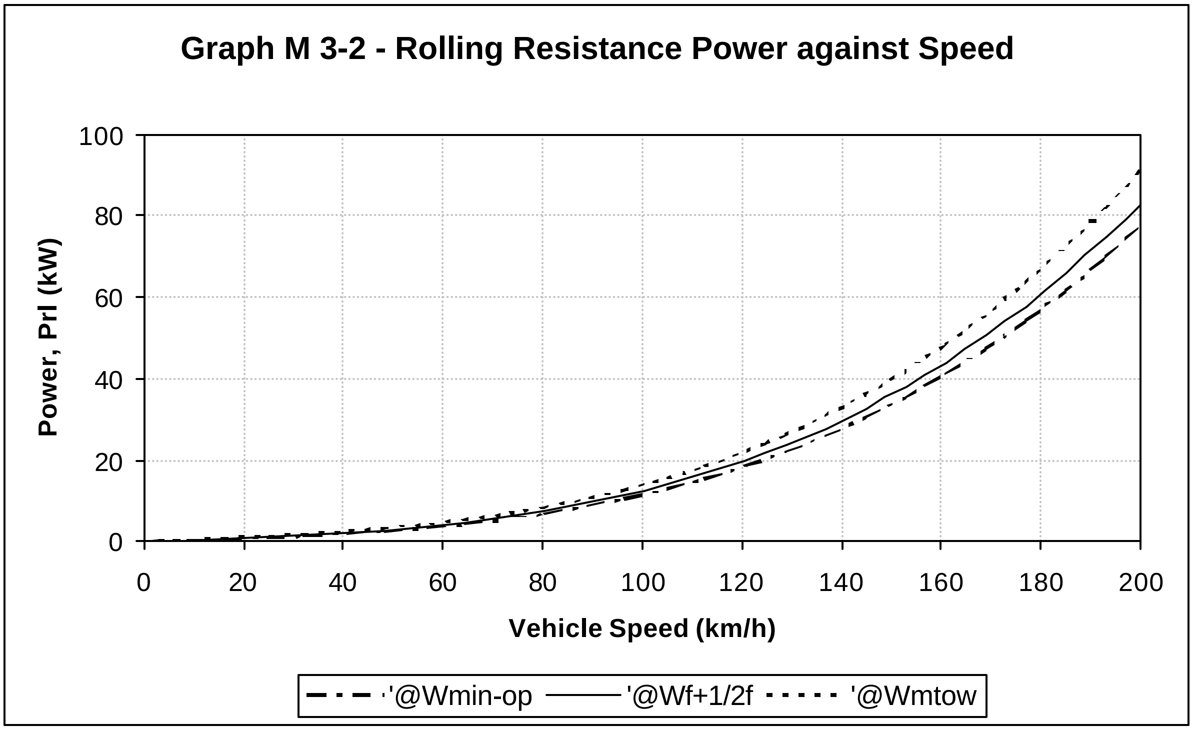

Figure M.3-4 Roling Resistance Power vs. Speed

The maximum available power can be determined from Eqn M-24:

(M-24) $$P = T\boldsymbol{w}$$

This gives a value of 40.7kW, using a constant engine speed (due to the CVT) of 2700RPM. The maximum speed can now be read from Graph M 3-2 as 160km/h (99mph) at minimum operating weight.

Graph M 3-2 shows the power required to overcome the road load forces, and at a cruise speed 105km/h (65mph) a power of approximately 15kW is required at MTOW.

M.3.3. Aerodynamic Lift

In order to ensure the safety and stability of the vehicle it is necessary to calculate the lift force caused by the inboard wing of the vehicle. The suspension is designed such that the fuselage is at 0° incidence at the minimum operating weight, and pitches slightly nose downwards as the loading increases. Using Eqn M-25:

(M-25) $$L_A = \tfrac{1}{2}\rho V^2 C_L A$$

Given that the lift coefficient is 0.143 (based on 2° wing incidence) for a stub wing reference area of 5.7m^2 (61.35 ft^2), the lift force may be calculated as 997N (224.1 lbf) at 160km/h (99.4 mph). In the worst case, with the front suspension at full rebound and the rear at full bump, the fuselage is at 2.4° incidence and the lift coefficient is 0.204 giving a lift force of 1422N (319.7 lbf) at 160km/h (88.4 mph). The lift force therefore causes a maximum of a 14% reduction in effective body weight; this should not adversely effect the vehicle's road performance.

Given that the lift coefficient is 0.143 (based on 2° wing incidence) for a stub wing reference area of 5.7m^2, the lift force may be calculated as 997N at160km/h. In the worse case, with the front suspension at full rebound and the rear at full bump, the fuselage is at 2.4° incidence and the lift coefficient is 0.204 giving a lift force of 1422N at 160km/h. The lift force therefore causes a maximum of a 14% reduction in effective body weight; this should not adversely effect the vehicle's road performance.

M.3.4. Acceleration

Using Eqn's M-26 & M-27:

(M-26) $$ma_x = F_x - R_x - D_A$$

(M-27) $$ma_x = \eta \frac{T_e \omega_e}{V} - \tfrac{1}{2}\rho V^2 C_D S - \mathrm{f_r.W}$$

The acceleration over a range of speeds may be determined, using values for engine torque of 180Nm (132.7 lbf-ft), a drive efficiency of 0.8, and a constant engine speed, due to the CVT, of 2700RPM. The maximum acceleration of the vehicle is plotted in Graph M 3-3, for the specified operating conditions across a range of velocities:

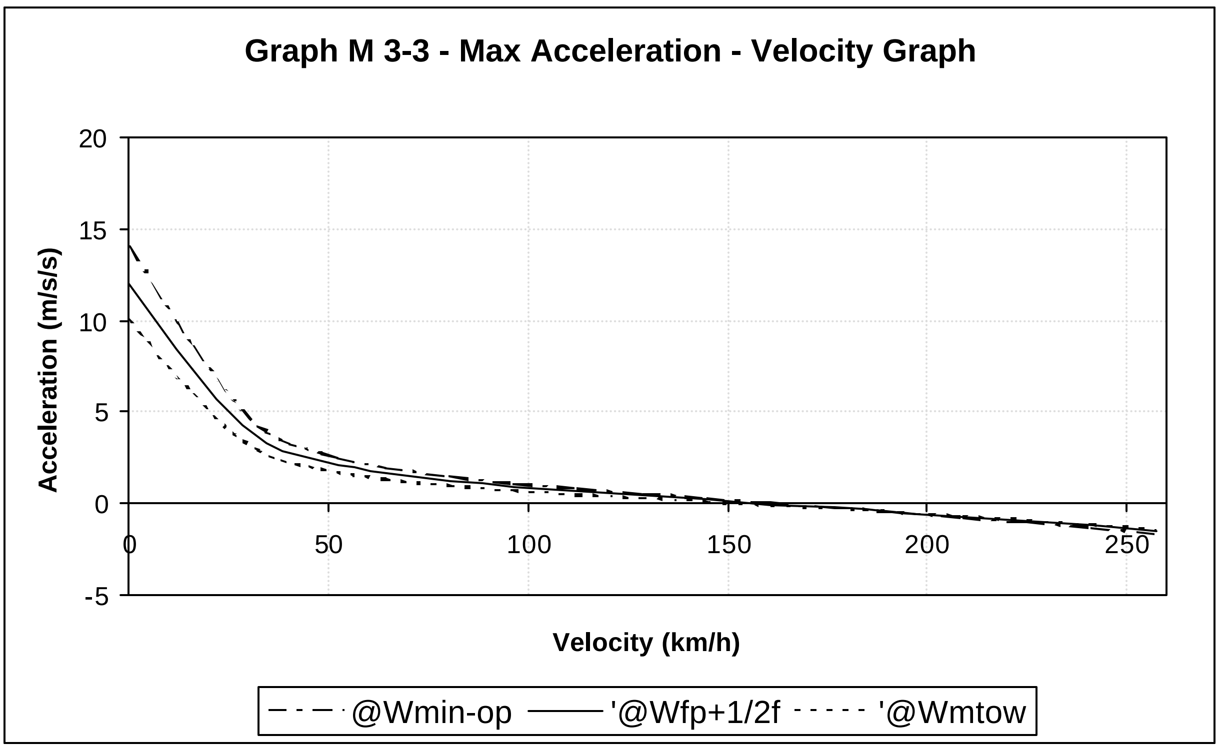

Figure M.3-5 Maximum Acceleration vs. Velocity

From Newton's Laws of Motion an acceleration-time graph may be produced (Graph M 3-4) that shows a minimum 0-100km/h (0-60 mph) time of approximately 11 seconds at minimum operating weight, and 16.5 seconds at MTOW. This model is extremely crude for initial accelerations and does not take into account loss of traction effects; hence these values should be used for guidance only.

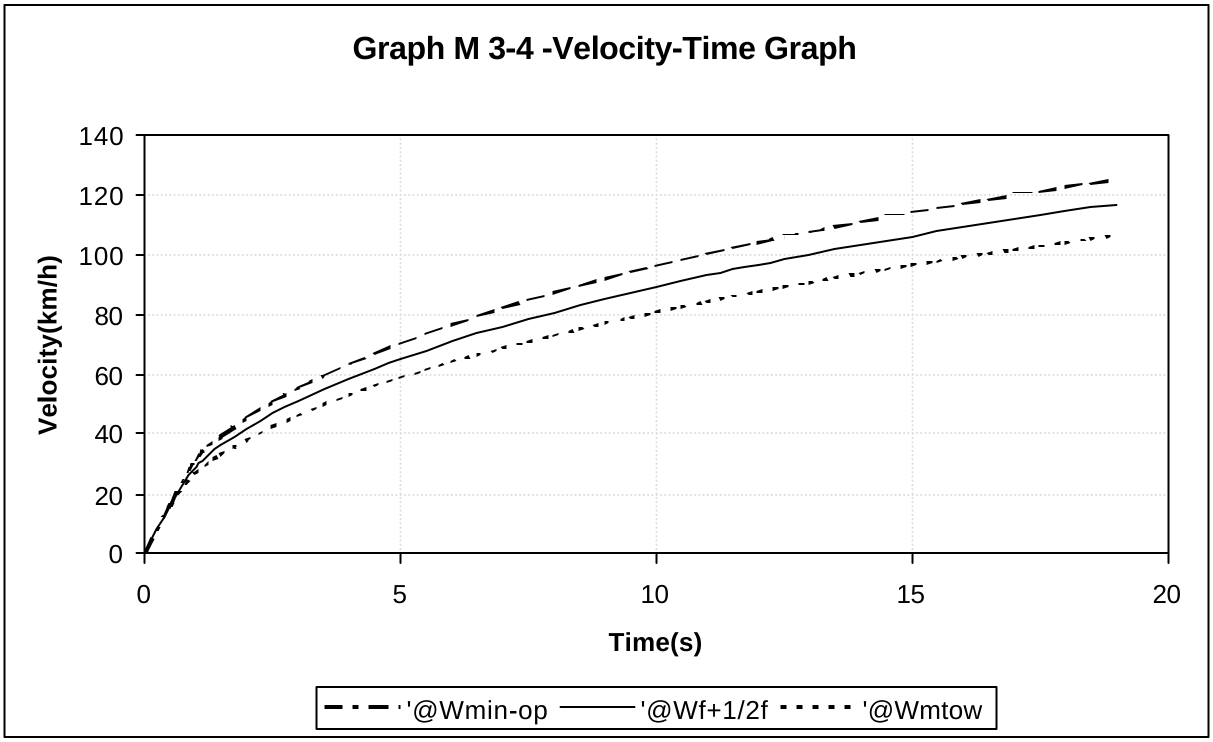

Figure M.3-5-a Velocity-Time Graph

M.3.5. Braking

The requirements of EC Directive 71/320 and ECE Directive 13 stipulate that for a M1 classified vehicle:

> With the engine disengaged the required stopping distance, SD (m) may be calculated from the velocity, v (km/h) using:
>
> $$SD = 0.1v + v^2/150$$
>
> which at a test speed of 80km/h (49.71 mph) gives a stopping distance of 50.7m (166.3 ft). The brake control force must be no greater than 500N (112.4 lbf).

The EC requirement includes a component for driver reaction time (SD = 0.1v), hence removing this component gives the braking performance of the vehicle from the application of the brakes to a complete stop. The stopping distance of the vehicle from the application of the brakes is SD = $v^2/150$ = 42.66m (140.0 ft). Using Eqn's M-28 to M-31:

M-28) $$ma_x = -F_b - R_x - D_A$$

(M-29) $$D_x = \frac{F_{xt}}{m} = -\frac{dV}{dt}$$

(M-30) $$V_0 = \frac{F_{xt}}{M} t_s$$

(M-31) $$SD = \frac{V_0^2}{2\frac{F_{xt}}{M}} = \frac{V_0^2}{2D_x}$$

The minimum vehicle deceleration, total deceleration force, and stopping time may be calculated as:

D_x = 5.8m/s^2 (19.0 ft/s^2)

F_x = 8738N (1964.4 lbf)

t_s = 3.84s

This analysis is based upon the engine disengaged case at MTOW, with no retarding force being supplied by engine braking.

A more complex analysis, Eqn's M-28 and M-32, takes into account aerodynamic drag and rolling resistance forces, giving a retardation force from the wheel brakes of 8671 N (1949.3 lbf).

(M-32) $$SD = \frac{m}{2C} \ln\left[\frac{(F_b + R_x) + CV_0^2}{(F_b + R_x)}\right]$$

Including a margin for error and to allow for brake wear, the total braking force to be supplied by the brakes is set at 9000N (2023.3 lbf). Using Eqn M-32, and setting a constant value for the rolling resistance coefficient of 0.015 for passenger cars on a concrete surface[3], the stopping distance can be plotted against initial velocity (Graph M 3-5).

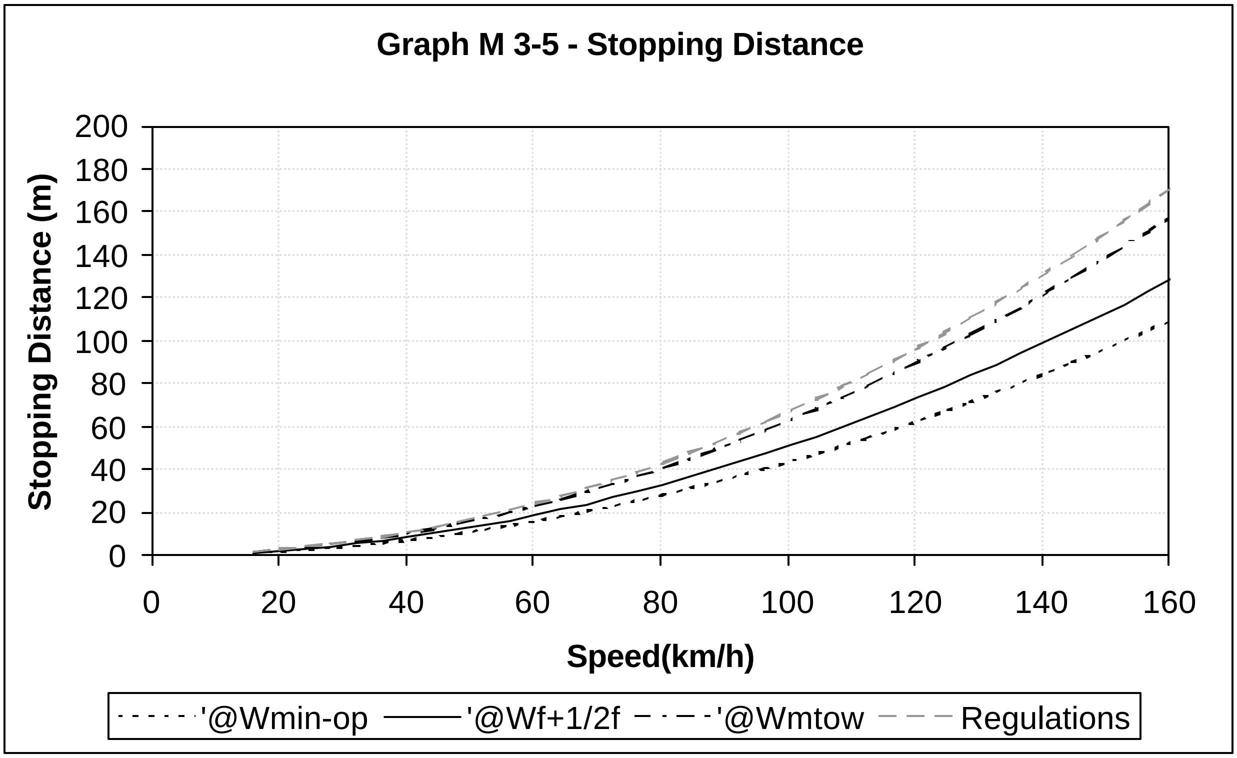

Figure M.3-6 Stopping Distance vs. Speed

M.3.6. Steady-State Cornering (Simple Analysis)

The cornering behavior of a motor vehicle is often equated with 'handling'. Handling is a loose term that refers to the subjective measurement of the vehicles response by the driver, as part of a 'closed loop' vehicle-driver system. For determining the behavior of the vehicle alone, the 'open loop' system, the vehicle's directional response may be measured. The most commonly used measure of the vehicle's open loop response is the understeer gradient, which is a measure of steady-state performance that can be used to infer performance in quasi-steady-state conditions[3].

Eqn M-33 presents a simplified steady-state cornering model based upon a bicycle-type vehicle, and uses tire cornering stiffness to calculate the understeer gradient.

(M-33) $$\boldsymbol{d} = 57.3\frac{L}{R} + \left(\frac{W_f}{C_{af}} - \frac{W_r}{C_{ar}}\right)\frac{V^2}{gR}$$

(M-34) $$CC_a = C_a / F_z$$

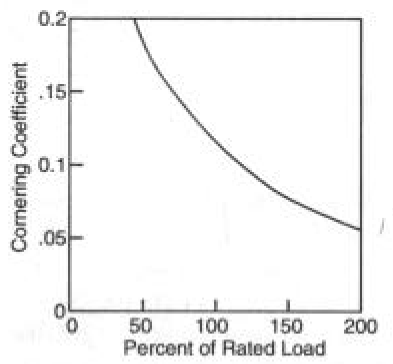

Figure M.3-7 Cornering Coefficient

The single-tire cornering stiffness' for the roadable aircraft were estimated, based on the cornering coefficient (Eqn M-34), which may be calculated using the tire load as a percentage of the rated load. Using Figure M3-3, the following values can be obtained:

Operating Condition	**Mass (kg ,lbs)**	**C_{af} (N/deg,lbf/deg)**	**C_{ar} (N/deg,lbf/deg)**
Min. Operating	1047,2308	405,91.05	479,107.7
Front passengers	1229,2709	472,106.1	507,114.0

+ ½ fuel			
MTOW	1510,3329	500,112.4	533,119.8

When using the bicycle model (Eqn M-33) the values for single-tire cornering stiffness must be doubled to obtain the tire cornering stiffness' across the front and rear axles. The understeer gradients, K, may now be determined:

$K_{min\text{-}op} = -0.12deg/g$

$K_{f+1/2f} = 0.17deg/g$

$K_{mtow} = 0.95deg/g$

The effect of the understeer gradient is as follows:

Table M.3-2 Understeer Gradient

	Understeer gradient, K	**Slip angles, a**	**Behavior on constant radius turn**
Neutral Steer	K = 0	$\alpha_f = \alpha_r$	Slip angles equal with increasing a_y hence no change in steering angle required.
Understeer	K > 0	$\alpha_f > \alpha_r$	With increasing a_y front wheel slip increases compared to back, increasing steering angles required.
Oversteer	K < 0	$\alpha_f < \alpha_r$	With increasing a_y back wheel slip increases compared to front, decreasing steering angles required.

Understeer reduces the lateral acceleration gain and the yaw velocity gain (rate of change of heading angle) and hence too much understeer will produce a sluggish vehicle response. A certain degree of understeer is favourable as it provides safe handling characteristics compared to the oversteer case in which the vehicle can become unstable, typical values are in the region 1deg/g.

M.3.7. Yaw Velocity Gain and Characteristic Speed

The yaw velocity, or yaw rate, of the vehicle is the rate of change of heading of the vehicle (deg/s). The yaw velocity gain is the ratio that represents a gain that is proportional to velocity in the case of a neutrally steered vehicle, and will effect the subjective evaluation of the vehicles handling by the driver. Using Eqn M-35:

(M-35) $$\frac{r}{d} = \frac{V/L}{1 + KV^2 / 57.3Lg}$$

The yaw velocity gain may be plotted as a function of speed for the roadable aircraft across the specified load range (Graph M 3-6).

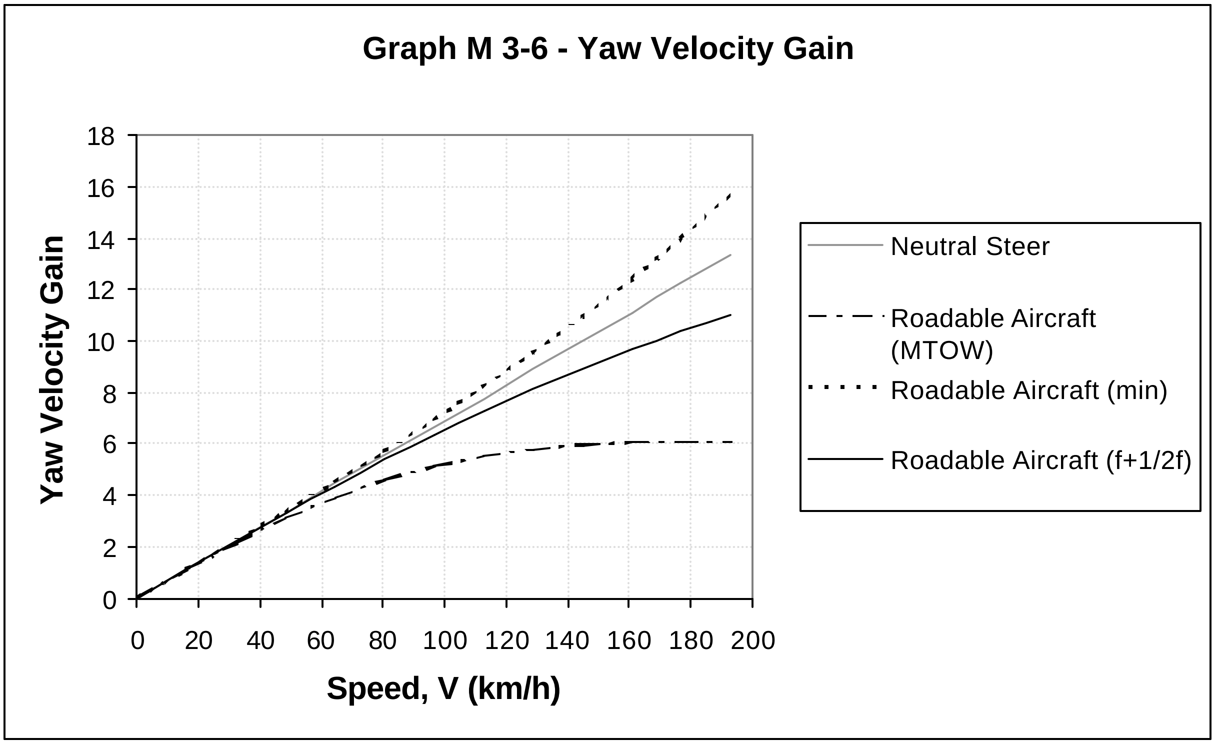

Figure M.3-8 Yaw Velocity Gain

Graph M 3-6 shows a wide variation in the Yaw Velocity Gain with vehicle weight. As a result, the handling of the vehicle will change significantly with weight, from sharp handling at the minimum operating weight to sloppy handling at MTOW.

The characteristic speed is the speed at which the vehicle is most responsive in yaw. Above the characteristic speed the vehicle has good straight line stability but its turning performance will be poor. The characteristic speed can be calculated using Eqn M-36, for MTOW, as approximately 176km/h (109.36 mph), which is above the maximum speed of the vehicle.

(M-36) $$V_{char} = \sqrt{57.3 L g / K}$$

This means that the vehicle will have good steering response across its speed range.

M.3.8. Side Slip Angle

The sideslip angle, β, is defined as the angle between the longitudinal axis and the local direction of travel, at the center of gravity. At higher cornering speeds the rear of the vehicle drifts outwards to generate the necessary slip angles on the rear tires, and this will cause the sideslip angle to move from positive (towards the turn center) to negative (away from the turn center). The speed $V_{\beta=0}$ at which this transition occurs is independent of the radius of turn and may be calculated using Eqn M-37:

(M-37) $$V_{b=0} = \sqrt{57.3gc\,C_{ar}/W_r}$$

This gives a zero sideslip velocity of approximately 36km/h across all operating conditions. Above this speed the rear of the vehicle will slip outwards during turning. For a 50m (164.0 ft) radius turn the sideslip angle with a lateral acceleration of 0.4g is 4.9° at MTOW; this angle will be noticeable but not significant.

M.3.9. Steady-State Cornering (Complex Analysis)

The complex analysis of steady-state cornering uses a four-wheel model, based upon Eqn's M-38 to M-44:

(M-38) $$K = K_{tyres} + K_{llt} + K_{at}$$

(M-39) $$K_{llt} = \frac{W_f}{C_{af}}\frac{2b\Delta F_{zf}^2}{C_{af}} - \frac{W_r}{C_{ar}}\frac{2b\Delta F_{zr}^2}{C_{ar}}$$

(M-40) $$\Delta F_{zf} = \frac{1}{t_f}\left[K_{ff}\,\frac{Wh_1}{K_{ff}+K_{fr}-Wh_1} + W_f h_f\right]\frac{V^2}{Rg}$$

(M-41) $$\Delta F_{zr} = \frac{1}{t_r}\left[K_{fr}\frac{Wh_1}{K_{ff} + K_{fr} - Wh_1} + W_r h_r\right]\frac{V^2}{Rg}$$

(M-42) $$K_f = 0.5 K_w t$$

(M-43) $$F_y = C_a \boldsymbol{a} = (aF_z - bF_z^2)\boldsymbol{a}$$

(M-44) $$K_{at} = W\frac{p}{L}\frac{C_{af} + C_{ar}}{C_{af}C_{ar}}$$

This analysis takes into account the lateral load transfer effects of the suspension, where load is shifted to the outer wheels, and also the aligning torque effects, caused by lateral forces being developed in a tire behind it's roll center. The model does not account for tire camber or steering effects.

Given an empirically estimated value for the second polynomial of cornering stiffness as 0.00036, a CoG height of 0.54m (1.77 ft) above the bottom of the fuselage, a front roll center calculated as the bisection of a line parallel to the suspension arms running through the tire contact patch with the vehicle center-line, and a rear roll center height taken as the roll center of the rear wheels, the following parameters were obtained:

Table M.3-3 Load Cases

Load Case	**h_f (m,ft)**	**h_r (m,ft)**	**CG_x(m,ft) *1**	**h_1 (m,ft)**	**DF_{zf}/a_y (N/g,lbs)**	**DF_{zr}/a_y (N/g,lbs)**
W_{min-op}	0.41,1.35	0.324,1.06	2.2,7.22	0.577,1.89	3012,6640	2936,6472
$W_{front +}$ ½ fuel	0.34,1.12	0.324,1.06	2.05,6.73	0.624,2.05	3417,7533	3398,7491
W_{mtow}	0.26,0.85	0.324,1.06	1.93,6.33	0.585,1.92	3927,8657	4130,9105

**1 From the front axle*

Using these values and Eqn M-39 & Eqn M-44 and a value for the pneumatic trail of 0.01m, the understeer gradients can be recalculated:

- $K_{total} = K_{tyres} + K_{at} + K_{llt}.a_y$
- $K_{Wmin\text{-}op} = -0.12 + 0.10 + 0.72a_y$ deg/g
- $K_{Wf+1/2f} = 0.17 + 0.11 + 0.53a_y$ deg/g
- $K_{Wmtow} = 0.95 + 0.13 + 0.79a_y$ deg/g

These values show that both the effects of aligning torque and lateral load transfer contribute to increasing the total understeer gradient of the vehicle. The understeer gradient is plotted against lateral acceleration for all three operating conditions (Graph M 3-7).

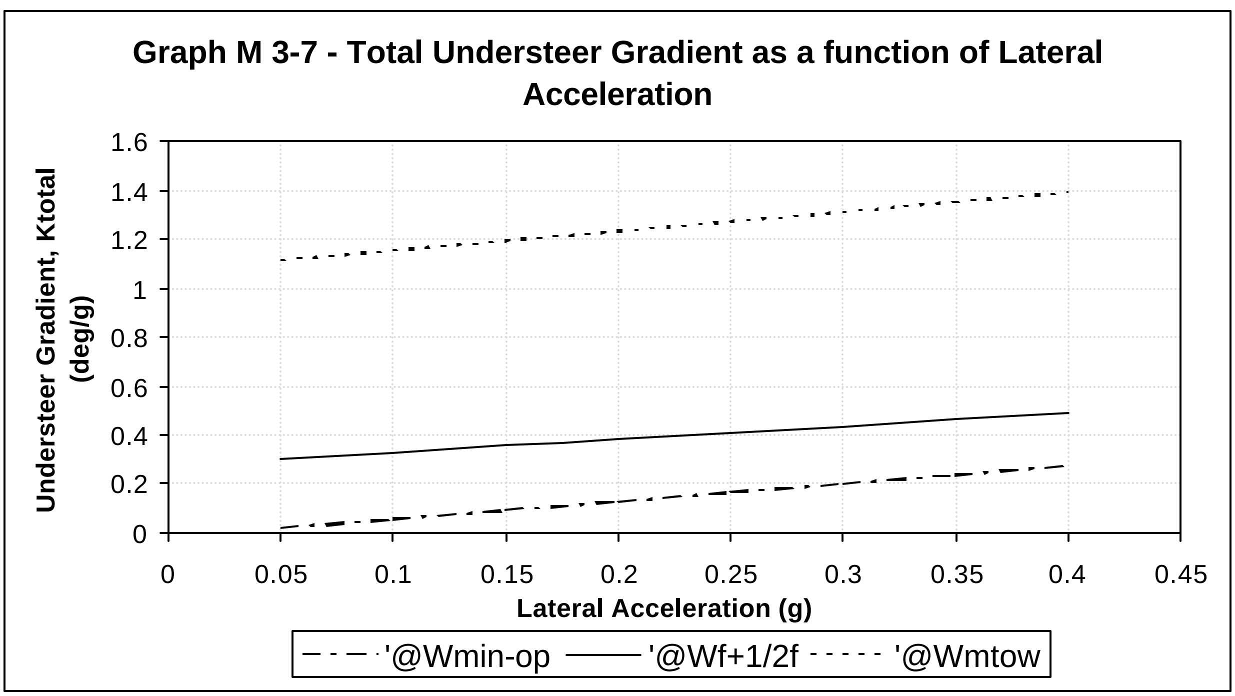

Figure M.3-9 Understeer Gradient

The graph shows steadily increasing understeer across all operating conditions. The steering angles are depicted for an example turn of 50m (164.04 ft) radius (Graph M 3-8).

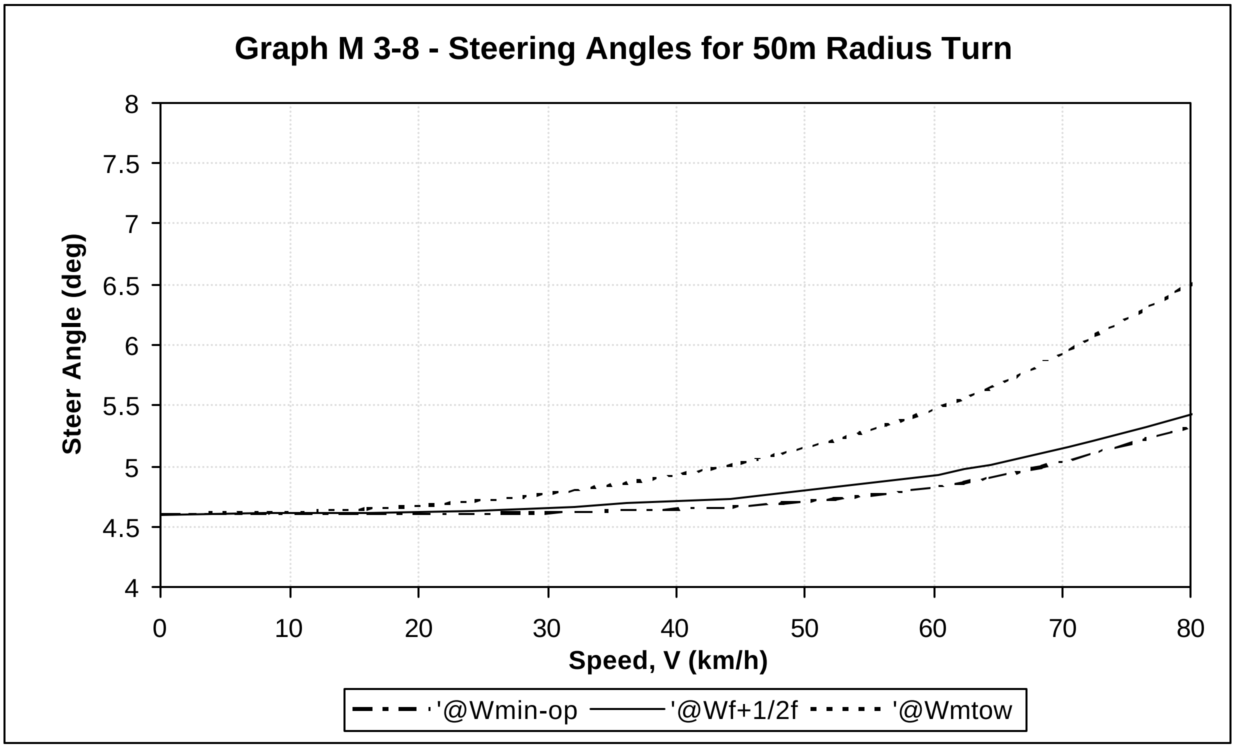

Figure M.3-10 Steering Angles for Fifty Radius Turn

M.3.10. Rollover

Using Eqn's M-45 & M-46:

(M-45) $$\frac{a_y}{g} = \frac{t}{2h}\frac{1}{\left[1 + R_f\left(1 - h_r/h\right)\right]}$$

(M-46) $$R_f = {d_f}/{a_y} = \frac{Wh_1}{\left(K_{ff} + K_{fr} - Wh_1\right)}$$

The lateral acceleration required to induce rollover can be calculated as ranging between 0.98 to 1.00g's of lateral acceleration, from minimum operating to maximum take-off weight. Given that maximum cornering accelerations usually exceed no more than 0.4g, the rollover case presents no threat to the vehicle or it's occupants.

M.4. Transport Regulations

As a roadable aircraft, the Pegasus must meet the US and European driving regulations. Due to the similarities between these regulations, the Pegasus needed to comply with only one of these. The UK regulations were used as specifications for the design as outlined in section M.4.2.

M.4.1. Example UK/EC Regulations

The Roadable Aircraft is classified as a Motor Car, according to UK Construction & Use Regulations, and is categorized as an M1 type vehicle according to the EEC Classification, whereby:

Category M : Motor vehicles having at least four wheels, or having three wheels when the maximum weight exceeds one metric ton, and used for the carriage of passengers.

Category M1 : Category M vehicles used for the carriage of passengers having not more than eight seats in addition to the drivers seat.

The Construction & Use Regulations[1 & 6] are briefly summarized below in three categories: dimensions, performance, and required equipment. The regulations presented no major problems to the configuration chosen.

M.4.1.1. Dimensional Regulations

- Maximum Length = 11m
- Maximum Width = 2.5m
- Rear Overhang must not exceed 60% of the wheelbase.
- Exterior mirrors must not project more than 20cm from the vehicle (if placed under 2m above the road surface).
- Positioning of lights – see Toyne[XXXM6].

M.4.1.2. Performance Regulations

- Capable of powered reverse travel.
- Power must be at least 4.4kW for every 1000kg of the max. gross weight.
- Must comply with EC directives for emissions.
- Noise emission no greater than 80dB under test conditions.
- The driver must have a clear view of the road in front of him
- Must comply with the EC Directives on performance of service, secondary and parking brake systems (see Bosch Automotive Handbook[XXXM1]).

M.4.1.3. Required Equipment Regulations

- Springs must be provided between the body and the wheels.
- A protective steering mechanism must be provided.
- Door latches and hinges must be fitted and capable of absorbing crash impact
- The vehicle must be fitted with windscreen wipers & washers, a speedometer (10% accuracy), an audible warning, mirrors (interior and offside *or* two exterior), a silencer, manufacturers and ministry plates, parking brakes, seat belts and pneumatic tyres.
- The petrol tank must have national type approval.
- Specified Safety Glass must be fitted to the windows in front and either side of the driver. Other windows must be fitted with Specified Safety Glass or Safety Glazing.

1) Bosch(1996) *Automotive Handbook 4th Edition* Robert Bosch GmbH

2) Dunn (1999) *Suspension Design* AAETS, Loughborough University.

3) Gillespie (1992) *Fundamentals of Vehicle Dynamics* SAE Inc.

4) Spring Design AE-21 (1996) SAE Inc

5) Stinton (1983) *The Design of the Aeroplane* Blackwell Science Ltd

6) Toyne (1982) *Motor Vehicle Technical Regulations 3rd Edition* Ruislip Press Ltd.

Appendix N. Human Factors and Safety

N.1. Interior Layout

N.1.1. CabinLayout

The design of the cabin was the result of two key requirements; the need to accommodate four passengers and also be capable of travel in both the plane and car modes. The environment created had to be spacious enough to fit the crew in comfort while, also compact enough to meet the constraint imposed on the length of 2.2m from the foot well to firewall. The cabin can be seen in figure N.1-1. This distance was chosen following the analysis of centre of mass calculations regarding the avionics in the nose and the implications of increased profile drag with fuselage length.

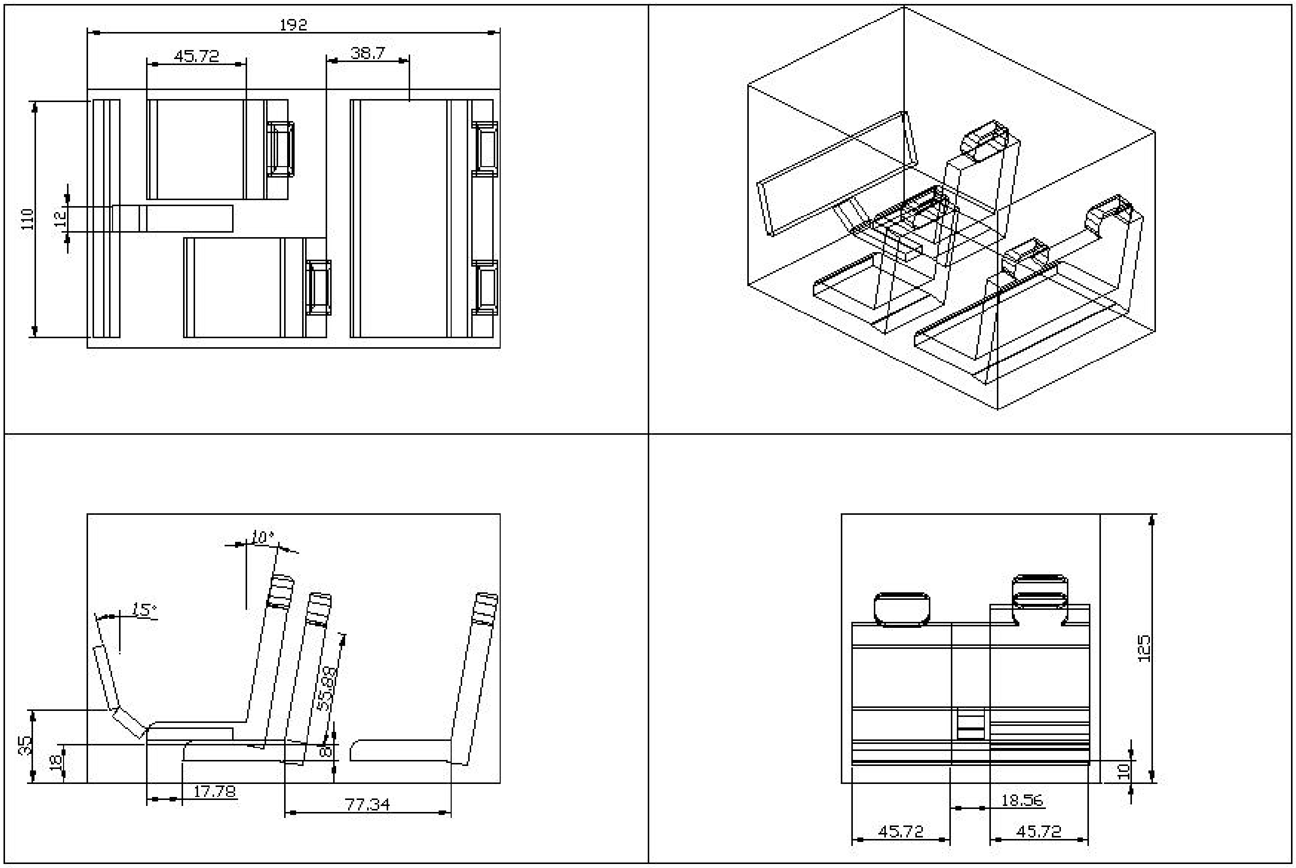

Figure N.1-1 3-view of cabin layout

The allocation of the space can be viewed in Figure N.1-2, which shows a 95th percentile male in the front of the cabin. The JACK anthropometrics software, developed by Pennsylvania University, was used to immerse virtual humans in the CAD layout drawing of the cockpit. The virtual humans used by the software are based on anthropometric data supplied by the US Army(1) and NASA(2).

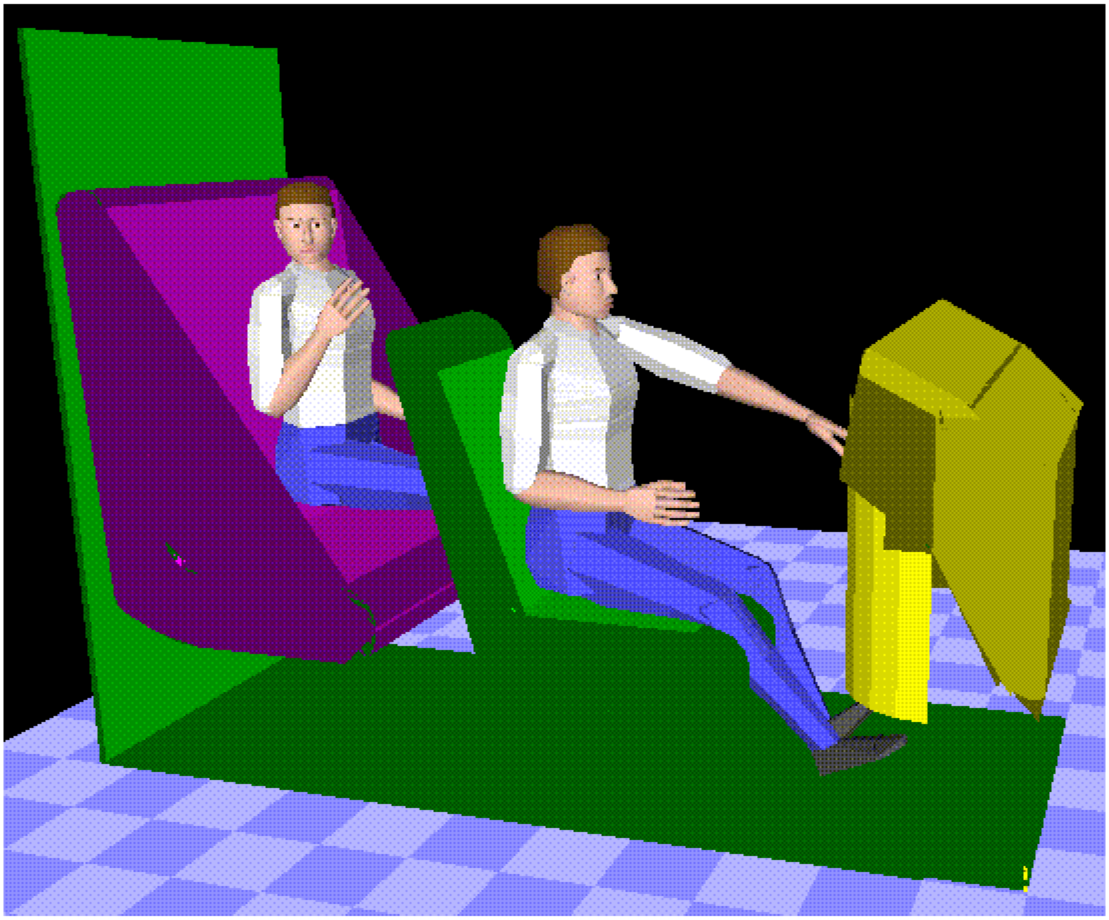

Figure N.1-2 JACK Software Cabin Rendering

(1) Anthropometric Source Book, Vol. 2:A, Handbook of Anthropometric Data, Technical Report NASA RP-1024.

N.1.2. Anthopometric Data

The data available on the sizes of the population as a whole is common and freely obtainable. To conduct a separate study into the different sized groups using the vehicle was both time consuming and of little use. Instead Motor Industry Research Association (MIRA) data sheets provided the sizes of various percentile male and females from which to create the seating size and cockpit internal dimensions.

The anthropometrics were grouped into geographical regions as European sixty-fifth percentile individuals were of different stature to, say, people of Latin American origin. Knowing this, the European and American sectors were studied and the heights compared. The variations between regions were slight and so the European data was chosen as the reference user group. From there the ninety-fifth percentile was chosen for the design to maximize the number of satisfied user groups without compromising the size of the aircraft significantly. The hundredth percentile was not considered a viable user group, as the probability of selling to this group was statistically low enough to ignore. Nevertheless, the one hundredth percentile could still fit into the concept, although the legroom and ceiling height may well reduce their comfort level.

Once the 95^{th} percentile was chosen, the reach of their arms defined the positions of the Multifunctional Displays (MFD) for the front passengers. The legroom needed by the rear occupants then defined the length of the space from front pedals to firewall. The width of the front seats were taken as the hip size of the males. The gap between the center of the seats where the throttle was to be housed was the result of actual mock-ups conducted in person. Initially, a one meter wide cockpit was proposed but this left too little room between the occupants. The feeling of claustrophobia was a concern due to the overall compactness of the design. The risk of knocking the central throttle was also a point to be aware of. The width was then increased to a value of 1.1 meters, which increased the gap and made throttle operation safe. The plan of four independent seats to maximize comfort were dropped in favor of an automotive interior, with a rear bench seat, divided by base contours. This was a better package for the family market as three children could be transported instead of two. It also gave increased luggage storing capacity, under the rear seats.

N.1.3. Seats

The sizing of the seat was done using the anthropometric MIRA data for a European 95% individual. Using the relevant limb measurements the following front seats and rear bench was constructed. The seats had to be designed with a high degree of sizing flexibility, as the initial design was liable to frequent change. The seats were modified many times within a set environment without exceeding the cockpit floor pan. The front two seats were modeled in a separate file so that their position could be manipulated independently. This property would be useful for ingress egress study using the JACK anthropometric software.
The final seat dimensions were confirmed following the successful integration of the CAD simulation to the anthropometric tests.

It was determined that the seat pan should be short enough that the front-edge does not press into the sensitive tissue near the knee during flight, which can be quite uncomfortable for the pilot and can even cause blood clots. The height, measured from the floor, should be variable between 20.32-27.94cm (8-11 inches) and the width should be larger than 44.98cm (17.71 inches) wide. The backrest should be at least 29.97cm (11.8 inches) wide. It is important for the backrest not to be a 90-degree angle. It should have an angle of no more than 30 degrees and no less that five degrees as measured from the vertical(3). Based upon these considerations, the front seats in the aircraft have a seat pan of 45.72 x 48.26cm (18 x 19 inches), a backrest of 45.72 x 55.88cm (18 x 22.5 inches) with a 10-degree range of motion as measured from the vertical. In order to accommodate the 95th percentile the horizontal range of motion is 17.78 cm (7 inches), and the vertical range of motion is 8.26cm (3.25 inches).

The complexity of the seat was again a function of the budget of the design team. Variants ranged from a basic single back rest angle adjustment to the most complex electrically controlled unit with adjustable lumbar support, recessed fans for cooling and base pitch adjustments. A one-piece composite backrest was initially specified as this reduced the room needed between front and rear passengers and shortened the cabin length. This idea was worked with until the problem of egress emerged. The only viable way of exiting the vehicle in the manner as described in the ingress/ egress section was to hinge the seat across the base of the backrest and mount the whole unit on runners. By having the doors so far forward of the rear seats, in a style similar to that of hatchback cars, the rear occupants could slide the front seats forward and rotate them upwards and over the dash. The possibility of using four doors was quickly ruled out along the decision making process as the occupants would have to leave by walking across the wing leading edge. This was deemed unacceptable when viewed against the final design.

Another factor to consider is the upholstery of the seats. Two options will be available for the consumer. The more economical choice will be fabric. Fabric breathes well when compared with vinyl and is very durable. Fabric also reduces sliding forces of the body with relation to the seat, which is a potential safety problem. The design on the seats drew influences from the prestige car market, and leather will also be an option for the high-end customer. These customers are willing to pay extra for a more luxury vehicle.

Safety is also a major factor when choosing seats. Aircraft seats that merely hold the occupant rigidly in place are satisfactory when there is only a horizontal or lateral deceleration; but they do not provide protection when accidents occur resulting in large vertical deceleration. This deficiency can be corrected by using energy-absorbing seats, which would utilize the space between the seat bottom and the floor to absorb impact energy and reduce acceleration, thereby increasing occupant survival potential in a crash[4].

N.2. Cockpit

N.2.1. Pilot Interface

Much consideration was put into the design of the control panel of the Pegasus. The width of the fuselage caused some difficulty, being only 1.10 meters wide. This small length posed a problem for a designer to place controls for both an aircraft as well as an automobile. Therefore, the placement of certain controls becomes critical. The final cockpit layout can be seen in Figure N.2.1-1.

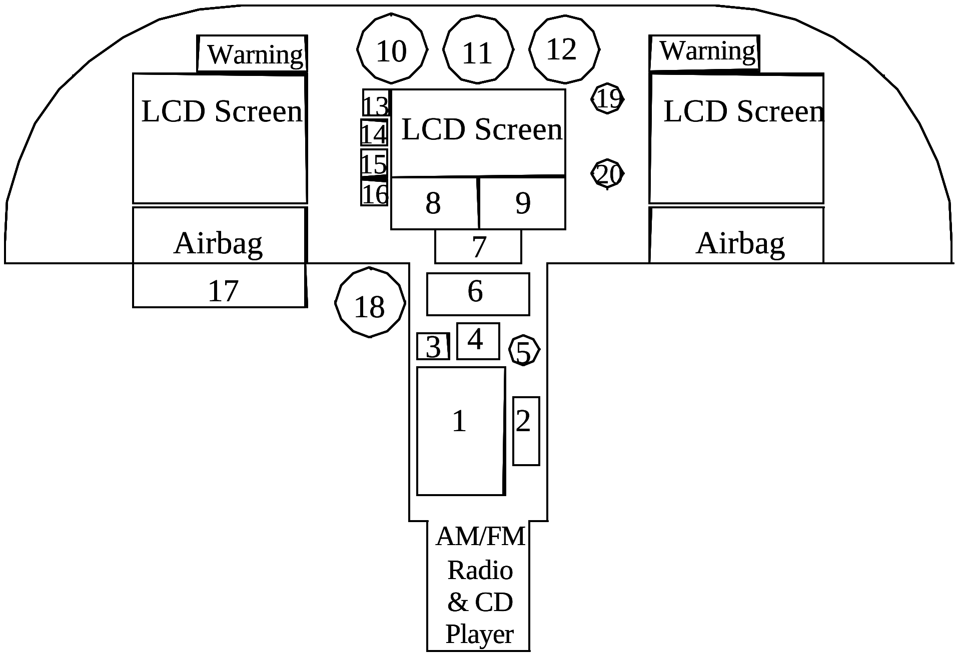

1	Throttle Gear Stick	11	Artificial Horizon
2	Flaps	12	Altimeter
3	Mode Change Button w/ Guard	13	Fuel Cutoff Button
4	Wing Flap Switch and Indicator	14	Engine Fire Extinguisher Indicator and Switch
5	Ignition Switch	15	Built in Test Button
6	Climate Controls	16	Hazard Warning Button
7	Audio Control Box	17	Circuit Breaker
8	Transponder	18	Brake
9	Radio	19	Lights Switch
10	Air Speed	20	Windshield

Figure N.2-1 Instrument panel

To enable flight from either front seat it was necessary to provide both sets of displays and controls on both sides of the cockpit. For the Multi-functional Display (MFD), touch screen Liquid Crystal Displays (LCD) were felt to have more advantages than conventional buttons and instruments. It was recognized that if conventional displays were used it would present the operators with a very congested and high workload solution. In order to provide an easy to use and low workload solution, Cathode Ray Tubes (CRT) or LCDs were considered, as this would enable only symbology required for each mode to be displayed. LCDs were chosen due to their smaller depth size, which would enable more freedom in the design of the fascia.

The cockpit panel consists of three LCDs. The two outer displays will present information for flying and driving and a center screen will provide the pilot or driver with secondary information including moving maps, weather and traffic information. The screens will display various things depending on the mode that the vehicle.

In aircraft mode, these main displays are split in two halves, providing a Primary Flight Display (PFD) on one side of the display and an Engine and Fuel Display System (EFDS) on the other. The PFD half provides all the flight information consisting of an Artificial horizon, a turn co-ordinator, an altimeter, a Vertical Speed Indicator, an airspeed indicator, a compass-heading ribbon, and an Instrument Landing System (ILS) overlay. The EFDS provides all the necessary engine and fuel information required for all the phases of flight. The following parameters are indicated on the display; engine rpm, engine manifold pressure, oil pressure, oil temperature, vacuum suction, fuel flow, fuel contents, voltage, current and outside air temperature.

The engine dials have amber and red regions marked on them, which become solid to indicate to the pilot that system is operating outside its normal parameters. In addition to the colored arcs, the pointer needle, the digital readout and its surround change color to further indicate the situation to the pilot.

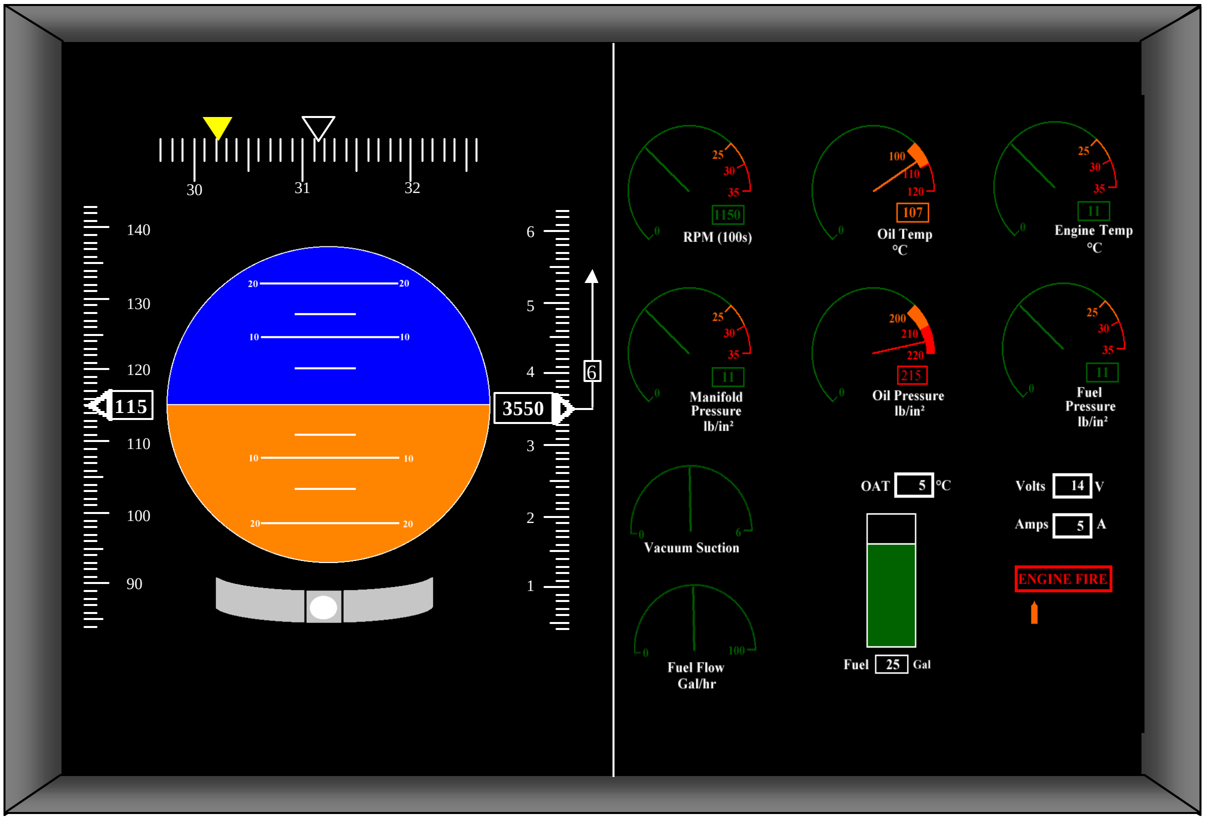

Figure N.2-2 LCD Screen in Aeroplane Mode

By displaying the information on both screens it not only allows the vehicle to be flown from either seat, but it also provides a degree redundancy in the event of a single screen failure.

When the vehicle is in car mode the LCD on the driver's side of the vehicle will display the standard car instruments, including speedometer, rev counter, fuel contents and water temperature, plus all the normal annunciators. The other LCD will be automatically switched off. The operator can change which side the vehicle can be driven from via a guarded toggle switch on the fascia, to allow operation in any part of the world.

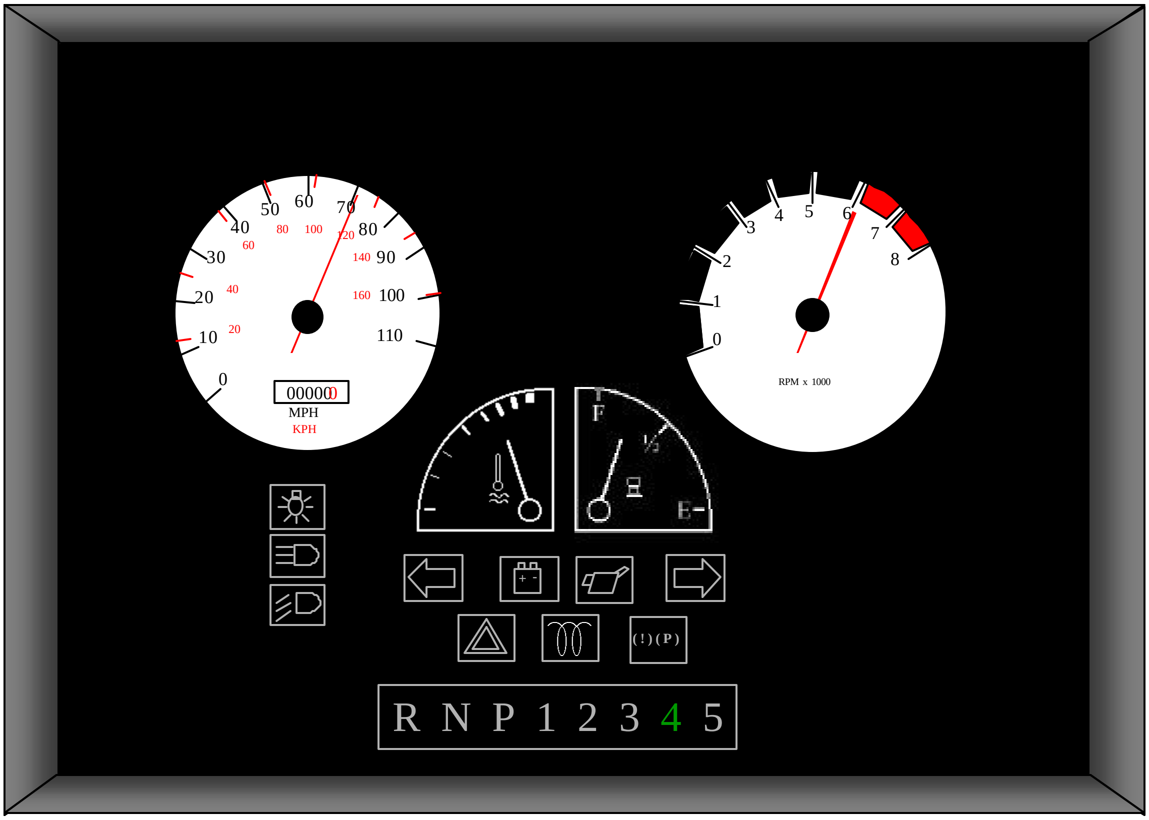

Figure N.2-3 LCD Screen in Car Mode

The MFDs provide secondary information to the operators to assist them, via a touch screen interface. This allows the design to be tailored specifically to the Pegasus's requirements without incurring excessive design costs that would be encountered using more traditional systems. The different displays can be selected via buttons down the left hand side of the screen and systems such as traffic or weather information can be activated via a set of buttons down the right hand side of the screen.

In aircraft mode the MFD allows the operator(s) to view any of the following information at a touch of the screen:

- Standard Navigation display with VOR, flight path etc
  - Weather information overlay

    - Traffic information overlay
- Moving map with standard Navigation overlays
    - Weather information overlay
    - Traffic information overlay
- Airfield info
- Vehicle status/failures
- Checklists

In addition to these different displays, flight navigation data can be entered prior to or during flight via the touch screen interface.

In car mode the MFD will allow the operator(s) to view any of the following:

- Moving map
- Navigation information
- Airfield info
- Vehicle status/failures

In addition to these functions, when the vehicle is in car mode the MFD automatically displays a video feed from a camera mounted in the rear of the vehicle, to assist the driver in reversing the vehicle, as a rear view is needed at all times.

In case of a power or total display failure, a set of secondary 'get you home' instruments have been included, consisting of an altimeter, airspeed indicator and an artificial horizon display. These instruments are pitot static driven so that they will remain functional at all times. As these displays are not intended for use except in an emergency, a cardholder will cover them during normal flight. When they are required the cardholder can be rotated up into the fascia to expose the instruments.

Figure N.2-4 Emergency Instruments

As discussed in section 2.1.1, a joystick is used for flying and driving. The drive-by-wire controls were placed on each side of the cockpit. They were placed on the door for ease in access and comfort of the pilot or co-pilot as the case may be. It was taken into consideration that people are generally not ambidextrous; therefore the controls were placed identically on both sides. A control button was placed on the dash to disable the co-pilot controls until activated.

The climate controls were placed on the console along with the CD player to allow for the passenger interaction as well as the pilots: this allows for the pilot to concentrate on his task and allow the passenger to control the comfort levels, while still allowing the pilot to adjust the controls when flying alone.

The master controls to transfer the aircraft to automobile mode were placed within reach of the pilot, with a guarded switch. This was done to avoid accidental transition in mid-flight.

By not being in a position of constant attention, the switch is less likely to be accidentally activated. For this reason, other ideas for placement were overruled. As far as the control itself, it was thought that some sort of button would be the most preferable rather than a lever. Other safety factors that control switching from one mode to another based on the weight of the wheels are discussed in the Appendix O.

N.2.1.1. Control Methods

From the outset two main designs were considered for the vehicle control system; a standard mechanical link or a 'Fly-By-Wire' strategy.

Mechanical Link.

The use of a mechanical control linkage involves *'Side by side Operation'* where the control columns are split for road driving on one side, airplane control on the other. The decision to drop this approach was the result of the duplicated controls and poor use of cabin space. The simplest way to overcome this problem was to utilize a digital link to some areas of control. It was not inconceivable that a solution to the mechanical link route could have been found. Nevertheless, due to the introduction date of 2010 the fly by wire system should be an approved technology and as such a realistic alternative.

FBW.

The first option discussed was a '*Detachable steering wheel'*. If the fly by wire solution was agreed on, the steering wheel could be attached on the dash and control the vehicle digitally on ground mode. This concept drove towards the next model of *'Sidestick with an outboard throttle'*. Here the aircraft control inputs would also control the vehicle on ground mode. Finally the '*Sidestick and center throttle'* was conceived. This was a variation on the above solution, but reversing the position of the sidestick and throttle.

The side-by-side operation was by far the easiest solution to the problem. By having mechanical links the cost would be reduced dramatically and operation in each mode would be more akin to what the operators were used to. Unfortunately, by splitting up the control systems, this would determine which side the vehicle had to be controlled from in each mode. The flexibility for the pilot preference was gone. A greater problem was the efficient use of interior space. The Pegasus represents a technological breakthrough and to have two sets of equipment gave an indication of a half-thought out design. It was not the image to sell the vehicle. However, by far the greatest problem was the mechanical links. To route the cables and pulleys in a standard aircraft is relatively easy due to the hard points and fixed structure. In the case presented, the wing section telescoping in and out made a cable link more difficult to implement. Hydraulic operations were considered but again the decision not to use them fell down to weight penalties. Also, the area forward of the two front seats was at a minimum. The avionics packages sat behind the fascia and the front undercarriage and steering mechanism all had to be housed in a very compact space.

Realizing the problems that would be faced with a mechanical link brought the fly by wire system to our attention. Although the costing was known to be higher than the existing mechanical solution, the application was far better suited to the aircraft's airframe. A large cost of FBW equipment comes from the level of authority given to the system. By reducing the complexity (and hence the authority) it was anticipated that the costs would also decrease.

Another advantage was the reduction of mechanical parts, which would wear with time. The simplicity of the FBW solution negates the utilization of any clutch system needed to engage the different drives from one mode to the other. This would reduce the servicing costs, as the only serviceable feature would be the electrical actuators.

Many aircraft in existence already utilize FBW technology, so it was more an issue of applying it to a light aircraft. Many motor manufacturers have already used drive by wire for some features, and Mercedes Benz has also studied the possibility of making a car completely drive by wire with their F200 concept car(7), so the idea was technically feasible. Accepting the higher costs and increased complexity of electrical actuators were deemed the way forward.

This led on to the idea of a detachable steering wheel. The concept used a steering wheel, which could be removed from its boss on arrival at the airport where the side stick in the door could then come into effect. The steering wheel boss used electrical displacement sensors to monitor the rotation of the wheel, and transducers mounted in the dash, (within the collar the boss secured into) supplied the input to turn the steering rack accordingly. The wheel when not in use could be stowed under the rear seats. Again the technology existed to remove steering wheels and Formula One Motor Racing cars show the level of complexity that can be successfully implemented. Displacement transducers work to a high degree of accuracy but in the case of the steering wheel suffer from poor feedback. Further research showed that the single biggest factor why steer by wire had not come into effect was the problem with driver feedback. Much of the sensory information available to the driver is a result of what feel the car has with the road. In extreme driving conditions the driver feels the lightness of the steering wheel is possibly the result of ice. Also heavy rain causing aquaplaning is felt by the sudden loss of feedback from the steering wheel. Perhaps the biggest problem is during the limit of tire performance. When cornering heavily the driver is normally aware of the twitching of the front wheels as they gain and loose traction moments before the car enters a skid. This may be lost with digital control. Unless adequate feedback was introduced, the control mechanism was too vague for serious consideration. What was needed was a solution where the feedback in car mode did not disagree with the feedback that exists in standard car steering mechanisms.

To use a side stick in flight over a traditional yoke increased the feeling of room inside the cabin and left an uncluttered environment in which to work in. The success of the Cirrus SR20 (figure N.2-6) shows the realistic application of the technology in GA aircraft control. The possibility of linking up this style of operation with the car controls was of great significance. Side stick for aileron and elevator control leaves an unobstructed view of the instrument panel.

Figure N.2-5 Cirrus SR20 Cockpit[8]

Side sticks are also noted for their reduction to Pilot Induced Oscillations (PIO) in flight. This is due to the user repeatedly over correcting the attitude of the aircraft or not allowing the effect of the input enough time to alter the behavior of the aircraft. Throughout the duration of the flight, the pilot can rest his arm on the side rest and reduce his fatigue. This effect is most noticeable through flights of considerable G-maneuvers. Under heavy accelerations where the forces are increased on the pilot, the armrest significantly alleviates this and the workload is decreased. The side stick is also the instrument for the next generation pilots, raised on home computer flight simulations.

However, using one set of controls for both modes, flying and driving, creates a possible overlap of functions for both the stick and the pedals. One idea was to utilize the stick for steering (left and right) and speed changes (braking and acceleration) whilst in the drive configuration. This idea was swiftly rejected when severe retardation forces were considered. In the case of a crash, the occupant would force the stick forwards, giving the command to accelerate. Reversing the commands so that forward slowed down the vehicle was considered too unorthodox for the general public. The action of braking the vehicle with forward pressure on the stick is not an intuitive action. Every effort was made to make the operation of the vehicle as natural and instinctive as possible to reduce the workload and increase safety.

The side sticks will control roll and pitch in aircraft mode. The stick will also be outfitted with a four way coolie hat to control rudder and elevator trim. In car mode those controls are for turn signals and the high beams lights, and the side stick will control steering. Mercedes has improved side stick steering in its SL roadster research vehicle. For steering the stick moves 20 degrees in each direction and uses force feedback found on modern computer joysticks. The steering is also speed sensitive, so the faster the car is moving the more the joystick needs to be moved. [(9)]

The decision of throttle position was then determined to facilitate operation of the vehicle in both modes from both front seats. One possibility was to duplicate the stick controls in the door and have a centrally mounted throttle selector. The other possibility was to have a duplicated throttle control in the door and a single centrally mounted control stick. For a single engine, side by side seat aircraft FAR section 23.777 states that the throttle should be at or near the center of the cockpit and so the decision to go this way to save certification time and money seemed sensible. There is an extra cost of producing two side sticks but the flexibility the vehicle gave was rated as more important.

The control method of the pedals in each separate mode posed few problems. Independently the method of control was easy to implement. However, when trying to satisfy both motions of travel, for both modes of transport and on the same set of pedals, the problem was more difficult to solve. In a standard automatic car the motion of the brake and accelerator are independent however in an aircraft the rudder acts antagonistically. Secondly, the travel of the pedals found on a car are rotating about the top of the pedal arm. In an aircraft the motion is purely translational, front to rear. Finally the weighting of the brake, accelerator and rudder was all different, as was the feedback. The final design utilizes a three pedal system with only two pedals being operational throughout each mode. In flight the Pegasus uses standard rudder pedals linked to electronic transducers which monitor displacement. Between the rudder pedals lies the standard brake pedal. It was decided that the feel of the brake was of paramount importance and so is hinged in a standard manner to give rotational displacement. The braking is controlled electronically, with the feel of the brake is provided by a mechanical spring and damper system. The brake pedal box was developed from a car modifications and accessories supplier where a unit existed which could be adapted to our purpose [(8)]. To use a different pedal arrangement from air to ground mode duplicated the controls and was inefficient use of equipment. The pedal box used digital sensors to monitor which mode the vehicle was in before disconnecting the travel in the left rudder for road operation. In flight the rudder controls are similar to the accelerator in feel due to their light loads. The toe brakes at the top of the pedals are hinged as in standard aircraft. In road mode the aircraft toe brake pedal on the accelerator becomes inoperable.

The final control mechanism studied was the throttle and gear selector unit. Again the drive was for one amalgamated unit, which utilized hardware from both modes. The most efficient way to do this with minimal changeover problems was to create a simple 4-gate for the lever to sit in. The vertical slit on the left was chosen for the throttle setting in flight and the right slot was the one used for the automatic gear selection on ground mode. The drive position on the automatic transmission was placed on the opening to the gate so that moving the throttle from one mode to the other ensured the vehicle was in Park mode. This reduced the possibility of the car moving off during a changeover. When shifted from drive position on the right to aircraft throttle setting on the right, the engine setting became ‘off’. To start the engine in aircraft mode the throttle had to be pushed forward to select a positive throttle setting, and the engine started with a conventional push button dashboard switch. All switches for mode changeovers are protected by flip top coverings.

The final operation is summarized below in table N.2-1.

Table N.2-1 Control Methods

Maneuver	**Aircraft Mode**	**Road Mode**
Left Rudder Depressed	Yaw to Left	
Middle Brake Pedal		Vehicle Brakes
Right Rudder Depressed	Yaw to Right	Vehicle Accelerates
Stick to the left	Roll to the left	Vehicle steers to the left
Stick to the right	Roll to the right	Vehicle steers to the right
Stick forward	Nose lowers	No action
Stick back	Nose raises	No action

Coolie Hat Up and Down	Elevator trim	Main and dipped light beam
Coolie Hat Left and Right	Rudder trim	Turn signal

N.2.1.2. LCDs

A new technology in touch screens and displays is Liquid Crystal Display (LCD). The traditional monitors that have been used for years are Cathode Ray Tubes (CRT). LCD screens are becoming more popular and as the increasing popularity of laptops increases the costs will come down in the future. LCDs are very thin compared to CRT monitors, which allows the display to take up less room behind the control panel. Another advantage of an LCD displays is that they consume much less energy(11). The only disadvantage that must be overcome with an LCD display screens is the smaller viewing angle. It must be more directly viewed from the front.

Active Matrix Liquid Crystal Displays (AMLCD) were chosen for the Pegasus because they alleviate the smearing problem associated with display movement on LCDs. The specification AMLCDs is based on displays used by Archangel Systems(10). The outer AMLCDS have a diagonal screen size of 26.42 cm (10.4 inches), equating to an overall physical screen size of 15.25cm by 21.59cm (6in by 8.5in). They have a horizontal viewing angle of ±40º, which means that the information displayed can be read from the opposite seat, and a vertical-viewing angle of ±30º. The MFD LCD display is equipped with hardware and software that allows for touch screen interaction from the pilot. The pilot has the ability to choose what functions he would like displayed. These allow for the pilot to configure a setup that will best suit his needs. It is important that the pilot familiarized himself with the system to reduce the chances of error in emergency situations.

The display system was designed in accordance with the FAR 23 and Advisory Circular N^{o} AC 23.1311-1A regulations, in order to reduce the costs and time scales required to certify it.

N.2.1.3. GPS

Global Positioning Systems (GPS) are becoming more commonplace in the general aviation market. GPS is a navigation system made possible by a constellation of satellites operated by the Department of Defense. The satellites send out signals that are processed by a GPS receiver, which then displays the user's latitude, longitude and altitude based on the information received. This system is extremely useful to pilots because it allows them to plan their flight and to pre-program waypoints along the flight route. Location information provided by the GPS receiver will insure that the pilot is flying in the correct direction. The GPS receiver can also be integrated with moving maps and weather information. By adding a moving map system the pilot will have instant access to a database of maps showing airports, roads, navigational aids, and pre-planned flight paths. Thus, once in car mode the GPS will be valuable to the driver as well. The position of the aircraft will always be known and the pilot will be able to adjust to unanticipated changes in the flight plan. The maps can be overlaid with a variety of different databases chosen by the pilot. In emergency situation this can be extremely helpful.

Incorporation of the system will allow for direct flight planning and instrument approaches. For bad weather or night landings the system reduces the reliance on ground support (12) Integration of the weather system with GPS and moving maps help the pilot make quick and accurate changes to the flight plan in order to avoid turbulent conditions. Also if weather requires landing, the pilot will be able to continue on with the help of moving maps.

N.2.1.4. Weather Link

ARNAV Systems' [13] WxLink is being used to provide weather information. This is a one-way data link that periodically broadcasts weather information to an aircraft while in flight. The aeronautical network can be used to provide real-time weather information to all equipped aircraft operating in the coverage area. Local weather for a radius of 150 miles from the closest facility is transmitted to the aircraft while in flight to provide the pilot with current Meteorological Aviation Routines (METAR) and Next Generation Weather Radar (NEXRAD) ground weather radar information. Pilots also receive additional weather information for areas outside the 150 mile area, including METARs for most air carrier airports and a CONUS (Contiguous United States) national NEXRAD mosaic image that provides clear visual information pertaining to weather fronts, isolated thunderstorms and other convective events.

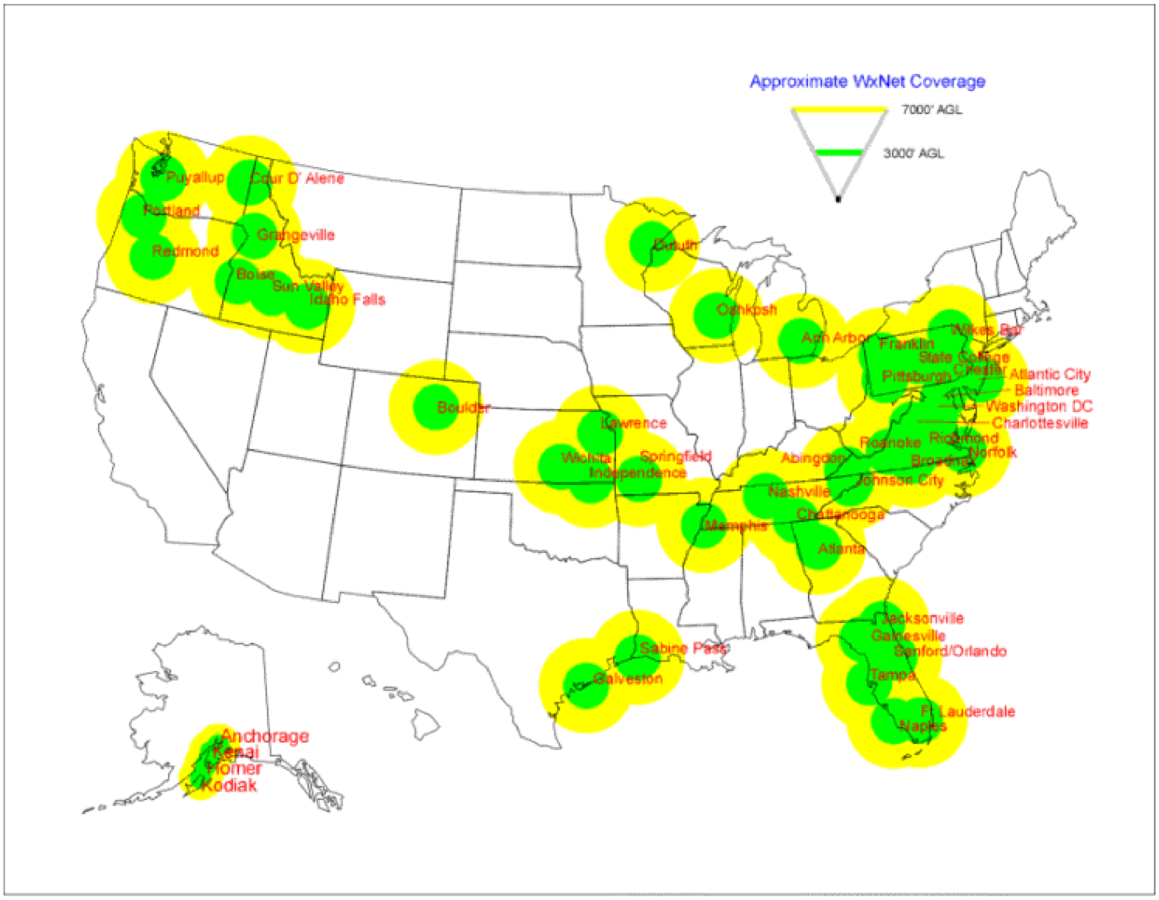

Figure N.2-5 The current WxLink network coverage.

From the figure above, it can be seen that the current coverage of this system is relatively limited. However, in the years leading up to the release of the Pegasus this should expand, particularly so with the revitalization of general aviation.

N.2.1.5. Switching from Plane to Car

The changeover between the two vehicle modes is initiated by pressing a single guarded push button switch on the dashboard. The guard is to prevent inadvertent operation of the switch, however there are several other conditions that must be met before the system will initiate the changeover, details of which are further discussed in the Appendix O.

Ground to air changeover

When a changeover from car to aircraft mode is initiated the ‘outer LCDs’ display the PFD display detailed in section 2.1.

The avionics system computer reactivates the transmission capabilities of the Transponder and VHF radio ready for flight, and provides the controls with the flight control functionality.

Air to ground changeover

When a changeover from aircraft to car mode is initiated one of the outer LCDs switches off and the other displays the car symbology discussed in section 2.1.

The avionics system computer deactivates the transmission capabilities of the Transponder and VHF radio so that no inadvertent transmissions can be made whilst in car mode. It also changes the control system so that it provides the car control functionality.

N.2.2. Radios

The radio system for the Pegasus not only provides a VHF communications facility but also provides a complete entertainment and intercom system for the vehicle.

In car mode the system allows the occupants to listen to the radio or a Compact Disk. In aircraft mode the system allows the pilot and co-pilot to transmit on VHF when the 'press to talk' button is pressed. When it is not pressed the system provides all four occupants with an intercom facility.

N.2.3. Extra Features

N.2.3.1. Fire Extinguisher

In order to comply with section 23.851 of FAR part 23, a hand CO_2 fire extinguisher is mounted under the pilot's seat to combat any cabin fires. A CO_2 extinguisher was chosen over a conventional water extinguisher, because of the electronics in the cockpit.

In addition to the cabin fire extinguisher, an engine fire extinguisher system has been fitted that allows the pilot to 'fire' two shots of CO_2 in the engine compartment to extinguish an engine fires. The system is activated via a guarded switch on the fascia.

N.2.3.2. CD Player

A CD player and AM/FM radio is located on the console between the seats; see Figure N.2.1-1. The CD player allows rear and front passengers to listen through headphones during flight. As many cars today are equipped with stereo systems, while in car mode the CD player and radio can be listened to by the entire cabin.

N.2.3.3. Window Opening Mechanism

The Pegasus has a window opening mechanism, only responsive in car mode. The current car market has a window lock available. The window opening mechanism is like those found in cars and while in flight the mechanism will be disabled. This feature allows for a more pleasurable road experience in the case of landing and having to travel some distance to the next destination.

N.2.3.4. Color Schemes

The need for individuality is recognized in the design of the aircraft. Every color option starts with the consumer's desire for a vehicle that reflects their personality. A choice was essential to the customer. Different exterior colors could reveal subtle nuances, adding vitality to an extraordinary shape. Aimed towards the business sector, the seats and door panels can be trimmed to customers own leather color choice. A selection of different Alcantara hides with different grain finishes is available as an optional extra. All options are included in the design to promote an environment with natural character. As all consumers have to be thought of as unique, so the product sold to them must be tailored to that personal level. With an aircraft as complex as this, the cabin space was aimed at being as natural as possible; calm colors were suggested to reduce an overwhelming feeling. Above all the emphasis had to be with consumer choice.

N.2.3.5. Other

Other features available in the Pegauss inclued:

- Air conditioning
- Front and rear cup holders

- Power outlet

N.3. Visibility

The visibility analysis was run in parallel with the cockpit design. The first draft on seating using the anthropometrics data gave a solid foundation from which to construct the visibility study. The prime area of concern was the dual mode experienced with the aircraft. The visibility while in air mode was to be designed on existing data. The recommended visibility is 240^{o} around the horizon and 13^{o} down over the nose[(15)]. This gave rise to the configuration shown in figure N.3-1.

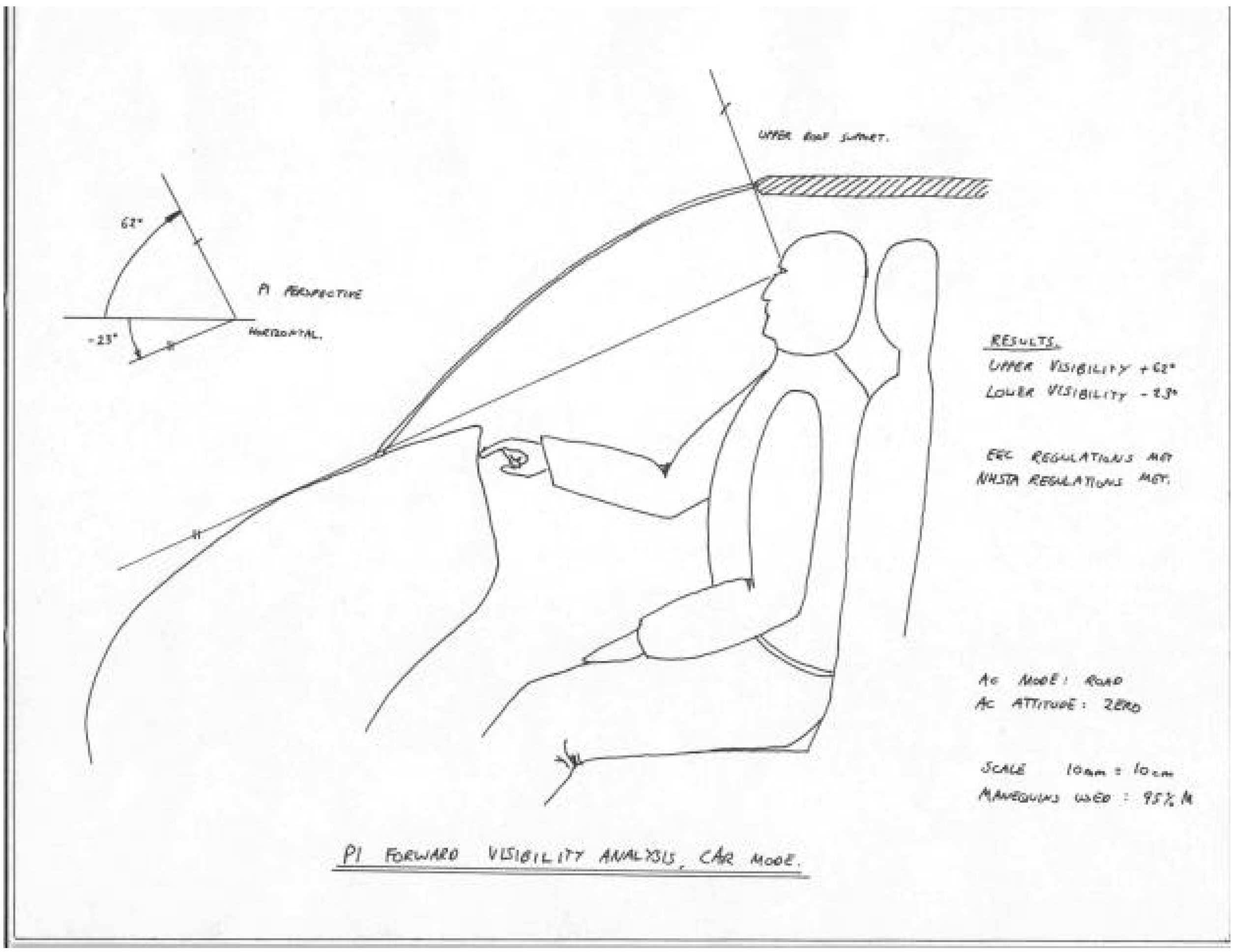

Figure N.3-1 visibility down over the nose

The primary region obstructing vision towards the front of the aircraft was the top of the dash. To adequately improve the range, the instrument panel was lowered by 150mm. This when redrawn showed the front of the nose to be the new determining feature. This was considered a satisfactory solution to the problem as many cars have the problem of the bonnet obstructing the immediate line of sight to the road below. On the ground the Roadable aircraft has two major increases to its field of forward vision, both due to the uniqueness of the vehicle. The first is the additional height gain for a car of its class. The travel needed in the front undercarriage on landings meant a large distance from full extension, no load on wheels to wheels at bump stop; no more extension possible. The hull of the fuselage could not foul the runway in the latter state and so this determined the fuselage ride height. Consequently the occupants have an elevated forward view from their cockpit. Quantitatively, the ride height on taxi is not dissimilar to that of an off road vehicle, such as the Land Rover Defender. The advantage that the aircar has over standard road vehicles is the inclination or attitude adopted on the road. When driving, adjustable suspension sets the aircar in a slight nose down attitude to reduce lift. This has the added advantage of elevating the occupants up behind the front wheel and increasing their field of ground vision. The visibility above would obviously be reduced slightly but this would not be a significant reduction and even taking that into consideration there would be no instances where this would hinder the vehicle in car mode.

In both road and air mode the biggest disruption of the forward field was through the A-posts needed to support the doors. Several attempts were made to reduce their impact by moving them both aft and increasing the door size but the final position of the members was stipulated by the Structures subgroup. The front pillars form the primary roll hoop in case of an accident. To move them backwards could compromise passenger safety hence the move was to work around them and minimize their intrusion.

The only way to remove the doorpillars was to have a single piece wrap around windshield, which met up with the two side doors further behind. This gave unrestricted viewing for 160° in the forward region. The problems with this solution were the effects on structural integrity along with the problem incurred with ingress and egress. Having the doors further back meant their opening was behind the front seat and in front of the rear bench. This created more problems than it actually solved. The second considered design was to reinforce the nose so that in the effect of a rollover, the fuselage sides acted as a protective tub with the firewall providing the aft roll hoop. The idea was based on the approach taken by the Formula One chassis design. To design a strengthened nose proved to be too difficult in the time allowed by the structures team. This point aside, there was also a problem with the weak cockpit caving in to the occupant space should a rollover occur. The final concept shows a traditional approach to the safety problem.

The biggest obstruction for the pilot in flight in the vertical direction was the roof fixings for the gull wing doors. The final design is a structural compromise but it has still better upper visibility than a *Cessna T206 Turbo Stationair* (studied for its visibility regions) due to its low wing. The low wing in flight should not pose much of a problem as the leading edge is positioned as far back as the rear seats backrest. In flight by far the biggest problem regarding visibility comes during landing where the nose is pitched up and the front undercarriage protrudes significantly from the sides of the fuselage. Conventional aircraft generally have much smaller undercarriage housings, most of which are mounted directly or behind the pilot. This was simply not an option.

The visibility to the sides was easily determined by the window size. Both front and rear passengers had separate windows and it was a case of increasing the window size until the level of vision required had been achieved. For the rear passengers the front edge of the window must be around 60° from the centerline of the aircraft[C].

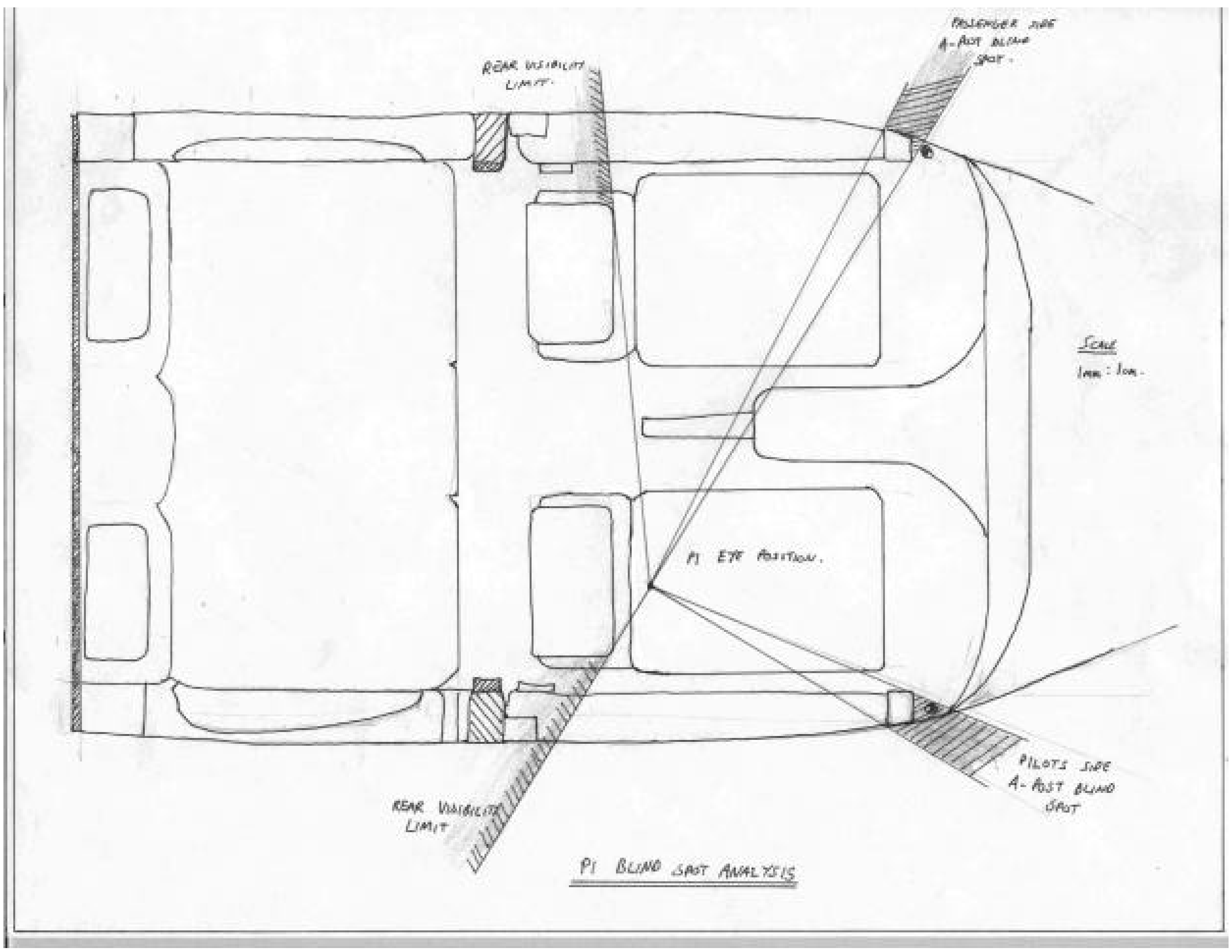

Figure N.3-2 **A plan view of the occupant's horizontal field of vision**

Reference material had shown that the effects of increasing visibility by moving the frame out induced a feeling of separation of the occupants from the vehicle. The edge of the rear frame was fixed to be in line with the center line of the backrests, in front of the firewall.

The rear visibility was deemed of limited interest in flight mode but on the ground obviously had great effect with maneuverability. A camera mounted within the fin utilizing the LCD in the cockpit was a primary solution and would make use of the extensive software available on ground mode. The final proposal was for two simple clip on mirrors, mounted of the front undercarriage legs, which could be removed for flying. This decision to choose the simpler solution was cost related. It was decided though that if the vehicle was to be introduced as a technological platform to show its avant-garde approach then the rear camera could easily be fitted. Once in production the clip on mirror would be implemented although a retrofit would not be impossible, possibly for variants on the design for different consumers.

Studying the real life visibility envelope without using scaled drawings was the ultimate aim for the analysis as the charts produced were not totally accurate due to the number of estimations that had to be made regarding occupants height and mode of transport. The software package JACK had the option to 'view environment' when given the virtual cockpit. The position of the pilot's eyes could be defined, as could the range of movement available. A 'dummy camera' would then show the real surroundings as seen by the virtual occupant.

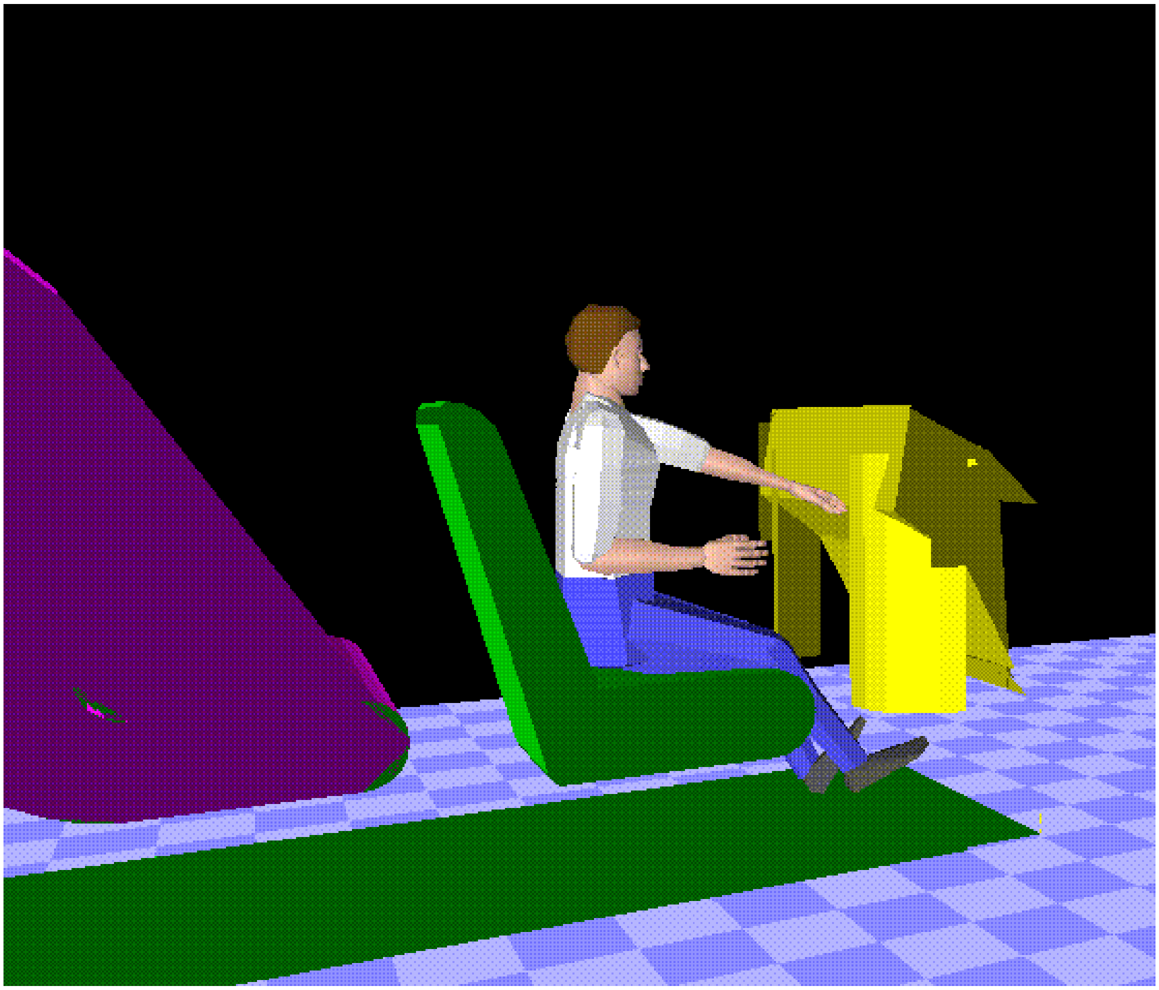

Figure N.3-3 JACK image of the cabin

N.4. Ingress/Egress

Regardless of the aircraft's performance, if the vehicle was difficult to get into or out of it would be harder to sell. The seats had already been assigned a position relative to the leading edge of the wing. One major problem with working on components of the aircraft was the failure to recognize the surrounding structures effect. The initial concept had four doors, as this would be the most functional option for a full crew load. However, on integrating the cockpit with the main fuselage it became apparent that the rear of the aft doors, when hinged about the forward edge swept through the wing. This was technically very complex to accomplish. The occupant would also be faced with a leading edge; halfway across the exit they were leaving from. Again, not a good solution. The rear doors were eventually dismissed after no viable egress solutions emerged. This left the aircraft with two front doors for four occupants. The method used to move the front chair was taken from a three-door hatchback already in production in the car market. The MkII Nissan Micra proved to be the most ideally matched as moving the seat initiated three separate actions, all needed by the Pegasus. On pulling the backrest mounted handle, the first action is the rotation of the backrest forwards. This is coupled with the sliding mechanism to move the whole unit forward along runners. The seat is sprung loaded as this minimizes the effort needed to move it and is particularly advantageous where small children are concerned. The third action is a rotation of the seat about the front two floor mounts. This moves the seat onto the dash, or steering wheel in the driver's case. The end result is a chair free corridor, which allows easy and uncluttered access in and out of the aircraft rear seats, all from one easy to use handle. The option of having the chair perform these rotations electronically was considered but dismissed for two main reasons: The chair functioned perfectly well as it stood; the inclusion of motors was heavier and probably more expensive.

The next feature to be considered was the actual hinge line of the door. The possibilities were numerous. Front hinged, split upper and lower (as on the Lear Jet), suicide (rear hinged), scissor and gull wing were all developed and drawn to fit the fuselage. A decision matrix was the most sensible way to determine the best solution as each had its own merits and drawbacks.

Table N.4-1 Door option decision matrix

Type	Cost	Ingress/Egress	Safety	Aesthetics	Legislation		Totals

Fwd H	4	3	3	3	5		18
Rear H	3	3	3	1	5		15
Scissor	2	3	2	4	2		13
Gull wing	2	4	2	5	2		15
Split Upper and Lower	2	4	2	4	3		13

Although close, the gull wing doors were not chosen due to the legalities involving rollovers. A standard front hinge is shown on the final model. The front A-frame was already reinforced due to the rollover considerations and provided the ideal fixing point and still gave a clear area to climb in and out of the cockpit.

N.5. Safety

The aircraft and automobile regulations specify a minimum level of safety that must be met by the Pegasus. In addition to these minimum requirements it was recognized that by increasing the level of safety afforded to the occupants of the Pegasus, it would also make it more marketable.

N.5.1. Seat Belts

Both the relevant aircraft and automobile regulations require seat belts to be fitted to the vehicle in order to protect the occupants in the event of a crash. It was felt that the three-point belt system of the type fitted in cars should be used, as it would offer a greater level of protection for the occupants. In addition car seat belts have been continually developed to maximize the protection offered to the wearers in all crash conditions.

The seat belt system fitted to the Pegasus consists of many features that can be found in practically any automobile.

Although seat belts reduce the likelihood of injuries, in high-speed collisions rib and abdominal injuries may be suffered, especially if the seat belt is not correctly positioned. In order to reduce these risks, devices to ensure the seat belt is in the most effective position are included such as seat belt height adjusters, pretensioners and load limiters

N.5.1.1. Height Adjusters

Height adjusters improve the seat belts' protective effect by achieving correct belt geometry. They also increase the ease and the comfort of use for car occupants of above or below average height. This system can be seen in figure N.5-1.

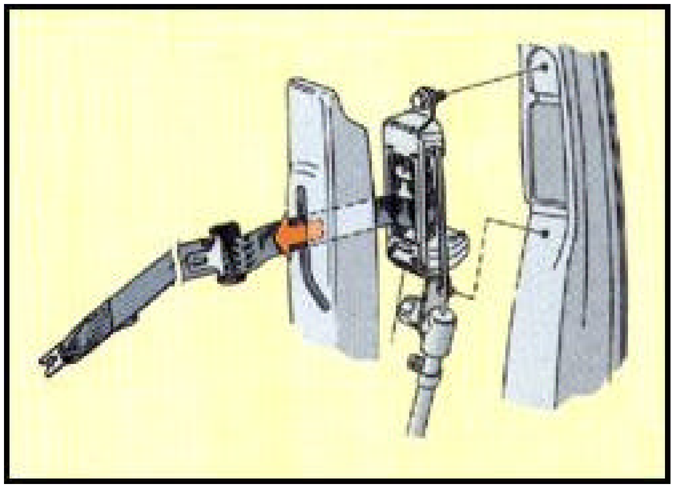

Figure N.5-1 Height adjuster system [16].

N.5.1.2. Pretensioners

Pretensioners have been developed to tighten the belt during the very first fractions of a second in a crash. This ensures that the seat belt starts to restrain a car occupant as early as possible in a crash and thereby reduce the load on an occupant's chest in a violent crash. Figure N.5-2 show the seat belt pretensioner.

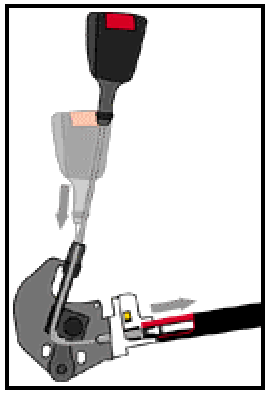

Figure N.5-2 Seat Belt Pretensioner [17].

They also reduce the risk of "submarining", when the car occupant slips under a loosely tightened seat belt. The pretensioners use the same sensor as the airbag and the two systems have been tuned to maximize the protection for the occupant.

Depending on the slack in the seat belt system, pretensioners can tighten the belt up to 15 cm (6 inches) by using one gram of a pyrotechnic propellant, either by pulling the seat belt buckle towards the floor or by operating the retractor.

N.5.1.3. Load Limiters

If the load on an occupant's body becomes too high in a violent crash, a load limiter mechanism in the retractor allows webbing to be pulled out slightly. This is especially important for elderly, since studies have shown that a sixty-year-old person can only take half as much load on their rib cage as a twenty-year-old person.

The load limiter is integrated into the retractor, where a specially designed bar holds the spindle with the webbing. When the force from the webbing exceeds a pre-set limit (approximately 4kN), the end of the bar turns, twisting the bar and thereby gradually reducing the load on the occupant's chest.

N.5.2. Airbags

To further increase the safety of the front seat occupants, front airbags have been fitted to the vehicle. These are now commonly fitted to automobiles for both the driver and passenger. Due to the use of sidesticks the risk to the people in the front seats is already significantly reduced, but this can be reduced further by the use of automotive passenger seat style airbag systems, shown in the figure N.5-3.

Figure N.5-3 Car Front Passenger Airbag [18].

Research carried out by the National Highway Traffic Safety Administration has shown that deaths due to frontal crashes have been reduced by about 14% among front seat passengers wearing seat belts and 23% among passengers without belts. The combination of an airbag and seat belt has reduced the risk of serious head injuries by 81%, compared with a 60% reduction for seat belts alone.

N.5.3. Firewalls

Safety was a critical issue considered in some detail. The safety aspects of the vehicle were considered more in the capacity of the Structures Subgroup but however these impacts on the occupants were analyzed. The role of the firewall was two fold. The first as the name suggests was to protect the passengers from a fire, started in the engine bay. The second was to protect the passengers in the instance of a rear end shunt or heavy retardation where the engine may break free from its mountings. Addressing the issue of fire risks, the composite structure behind the rear passengers must be able to withstand high temperatures without burning. Using techniques already employed by light aircraft manufacturers, the composite best used for the application is Sperotex and is treated with a phenolic resin. This resin application is sufficient to satisfy all fire regulations.

The shape of the firewall derives from principles pioneered in small car production(19). In the event of a force great enough to dislodge the inverted engine from its original position, the floor pan is designed in such a way to force the block down, and under the base of the aircraft. Strong tubular members are woven about weaker elements so the engine movement absorbs energy on its route out whilst remains constrained to travelling on the safest path; away from the occupants. In extreme load cases the engine would break the firewall within the wing center section (inside the low aspect ratio box) before leaving the fuselage. This passenger compartment would be forced upwards in this instance to accept the increased travel. The whole aim behind this is energy dissipation. By allowing the massive elements of the vehicle to come to rest, separate to the occupants, the deceleration forces will be minimized resulting in a likely reduction of injury.

N.5.4. Traffic Collision Avoidance

The Ryan Traffic and Collision Alert Device (TCAD) greatly reduces the possibility of a midair collision by enabling the pilot to quickly identify, monitor and respond to collision threats before they become critical. The TCAD system alerts the pilot to the presence and location of traffic in their proximity, along with information that indicates potential problems.

The inclusion of this system combined with the weather information provides the Pegasus with a complete freeflight capability.

N.5.5. Warning Systems

It was decided that speech warnings would be used to alert the pilot to the major situations requiring immediate action, in addition to the visual cues. The major alerts were considered to be stall warning, traffic collision and engine fire alerts.

In addition to these major alerts, additional alert indications are provided by an audio tone and/or visual cues on the displays and warning panels.

In accordance with FAR 23.1322 the following colors have been used:

- Red to indicate a hazard that may require immediate corrective action.
- Amber to indicate the possible need for future corrective action.
- Green to indicate the system is operating within its normal parameters.

Training

One of the AGATE objectives was to develop a computer based training system. Training the pilot to be familiar with the instrumentation and warning system of the aircraft will take a minimal amount of time due to the user friendly design which has been developed. The computer training program will be organized into two sections where the first section will familiarize the pilot with the cockpit and the second section will test the pilots introduced as well as how to read any “non standard” instruments or gauges. During this section the pilot will also have a chance to practice reading the gauges and to operate the controls. The next step of the training program is to test the pilot’s knowledge. This is done via event simulation. The pilot will be presented with a situation in which he will have to interpret the warning and also indicate the value on the gauge that the warning represents. To increase the realism the pilot will also be performing a secondary task such as reading the GPS. In the air the pilot will not be waiting for or anticipating a warning signal or some other event because he will be involved wit radio communication, communication with other passengers, or insuring that he is aware of the surroundings. Each response during the event simulation will be timed and the pilot must answer each response in a specific time limit or else he must go through a review and take a re-test. This is important, because in the air quick and correct decisions can be the difference between a critical situation and a fatal situation. An advantage to using a PC based training program is the cost. The pilot does not have to purchase special equipment because the program runs using a Macintosh or IBM compatible computer with a port for a headset to be used.

It is important to simulate distractions. Flying an airplane or car with unfamiliar equipment can be a distraction[20]. The incorporation of the joystick may be unusual to pilots and drivers and will be incorporated into the training. A pilot and driver will need to log several hours using the joystick to ensure its familiarity.

N.6. Noise

It is important to keep noise in the cabin at a minimum. Continuous vehicle noise experienced over a long period of time can cause increased fatigue and passenger discomfort. (M1) The initial concept specification required the vehicle to replace the standard car for long journeys, across the USA. Clearly duration in the order of several hours was planned for the occupants. The limits on the maximum length of the journey were dictated by the ability of the operator to remain focused and alert, and also, how long passengers could go without breaks for refreshments and toilet stops. The requirements were obviously to minimize the sound transmitted into the cockpit from the engine and the road without penalizing the operational weight empty with bulky sound absorbent padding. The aspect of road noise from the vehicle to other road users and pedestrians was also an issue to focus on.

The noise originates from two generators, the engine and propeller. The propeller emits increasingly high and penetrating frequencies as tip speeds approach the speed of sound. The propeller-tip speed noise could be decreased with a reduction in propeller diameter. Yet, this creates a trade-off as the weight and cost of the propeller.

There is little that can be done to reduce normal propeller noise.(M1), but knowing the engine data the levels of noise from propulsion could be predicted and effectively lowered.

The engine provides many alternatives for noise reduction. There were a number of options considered but many available off the shelf solutions are applied primarily with automobiles in mind. The best solution was considered to use Dynamatting around the upper engine bay and throughout the cockpit. Normally sound proofing material is heavy but at only 0.7mm deep, the trade-off on mass was minimized. The cockpit floor was coated, as was the instrument binnacle and firewall front. The matting minimizes noise interference by damping out the structural resonances experienced by composites.

Another viable option for the Pegasus was the incorporation of a muffler. Since the vehicle will function as a car and will be required to have a muffler. Automobile mufflers do not work on aircraft engines, because the automobile is normally operating at a small percentage of total power, while an airplane is at or near maximum output. The Pegasus is equipped with a low back pressure muffler compatible with the engine.

The placement of the propeller and engine in the back of the aircraft will also reduce some of the noise level in the cabin. General placement of the accessory sections and driven accessories tend to be directly ahead of the firewall in the average airplane. This permits all accessory noise to be reflected from the engine right back into the cabin area. The cabin will be separated from the engine deck by the bulkhead and firewall, which will absorb some of the reflected noise levels.

The road noise was reduced to minimal levels by the inclusion of rubber door seals and well-fitted windowpanes. To reduce the noise effect of the engine, the mountings were designed to use rubber bushes and grommets as well as the traditional steel bolts and rubberized collars on engine steadies.

The exhaust note was minimized through a conventional silencer arrangement. By placing the exit towards the rear of the aircraft the possibility of exhaust noise was decreased for the occupants. Unfortunately due to the unclean lines on the vehicle with the fin protrusions and sharp wing fences, when driving in road mode it is anticipated that the cabin noise will be markedly higher than conventional vehicles. The technology clearly exists to reduce noise levels even more, but they carry with it large weight and cost penalties. It was therefore a compromise on other issues that left the road noise levels at this higher than average values.

It is beneficial for the pilot, in flight, to wear a headset that will serve as both a communication and noise-attenuating device. Technologies that would allow the pilot to communicate without a headset were considered, however after researching the human factors side of the issue it was decided that headsets would make the aircraft safer. It is necessary to equip the aircraft with headsets is because the market that we are attracting contains many older individuals and those concerned with safety. Statistics show that pilots, especially older ones, must turn up the volume relatively loud on their headset in order to hear auditory warnings and radio communication. The assumption cannot be made that all pilots possess the same hearing level because current legislation has lax hearing requirements. In a study of causes for disqualification in USAF pilots and navigators over a two-year period in the 1980's only three were grounded for hearing loss[(21)]. The FAA has imposed regulations, yet current legislation has lax hearing requirements on pilots and the noise that they can be exposed to in the cockpit. Small propeller driven aircraft will have to meet FAA standards with external sound levels at 80 dBA at 1000ft[(15)]. It is not necessary to insist on tougher regulations, however, it would be more beneficial to the market of older pilots with increased potential for hearing loss and to the family buyer, to accommodate these pilots and the passengers with headsets. The headsets for the all passengers would have the potential to be plugged into the CD player. The availability of the headsets would provide for a more comfortable and quality trip in the Pegasus.

N.7. Car Features

N.7.1. Climate Controls

In order to comply with the aircraft and automobile regulations the Pegasus must be fitted with various sets of external lights. In order to control these various lights, a switch, N^o 19 on figure N.2-1 in section 2.1, is provided on the fascia.

To comply with the automobile regulations, the vehicle must be fitted with headlights, indicators and rear lights. The vehicle is fitted with xenon headlights. These lights provide more illumination than the standard halogen headlamps and are cheaper as well.

The xenon lamps have a luminous flux 2.5 times that of halogen light and use 35% less energy and the color of the light is similar to that of Natural Daylight.

For the indicators and rear lights, Light Emitting Diodes (LED) have been used. LEDs have a quicker illumination time than conventional lamps, and although this time is only fractionally quicker it allows following traffic to react to the vehicle braking quicker and therefore reduce the risk of rear end collisions. It also provides some redundancy because several of the LEDs can fail without degrading the overall effect.

N.7.2. Car-specific Controls

To increase the level of comfort for all the occupants an air conditioning system has been included. It provides the standard types of ventilation found in an automobile, such as windscreen demist, cabin air, etc. The controls for the system are mounted on the dash as shown in figure N.2-1 in section 2.1.

N.7.3. Other

- *Wipers - control 20*
- Horn – on joystick

- Indicators – on joystick coolie hat in automobile mode
- Hazard Warning – control 16
- Headlight Dipped/Main beam selector– on joystick coolie hat in automobile mode

Appendix O. Systems

O.1. Introduction

Every complex system that is developed relies on a collection of sub systems operating together to fulfil the requirements of the system as a whole. For this particular vehicle the systems section is particularly important because two individual systems are being combined into one. This means that there will be an element of duplication that has to be removed and a lot of areas that will have to be included to allow the vehicle to operate safely as a car and as an aircraft. In order to ensure that all of the elements are covered we have decided to adopt a systems approach to design. This is illustrated in the V-Diagram below:

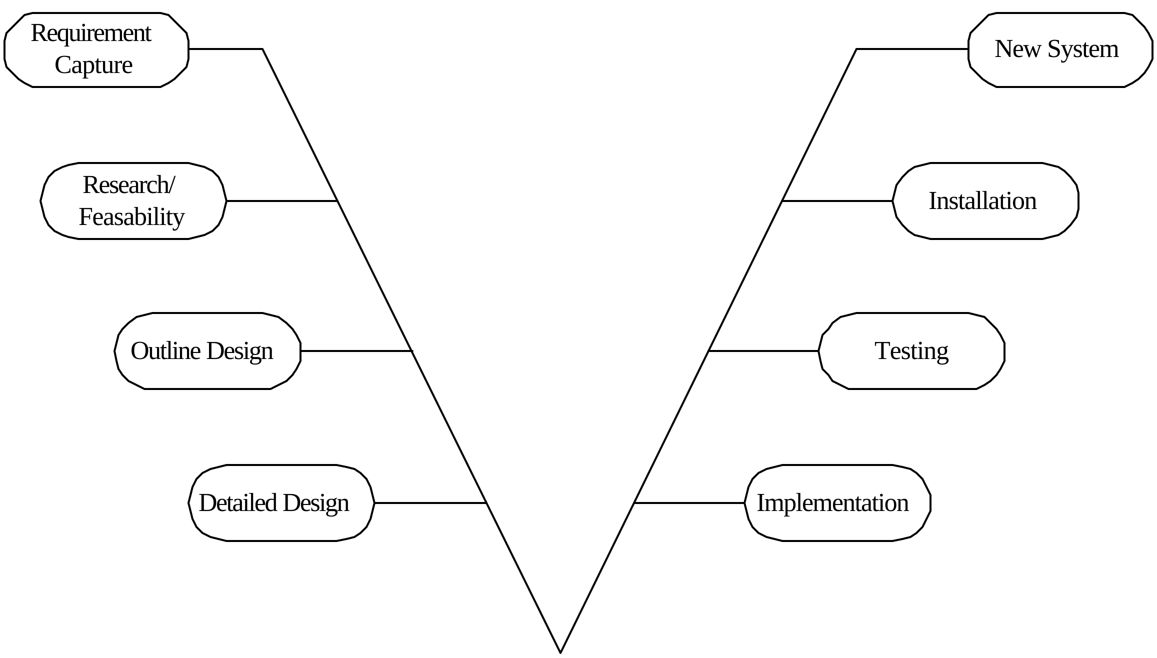

Figure 0.1-O.1-1: V diagram of System Design.

This diagram not only identifies the philosophy behind how the systems elements of the vehicle were designed but also lays out the format of the remainder of this appendix. The initial step is to identify the requirements from each of the sub groups as to the electronic and power requirements that they require. Primarily this covers the monitoring of propulsion systems and the gathering of the vehicle performance data so that it can be displayed and the generation and supply of the necessary power to keep the vehicle running smoothly both electrically and from a fuel point of view. Once these requirements have been identified it is then possible to outline the design for the avionics system and for the utilities system as individual elements. These two systems can then be integrated to give an overall systems design that will be implemented into the PN design. The system can then be tested independently through to fully operational in the Pegasus vehicle environment before final installation and the completed Pegasus system.

The systems design process that was undertaken only addresses the first half of the process described in the diagram above – from requirements to outline/detailed design.

O.2. Comparison of Aircraft and Automotive Systems

In this section of the appendix, existing GA aircraft and automotive technology is assessed and compared so that any duplication between the two vehicles can be combined and to ensure that all of the systems necessary for a roadable aircraft are included in the Pegasus design. From this brief assessment it will be possible to derive a list of system requirements that can then be compared to the lists generated by each of the other technical sub groups. This will ensure that all aspects of the design are covered and that all of the inputs and outputs to the system are included.

O.2.1. Avionics

In order to compare the two vehicles systems this section is separated into six key areas: Controls, Navigation, Monitoring, Communications, Safety and Lighting. Each of these will now be considered in turn and a requirement derived that can be developed as the design is progressed.

O.2.1.1. Controls

Aircraft

A standard GA aircraft is controlled using a control column for pitch and roll and a set of rudder pedals for the yaw control. Both pitch and yaw controls are complemented with trim control devices. These allow the pilot to set the aircraft up for various stages of a flight. The engine is controlled primarily by the use of a throttle lever and additional controls can be included to control the mixture. These control inputs then operate either simple cable mechanisms to the relevant surface or engine or it can send electrical signals along wires to operate electrical actuators. There is also the facility to incorporate a simple autopilot that can hold a heading, speed and height for longer legs of a flight.

Automobile

An ordinary car is controlled using a steering wheel for directional control and two pedals for acceleration and braking (assuming an automatic gearbox is used). It is also fitted with a gearshift selector for selecting the various modes of the automatic transmission. Behind the controls an automobile has many systems fitted that improve the control that the driver has over the vehicle. These include active suspension to improve the ride that the occupants feel and traction control to ensure that the vehicle holds the road without locking the wheels to improve both the comfort of the occupants and the safety of those in the vehicle. Traction control can also be used in a straight line to stop the wheels locking under heavy braking and hence improve the stopping performance of the car.

O.2.1.2. Navigation

Aircraft

Navigation has developed significantly over the years. The basic requirements are fairly simple, all the pilot really needs is a map, a compass, and a stopwatch. These days the navigation systems fitted in aircraft are fairly complex comprising of a GPS receiver and a transponder to provide air traffic control with information on the aircraft's type and height. In addition to this, a system called TCAS can be installed to provide collision avoidance information that backs up the standard lookout that a pilot would normally carry out, and allow for smaller separation in non-VMC conditions. In addition to these a typical GA aircraft will also be fitted with VOR/DME and ILS antennas so that it can fly from radar beacon to beacon and also use the Instrument Landing Facilities at airfields that have the necessary equipment.

Automobile

Navigation in automobiles is slightly easier in that most roads are fitted with signs and hence the need for navigation data is not so great. It is however becoming popular to have electronic route guidance systems in the car. These inform the driver as to the best direction to go in to maximize the efficiency of the journey and avoid traffic congestion. This also works off a system of GPS coordinates and standard road traffic information provided by a network provider.

O.2.1.3. Monitoring

Aircraft

Systems monitoring is essential in aircraft as they are not easily able to pull over at the slightest hint of something going wrong. Each main component in an aircraft is monitored and various temperatures, pressures, and equipment statuses are displayed to the pilot. These include the engine temperatures and pressures, the electrical systems status, the fuel system pressures and contents. It is also under this section that the primary flight data is acquired and displayed via pitot static systems and basic gyroscopic outputs, as well as sensors for items such as flap position.

Automobile

Unlike aircraft the driver of an automobile can stop a car at any point if a failure occurs and hence the monitoring is not so safety critical. It is however essential to ensure that any problems can be spotted to minimize the damage caused to the particular system and the inconvenience of larger repairs for the owner. A standard car will monitor the engine fluid temperatures (Oil and water) and also the fuel contents. The system also monitors the engine speed and the ground speed of the automobile. In addition to the engine the electrical system is also monitored, as this is essential for most of the features in a modern car. To improve the driver's comfort some cars are fitted with environmental control systems that can control the internal temperature of the cabin and the humidity.

O.2.1.4. Communications

Aircraft

Fundamentally, an aircraft has to be fitted with a VHF radio in order that the crew can stay in touch with air traffic control. This is so that the crew can inform the controllers of their intentions and to accept commands from the controllers to ensure the safe operation of the aircraft and its interaction with other aircraft within its vicinity. It is also necessary as an aid if the aircraft should get into trouble and require assistance from the ground.

Automobile

As a standard fit an automobile is not fitted with a VHF transmitter although it will have a receiver for the purpose of in car entertainment.

O.2.1.5. Safety

Aircraft

These systems are heavily interlinked with the monitoring systems and generally take their control inputs from monitoring sensors. In a typical GA aircraft the pilot will have some form of warning panel or indication to inform them of component failures. As a back up the aircraft electrical circuits will be fused to prevent damage and allow for load shedding if the situation arises. As a last resort some GA aircraft have a fire extinguisher system in the engine compartment and all are fitted with a three-point harness to hold the crew in their seats.

Automobile

Safety is a far bigger issue in automobiles and the consumer is now after a safe car as opposed to a high performance model. Safety in an automobile includes the entire chassis design and load distribution network as well as specific in cabin features such as airbags and intelligent seat belts. The automobile is also fitted with a fuse box to protect the electrical circuitry and has several displays to alert the driver to overheating engines (high oil and water temperatures).

O.2.1.6. Lighting

One of the major systems that has not been mentioned so far is the lighting system. Both types of vehicles have internal as well as external lighting for various roles during the day and night. The aircraft will be fitted with navigation lights on the wing tips, a high-visibility identification strobe, taxi lights and a landing light. Automobiles on the other hand are fitted with headlights both front and rear and occasionally sidelights. In addition they have indicators, brake lights, reversing lights and fog lights to cope with the various driving environments and aid other road users to the intentions of the driver.

O.2.2. Utility Systems

The functional backbone of any vehicle can be considered to be the control and management of systems that deliver supplies of power on demand. Systems that perform these tasks are generally referred to as vehicle utility systems. Typical power requirements on aircraft and motor vehicles will include:

- Electrical power generation and distribution.
- Hydraulic power distribution.
- Environmental control.

For the design of the Pegasus aircraft it is necessary to provide a generic utilities system that covers the requirements of both a motor vehicle and an aircraft, which in essence prove to have a many similarities, however have very different operational environments and conditions.

The aim of this section of the report is to summarize the utilities requirements of both a car and a light aircraft, then highlight the commonality to remove repetitive functionality, and finally arrive at a set of requirements that we can develop into a utilities system design.

As well as the requirements to supply power to various vehicle systems, the other design drivers for the utilities systems are derived from original customer specifications and requirements such as:

- Operation from remote unserviced airfields.
- Fully self-contained vehicle (i.e. requires no ground power unit or starter).
- Ease of maintainability.
- High level of reliability.

O.2.2.1. More Electronic Aircraft Introduction

A current trend in aircraft design throughout the western world is the concept of a More Electric Aircraft (MEA – Replacement of hydraulic flight control channels with electric channels), and eventually an All Electric Aircraft (AEA – Replacement of all hydraulic channels with electric channels). Under development in several US and UK agencies and aircraft manufacturers (TRW Aeronautical – Lucas Aerospace), the aim is to develop an aircraft that has a single power source to supply all onboard equipment, which is derived from the engine.

There are several advantages in having a single power source. These are mainly the increase in reliability obtained from a single ‘clean’ power distribution system, but also include increased ease of maintainability, reduced lifecycle costs and reduced amount of vehicle support. A recent study by TRW Aeronautical concluded that the removal of a single hydraulic system and replacement with an electric channel would save 100kg (220lb) without additional costs.

Obviously there are also several clear disadvantages that will need addressing before the concepts become a reality. Such issues include the increased necessity to consider and control electromagnetic compatibility with safety critical systems, and also the increased criticality of maintaining the power supply to the demanding systems.

Also, there are issues regarding actuator miniaturization which will need to be resolved for these ideas to become a reality. One of the main reasons hydraulic actuation is still the most preferred method of power transfer is the compactness of the actuating unit. As technology progresses, the size of comparable actuator units will reduce.

With these issues in mind, considering the operational environment and the proposed end user, when designing the utilities for the Pegasus aircraft, the primary design criteria will be the optimization of the utilities by aiming to make use of electrical technologies.

O.2.2.2. Electrical Systems

Electrical power makes up the majority of the power requirements on both a car and an aircraft.

Aircraft

The electrical distribution system on an aircraft in general provides similar service to that of an automobile system in that it is the main source of power, feeding equipment such as avionics, lights and the engine's starter.

Aircraft with comparable performance and functional requirements (Cessna Skylane) operate a 28 volt DC system, which is derived from an engine-mounted alternator. In addition to this, aircraft are fitted with a battery backup supply, a 24 volt 12.5A/hr rechargeable supply, which is used in emergency situations to feed essential loads such as navigation and communication systems, and when the aircraft is on the ground without the engine running.

When considering designing an aircraft with a fly-by-wire system, as the Pegasus is, it will be necessary to implement some kind of control surface actuation. Full use of a set of electric channels will be utilized to provide this power actuation, for the reasons as outlined in the More Electric Aircraft concept.

Electrical actuation, or in fact any electrical system which is involved in a large amount of energy transfer (motors, actuators, heaters), will utilize a high voltage AC system to optimize efficiency by reducing power losses. This places a requirement on the Pegasus electrical generation system to provide a source of DC and AC electricity.

The major difference in the electrical system on an aircraft compared to the automobile is the use of twin power systems – AC and DC. The majority of modern aircraft operate a regulated 28 volt DC system (for systems that require a steady low voltage, i.e. digital electronic circuits), which is derived from a 115 volt 400Hz 3-phase AC system. The main reason for utilizing two power distribution methods is the advantages that a high voltage AC can provide when it comes to distributing power around the aircraft. In general, to transmit an equivalent power, a high voltage means a lower current. The lower the current, the lower losses such as voltage drops are, and the lower the power losses are (power losses are proportional to the current squared). Also as current conductors are heavy it can be seen that the reduction in current will save weight, due to the reduced thickness of the required conductors, which is a very important issue when designing an aircraft.

Automobile

In a car the electrical system is usually derived from a 12 volt DC lead-acid type battery, which is charged by the alternator. Power for all equipment such as the lights and all electrical systems is supplied directly from the battery and no other source.

The battery is the sole source for a number of independent parallel circuits, which normally consist of isolating fuses, relays, switches and the specific system equipment.

In standard automobiles the electrical distribution system provides no facility for load shedding, as there is no general safety or performance requirement that might be expected in an aircraft architecture.

When designing a common architecture for both modes of travel for this particular vehicle it is necessary to provide a reliable source of power that is driven by the requirements of the most safety critical mode. In the case of the Pegasus vehicle it is the airborne mode that will establish and govern the design.

As mentioned above one of the design triggers for the design of the electrical system is the aim to provide a More Electric Aircraft. For aircraft that can be considered to be similar to the Pegasus vehicle it is not uncommon for there to be an absence of a complete hydraulic system (Cessna, Bulldog). This is because the largest requirements for a hydraulic system on an aircraft are the control surface actuators and landing gear. This type of aircraft generally has a fixed undercarriage and utilizes mechanical linkages to move actuator surfaces. This will be discussed later in this section of the report.

A summary of the differences in electrical power generation and distribution between car and automobile can be found in Table O.2-1:

Table 0.2-O.2-1: Comparison of Power Generation Methods – Aircraft vs. Automobile

Attribute	Automobile	Aircraft with electric actuation
Electrical power generation method.	Alternator driven mechanically from engine.	Alternator/generator driven mechanically from engine.
Distribution supply.	12volt DC from battery which is recharged from	115volt AC derived from a constant/variable speed drive.

	alternator.	28volt DC derived by transformer from AC system. 24volt battery backup.
Electrical power control.	Simple fuse isolation system.	Fuse isolation system, load shedding utilizing mechanical contactors.

O.2.2.3. Hydraulic Systems

Although it is not planned to have a dedicated hydraulic power distribution system as such, it is still worth noting the comparisons for the automobile and aircraft functional requirements.

Aircraft

Similar aircraft to the Pegasus, such as the Cessna Skylane only rely on hydraulic power for independent wheel braking. As aircraft increase in size and/or implement fly-by-wire control systems hydraulic electrically triggered hydraulic actuators become necessary. Additional complexities such as retracting undercarriage will also increase requirements on the hydraulic systems.

As the number of hydraulic systems increase it becomes more efficient to implement a distribution system rather than using a number of independent self contained entities.

Automobile

Most modern automobiles will use hydraulic power for power assisted steering and braking systems, as these demand high power transfer. These systems are isolated from each other and require completely different maintenance and fluids.

The basis for using a hydraulic distribution system is determined on the aircraft's size – its control surface power requirements or the introduction of a fly-by-wire system.

However all functions of a hydraulic system could be feasible replaced by an electrical power system.

O.2.2.4. Environmental Control Systems

Aircraft

The Environmental Control System on a light aircraft is fairly similar to that of an automobile. It will provide a simple, controllable supply of hot/cold air to the passengers. The engine on light aircraft is commonly placed at the front of the aircraft allowing ram-air cooling through large ducts behind the propeller.

Automobile

Most automobiles do not require sophisticated Environmental Control Systems. The fundamental components that such a system must provide are passenger air supply, which may include air conditioning, avionics and systems cooling, and engine cooling.

To provide engine cooling one of two methods are usually used, direct air cooling and indirect air cooling. The simplest form of cooling available is direct cooling or air cooling. This became a notorious problem for car designers such as Porsche, who through lack of space and complexity in the engine bay area could not afford to implement a method more complex than just blowing cool air through the engine. As significant advances in the engine/automotive community have developed, indirect cooling, more commonly known as water cooling has become more widespread, and more effective. Indirect cooling utilizes a liquid coolant to pass through the engine and remove heat from sensitive areas. This heat is then dissipated to the air through a heat exchanger or radiator. This technology is valid for both automotive and aerospace engine applications. A summary of the different cooling methods used in automobiles and aircrafts can be found in Table O.2-2.

Table O.2-2: Comparison of cooling methods – Automobile vs. Aircraft.

Attribute	Automobile	Aircraft with electric actuation
Engine cooling	Air or water cooled engine using a radiator as a heat exchanging device.	Air or water cooled engine using a radiator as a heat exchanging device.
Passenger cooling	Air available direct from external supply. Can be heated from engine cooling system. Refrigerated air commonly available on even basic cars. No pressurization required.	Air available direct from external supply. Can be heated from engine cooling system. No pressurization required in operational environment of many light aircraft.
Systems cooling	Not commonly found in automobiles.	External air ducted over avionics equipment by using electric fans.

O.3. System Requirements for the Pegasust

This section of the appendix summarizes both the requirements that were obtained from the requirements capture process in sections N2.1 and N2.2 and also the additional requirements that are necessary due to the nature of this vehicle being a combination aircraft and automobile.

In order that all of the requirements are captured, the Systems team has engineered the problem in the normal manor. This was complemented by the Human Factors team who specified the data that they needed to be displayed in the cockpit and hence the data that had to be collected by the various systems. By comparing these lists the chance of missing any vital data was reduced and the overall system was then designed without the need for further modifications.

O.3.1. Avionics Requirements

O.3.1.1 The main control system had to cater for driving and flying through the same controls. These controls are specified in section O.3.3

O.3.1.2 The vehicle required mechanisms to allow for auxiliary controls to be operated. These controls are specified in section O.3.3

O.3.1.3 The vehicle had to be fitted with a system that would allow the pilot to navigate safely and to avoid other air traffic. E.g. GPS and TCAS.

O.3.1.4 The vehicle had to be fitted with standard VOR/DME and ILS equipment for the purpose of navigation and poor weather flying.

O.3.1.5 A monitoring system had to be fitted so that the engine, electrical, fuel and flight data status' could be displayed to the pilot.

O.3.1.6 The vehicle had to have a means to communicate with the ground via a radio.

O.3.1.7 The vehicle had to be electrically safe and display to the pilot any possible emergency warnings as and when relevant.

O.3.1.8 The vehicle safety system had to be able to support the safety features specified by the human factors sub group. See section O.3.3

O.3.1.9 The vehicle had to have both an internal and external lighting system that included the lights specified in both flying and road regulations.

O.3.2. Utilities Requirements

O.3.2.1 *The vehicle required power actuators to move the control surfaces.*

O.3.2.2 The vehicle required power actuators to move elevator and rudder trim tabs.

O.3.2.3 The vehicle required power actuators to raise and lower front and rear undercarriage and adjust the suspension damping.

O.3.2.4 The vehicle required power actuators to brake the vehicle in road mode and on landing.

O.3.2.5 The vehicle required power actuators to steer the vehicle in road mode.

O.3.2.6 The engine required an air supply for cooling.

O.3.2.7 The vehicle had to be completely independent i.e. it must be able to start on its own.

O.3.2.8 The electrical system implemented had to be able to provide sufficient power to essential systems for a limited period after loss of generated power.

O.3.2.9 To minimize pilot workload the utilities will be managed by an advanced control system.

O.3.2.10 The vehicle makes use of solid state power controllers to optimize and make the electrical distribution more reliable and controllable.

O.3.2.11 The passengers had to have a supply of cooling/heating air.

O.3.2.12 The avionics had be supplied with cooling air.

O.3.2.13 The electrical system had to provide power for interior and exterior lighting

O.3.2.14 The electrical system had to provide power for all avionics and display equipment.

O.3.2.15 The fuel system required electric pumps to move fuel around the vehicle.

O.3.3. Human Factors Controls and Displays Requirements

In addition to the requirements specified in sections O3.1 and O3.2 of this section, there are road and aircraft regulations that specify the information that the pilot or driver must be able to see during the journey. Using these two regulation sources the Human Factors group have selected the data that they wish to be able to display to the pilot using a number of LCD displays and standard dial standby instruments. It is therefore necessary to ensure that the systems are in place to collect and process the necessary data for these displays. The following is a list of the controls and data that the Human Factors sub-group have specified for the cockpit.

Aircraft	Car	Aircraft and Car
Artificial Horizon	Car speedometer	Pedals
Altimeter	Rev counter	Joytsick
Vertical Speed Indicator	Fuel Contents	Wing Position
Air Speed Indicator	Radiator temp	Fly or Drive Mode

Compass	Indicator control and display
RPM Gauge	Headlight control and indication
Fuel contents	Hand/park brake control and display
Fuel Pressure	Glow plugs display
Oil temp	Battery display
Oil pressure	Oil display
Engine fire	Hazard warning control
Fire extinguisher status	Heater and ventilation controls
Fire extinguisher discharge button	Front windscreen demister button
Radiator gauge	Radio and CD player
Amps volts	Airbag and seat belt pre-tensioners
Vacuum suction	Gear selection and display
Outside air temp	Wipers control
GPS + control	Foglight control and display
TCAS + control	
Weather + control	
Radio	
Transponder	
BIT buttons	
Warning panel	
Trim PTT switch	
Hand Throttle	
Flap Position	

O.4. Top Level Subsystem Design

Every system, no matter how simple, is composed of three main components, input devices, processing units and output devices. Through the requirements defined in sections O.3.1, O.3.2 and O.3.3 the inputs to the various systems were specified and the processing necessary for each unit was divided into various sub systems depending on the data processing and the type of data being processed. The various sub-systems are linked using a standard digital data transmission of an ARINC 629 standard. The databus selected for the Pegasus is a Multiple Source/Multiple Sink, which means that the system has multiple transmitting sources that supply data that can be received by multiple receivers. The databus structure has many advantages over the standard discrete wire connections and allows for easy maintainability and expansion for future generations of Pegasus's. Because of the fact that there is a single cable connecting all the sub-systems, this method saves weight and cost while performance is improved. The databus connection technique is also very reliable and has an automatic built in redundancy (i.e. duplex). Due to the easy maintainability and upgrading made feasible by the data-bus, total lifecycle cost is also reduced. The next three sections look at the various sub-systems and consider the inputs and outputs to the sub-systems and the inter-dependencies between the sub-systems.

O.4.1. Sensor Types

The main objectives of the inputs to the avionics system are to acquire the real world data using an array of sensors. These sensors are predominantly excited by electrical means, and ultimately output electrical signals. These signals are then passed through signal conditioning circuitry, such as filters and amplifiers, to the information processing elements of the system. The sensors used on the Pegasus fall into four main categories, which are discussed in detail in the rest of this section.

The first category of sensors is used to capture the air mass data, such as air temperature, pressures, and density. For the Pegasus air data is collected using a pitot static probe that is fitted to the vertical tail sections of the aircraft in clean airflow so as to avoid being dangerous to pedestrians when the vehicle is in road mode. The pitot static tube and static port allow for the measurement of total and static pressure, which is then used to calculate the airspeed and the altitude of the aircraft. This pressure data is then split so that the pressures can be converted into electronic signals for the vehicle control computer to use and also provide the mechanical flight backup system with the standard pitot static inputs.

The second batch of sensors used in the Pegasus is used to measure the inertial data, such as changes in position and acceleration. These consist of a set of gyros that provide attitude and heading information, which are supplied as electrical signals that can be interpreted by the Vehicle Utilities Sub-System. This is very similar to the Inertial Navigation systems used in commercial and military aircraft. The information from the gyros is processed according to a set of rules that allow it to provide the necessary navigational information.

In order for the information to be transmitted and received it was also necessary to include a number antennas. For the Pegasus these consist of blade antennae for the VHF radio, Transponder and the weather and TCAS systems. When the vehicle is converted to its automobile mode a standard automobile radio antenna is used to provide the in-car entertainment system with radio information.

Finally a number of sensors are incorporated to sense the position of vehicle components such as the wings and the undercarriage. This also includes items such as the contents of the fuel tank and the oil sump. These sensors are simple microswitches, which are either open or closed to indicate the position of the component being monitored. Table O.4-1 summarizes the various data that is collected and the type of sensor that is used to collect it.

Table O.4.1: Summary of Various Sensors and their Uses

Sensor	Information Provided
Pitot Static probe	Provides pressure information that is used to give airspeed and altitude information
Pressure Sensors	These are used to sense the flow of a fluid through a pipe. In the Pegasus these are used for fuel flow and oil pressure
Temperature Sensors	Oil and radiator temperatures are monitored using these electrical devices
Gyroscopes	A selection of gyros provide attitude and rate of change information for the Artificial Horizon and the Vertical Speed Indicator
Rotary Encoders	The engine rpm, wheel speed, and drive by wire system use these sensors to provide rotational velocities
Antenna	VHF radio signals, GPS data, IFF transponder data and the in car entertainment system all use these sensors for aerials and

	antenna.
Microswitches	These are used to provide information on the wing position, the Weight on Wheels signal and the fuel and oil contents.
Voltmeters and Ammeters	Used to provide information on the battery health and the charging rates of the electricity being produced.

O.4.2. Data Processing

Once the data has been collected it is converted into electrical signals at the sub-system stage and then transmitted to the vehicle's main computer (VMC). This transfer is made possible due to the simple data-bus, controlled by the MC, linking all of the sub- systems. Once the necessary sub-systems have been allocated with the data that they need, the displays are refreshed and any feedback commands are sent to the side-stick and the pedals. The three main displays in the cockpit are the Liquid Crystal Displays (LCD's) that provide the pilot and co-pilot with all the flight and aircraft status data that they will require while flying the vehicle safely. An individual symbol generator drives each display so that the crew can be guaranteed displays even after a maximum of two signal generators fail.

In order to fulfil the reliability requirements for aircraft the VMC is a triplex system and contains three separate processors each programmed by separate software teams. Data is also provided for the back up instruments from a stand by non-electric system that runs off the traditional pitot static inputs to provide altitude, airspeed and attitude data.

O.4.3. Output Data

The main outputs for the Pegasus avionics system are the displays in the cockpit and feedback to the controls so that the pilot can get a sense of how the vehicle is flying or driving so that they can make correcting inputs. These were explained in Appendix N.

O.4.4. Subsystem Definition

Once the sensor and outputs had been selected they were grouped into a number of avionic sub systems so that the processor in the VMC could be programmed to collect and distribute the data between the inputs and outputs. It also allows the systems to be developed and tested independently prior to integration to make the debugging process simpler and quicker hence speeding up the development process. Finally it allows all of the necessary equipment for that sub system to be collected together and makes the process of maintaining and repairing the vehicle easier. For the Pegasus the following sub systems were selected for the avionics system:

1) Main Computer: This is the heart of the vehicle avionics system and is responsible for ensuring that all of the data that is transferred between systems via the databus is done so correctly. For this reason it also contains the Bus Controller that is used in everyday travelling.

2) Displays and Controls Sub-System: As its name suggests this sub-system is responsible for the control inputs for the vehicle and the outputs for the displays.

3) Navigation Sub-System: This sub-system is responsible for providing all of the navigation information for the vehicle from the GPS antenna, the ILS/VOR/DME receivers, the weather data-link and the TCAS system

4) Communications Sub-System: Again as the name suggests this sub-system contains the air to ground radio, the transponder and the automobile in car entertainment system.

5) Vehicle Utilities Sub-System: This sub-system is responsible for controlling the utilities that are present in the vehicle such as the electrical and fuel distribution around the vehicle, as well as monitoring the status of the other components that build up the avionics system.

6) Vehicle Control Sub-System: This sub-system takes inputs from the control devices and transfers them into actuator movement, which is monitored and then transferred into feedback inputs to the control devices to provide the driver/pilot with the "feel" of the vehicle.

Having defined the sub-systems required for the Pegasus in order that the requirements were fulfilled a top level design diagram was produced showing clearly the early schematic for the avionics and electrical system. This is illustrated in Figure O.4-1.

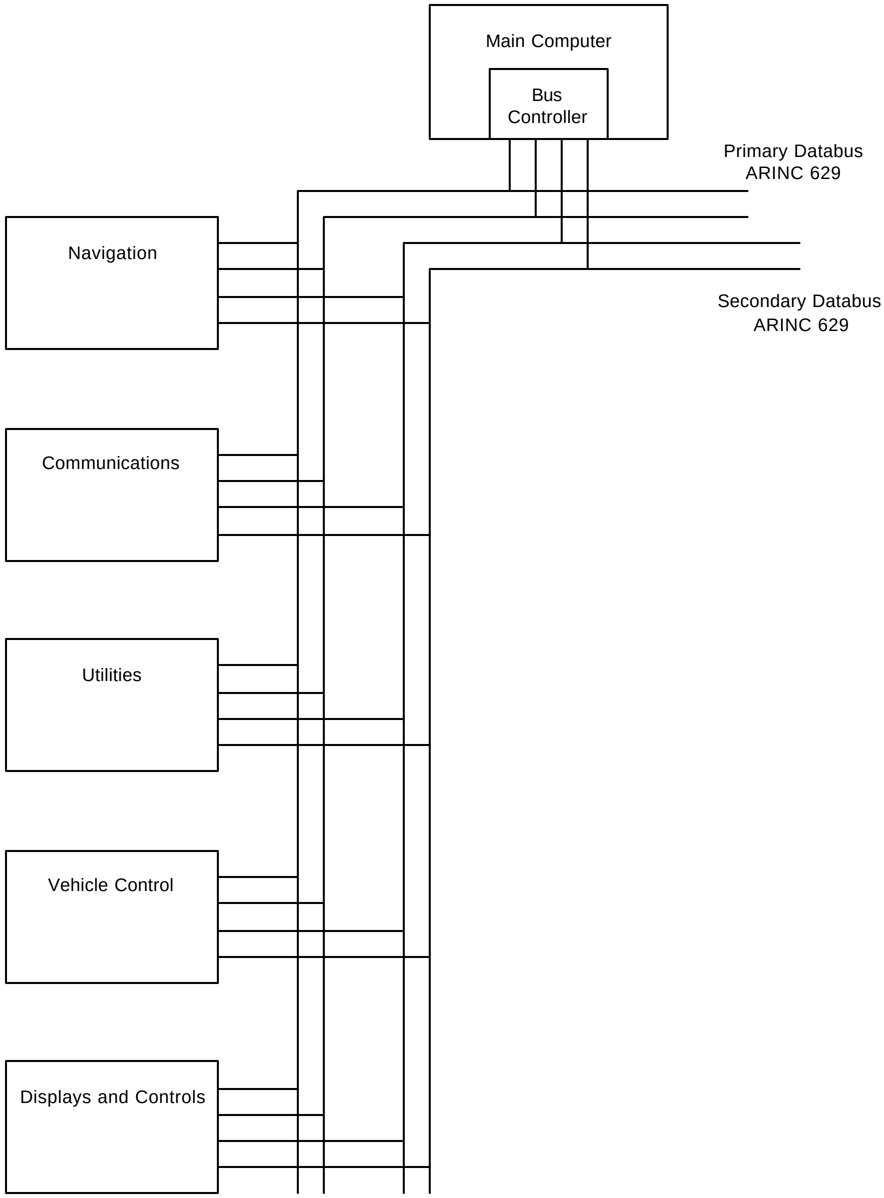

Figure O.4-O.4-1: Top Level Data-bus diagram.

O.5. Utilities Design

The electric utilities system has clear benefits such as reliability, increased ease of maintainability and weight reduction. Wherever possible the design will utilize electrical/electro-hydrostatic actuation. The implications such as criticality and redundancy associated with these technologies will be addressed in this section of the design document.

A critical design decision for the Pegasus aircraft was the choice of powered actuation system, which in turn would provide a requirement on a particular power system. The pros and cons are discussed in more detail in section O.6.1.6, but can be summarized as the need to control the complex flaperons within the telescoping wing structure and to ease pilot control effort. For these reasons it was decided to incorporate powered actuation under the management of a vehicle control system.

The next three sections look at the various sub-systems that fall under the umbrella of aircraft utilities and consider the inputs and outputs to the sub-systems and the interdependencies between them. The aim is to derive a simplified top-level design based upon the requirements detailed in O.3.2.

O.5.1. Electrical PowerGeneration

The role of the Electrical Power Generation System (EPGS) is to obtain the needed power supply from the aircraft engine in a safe and controllable manner.

On any vehicle the means of generating reliable electrical power are extremely limited and are confined to systems that are based around engine mounted generators. Generally this is accomplished using an alternator to generate a sine wave of a given voltage at a constant frequency, normally 400Hz. To produce an AC output that can be used by vehicle systems it is necessary to condition the alternator output voltage. To accomplish this, the alternator must output at a constant frequency, however the speed of the engine is variable with throttle demand. To get around this problem a Constant Speed Drive (CSD) is mounted on the engine to output a single-frequency rotating shaft. The alternator is driven by this shaft, which then outputs a constant frequency voltage. A diagram of the craft's power generation system can be found in Figure O.5-1.

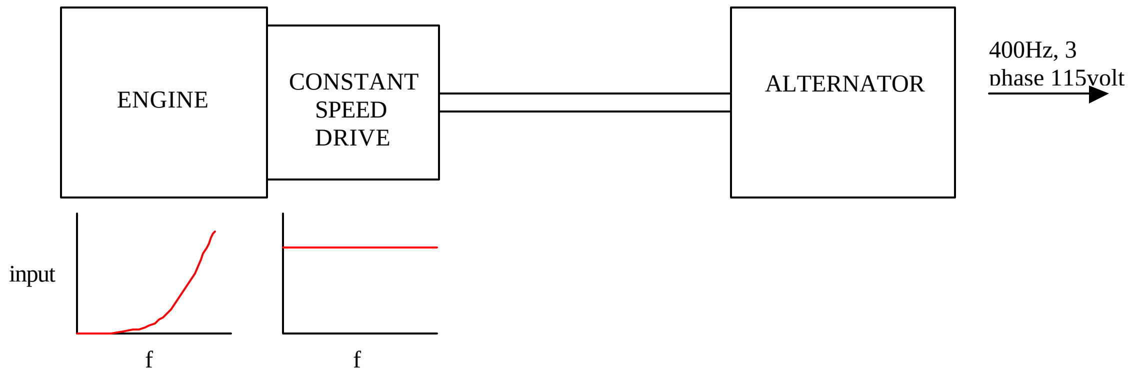

Figure O.5-1: Electric Power Generation System Schematic.

It is estimated that the CSD will draw a small percentage of power from the engine, in the range of less than 5%. The proposed engine for the Pegasus is slightly overpowered for the application, so the addition of the CSD to the engine should not present much of a problem to other systems.

When designing a common architecture for both modes of travel for this particular vehicle, it will be necessary to provide a reliable source of power that is driven by the requirements of the most safety critical mode. In the case of the Pegasus it is the airborne mode that will establish and govern the design.

AC electrical power generation will be used as the primary source as it is simple to derive from a turning alternator, in comparison with DC. Many of the proposed devices on the aircraft, such as control surface actuators, will use an AC supply. For sensitive avionics equipment it will be necessary to provide some kind of low voltage supply. This could be derived locally by the individual equipment concerned, or as a separate busbar supply that has been conditioned from the AC source.

There are three major electrical generation technologies that were considered for the primary power source on the Pegasus vehicle.

- Standard 115volt, 3 phase, 400Hz AC.
- Variable speed constant frequency 115volt, 3 phase, 400Hz AC.
- 270volt DC.

The 270volt DC supply is based on the principle of a usable, high voltage-low current source (weight reduction). The disadvantages of this method are the high voltage potentials, which can lead to arcing between conductors (the airframe is often used a current carrier – grounding point). For these reasons this generation method was discarded and it was decided to proceed with a proven standard design. The chosen generation method for the Pegasus aircraft will be a standard alternator providing 115volt, 3 phase, 400Hz. From this a 28volt DC busbar will be provided via a transformer rectifier unit to service avionics equipment. The generator of choice is provided by Allied Signal Aerospace, meeting the requirements exactly. This generator is shown in Figure O.5-2 (1) and with control unit (2):

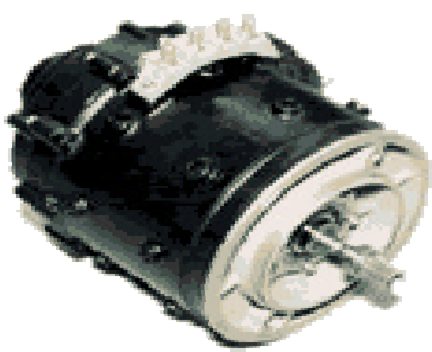

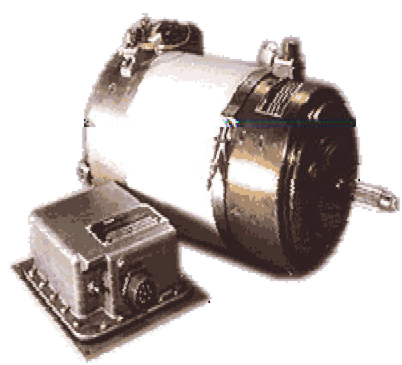

Figure O.5-2 (1,2): Allied Signal Aerospace Electrical Generators.

If necessary it will be possible to apply load shedding to the electrical system. In situations such as engine failure it will be possible for the pilot to turn off supplies that are deemed non-essential. From the cockpit the pilot will be able to manually shed load via a set of switches. These commands are interpreted by the utilities control system, which in turn switches contactors to either apply or remove the power. In emergency situations the load shedding will be handled automatically by the utilities control system.

Once a source of electricity has been generated, the internal function of the EPGS is to produce and distribute a safe controlled power supply. This is commonly achieved by implementing a distribution architecture, which is made up of different branches known as busbars. The main reason for a distributed architecture, is the ability to control which pieces of equipment have a power supply to them. For the Pegasus vehicle this control is managed by the utilities system. The distributed architecture will segregate the electrical system into three separate supplies:

- AC busbar.
- Non-essential DC busbar.
- Essential DC busbar.

The segregation of the electrical system is made possible by utilizing some kind of switching devices. New developments in switching technology have led to the replacement of heavy mechanical contactors with state of the art solid state devices, much like large transistors. The benefits of this are that there is a considerable reduction in size and weight of the switching devices. The devices are known as Solid State Power Controllers (SSPC's). This technology is currently available on the market. A comparison between standard electro-mechanical contactors and SSPC's can be made from the pictures found in O.5-3,4.

Figure O.5-3: Electro-mechanical contactor.

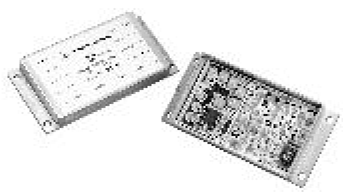

Figure O.5.4: Solid State Power Controller.

The operation of the SSPC's are controlled by the utilities control system, on a 'utilities bus', a dedicated databus which will control all utilities including the environmental control and the electrical power supply. Figure O.5-5 demonstrates the control of the SSPC's by a Utilities Control System:

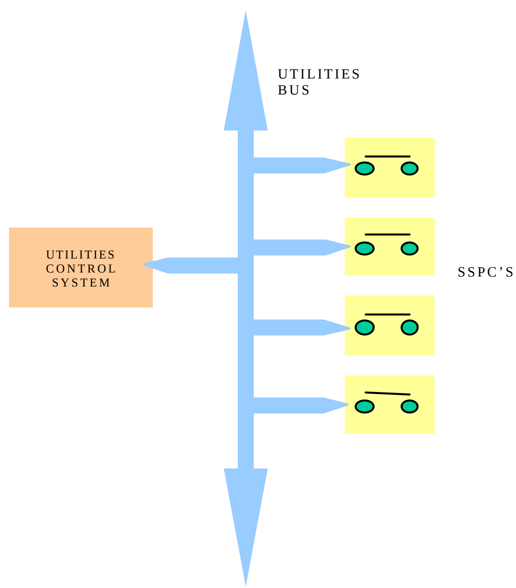

Figure O.5-5: Utilities Control System.

The specific processes of the EPGS can be defined as follows:

- Conversion of AC voltage to DC voltage.
- Control of the busbars - load shedding.
- Charging of an emergency backup battery.
- Regulation of the supply voltages.

The EPGS will provide status information, which will be displayed to the pilot in. This information will include:

- System health.
- Details of load shedding.

Figure O.5-6 shows the basic top level EPGS architecture:

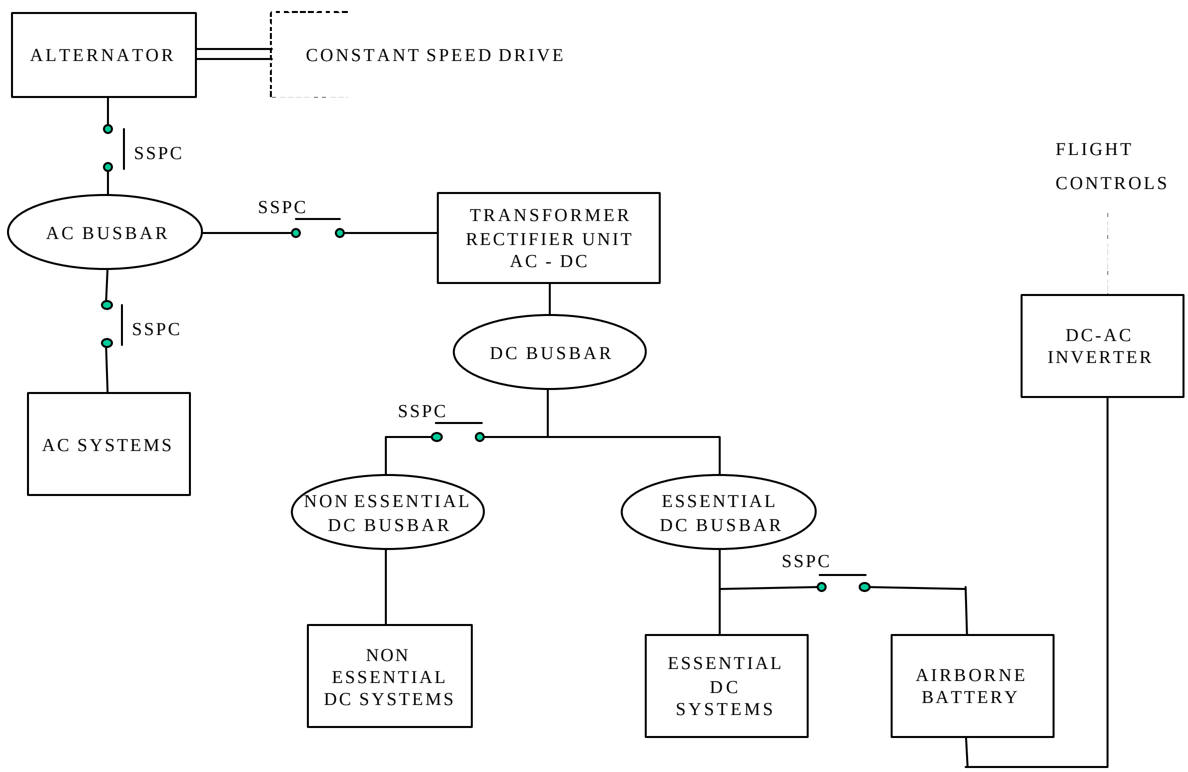

Figure O.5-6: Schematic of EPGS Architecture.

The internal function of the EPGS is to produce and distribute a safe controlled power supply. This is commonly achieved by implementing a distribution architecture, which is made up of different branches known as busbars. The main reason for a distributed architecture, is the ability to control which pieces of equipment have a power supply to them. For the Pegasus vehicle this control is managed by the utilities system.

The specific processes of the EPGS can be defined as follows:

- Conversion of AC voltage to DC voltage.
- Control of the busbars - load shedding.
- Charging of an emergency backup battery.
- Regulation of the supply voltages.

Mission Criticality/Emergency Situations

One of the most important issues that needs addressing when designing an aircraft that relies on a single engine as a power source to generate the electrical power for the entire craft is what happens when the generation of electrical power fails? It is not acceptable to disregard or design around situations that no matter how unlikely may eventually occur.

As a basic requirement, after loss of an engine or generated electrical power the pilot of the vehicle must be able to retain a degree of control of the vehicle for a limited time and/or be able to reach the ground in a safe manner. The responsibility for this lies on the shoulders of several design groups with the Pegasus design team, aerodynamics for glideability, stability to retain control and electrical power generation to retain control of the flight controls.

For the customer in consideration, it is not viable based on cost, complexity, physical ability of the passengers and space within the vehicle to implement any kind of ejection mechanism.

A solution to this that will be implemented on the Pegasus, will be the ability to retain control of essential systems within the aircraft for a limited period of time after loss of generated power. To do this an airborne battery will be placed with in the electrical system. This battery will not supply power at any time unless an emergency situation is encountered. The battery will be continuously trickle-charged during vehicle operation from the regular generation system. In an emergency situation the utilities control system will isolate the essential systems and apply 28 volts DC power to them. A DC-AC inverter will be used to provide power to the control surface actuators. This will enable the pilot a limited period of time to execute an emergency landing using simple instruments and all flight controls.

Summary

Due to the complex nature of the vehicle, primarily brought about by the dual functionality it has been necessary to implement a full electric system that provides power for:

- Control surface actuators.
- Avionics equipment.
- Wheel brakes.
- Road control functions (Steering, throttle actuation).
- Cooling fans (for engine intake mounting, avionics cooling).
- Interior/Exterior lighting.
- Mode change devices (Aircraft to road vehicle, and vice-versa).

Utilizing a vehicle that would have implemented mechanical linkages would have required a highly complex and less reliable mechanical structure. By removing the hydraulic system and utilizing electricity as an alternative, space, reliability and maintainability have all been increased, and aircraft weight reduced.

Of primary importance is maintaining a reliable power supply. In abnormal conditions where there has been a total loss of generated power, the system will provide a limited source of electrical power to essential systems, by utilizing a set of airborne batteries such as below, from Page Aerospace.

Figure O.5-7: Page Aerospace Backup Batteries.

O.5.2. Environmental Control System

The Environmental Control System (ECS) for the Pegasus aircraft will be a simple design, as the operational environment does not require high altitude pressurized flying. The ECS will perform three tasks:

- Engine cooling.
- Avionics cooling.
- Passenger compartment air conditioning.

Both in an airborne mode and in road mode the Pegasus vehicle has a requirement to provide a fresh air supply to the passengers and also a cooling/heating supply to various pieces of equipment. The operational environment of the vehicle means that the provision of a pressurized air supply is not required, however there will still need to be some ducting to supply a controllable airflow into the cabin. An air conditioning system will operate to provide cooler and dehumidified air to the passenger compartment.

The air conditioning will be operate from an engine driven compressor, which will pump pressurized coolant around the refrigeration system

The primary requirement for an Environmental Control System is to provide a cooling supply to the engine and to the avionics and electrical power equipment, which will include brakes and other actuating devices.

Mounted on the side of the fuselage are two intake ducts that are used to supply an cool external air to the engine heat exchanger. The diagram below illustrates the position and method of airflow.

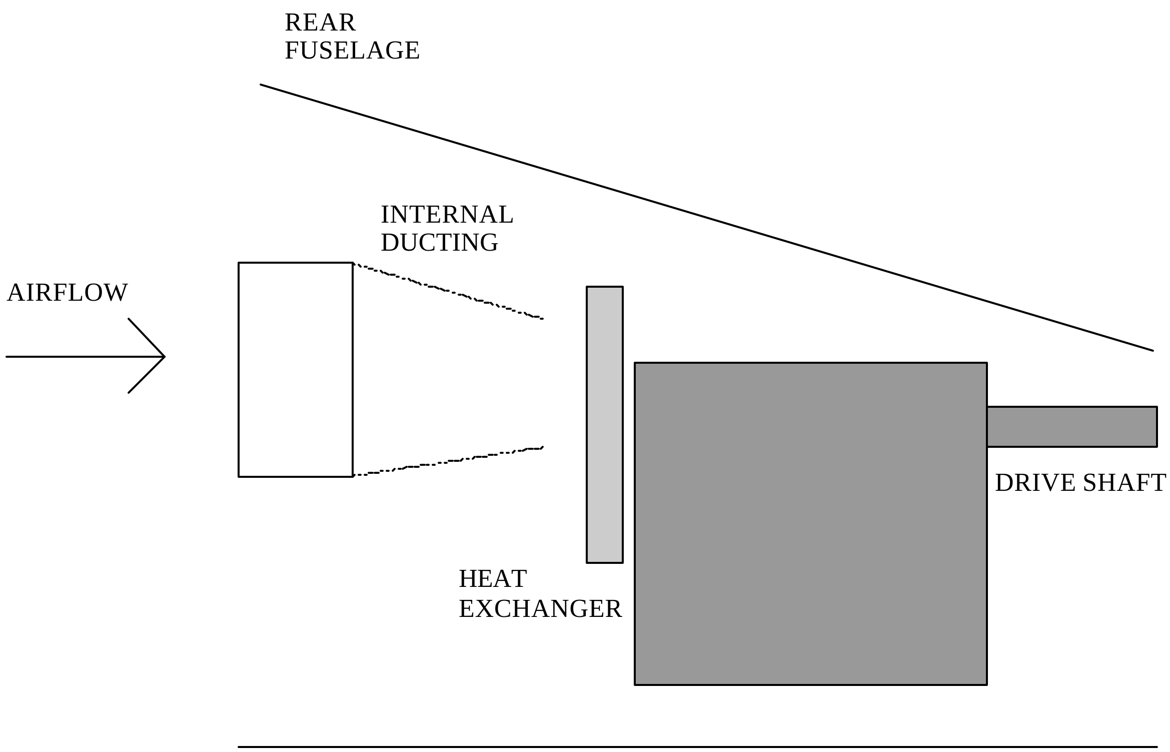

Figure O.5-8: Diagram of Airflow Through Engine Compartment.

The Pegasus vehicle will use indirect water cooling to remove excess heat from critical areas of the engine. That is to say the engine will be water cooled. The main reasoning for this design decision is the fact that the proposed engine is an extremely powerful diesel engine that is operating under normal loading conditions, i.e. governed. It was necessary to employ a highly effective method of removing all of the excess energy from the engine to prevent excessive overheating. A less complex direct air cooled method would not have provided satisfactory results.

However complex this may appear, this method is identical to existing automotive and aeronautical internal combustion engine cooling systems.

O.6. Detailed Design

Having detailed the top-level layouts for the avionics and utilities systems the two systems were developed and integrated into a single system. These two sub-systems are actually heavily dependent on each other and one would be unable to operate without the other. The utilities system provides power for the avionics system and the rest of the vehicle and this in turn sends commands to the utilities system to control the amount of power distributed and the actuator movements required.

O.6.1. Avionics

This section contains the detailed description of the various sub-systems that combine to make the avionic sub system and how these sub-systems interact with each other and with the electrical sub system.

O.6.1.1. Utilities Subsystem

The main sub-system in the Pegasus is the Vehicle Utilities Sub-System, which is an integral input to the main computer. This sub-system is responsible for monitoring all of the various sub-systems, collecting the various data to provide the other sub-systems with their necessary inputs, and controlling the electrical power supplies (load shedding).

In order to ensure the safe operation of the Pegasus there are a number of built in safety features that ensure that the aircraft can be safely operated. These include a weight-on-wheels sensor and a wing position sensor. Between these two signals there is no way that the pilot can inadvertently retract the wings while in flight or extend them while driving on the road. This takes some of the pressure off of the pilot and makes the Pegasus easier and safer to operate.

The utilities sub-system is the main monitoring system as was mentioned earlier in this section. In order to fulfill this role, the sub-system monitors: fuel system status, the various engine parameters and fire indications, as well as various electrical power system parameters. In the case of a fire two CO_2 bottles stored in the engine compartment are released to put out the fire and the system immediately reverts to the emergency status. It then sheds the non-essential electrical items in order to conserve maximum electrical power for the purpose of flying the aircraft. Section O.6.4 contains more information on emergency actions in the Pegasus. Also included in the utilities sub-system are the environmental systems and the car safety features such as the airbags and the seat-belt systems. A schematic of the electrical system's wiring can be found in Figure O.6-1.

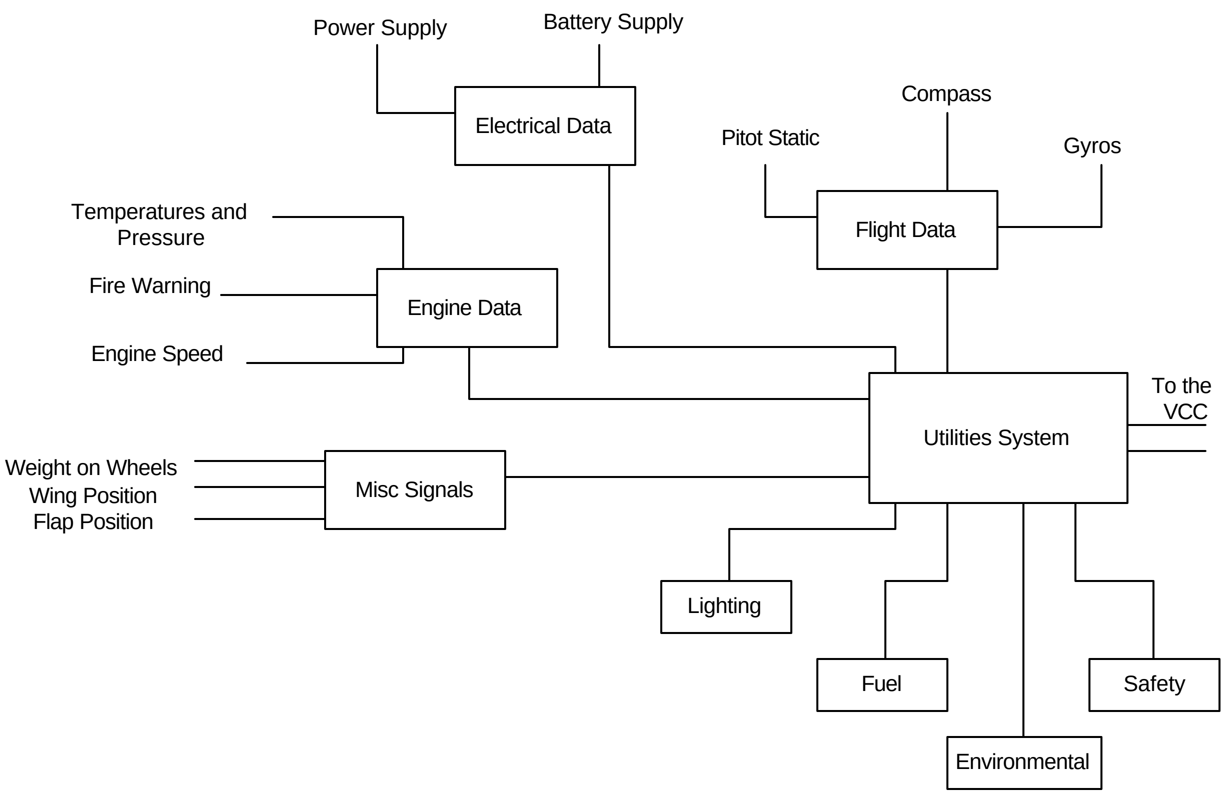

Figure O.6-1: Electrical System Wiring General Wiring Schematic

One of the key areas of this sub-system not yet discussed in detail is the lighting aspect of the vehicle. In both automobiles and aircraft, lights are fundamental to the design to fulfill legal requirements. This vehicle had to have the lights that would fulfill the role of an automobile and that of an aircraft with minimal duplication to save on weight. To this end the Fig O.6-2 shows the lighting schematic was developed illustrating the various lights and the switches that control them.

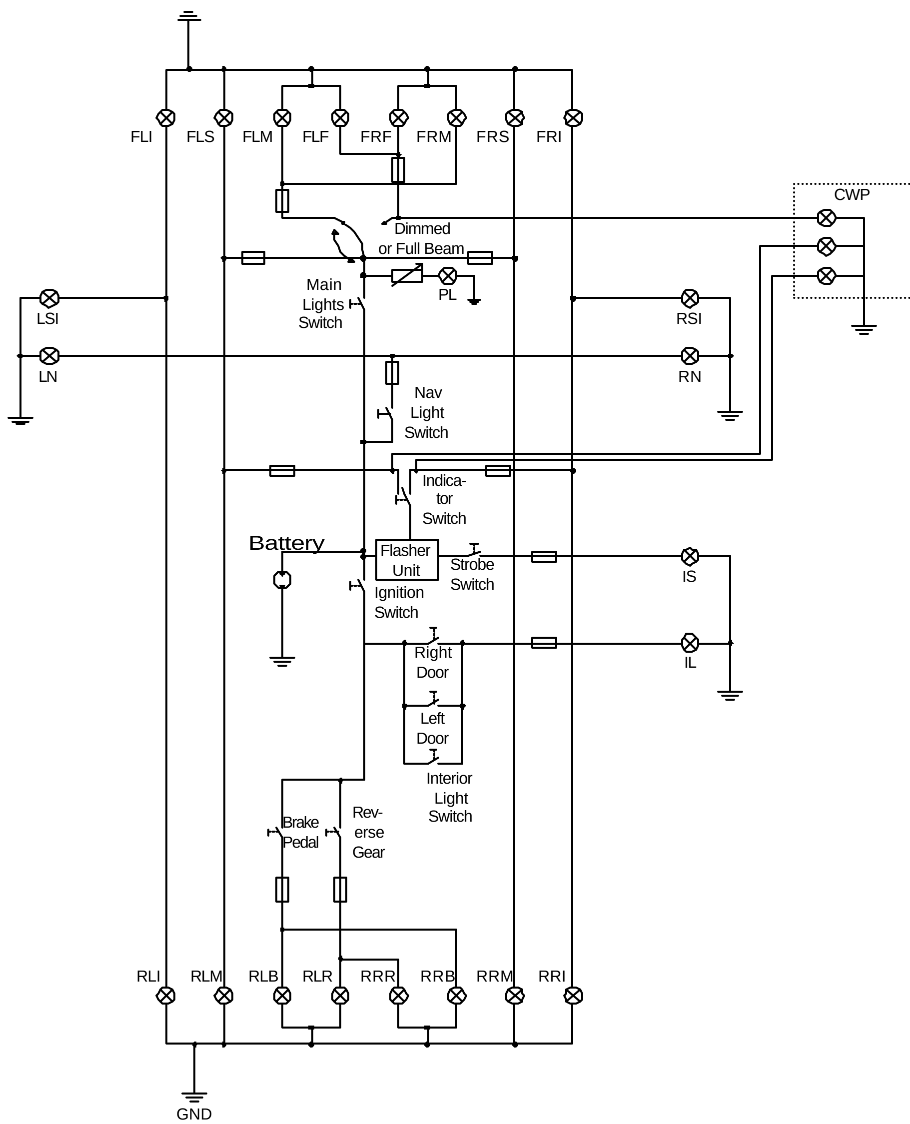

Fig O.6-2: Lighting schematic for the Pegasus.

Table O.6-1: Abbreviation Key for Figure O.6-2.

FLI	Front Left Indicator	FRI	Front Right Indicator
FLS	Front Left Sidelight	FRS	Front Right Sidelight
FLM	Front Left Main light	FRM	Front Right Main light
FLF	Front Left Fullbeam	FRF	Front Right Fullbeam
LSI	Left Side Indicator	RSI	Right Side Indicator
LN	Left NavLight	RN	Right NavLight
RLI	Rear Left Indicator	RRI	Rear Right Indicator
RLM	Rear Left Light	RRM	Rear Right Light
RLB	Rear Left Brake Light	RRB	Rear Right Brake Light
RLR	Rear Left Reversing Light	RRR	Rear Right Reversing Light
IS	Identification Strobe	CWP	Central Warning Panel
IL	Interior Light		

The lights on the Pegasus have been specially blended into the vehicle's body at the front and rear in order that the aerodynamic characteristics not be altered with their addition. This means that the lights at the front are blended into the nose cone with molded plastic covers that also direct the light from the main lights onto the road surface. On the wingtips the Pegasus has a combination indicator and navigation light which contains both orange LED's for the indicator and red or green LED’s for the navigation lights. Depending on the mode in which the vehicle is in the respective light will flash as required.

Utilizing a computer operated databus system to control all the utilities on the aircraft simplifies the tasks of a pilot and removes workload. Utilities Control Systems are available on the market today. Figure O.6-3 shows components of the Utilities Control System and gives an idea of the size and on-the-surface simplicity of such a system controller (From Airsigna Gmbh).

Figure O.6-3: Utilities Control System.

In order to give an appreciation of the size of these components the connector on the middle device is roughly the same size as a dollar coin.

O.6.1.2. Displays and Controls Subsystem

The Displays and Controls sub-system is one of the safety critical systems in the aircraft as it is responsible for controlling the vehicle and displaying the aircraft data to the pilot. The vehicle uses a very basic fly-by-wire system in the aircraft mode. In this form the electrical system simply replaces the mechanical links found in a standard GA aircraft. Instead of a cable, voltage is sent to an electrical actuator in amounts relative to the distance that the control device has been moved. The actuator will then move the control surface unless an external force prevents it, such as a gust. This force is sensed on the control surface and a signal is sent back to the control device so that the pilot can feel that there is need for a greater input, in much the same way as they would in a mechanical link. When the vehicle is in automobile mode the inputs from the control device follow a set of rules designed to activate the drive-by-wire system controlling the front wheels. In the same way as the flying surfaces provided feedback the steering forces are also transferred back to the control device so that the driver has a “feel” for the performance and handling of the vehicle. In Figure O.6-4 the Primary controls are defined as the main control device, the pedals and the throttle device. The secondary controls are defined as those that are independent for each vehicle, such as windscreen wipers and the various external light controls.

The control signals are sent to the Main Computer through the aircraft data-bus and the display signals are received through the same data-bus once the raw data has been converted from the various discrete inputs that are collected in the various sub-systems. The electrical signals are sent to the three symbol generators to provide the displays on the three main LCD’s. Also included in the displays are the backup instruments that function even after the main electrical supply is compromised and the LCD’s have to be switched off for load shedding purposes. These are: an artificial horizon (run off standard gyros and mechanical links and powered by the battery), an airspeed indicator (Comparing static and dynamic air pressures directly from the pitot tube using mechanical links), and an altimeter (Again run from the pitot static data). In addition to this a standalone compass is also fitted to provide an idea of heading, although it will be effected by magnetic variation and hence the readings will be fairly rough. Figure O.6-4 shows the control and displays sub-system diagram.

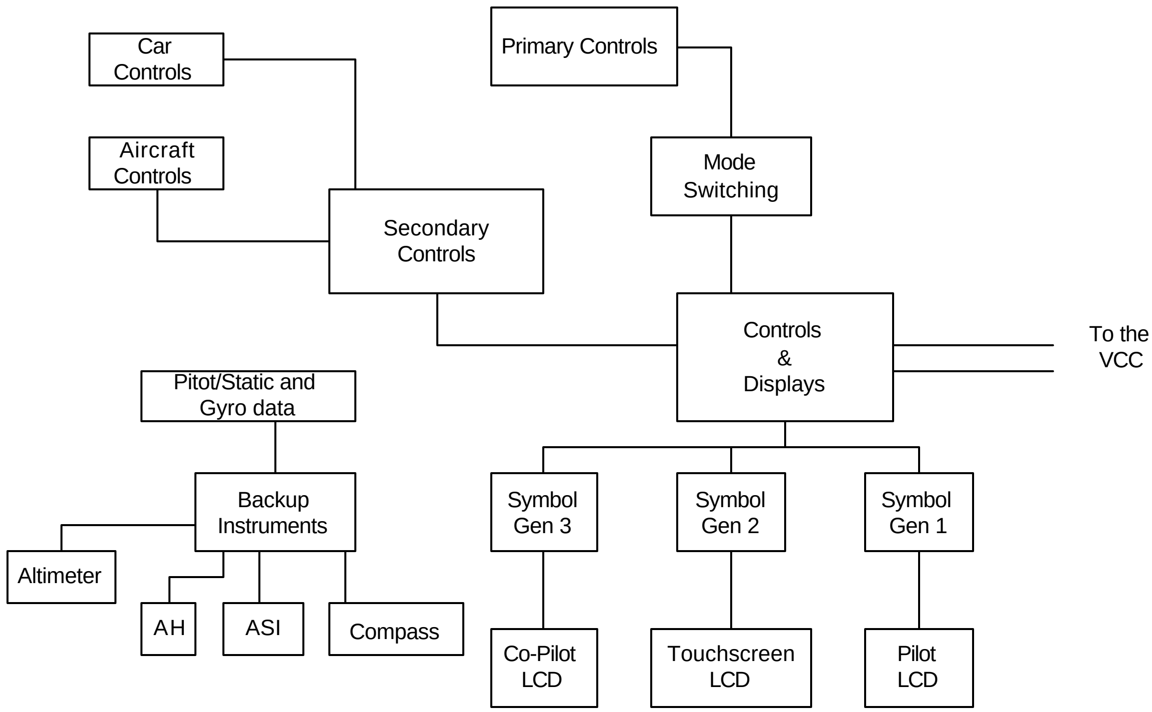

Figure O.6-4: Control and Displays sub-system diagram.

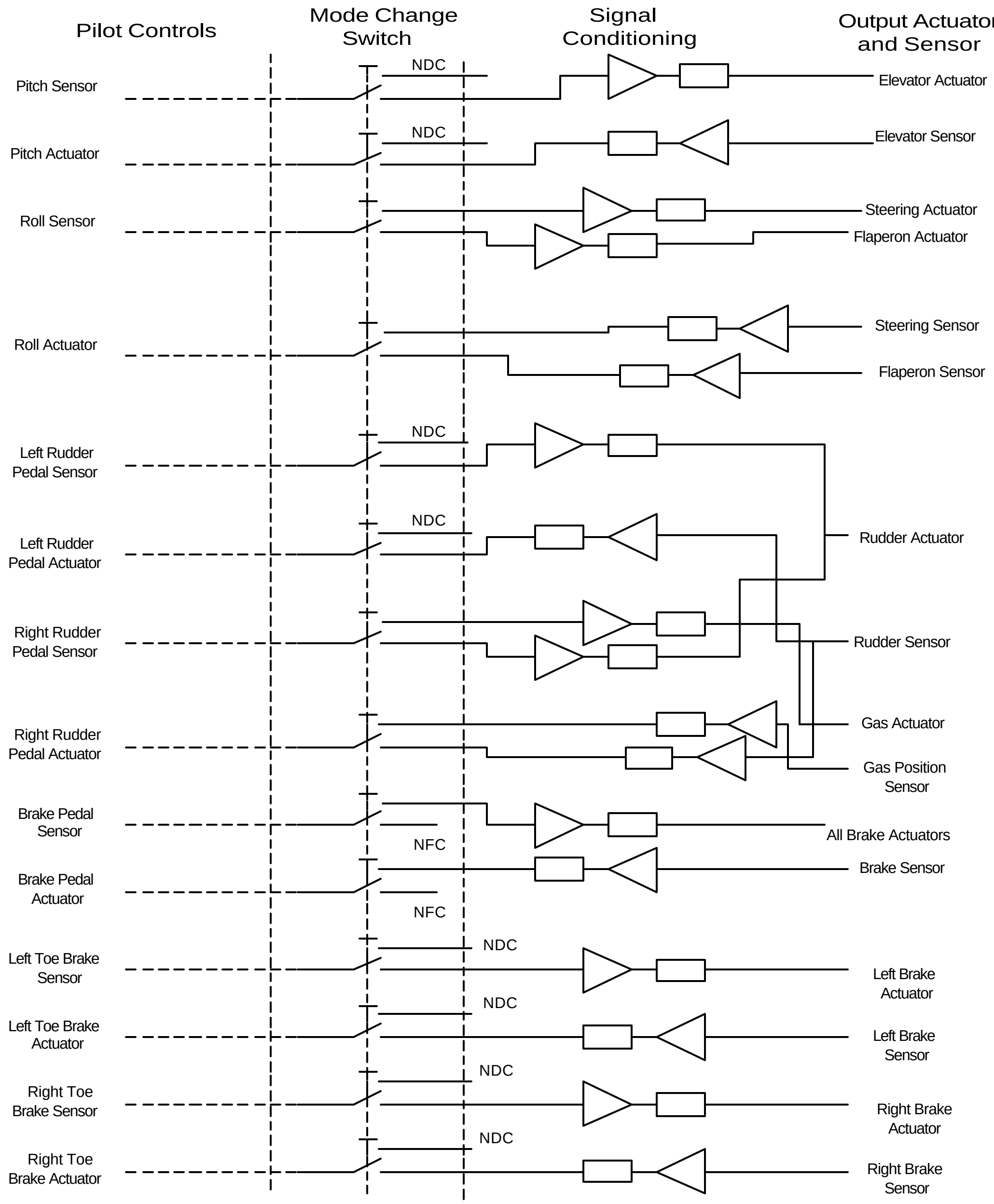

Figure O.6-5: Electrical System Mode-Switching Schematic.

The key area of interest with this subsystem is the mode change circuitry, which allows the Pegasus to operate in two modes with a single set of controls, both safely and utilizing an electrical system to save weight. Fig O.6-5 shows the mode switching in a semi-schematic form illustrating the control inputs, the mode switch, the signal processing and the control surface controlled. In the diagram the vehicle is in drive mode when the switch is in the uppermost position and aircraft mode in the lower position.

The abbreviations in this diagram are NDC and NFC and stand for no drive connection and no fly connection respectively inferring that the particular control is not responsible for any controls while in that mode of transport.

O.6.1.3. Navigation Subsystem

The navigation sub-system for the Pegasus is fairly basic and follows a similar design to the standard GA aircraft. Typically automobiles do not contain much in the way of navigation equipment and rely on road signs and driver knowledge for navigation. The Pegasus contains the standard VOR (VHF Omni-Directional Radar), DME (distance measuring equipment) and ILS (instrument landing system) receivers so that the aircraft can be navigated via standard radio beacons and navigated in bad weather safely using both the beacons and airfield ILS systems. VOR provides the pilot with heading data to radio beacons that the pilot can tune into to aid with navigating the aircraft on the flight route. DME information is provided by the same beacon and gives the distance to that beacon utilizing the properties of electromagnetic waves to calculate the time to receive a response and hence the distance from the beacon. The ILS system in the Pegasus provides the pilot with information regarding the position of the runway centerline (localizer information) and also rate of descent information (glideslope data) from the transmitters on the ground. This data is displayed on the flight director, which is present in the LCD display screens. To complement these basic sensors the Pegasus is fitted with a GPS system so that it can obtain accurate position data which can either be used in case of the other systems failing or as the primary navigation aid depending on the competency and familiarity of the pilot.

As an additional flight planning and route monitoring aid the Pegasus has a weather data-link that informs the pilot of the weather in and around the area into which they are planning on flying so that an alternative route can be taken if necessary. Finally, to aid the pilot in the lookout task while flying, the Pegasus is fitted with TCAS (Traffic Collision Avoidance System) to alert the crew as to the presence of other air traffic. Not only is this a useful safety feature it also allows for the development of a free flight capability which could be the next step for the avionics system of the Pegasus as the aircraft develops in the future. Figure O.6-6 shows the navigation sub system diagram.

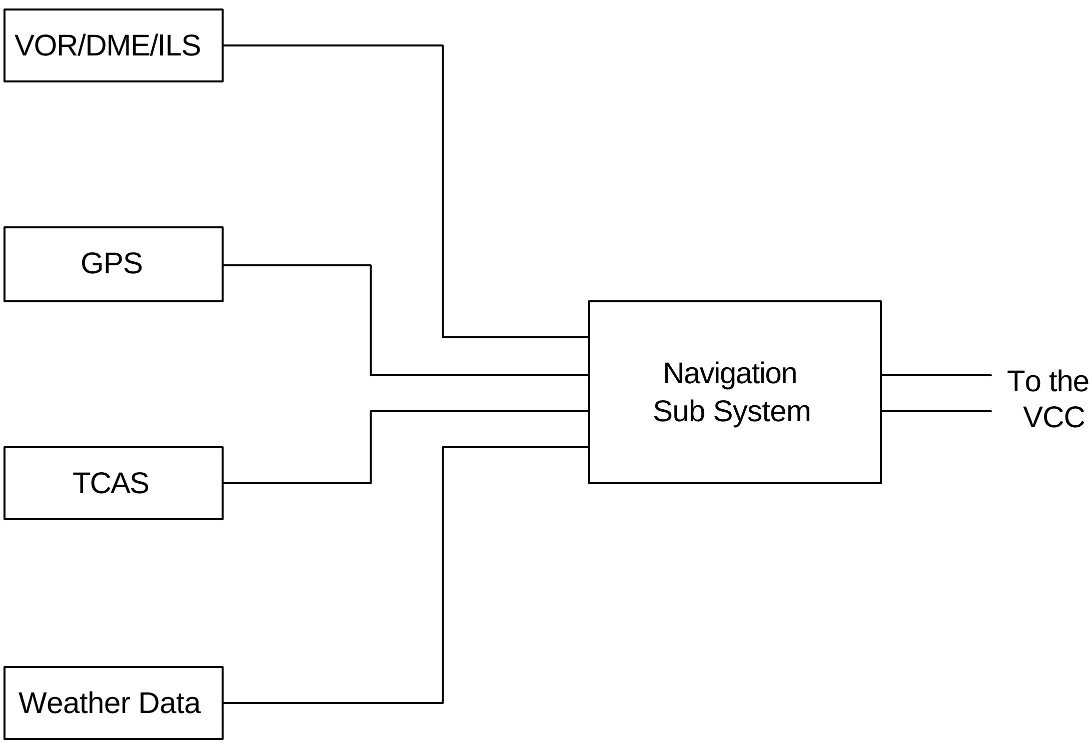

Figure O.6-6 Navigation Sub-System Diagram.

O.6.1.4. Communications Subsystem

A minor Sub-System in the Pegasus avionics system is that of communications. This sub-system is the most simple in the vehicle and consists of only four elements. The main component is a VHF radio that allows the pilot to stay in contact with the ground and obtain commands from air traffic control in order that the vehicle can be flown safely with other aircraft in the sky. This is complemented with a transponder which automatically (when switched on) provides aircraft type and altitude data to a ground interrogator situated at most major airfields. It also allows the pilot to notify the ground if he gets into difficulty or suffers a communications failure. Finally the in-car entertainment system is included under the communications sub-system. This consists of a standard FM/AM radio receiver and a Compact Disc player, which can be upgraded to cater for mini discs if the technology takes off in the next ten years. Finally the in-cockpit inter-comm wiring and controls fall into this sub-system. This allows all of the occupants to communicate when the engine is running at full power or to listen to the radio or a CD. The pilot is the only person that does not have access to the entertainment radio in flight mode as this would act as a distraction from their main role of flying the Pegasus. When the vehicle is being used as a standard automobile everyone can listen to the in car entertainment. Figure O.6-7 shows the communications sub-system diagram.

Missing O.6-7

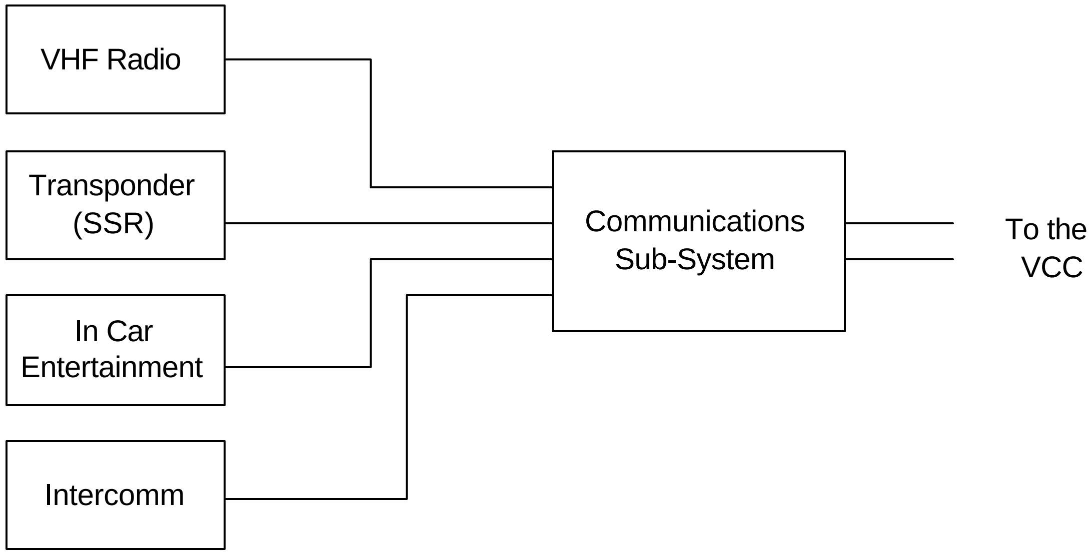

Figure O.6-1 Fig XXX Communications Sub-System Diagram

O.6.1.5. Vehicle Control System

The Vehicle Control System (VCS) will operate in two distinct modes, either airborne or road. The purpose of this system is to provide the electrical 'drive/fly-by-wire' link between the pilot/driver's control devices and the actuators that provide motion of the vehicle.

The need for a control system has come about due to the complexity of the pilot/driver interface, using one set of controls to accomplish two distinctly different functions. Another contributory factor is the difficulty that would be encountered when trying to use a simple mechanical control surface linkage, within the telescopic airfoil section for the flaperons. Instead of a mechanical linkage system electric actuation was implemented to provide a large amount of power transfer and increased reliability, within a restricted volume.

In road mode the responsibilities of the VCS are:

- Steering actuation through the side-stick.
- Acceleration/deceleration control through the two foot pedals.

In airborne mode the responsibilities of the VCS are:

- Control surface actuation through the side-stick and foot pedals.
- Acceleration/deceleration control through the hand throttle.

Although the system description defines the VCS as a drive/fly-by-wire system, this may be somewhat misleading. In the true sense of a flight control system, trim is automatic. The VCS on the Pegasus has been designed to reduce the level of complicated electronics and hence concerns with certification of such a system. Therefore manually adjustable trim surfaces are implemented. The result is a control system that is directly analogous to a mechanical linkage, but utilizing power actuation.

As with any artificial flight control system difficulties arise when the natural feedback to the pilot is removed. By using flight control surface actuation devices the pilot has no direct feel to what degree he is stressing the airframe. It is entirely possible that the pilot could try and instigate impossible maneuvers. For this reason it is necessary to employ force sensors on the control surfaces. These will sense the forces against the movement of the control surfaces, such as natural aerodynamic resistance, gusts etc. These will be translated into forces in the control device that will act against the pilots input.

The VCS can determine the mode of operation, i.e. either road or airborne, by sensors placed to detect wing position. For example when the wings are fully extended the vehicle is defined as being in aircraft mode, and vice versa. Figure O.6-8 summarizes the components of the VCS:

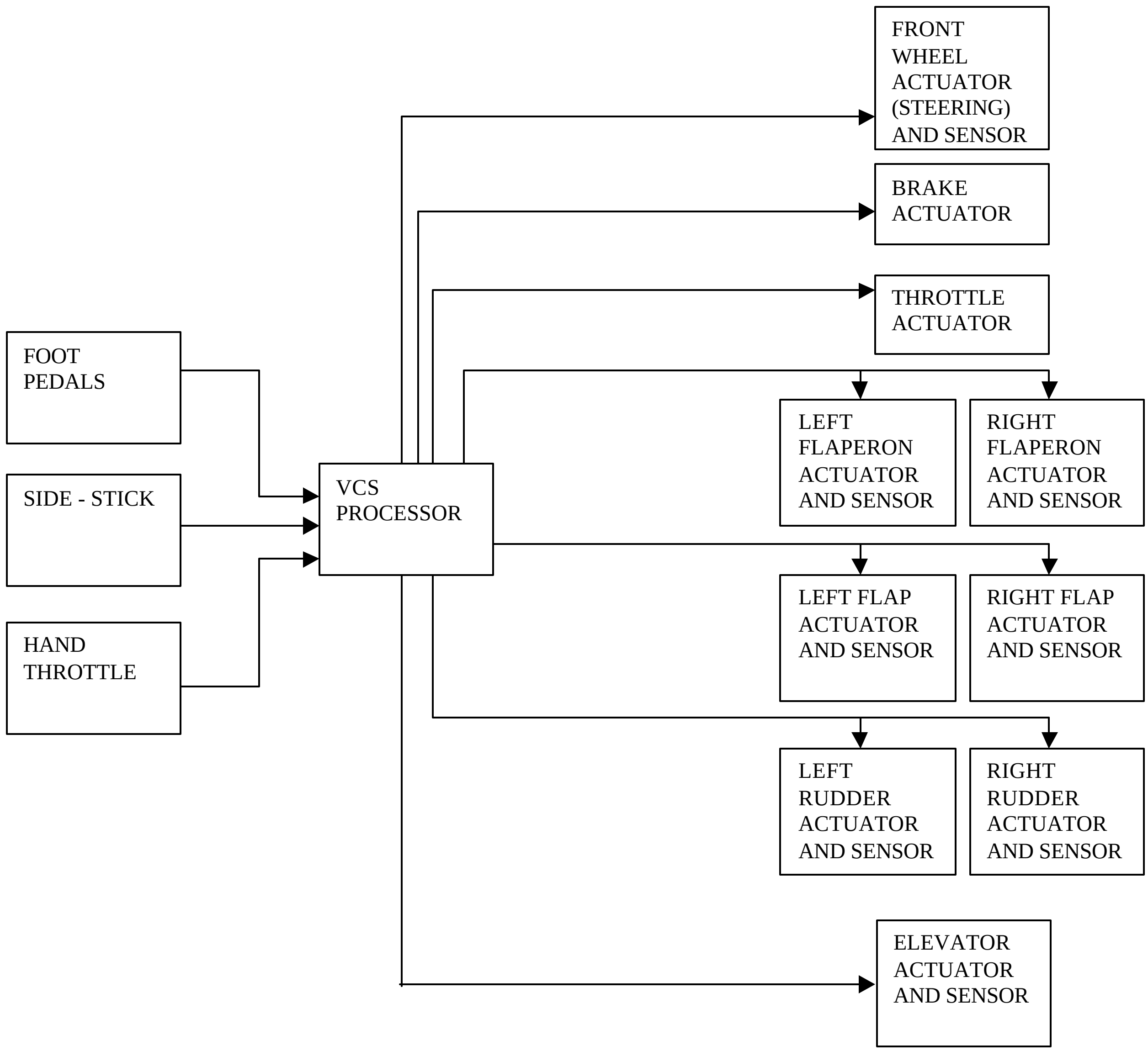

Figure O.6-8: Summary of Components of VCS and their Connecions.

For the Pegasus vehicle it is envisaged to to utilize electrical actuation for all vehicle control functions. One of the primary concerns identified is the actual size of the actuators which comes about by removing an efficient hydraulic system. As technology progresses equivalent electrical componets are becoming significantly smaller, therefore it is not anticipated to be a large problem. There are several manufacturers of electrical actuation devices for different linear and rotary purposes. Outlined below are actuators available for the Pegasus aircraft from Vickers Inc. and TRW Aerospace – Lucas Aerospace. The difference between an all-electric Electro-Mechanical Actuator (EMA) and a more-electric Electro-HydroStatic Actuator (EHA) can be realized. The EMA is acutally substantially larger than the EHA. For the Pegasus vehicle we will be using EHA's for this reason.

Figure O.6-9-O.6-1: Vickers Linear Electrical Actuator.

Figure O.6-10: Electro-Hydrostatic Actuator (EHA).

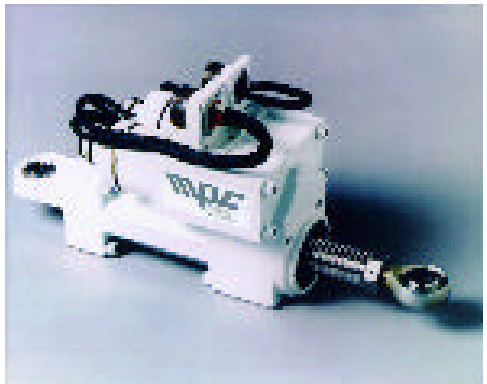

Figure O.6-11: Electro Mechanical Actuator (EMA).

Figure O.6-12: Cut away of an EHA.

O.6.2. Changeover and Emergency Actions Description

The Pegasus is a multi-purpose vehicle that is used both as an automobile and an aircraft. The pilot controls the changeover from one mode of transport to the other. If the vehicle starts in automobile mode the wings are retracted and the propeller is locked in a fixed position. The transmission from the engine is set to transfer motion to the rear wheels and the air data and aircraft sensors are stowed inside the vehicle. The control device determines the direction of the front wheels and the two pedals control the gas and brakes for the vehicle. When the changeover button is pressed the wings telescope out and are locked in the flight position. The control device inputs control the flaperons and elevator (i.e. pitch and roll as in a conventional GA aircraft) and the pedals operate as standard rudder pedals with toe brakes. This functionality is made possible through switching circuitry in the controls and displays sub-system. The automobile external lights retract into the nose of the vehicle and the aircraft lights become active. The transmission switches from the rear wheels to the propeller drive shaft so that power is provided for flight. During the flight the mode change switch is made inactive by the nature that the weight on wheels sensor is open and hence the changeover circuit is incomplete. This ensures that the wings cannot be retracted during flight and hence the safety of the occupants is guaranteed. When the flight is near completion the underside sensors rotate back into the vehicle at a predetermined height above the ground. When the four wheels are safely on the ground the mode changeover switch becomes active again and the vehicle can convert back to an automobile by retracting the wings, activating the vehicle lights and switching the transmission output.

With an all-electric aircraft the main emergency that is going to ruin the crews day will be an engine failure. If this occurs there is no longer any power being generated and hence the electric aircraft is reliant solely on the backup battery for power. Under these circumstances the aircraft relies solely on the essential bus-bar which runs the essential components necessary to fly the aircraft to the ground for an emergency landing. As the engine fails the pilot’s LCD display provides a single radio transmission that the pilot can repeat over the radio to alert the ground as to the current position, height, heading, altitude and nature of the failure. This eliminates some of the stress involved in making the initial radio distress call under the confusing extreme conditions of the immediate failure. The LCD then goes off-line and the remaining standby instruments are used to fly to the ground. At all times the Pegasus has been designed to provide sufficient power to the control actuators so that at the worst an emergency descent and landing can be performed if the power generation system fails.

O.7. Summary

In this appendix, the various systems within the Pegasus have been discussed and their evolution described using the systems process of development. The initial requirements have been considered and with the final systems architecture they have all been met or exceeded, ensuring that the Pegasus has a stable electronic and electrical basis onto which the rest of the design can build upon. Systems for this type of vehicle are complex in their nature due to the need to fulfill a dual role and the Pegasus has systems that maximize efficiency and minimize their total mass through eliminating duplication.

The Pegasus acts as both a vehicle and an aircraft utilizing only one set of controls and can be converted from one vehicle to the other at the press of a button. The dual role controls are the first of their kind and hence an innovation unseen in roadable aircraft to date. The aircraft produces sufficient power not only to power the onboard monitoring and display technology but also to power control actuators and charge a battery for use in emergencies. Although the aircraft utilizes electrical links between the control actuators with no mechanical back up the pilot will still have the same sensation as if they were flying a mechanically linked aircraft due to the simple electrical feedback system. Without pilot intervention the Pegasus monitors all of the utilities systems and ensures that when the pilot needs to be made aware of a certain system status they are made aware and hence the pilot is able to concentrate on the primary flying/ driving task which is hence more pleasurable.

Due to the inclusion of all electric aircraft technology the Pegasus will be one of the safest roadable aircraft on the market without the pilot having to lift a finger. However the use of an all-electric concept produces a great responsibility on the integrity of the electrical power generation system, which must be designed and tested to the highest possible standards and tolerances.

In emergency situations the vehicle responds and immediately sheds electrical loads and provides the pilot with the information that they require to make an intelligent emergency radio call and then fly the aircraft safely for an emergency landing.

References

Vehicle and Engine Technology – Heinz Heisler

Peugeot 106 manual – Haynes

Avionic Systems – D. H. Middleton

The Fliers Handbook – Pan Books

Avionics and Systems – lecture notes, Mr P. Reeves Hardcastle (Loughborough University)

www.vickers-systems.com

www.airsigna.com.

www.cessna.textron.com

Appendix P. Manufacturing and Maintenance

P.1. Manufacturing

Given the construction materials from the Structures sub-group, the task was then to provide a plan of how to manufacture certain components of the aircraft, determine which parts can be outsourced and provide a detailed factory layout of where the vehicle can be assembled in the most efficient manner possible.

The Design Process from Conception to Implementation.

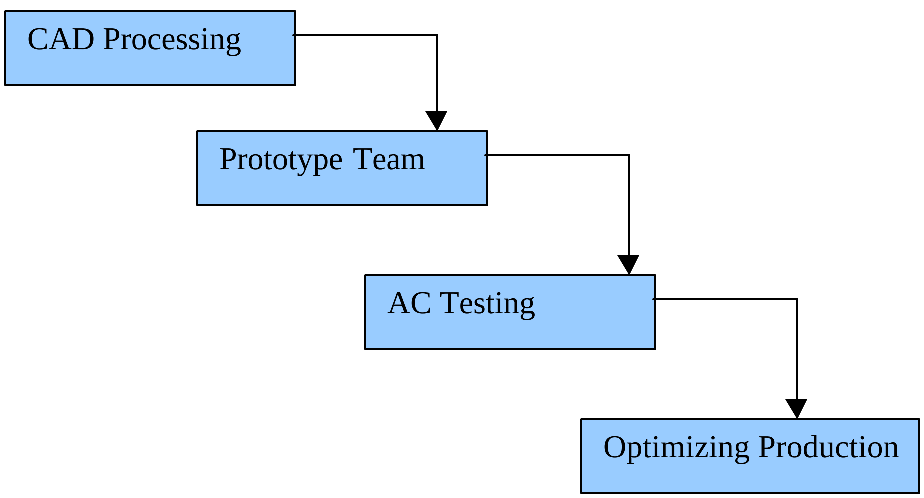

Figure P.1-1Solid Body Computer Modeling

The manufacturing process is basically the realization of a design concept; in this case a roadable aircraft. Once a final design has been reached, it is then passed to the Computer Aided Design (CAD) team who then create a model of the aircraft using a three-dimensional computer modeling package. There are various modeling packages used in the aircraft industry today such as Catia, Pro Engineer, Cadds 5 and UniGraphics; however, we plan on using Catia. These packages allow you create an entire aircraft in a virtual environment so that it can easily be seen how the various components are assembled. Obviously there are countless parts that make up an aircraft and although these computer packages do have the potential to model and assemble every single component on the aircraft this may not always be desirable, since cost and time factors will become heavily involved.

The power of Catia and similar packages is that once you have modeled a particular component, you can then use it to carry out finite element analysis (FEA) by incorporating it into a finite element package such as MSC-PATRAN/NASTRAN. This will enable the design engineer to carry out various stress and thermal analysis of the component i.e. stress distributions, temperature profiles, part deformation and dynamic behavior.

These analyses are of significant importance and needs to be carried before an aircraft enters manufacturing since problems not caught in the design phase may have costly if not catastrophic consequences in service if they are not resolved early. The benefit of using a system like Catia is that a lot of the analysis is done on computer which greatly reduces the amount of manufacturing and testing of components taking place, hence this significantly reduces the time and cost of production. Another application of Catia is that it has the capability of generating the necessary tooling requirements of a component simply from the model itself. It can in essence create a virtual construction plan for the aircraft.

P.2. Prototyping

Once the CAD team has completed their model and analysis of the aircraft with all it's components, they then produce a set of detailed part and assembly drawings, which are then passed onto the prototype team. Their task is to build a prototype of the aircraft; this may be several depending on the size and complexity of the project. We are projecting a series of four prototypes. The prototypes are then built, as closely to the drawings as possible assuming there are no fundamental flaws. The finished prototype can then undergo the various aircraft testing required to certify the aircraft. From the results of the testing, it will be evident if improvements need to be made to the aircraft depending on the type and number of component failures, if any occur. Even though complex FEA may have been carried out earlier on, the results will still need to be proved by physically testing the aircraft to see if it meets the necessary certification requirements.

The prototypes will pass through four phases that develop the plane to desired specifications while yielding valuable market data. These prototypes are called Demonstrator Aircraft's or DA's. Flight test information is then collected while the prototype performs in consumer fairs and expositions. Each phase tests, develops and proves a particular aspect of the final product.

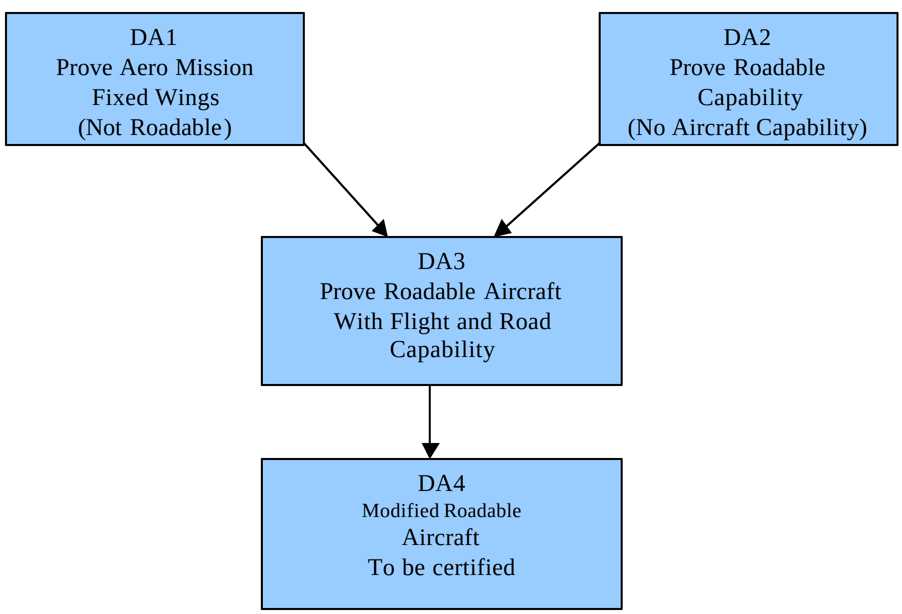

Figure P.3-1 Prototype aircraft test schedule

Demonstrator Aircrafts

The first prototype, DA1 is not roadable but purely an aircraft. It possesses all the same aerodynamic properties and geometry as the final product will have but the outboard wing will be one piece and permanently fixed. It also shares the same cockpit and controls. This craft is tested for stability and control and safety in the air.

The DA2 performs the other half of the vehicle testing by running in solely the car mode. While maintaining all the weight of the final product, this prototype tests roadable properties such as safety, acceleration, and cornering. After these two parallel prototypes tested are, the roadable aircraft prototype, DA3, tested to put into service to mesh the two main systems. This process will find compatibility errors and functional duality issues. This prototype will contain all fly by wire controls and avionics as will the final product as well all the roadable features: suspension, steering, and drive train system. Again the vehicle will be placed in the general public's eye with demonstrations at trade and shows and giving demo flights/rides to prominent VIP's. This gives the production model the opportunity to be adapted to the demand or requests of the potential market. The last prototype, DA4 will be for certification. This craft will continue its parallel mission of convincing potential buyers of its safety and road and airworthiness. As such, its flights will provide excellent feedback from the market itself.

P.3. Certification

The craft must pass FAR 23 Federal Regulations. This certification requires extensive testing and evidence of the aircraft's airworthiness. Initially, the company will need to establish the "applicability" of the certification. The "type" and category has to be defined. With that, it must be determined "eligible." Then the aircraft is inspected and tested to determine compliance to the regulation. This will include flight-testing, instrument calibration, and establishment of manufacturing faculties and the corresponding quality control procedures.

Following are the categories of inspections that must be met according to the FAR 23 for our Roadable Aircraft to allow certification:

Flight:

- Controllability
- Flight Characteristics
- Performance
- Spinning
- Stability
- Stalls
- Trim

Structure

- Ailerons and Special Devices
- Control Surfaces
- Emergency Landing
- Fatigue Evaluation
- Fire Protection
- Flight Loads
- Ground Loads
- Horizontal Stabilizers
- Vertical Surfaces
- Water Loads

Design and Construction

- Control Surfaces
- Control Systems
- Electrical Bonding and Lighting Protection
- Fire Protection
- Landing Gear
- Personal/ Cargo Accommodations
- Pressurization
- Wings

Power plant

- Cooling
- Exhaust Systems
- Fuel Systems/ Components
- Induction System
- Liquid Cooling
- Oil System
- Power plant controls
- Power plant Fire Protection

Equipment

- Electrical Systems and Equipment
- Instruments Installation
- Lights
- Misc. Equipment
- Safety Equipment

P.4. Manufacturing Processes

Once the aircraft is fully certified then it will have reached the stage where it can be mass-produced. This is where the production engineers become involved. Their aim is to assess the manufacturing process initially employed to build the prototype aircraft and see how those methods can be optimized for mass production. The production engineers will see how they can speed up the manufacturing process, hence reducing expensive labor costs. They will also investigate the most effective methods to construct the components on a large scale, most likely using a cellular manufacture approach. Where possible it will be desirable to use outsourcing, which involves using previously manufactured goods for some of the components.

There are many strategies which are employed by companies these days to try and achieve an optimum manufacturing process. However the one most frequently featured is lean manufacture. Lean manufacturing derives it name from the manufacturing systems and processes of the Toyota production system that are extremely effective at producing at low cost, high quality, and short cycle times. Lean manufacturing identifies waste and eliminates non-value added activities. Every step and process of lean manufacturing is designed to make the shop floor closer to the customer. However, it does not require a large capital investment. What it does require is a commitment and belief in the principles and the self-discipline to adhere to them. Lean Manufacturing will work in nearly any environment and under many circumstances.

These sorts of strategies are usually applicable to larger manufacturing organizations where small changes in the implementation of their production processes can have significant effects on efficiency of manufacturing.

A key area in the manufacturing process is quality control. Traditionally quality control has been concerned with detecting poor quality in manufacturing products and taking corrective action to eliminate it. However, quality control encompasses a broader scope of activities including statistical process control (SPC). The main aspect of quality control in a manufactured product is to ensure that it is free from any deficiencies. That means that the product does what it is supposed to do (within the limitations of its design features) and that it is absent of defects and out-of-tolerance conditions. Variability exists in the manufacturing process because of the physical variations that can occur. These can be due to random discrepancies e.g. human variability with each operation cycle, variations in raw materials, machine vibration, etc. Also exist predictable variations, which are discrepancies incurred because of changes in operating conditions e.g. operator mistakes, defective raw materials, machine malfunctions. This is where methods like SPC become involved, they make use of a range of statistical methods to assess and analyze variations in a process. SPC is based upon a control chart, this is a graphical technique in which statistics computed from measured values of a certain process characteristic are plotted over time to determine if the process remains in statistical control. If the sample values lie inside the lower and upper control limits, the process is referred to as being in ‘statistical control’.

P.4.1. Stage 1

The Control Surfaces and Doors.

The first aircraft components constructed are the horizontal stabilizers, rudders, ailerons and flaps. These are manufactured by the traditional laminated foam core process. The core of each component is cut using hot wire processing to sculpt the blocks into the desired profile. Initially human operators will do this although when full production runs are operational then CNC machines can be used. Once shaped, the blocks are applied with a resin that attaches the fiber sheets to the surface. The fibers used in this region are bi-directional so as to follow the complex surface contours of the foam inserts. Over surface areas where the no curves exist or the curve is only about one axis, the unidirectional weave is applied.

The doors are unique in that their construction is entirely from carbon fiber. The reason for this comes from their role as a roll over hoop. In order to achieve adequate levels of safety for the occupants, the carbon fiber skins resist extreme dynamic loads such as those experienced on rolling a vehicle. The tail fins at the rear were considered large enough to protect the rear end of the vehicle should it roll.

In a manner similar to the pre-pregs, the carbon fiber cloth is impregnated with a resin and laid into a mould of the door where it is smoothed to fit. It is the vacuum bagged and cured in the autoclave. The temperatures are carefully controlled and in keeping with current levels ensure that they do not fall below the recognized 15 C minimum. The humidity is kept to a 65% maximum. Dust can also be problematic so a Heaton Green dust extractor is installed, as used in the Europa Aviation plant. The department is equipped with various curing ovens and vacuum systems with paired mixing and cutting rooms and pultrusion rigs. This enables a continuos output of parts and improves the plants efficiency by reducing bottlenecks of production. Time must be spent finishing the surface of the end product due to the imperfections often created in this process. Any imperfections in the surface can lead to increased drag and reduced performance. They are also unsightly to the consumer.

P.4.2. Stage 2

The Wings.

The complexity of the wings necessitate a manufacturing process as efficient as possible to reduce costs. To do this a partial production line within the building is operated with increasing states of assembly being achieved towards the hangar entrance. This ensures that new wings are quick to be fitted and that the large amount of time needed to assemble the wings is kept to an absolute minimum.

The central rotating tubes used for extension of the wing are produced from carbon fibre, which are slotted into the stationary members made from stainless steel. The carbon fiber components are manufactured in house within the composites region of the plant. All the metal components are produced in a separate zone in keeping with the efficient factory ethic. The steel is outsourced as various sheet thickness to save manufacturing time. The skins produced from rolled aluminum are fitted to the ribs using an epoxy resin. The aluminum arrives in sheet form and has to be guillotined into correct profiles. The center box is also produced independently from the wings and is comprised of glass fiber and aluminum honeycombed sandwich plates (SEE APPENDIX H). The rotating tubes used to extend the wings are produced in paired sections to avoid material abnomalies in production. Milled steel sections are used as specified in the materials selection. The different bored tubes are machined from the same ingots to keep material uniformity. The internal threads are gun drilled to reduces tolerances. Unfortunately, this increases the tooling time and costs but the accuracy of the wing alignment is obviously critical. The spar support plates are fabricated form extruded aluminum and the end plates are sheet aluminum cut to size. Also by using aluminum on all the bearing bushes the material diversity is reduced which lowers production costs.

The wing rib sections are made a of carbon fiber sandwich. Due to the simplicity of the centrebox design, the sandwich boards required to build is bought in from external manufacturers. They are vacuum bagged on top of a glass plate during the curing cycle of the resin fiber layers. Although this process produces some waste materials, the process is cheap enough to warrant the technique. Finally, the separate wing halves can be sandwiched together then pressed and glued using 3M-Scotchweld.

P.4.3. Stage 3

The Fuselage

The fuselage is made from two separate moldings split down the water line of the aircraft. The twin boom assembly can be produced in a single sheet, using one mould and the latest pre-preg composites. Using pre-preg sheets lowers the resin content to the optimum level and reduces weight over the more traditional wet lay-up process. All laminating work is carried out in the designated clean room. The environment is strictly controlled to meet necessary requirements for limited contamination areas. During laminating operations, the room is continually monitored for temperature, humidity and particle count. The clean room controls the temperature at 22°C +/- 2°C. The humidity level affects the strength of the laminations and is kept at 40% +/- 10%. Dust creates similar problems as found in the carbon fibre curing process and is restricted to an upper level count of 0.5 micron particle. Finally, the process records the internal pressure to verify that the required level of 38.1mm water. All pre-preg materials used in the manufacturing process are stored at -18C within a cold room, which is divided into two sections: quarantine and 'ready to use' storage. This preserves the limited life of the material. The autoclave uses a hot compressed air technique operating at a maximum temperature of 200C and a maximum pressure of 7 bar. In order to produce high quality parts and limit the warping potential the maximum heating rate is 5°C per minute and a maximum cooling rate of 0.5°C per minute.

The formers between the two halves of the fuselage hold the top to the bottom and are primarily composites with two aluminum inserts on the central load bearing positions. The two central formers are load bearing and are of standard aluminum hoop design as specified by the structural loads. The hoops are designed in house and bonded using a phosphoric acid etching technique, as pioneered in cutting edge automotive design. The extruded aluminum panels are mated with Scotch-weld tape, manufactured by 3M and bought in on a ‘just in time’ (JIT) basis.

As the design is optimized with a single molded cockpit and integrated foot well, the firewall at the rear of the cockpit is made from the modern composite Sperotex and is treated with a phenolic resin to satisfy fire regulations. It is bonded to the cockpit floor in the lay up process. This involves building up the cloth layers and strengthening the material in hard point areas such as wing and engine attachment, undercarriage pick up points or seat belt fixings. When the correct depth of pre-preg layers has been achieved, the mould is vacuum bagged and cured in an oven. The process is identical to that of the previous pre preg method.

The cockpit floor is produced in a similar manner to the fuselage, the only difference being a different mould. The lay up incorporates all the hard points for seatbelts, wing fixtures, luggage space, and fuel stowage.[1]

P.4.4. Stage 4

The engine and ancillaries.

All the engine ancillaries are outsourced from Wilksch who also provides the engine. This was purely a cost saving venture. The engine comes ready made and merely needs oil feeds, water hoses and exhaust components. The drive from the gearbox to the propeller is finally attached before the completed unit is wheeled out ready for connecting to the airframe.

P.5. Final Assembly

The cockpit electronics are assembled in a controlled environment within the building. The hydraulic systems and electric actuators for the control surfaces are partially assembled and ready to be positioned within the glass fibre mould. Once the equipment has been checked, the avionics and cockpit apparatus are assembled behind the panel fascia. The steering mechanism and brake servo is then attached to a hard point on the back of the cockpit floor and the pedal attached to the servo housing. The recess in the fuselage hull is left free from the front undercarriage, which allows careful positioning of equipment during the assembly process. Upon completion, the cockpit floor is then lowered into the hull. The floor is attached using aerospace adhesives. The cavity in the undercarriage wells allow the bus bars to be connected and the wiring loom to the engine from the display to be positioned and secured. This allows the remaining electrical wiring to be connected through simple connecter plugs when in position without having any accessibility problems.

Formers are then positioned within the hull and bonded onto position. The wing fixing mechanism is then secured to provide a central root for the attachment of the root section. Following that, the electronics, fuel systems, and control mechanisms as well as the undercarriage electrical and hydraulic supplies are all routed within the channels cut into the formers. The assembled wings are then attached in their extended mode to the hard points and the wiring loom connected and tested. The advantage of assembling all the components into the hull before attaching the top surface is the ease of the work can be done in attaching all the subsystems without being hindered by the fuselage. It also allows the possibility of further mechanical automation for the futures should the sales exceed the proposed demand.

The engine is next secured onto its four fixing bolts behind the bulkhead and connected to its fuel feed, cooling systems and fire protection systems. The gearbox is pre-mated to the engine and the only drive to be connected is that of the rear wheels. Finally the monitoring sensors and electrical supply is connected.

In parallel to this process, the tail surfaces are put into place within the boom and the control actuators mounted to their hard points and wired in. The electrical looms for the port and starboard rudder are secured to the top of the inner boom surfaces and fed up the undercarriage recess where they are finished ready for mating to the lower aircraft. This allows the joining of the top of the fuselage with the hull.

The formers and lips of the hull are coated with a standard aviation epoxy adhesive, as are contact points on the wing. The top is then lowered to mate with the hull and aligned in a jig before setting commences. The recess for the rear undercarriage is still free from the rear wheels and allows electrical connection of the tail control surfaces to the wiring loom exiting the aft of the boom, secured in place earlier.

The drive from the engine to the propellers and the rear wheels is then fixed in position and tested for the full range of motion. The spring/damper units are then fitted to the booms on hard points and attached to the swing arms. This leaves the wheels and braking to be attached for rear undercarriage completion. Due to the cost saving strived for, the majority of the undercarriage parts are outsourced. This reduces the R & D costs and also saves expensive time that could be spent on assembling its constituent components.

At the front of the aircraft, the window mechanism is fitted along with the side stick controller-wiring loom into the doorframe. The door cards are then added to trim the interior surface and the side stick arm rests attached and connected to the exposed loom. Acrylics windows are then fitted and sealed in place. The doors are then connected to the fuselage. The whole structure is then raised on a hydraulic cradle to give access to the fixing points for the front undercarriage. Finally the front undercarriage is assembled to the fixing point within the front two floor pan cavities.

With an aircraft having systems as complicated as these, a computer test is run externally with all the systems to check their responses. This link is via the modem port used for out of factory servicing and is housed in the undercarriage cavity for ease of access again. The computer runs a data burst and monitors the expected output with that achieved using existing technology as pioneered by McLaren. This process is carried out within the factory shown in figure P.6-1.

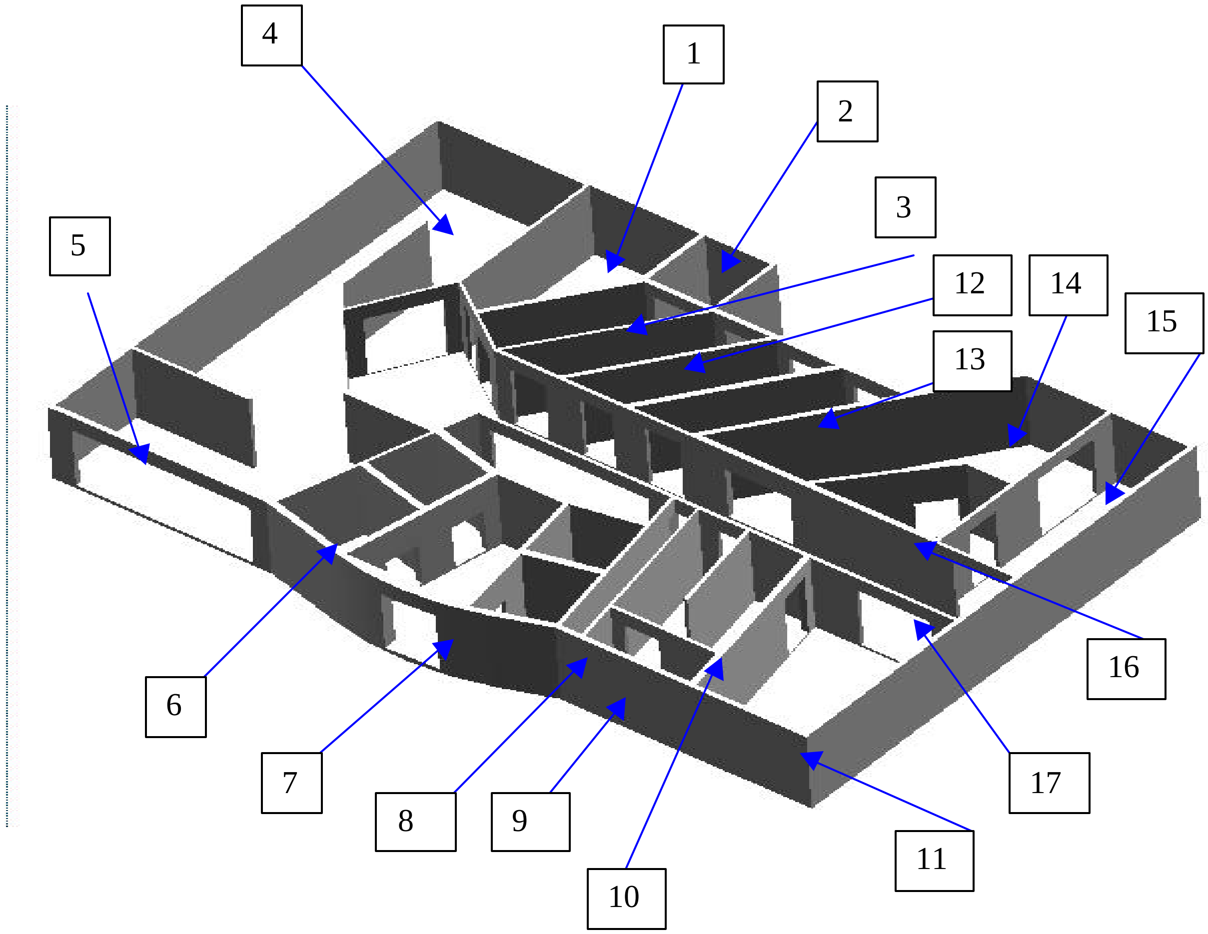

Figure P.6-1 Manufacturing Plant Layout

Key.

1. Systems test bay. Using methods mentioned earlier, this bay uses state of the art computer diagnostics to primarily test the FBW and electronic wing mechanisms. Other tests include noise measurement, propeller balancing and ASI calibration.
2. Outsourced stores. This zone is essential to run the JIT methods suggested.
3. Finishing shop. Doors, wing mirrors and final additions to the airframe are implemented here.

4. Paint shop. The paint shop has the facility for the spraying of polyurethane and epoxy paint systems, with the capability of baking up to 80°C. In addition, a combined preparation zone for spraying primers and undercoats is available.
5. Hangar entrance from Storage area.
6. Business offices and administration area. The running of the business is carried out in a region central to the manufacturing so the staff has a greater appreciation for the production of the product.
7. Main entrance.
8. Electrical loom assembly.
9. Avionics processing area.
10. Cockpit floor processing zone. The cockpit floor is fitted here with all hardpoints and surface panels before the addition of the avionics system.
11. Composite production zone. The shop, include lathes, borers, routers, radial drills and saws.
12. Front and rear outsourced undercarriage component assembly.
13. Outsourced engine assembly line.
14. Wing assembly line.
15. Metal component production zone.
16. Metal shop stores. Main fuselage hull assembly line.
17. Zone 17 is the main route the hull takes from start to finish and the attaching of the fuselage upper half.

P.6. Environmental Concerns

The company structure of the aircraft manufacturer along with the major departments within it, is shown in figure P.7-1.

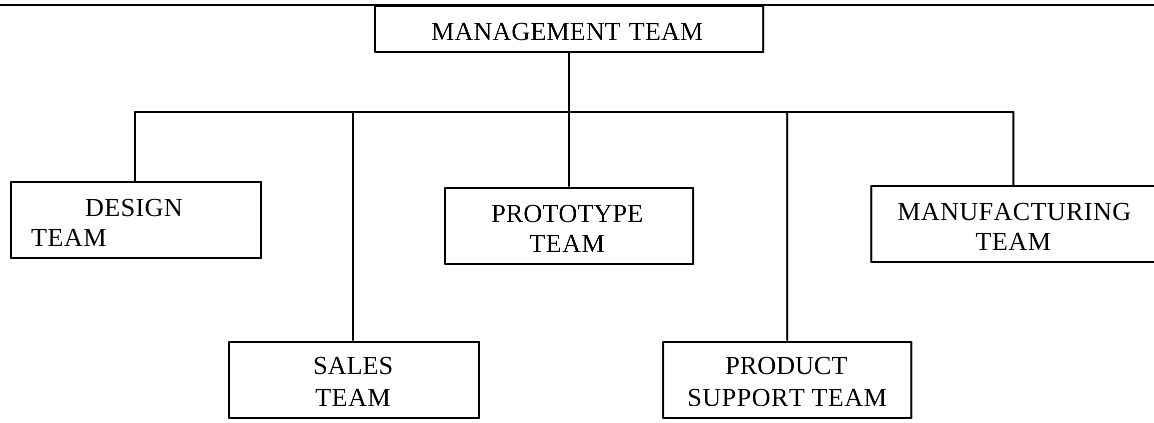

Figure P.7-1 Company structure

The management team will manage the entire process from the early conceptual design phase to the sales and product support. The roles of the design team, prototype team and manufacturing team have already been descibed in the previous sections.

The sales team will be an important factor to the success of the company. Their main objective will be to advertise and market the aircraft to all the potential consumers and establish public confidence in the idea of a roadable aircraft. After successful introduction of the aircraft into the American market then foreign markets must be targeted across the globe. The fact that the vehicle can be driven from either side in the radable mode enhnaces the international sale-ability.

The customer support team will be responsible in providing after market service to the consumers of the aircraft. This will mean having a twenty four hour service available so that the customers can contact the company at any time via telephone, fax or e-mail anywhere in the world. The customer support team will also be in charge of the maintence and servicing of the aircrafts, making sure the customer is always entirely satisfied with the product. Once the team has established itself in the marketplace and has a substantial user base, it will then be able to create a computer database cataloging all the aircraft in service and identifying any common faults which may be present. This information can then be relayed back to the design and manufacturing departments as well as to the management so that the overall design of the aircraft can be improved and optimised and changes can be made when necessary in the future.

Appendix Q. Cost Estimation

Q.1. Market

Marketing the Pegasus was very important to the design process. An extensive market survey was found on the AGATE web[1]. The survey participants included current, former, and potential pilots. Relevant information pertaining to our design indicates that a large majority of respondents currently:

- Travel 3 – 5 hours away
- Take 50% or more trips by car (more than 2 hours away but less than 1000 miles)
- Travel 5 or less days per month for business
- Travel 5 or less days per month for personal travel
- Travel on an irregular schedule
- Are not full owners of aircraft

The survey also addressed the most important benefits of a general aviation aircraft. The top three benefits indicated by the respondents were affordability, reliability, and increased safety. Almost 50% of the respondents to the survey would increase travel to more than 10 days per month if traveling were faster and cheaper. In comparison to commercial fights, the Pegasus reduces travel time by affording the convenience of driving to and from a local airport and not dealing with tickets and checking baggage. Increased travel would also increase the usage of the smaller general aviation airports around the country, which is one of AGATE's goals

According to 123 potential pilots that responded to the survey 21% indicated that the reason to learn to fly was for transportation. Another ten percent said convenience or business was a reason to learn to fly. The majority of respondents indicated that it was a lifelong dream.

Also, a majority of the respondents indicated that a desired key feature was a graphical pilot interface.

The main market of the Pegasus is small businesses that have the need to travel but cannot afford the cost of a business jet. As discussed in the next section, the cost of the Pegasus is well within the range of a small business.

Q.2. Technique and Discussion

Cost was a key factor in the design of a roadable aircraft since the cost needed to be competitive with other general aviation aircraft. It was imperative that the aircraft be designed with amenities and technological advances needed to attract small businesses as buyers, yet the cost had to be affordable. To produce the cost analysis of the Pegasus, a cost spreadsheet was generated[2].

The spreadsheet was utilized to make continuous changes to the cost as the aircraft was modified throughout the design process. Preliminary assumptions made during the cost estimation process included hiring highly qualified personnel for the design and manufacturing of the aircraft.

The final cost estimate was highly dependent on several factors including take-off gross weight, maximum velocity, and total number of aircraft to be produced. The estimated cost is the result of modern manufacturing techniques and good organization. A production rate of 1000 aircraft per year for 10 years is predicted leading to a total 10,000 vehicles produced. Normally, for general aviation aircraft, this rate is approximately 200 per year for 30 years. The 1000 aircraft per year production rate reflects the immediate need of the Pegasus to small businesses and is similar to that of an automobile production line. Figure Q.2-1 is a graph showing the relationship between production and cost of the Pegasus.

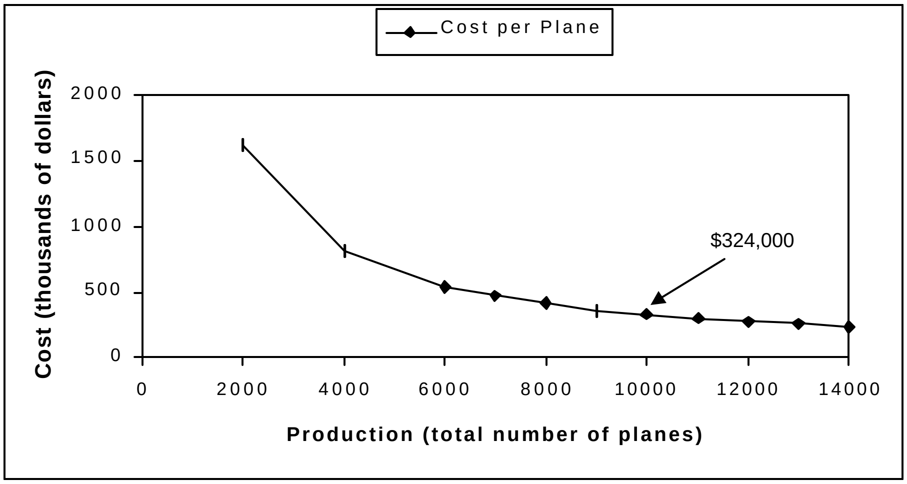

Figure Q.2-1 Cost vs Number of Aircraft Produced

Based on these calculations, a sale price of $324,000 is expected. In comparison to other general aviation aircraft, this is a reasonable price based on the amenities and technological advances the Pegasus offers. Table Q.2-1 shows direct comparisons in the standard equipped vehicle prices and features of the Pegasus versus other general aviation aircraft.

Table Q.2-1 Comparison of Features and Cost

VEHICLE:	Pegasus	Cessna 182 Skylane	Cirrus SR20	Mooney M20S Eagle	Piper Arrow
PRICE:	$324,000	$227,000	$188,000	$345,000	$230,000
FEATURES:					
4 Passengers	✓	✓	✓	✓	✓
Yoke		✓		✓	✓
Joystick Control	✓		✓		
Advance Avionics System	✓	✓	✓	✓	✓
Mechanical Instruments	✓	✓	✓	✓	✓
GPS (Moving Maps)	✓	✓	✓	✓	✓
LCD Pilot Interface	✓		✓		
Autopilot		✓	✓	✓	
TCAS System	✓				
Weather Data Link	✓				
Leather Seats	✓	✓			
Vehicle Entertainment	✓		✓		
Air Conditioning	✓				
Power Outlet	✓		✓		

As revealed by the table, the standard equipped Pegasus offers many features not found in the base models of the other aircraft. These advanced features such as leather seats, vehicle entertainment, and various navigation aids such as a weather data link system are available in these other aircraft but at extra costs to the buyer. Incorporation of these features into the comparator vehicles would considerably raise the price of each bringing its overall cost close to that of the Pegasus.

1) www.agate.larc.nasa.gov

2) - *Airplane Design, Part HIT Airplane Cost Estimation: Design, Development, Manufacturing, and Operation*, Chapters 3 and 4, by Roskam.

Appendix R. Model

R.1. Construction

Fuselage

The fuselage was constructed using a skeleton process. Scaled drawings were developed and used as templates. These drawings included the length of the fuselage and six cross sections that were strategically placed. The templates were placed on plywood and then cut to size. The pieces were slotted as to slide them together for a secure fit. Once the cross sections and the main length were connected creating the skeleton, foam was roughly cut to size using the cross-sections as templates to fit snugly within the gaps between the cross-sections. Once all the foam was cut to fit horizontally, the skeleton and foam were all glued using wood glue to secure the main body of the fuselage. A hot wire, wood files, and sand paper were used to shape the foam to a rounded edge, thus making the fuselage a smooth figure.

After the main construction of the fuselage body was complete, dry wall compound was used to create a smooth uniform surface. Several layers were applied, sanding after each.

Inner Wings

The inner wing was more of a mechanical construction. A mounting base was needed to enable mounting for testing, therefore it was thought that the best location would be in the center of the model and within the inner wing. The metal mounting base was attached to two blocks of wood that were the length of the inner wing. The ends of these thin blocks were attached to the inner wing templates with screws. This completed the internal construction of the inner wing.

The base was then covered with foam to create a uniform surface. The position of the mounting base was chiseled out of the foam from the inside allowing for a more accurate fit.

Once the foam was fitted perfectly between the inner wing templates and over the mounting base it was glued down and hot wired for shape. Very thin sheets of plywood were glued over the inner wing to create the final uniform surface. A hole was extruded down to the mounting base on the bottom of the inner wing to allow access.

Outer wings

The outer wings were created using a template to hot wire foam. Once the foam was to scale, the wing was covered with smooth cardboard to create a uniform surface. Two rods were secured through the inside of each wing, each protruding somewhat.

Horizontal tail

The horizontal tail was created the exact same way as the outer wings. A template was used to hot wire the foam to a smooth curved surface. The surface was then covered with cardboard, and the plywood templates were glued to the ends.

Vertical Tail

The vertical tail consisted of two plywood templates cut to scale. A thin layer of foam was glue to the outside of the plywood to create a curved aerodynamic surface. Dry wall compound was used over the surface to make it more uniform as was done with the fuselage, including sanding.

Attachment

The inner wing was attached to the fuselage first. During construction of the fuselage a space was left to allow for the placement of the inner wing. Because the inner wing was constructed uniformly, it was placed directly into its position and secured with glue.

The vertical tails were attached second. They were attached to the inner wing with screws as well as with glue to ensure security. The attachment of the vertical tail paved the road for the attachment of the horizontal tail. Screws were used to secure the horizontal tail to the vertical.

Attaching the outer wings posed the most difficulty, because they required an attachment angle. Holes were drilled at this angle into the inner wing on either side. The desire of the team was that once completed, when the outer wings were removed the model will appear as it would on the road. Because of this desire, copper rods were planted inside of the outer wing leaving an extrusion, and smaller rods within the inner wing at the desired angle. The rods were able to slide within each other snugly.

Finishing Touches

After much sanding, the model was ready to be painted. Two layers of a primer were brushed on initially finish off the smoothing process. Once dry, grey spray paint was used as the uniform base color. A combination of purples was used as the final color of the model, thus truly giving it the name “The Purple Nasty”.

R.2. Wind Tunnel Testing

The Pegasus was tested in the Virginia Tech Stability Wind Tunnel (VTSWT). The tunnel is a continuous, closed jet, single return, subsonic wind tunnel with 24-foot long interchangeable round and square test sections of six-foot cross section. It is powered by a 600 hp d.c. motor. A 14-foot propeller provides speeds up to 275 fps. Data from tests is analyzed via computer in the main testing room. Control of the wind speed is regulated by a custom designed Emerson VIP ES-6600 SCR Drive. A complete view of the VTSWT is shown in Figure R.2-1.

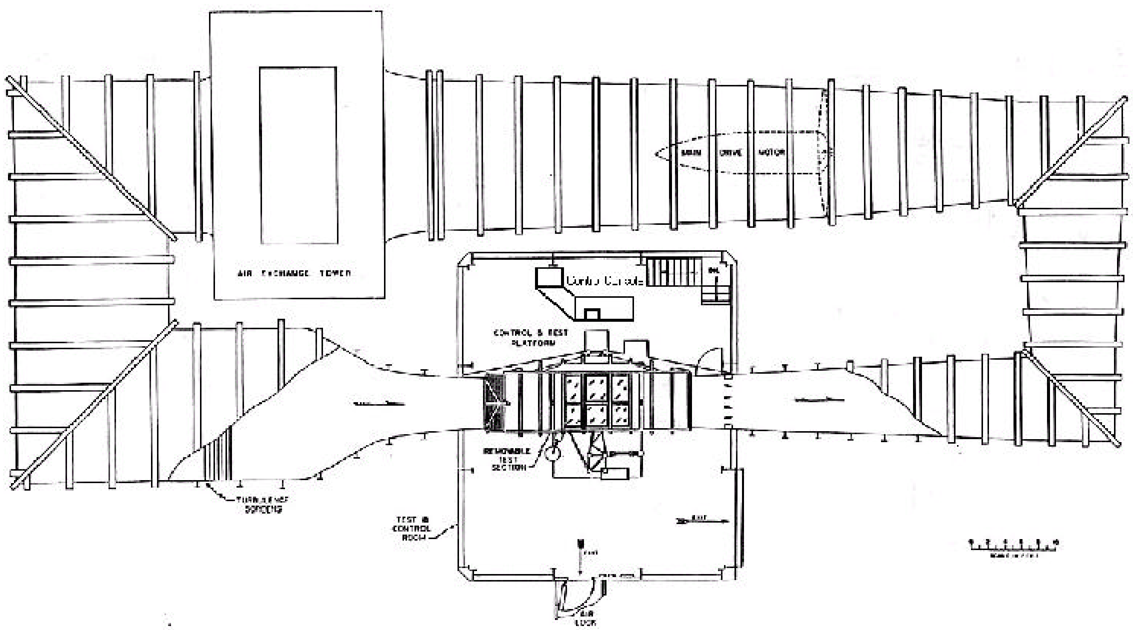

Figure R.2-1: The Virginia Tech Stability Wind Tunnel.

The model tested was 1/8 scale. The model had a wingspan of 1.11 m (3.66 ft) and an overall length of 1.22 m (4 ft). The model was built to this scale to maximum model size while avoiding blockage effects. The model is shown in Figure R.2-2.

Figure R.2-2: The wind tunnel test model in the tunnel.

The VTSWT has excellent flow uniformity with a low turbulence level, which has been recorded to be 0.05% or less. The VTSWT also contains 7 anti-turbulence screens along with other flow smoothing features, which allows for very clean flow.

The model was mounted on a NASA designed and manufactured 6-component strain gauge mount. All tests were run at a dynamic pressure of 493 N/m^2 (10.4 psf). Two force and moment data test series were run, one with the full model configuration and one with the outer wing segments removed. In all tests the model angle of attack was set manually using a digital precision inclinometer and wing template forms which provided a flat reference surface parallel to the inboard wing chordline.

All force and moment and wind flow data was taken electronically using LabView and electronic sensors. Measured quantities included tunnel static and dynamic pressures and temperature plus all six forces and moments. Each recorded data point was the average of 50 readings taken in less than five seconds. Lift, drag and moment coefficient results were displayed in real time and all data was stored for later use.

The third and fourth test runs were made with the model partially covered with wool 'tufts' to obtain a visual record of flow patterns around the model.

Analysis of Results

Test results are shown in Table R.2-1 and in Figures R.2-3 through R.2-7. Because our Reynolds numbers were lower than flight conditions, we expected lower values than theoretically predicted of the maximum lift coefficient, C_{Lmax}, lift to drag ratio, L/D, and angle of attack at stall, α_{stall}. The summary of these results is in Table R.2-1.

Table R.2-1: Wind Tunnel Test Results

Parameter	Experimental Results
α_{stall}	10°
C_{Lmax}	0.9
$\alpha_{L/Dmax}$	6°
L/D_{max}	7.1
$\frac{dC_L}{d\alpha}$ Wings On	3.048 /radian
$\frac{dC_L}{d\alpha}$ Wings Off	.7047 /radian
α_0 Wings On	-7.1316°
α_0 Wings Off	-7.74797°

The lift and drag coefficient profile is shown in Figure R.2-3. In this figure the lift and drag profiles are plotted for both the aircraft and car configurations. However, this car data is not representative of ground effects because no ground simulation was attempted. The car configuration was tested to independently assess the inboard wing's performance compared to that of the entire wing. The aircraft configuration's lift profile shows a gradual, non-precipitous stall performance, which indicates that the inboard and outboard wings stall at different times. The flow visualization photo (Figure R.2-7) corroborates this claim and suggests that the entire wing stalls from root to tip.

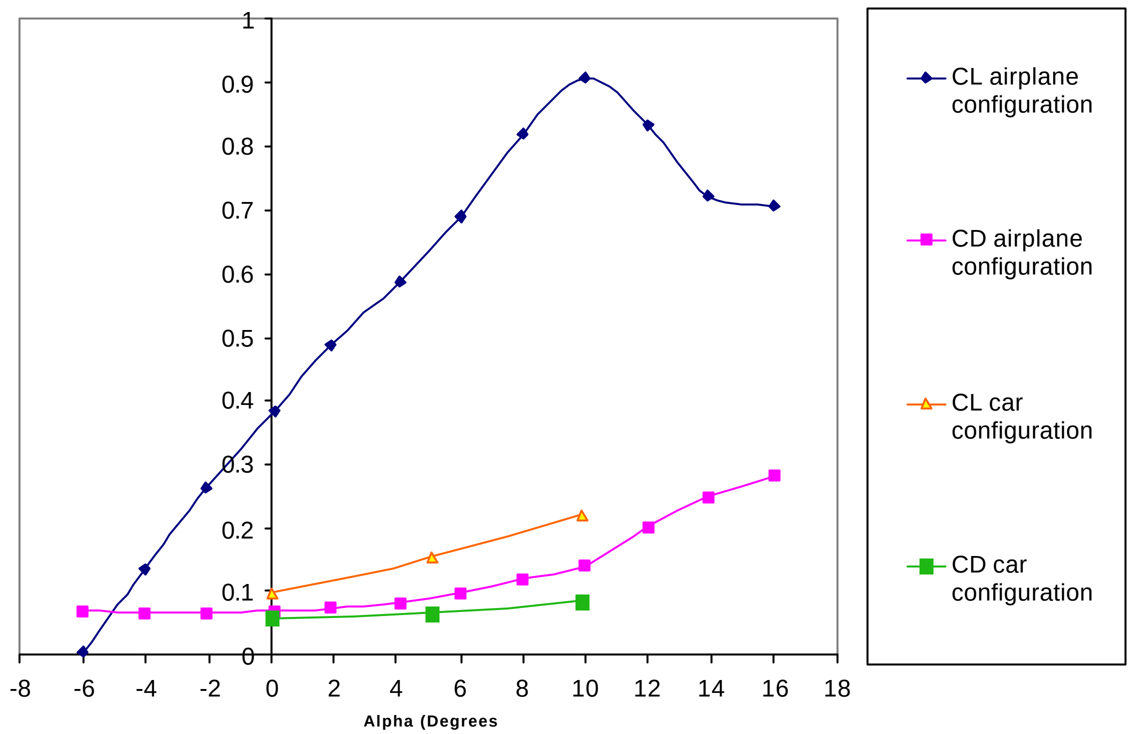

Figure R.2-3: The lift and drag coefficient of the model in both configurations.

The pitching moment coefficient is plotted in Figure R.2-4. The pitching moment coefficient has a negative slope in alpha; therefore, the aircraft is stable in pitch.

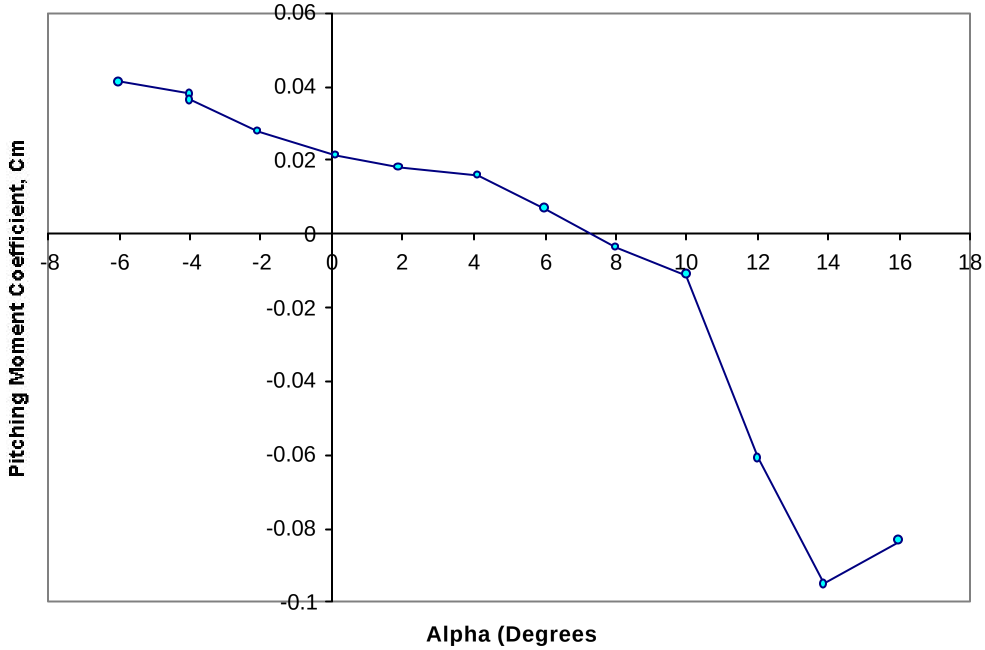

Figure R.2-4: The pitching moment coefficient vs. angle of attack.

The lift to drag ratio is plotted in Figure 5 for each configuration. The *L/D* curve for the aircraft configuration shows an encouraging plateau around L/D_{max} which indicates that cruise can be set nominally at 6°. However the pilot has a large range of cruise angles of attack (2° - 7°) in which the aircraft's range is optimal. The lift to drag coefficient of the car configuration is shown for comparison purposes.

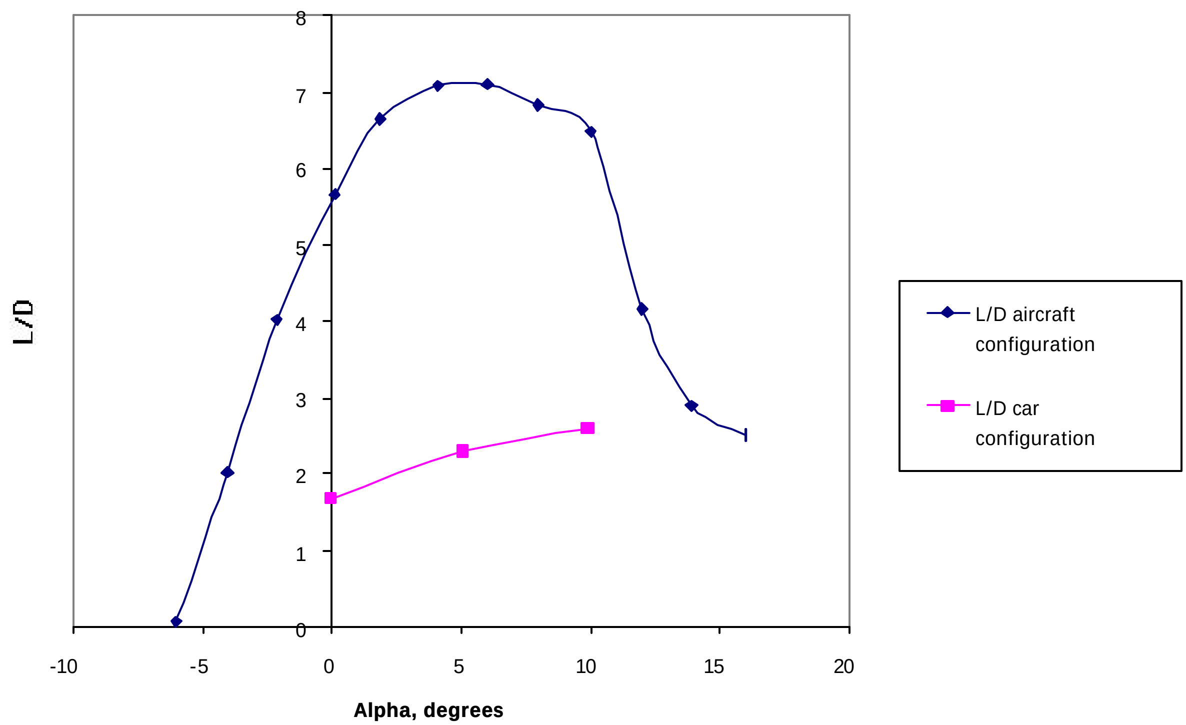

Figure R.2-5: The lift to drag ratio vs. angle of attack for both configurations.

The fraction of the lift from the inboard section to that of the entire wing is shown in Figure 6. This figure demonstrates the differences in the lift curve slopes between the two configurations as well as suggests the distinct stall patterns of the two wing configurations.

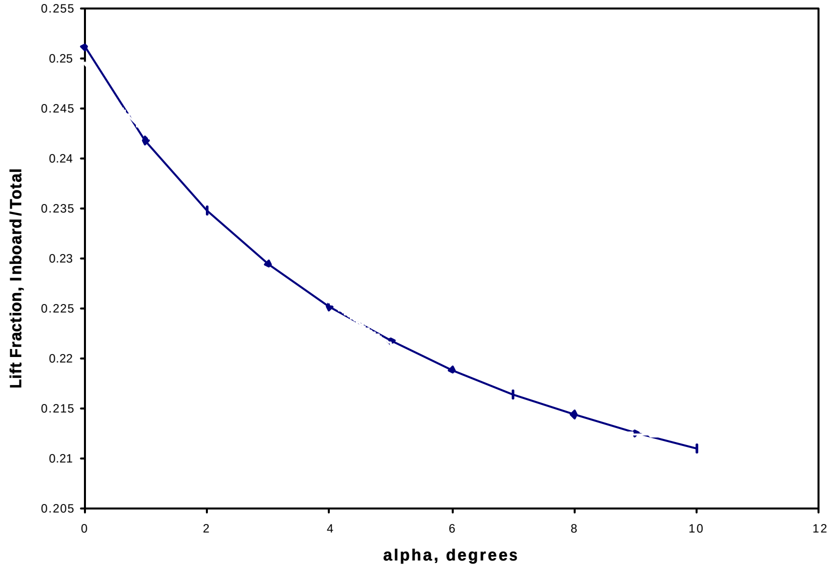

Figure R.2-6: The fraction of the lift generated by the inboard wing of the total lift vs. alpha.

As mentioned, the remaining wind tunnel time was used to perform flow visualization with yarn 'tufts'. The model was run at cruise, stall, and post-stall; the stall run is shown in Figure 7. This photograph demonstrates the appropriate stall pattern for the aircraft as the stall progresses from root to tip. Therefore, the ailerons are still usable at the onset of stall. Furthermore, the elevator is in attached flow at the onset of stall, which dismisses fear of deep stall. Pitch control is still intact when the wing starts to stall.

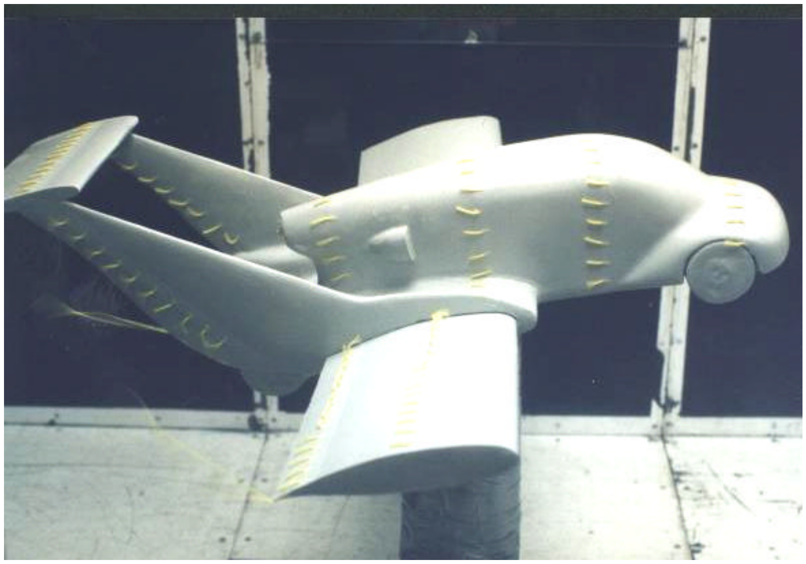

Figure R.2-7: The wind tunnel model beginning to stall. The root-to-tip stall progression is evident, as is the attached flow on the elevator.

Conclusions

The wind tunnel tests of the Pegasus demonstrated the performance and stability of the aircraft. Stall performance is acceptable and the aerodynamics of the car configuration were investigated.